Lib.

MAR 7 1949

REGISTERED No. M. 3121

PROCEEDINGS

OF THE

INDIAN ACADEMY

OF SCIENCES

VOL. XXVIII] *SECTION A* [No. 5

SYMPOSIUM ON

CRYSTAL PHYSICS

IN COMMEMORATION OF

THE SIXTIETH BIRTHDAY

OF

SIR C. V. RAMAN

NOVEMBER, 1948

PRINTED AT THE BANGALORE PRESS, BANGALORE CITY, BY G. SRINIVASA RAO,
SUPERINTENDENT, AND PUBLISHED BY THE INDIAN ACADEMY OF SCIENCES,
BANGALORE.

CONTENTS

PAGE

Sir C. V. Raman on His Sixtieth Birthday.
S. RAMACHANDRA RAO 253

Sir C. V. Raman as Physicist and Teacher.
B. S. MADHAVA RAO 254

Sir C. V. Raman and Crystal Physics.
R. S. KRISHNAN 258

Prefatory Note to the Symposium 288

The Vibrations of an Infinite Linear Lattice Consisting of Two Types of Particles.
N. S. NAGENDRA NATH AND SANAT KUMAR ROY 289

The Vibration Spectra of the Alkali Halides.
R. S. KRISHNAN AND P. S. NARAYANAN 296

The Theory of the Vibrations and the Raman Spectrum of the Diamond Lattice.
R. S. KRISHNAN 307

Some New Techniques in X-Ray Diffraction.
I. FANKUCHEN 312

The Dynamic X-Ray Reflections in Carbon Silicide.
C. S. VENKATESWARAN 316

Fourier Aspects of Implication Theory.
M. J. BUERGER 324

A Simplified Treatment of the Diffraction of X-Rays from Perturbed Lattices.
ANDREW D. BOOTH 332

Recherches sur les Cristaux dans le Spectre Infrarouge.
JEAN LECOMTE 339

Les Oscillations Externes du Reseau Cristallin de la Calcite.
ALFRED KASTLER 349

The Faraday Effect and Magneto-Optic Anomaly of Some Cubic Crystals.
S. RAMASESHAN 360

Theoretical Evaluation of the Acoustic Wave-Velocities in Diamond.
K. G. RAMANATHAN 370

The Photoelastic Properties of Ionic Crystals.
ELIAS BURSTEIN AND PAUL L. SMITH 377

The Infrared Properties of Magnesium Oxide and their Interpretation.
ELIAS BURSTEIN, JOHN J. OBERLY AND EARLE K. PLYLER 388

PAGE

Spectres de Raman du Chlorure et du Bromure D'Ammonium.
LUCIENNE COUTURE ET JEAN-PAUL MATHIEU 401

The Influence of Optical Activity on Light-Scattering in Quartz.
V. CHANDRASEKHARAN 409

The α–β Transformation in Quartz.
P. K. NARAYANASWAMY 417

A New Method of Calculating the Piezo-Electric Constants of α-Quartz.
BISHAMBHAR DAYAL SAKSENA AND KRISHNA GOPAL SRIVASTAVA .. 423

Variation of the Piezo-Electric Constants of α-Quartz with Temperature.
BISHAMBHAR DAYAL SAKSENA AND KRISHNA GOPAL SRIVASTAVA .. 437

The Thermo-Optic Behaviour of Mica.
T. RADHAKRISHNAN 447

The Dynamical Theory of the Vibration Spectra of Crystals. Part V. The Fluorspar Structure.
K. G. RAMANATHAN 454

Dynamical Theory of the Vibration Spectra of Crystals. Part VI. The Zinc Sulphide Structure.
K. G. RAMANATHAN 459

Photometry of Raman Spectra of Crystals.
P. S. NARAYANAN 463

Raman Spectrum of Ammonium Di-Hydrogen Phosphate.
P. S. NARAYANAN 469

A Modified Method for the Determination of Elastic Constants of Crystals.
R. V. G. SUNDARA RAO 475

lastic Constants of Ammonium Chloride and Ammonium Bromide.
R. V. G. SUNDARA RAO AND T. S. BALAKRISHNAN 480

Raman Spectra of Sodium and Potassium Tartrates.
V. M. PADMANABHAN 485

Raman Spectrum of Ethylene Diamine Tartrate.
V. M PADMANABHAN 494

Raman Spectrum of Sodium Chlorate.
C. SHANTA KUMARI 500

Der Einfluss des Kations auf die Intensität des Ramanspektrums von Salzpulvern.
VON OTTO THEIMER 506

C. V. Raman

SIR C. V. RAMAN ON HIS SIXTIETH BIRTHDAY

On the 7th of November 1948, Sir C. V. Raman attained the age of sixty. It was an occasion for public rejoicings all over India. For, more than any other Indian, he has raised the intellectual prestige of the country and placed her well and truly on the scientific map of the world. The respect, esteem, and affection with which he is regarded by his friends and scientific colleagues found expression in the many messages and greetings which reached him from far and near on his birthday.

It is a matter of the deepest satisfaction that the advancing years have laid their hands on him very lightly indeed. During the ten years that have elapsed since the publication by the Academy of the Jubilee Volume on the occasion of his fiftieth birthday, his achievement in research, as evidenced by the stream of published work from his laboratory, has been greater than ever, while the range of his scientific interests has continually expanded. Far from retiring from active research or changing over to less strenuous pursuits, Sir C. V. Raman has consistently refused offers of positions which would have diverted him from his chosen path as an investigator.

During the past few years, he has also perfected plans that would enable him to devote the rest of his life, and the whole of his time, to the pursuit of his scientific interests without having to suffer distractions. On a magnificent site overlooking Bangalore and the surrounding country for over thirty miles on all sides, an imposing structure of granite has been raised which will house a Research Institute of which he will be the permanent Director. The library, the lecture theatre, and the museum of the Institute, have been fitted up and the research laboratories are now being equipped. With the additional advantage of the climate of Bangalore, one of the finest in the world, the Raman Research Institute, on being fully equipped, will certainly attract many distinguished workers from all over the world.

It will be the earnest wish of all that Sir C. V. Raman lives many more years and enjoys the health and strength needed to achieve his aims in the fullest measure.

S. Ramachandra Rao.

SIR C. V. RAMAN AS PHYSICIST AND TEACHER

A BRIEF review of the investigations in the field of crystal physics, carried out by Sir C. V. Raman and his pupils, is given in the next article of the present issue. We only wish to indicate here a few characteristic features of the scientific work of Sir C. V. Raman, his approach to research, and his relationships with his pupils.

The most obvious characteristic is his great passion for physics coupled with an intense enthusiasm and volcanic energy. Even the most casual observer cannot fail to miss the fire in his sparkling eyes which seem to radiate this energy, and to be animated by the dynamic force of an active brain. He lives for his work as few men do, and by his exceptional tenacity of purpose, and of hard work in the pursuit of research he has set a shining example to others.

He has a deep insight into physical processes, and an intuitive sense of physical reality. He has often shown the ability to illuminate a whole subject with a few crucial ideas. His highest work shows the inevitable simplicity of all great work, and has been achieved by spontaneously taking the significant step at the right moment. He possesses in a remarkable degree the gift of seizing the vital point from apparently trivial observations. This genius for picking out the true significance of what to others would be an unimportant detail, and transforming it into a clue to the understanding of fundamental problems is brought out strikingly in his work leading to the discovery of the Raman effect itself.

Raman is a born experimental physicist, and has been guided by the conviction that real progress in physics can be achieved by the application of considerations based on experience and reason to experimental observations of properly chosen phenomena. He has advanced directly and successfully along this straight path without often branching into mathematical physics. Yet whenever occasion arose he has shown that he possessed the mathematical equipment essential to the interpretation of his work. He has also recognised and acknowledged the fundamental importance of ideas of a mathematical or deductive nature. Thus, in the realm of his researches in crystal physics, he has realised the importance of group theory, and the theory of group representations, and encouraged investigations based on such theoretical considerations. He has also shown facility in choosing the right type of mathematical technique needed in his work, and an uncanny faculty

for seeing clearly through a mass of complicated mathematical calculations. His theory of the diffraction of light by high frequency sound waves is a striking example of this. Like all great physicists, however, he has placed facts first, and hypothesis always second.

Though the work of Raman and his school has lain in apparently diverse fields it is easy to discern a coherence and unity in them. The central and guiding theme of all his physical research has been optics in all its aspects. His special love has been for crystal physics, and in particular, physics of the diamond, in which subject he is a recognised authority. He has recently struck new paths in crystal physics, and introduced new concepts regarding crystal structure.

Another noticeable characteristic of Raman's scientific work is its sturdy individualism which is a consequence of the fact that when he started his career he belonged to no particular school of physics, but had to build one himself. He is thus a true pioneer who has had the vision and courage successfully to explore unknown lands in physics. This circumstance has made him attach great importance to an independent approach to problems, and if his valuable example of striking out new and independent paths of research were to infect other scientific workers in our country, we are assured of a bright scientific future indeed. Further, the fact that he had to start work as an independent investigator without the facilities of an already well-equipped laboratory has brought out to the full his skill as an experimenter. Most of his experiments have required neither costly machinery nor any type of special techniques, but have been so simply devised as to be easily understood even by a layman. In fact, the apparatus with which he demonstrated the Raman effect is a model of simplicity and by no means a costly one, but nevertheless this simple experiment is one of the important milestones in the world's knowledge of nature.

It is perhaps not very well known that Raman has shown a fine æsthetic outlook in his research work. His choice of topics for investigation, and his way of handling them bring out clearly his innate artistic nature. His love of music, colour, light, vibration, symmetry, harmony, pattern, structure, and architecture is but the result of a deep appreciation of the beautiful in nature. His researches on musical instruments, numerous beautiful phenomena of wave optics, the colour of the sea, colour in the plumage of birds, iridiscent shells and mother-of-pearl, vibration in crystals, and above all his studies on the form, symmetry and structure of diamond based on fluorescence, phosphorescence and birefringence patterns are a few examples of his æsthetic tastes in research. He has one of the finest

private scientific collections of diamonds and other beautiful crystals, and loves them as only a true artist can.

None who has come in contact with Raman can have failed to notice his very wide and catholic interest in many branches of science besides physics. He has perhaps done as much for chemistry as for physics. His interest in geology based on deep knowledge, specially in the fields of mineralogy and crystallography, has been a stimulant for the geological research of many workers in India. Some aspects of plant life, and animal life, specially birds, have always had a deep fascination for him. He has shown keen interest in and appreciation of astronomical and astrophysical research, both observational and theoretical. Indicative of his wide interests are his plans to build an astronomical observatory, a biological research unit, and a mineralogical laboratory in the new Raman Research Institute. In spite of criticism from some quarters, it can be confidently said that by his collaboration and encouragement he has given the necessary incentive to studies in mathematics even of the purest type. It is safe to say that there is no branch of science in which he has not encouraged creative and original work, and this augurs well for the development of fundamental research in the country in its new set-up.

Raman is not only a great investigator but also a great teacher in the true sense of the word. His ideas and personality have attracted many young research students, and he has held their loyalty and affection by extending a never-failing friendship to them. He has not only taught methods of physical research to his students, but by his own shining example made them realise the necessity of endurance, steadiness and hard work in the pursuit of knowledge. While giving help and encouragement in plenty, he has always expected and sometimes demanded from his students the best that they could give. The writer of this article has had many occasions to see the great care with which he would supervise the papers of his students, sometimes going to the extent of re-writing whole sections. No paper ever leaves his laboratory until he is completely satisfied with it.

The feelings of respect and admiration which his students have towards him can be ascribed to his fairness and even generosity in acknowledging a pupil's ideas or originality. He is very liberal minded and gives away whole lines of research which lesser men would be tempted to keep for themselves. Whenever he discovers any originality in a pupil he will do all he can to develop it. His simplicity and informality are best seen in his discussions with students. Some penetrating remark made by him at such discussions has been the starting point, as some of his pupils have confessed,

of a complete line of investigation undertaken by them later. This has been true not merely in his own special field of research, but in other subjects as well.

Raman has rendered signal service to scientific advance in India as much by his contributions to knowledge as by his training of students in methods of research. He has exerted a profound influence on the work and outlook of not only his students but most of his contemporaries.

Unlike many scientific investigators who are giants in their own laboratories but dwarfs outside unable to take a due share in the national life of their country, Raman has fully participated in several walks of national activity, and is eager to serve the cause of scientific and technological advance in India. Possessing in a rare measure the extraordinary gift of making the most difficult problems in physics appear simple, and with a keen and irresistible sense of humour, he has admirably filled the role of an eminent popular lecturer on scientific subjects. Popularisation of science in the country owes not a little to his gifts of eloquence and exposition.

To have accomplished so much in one's own chosen field of research might have contented many men, but it is not enough for Raman. He has an unquenchable thirst for knowledge, and great energy for exploration, and for him " 'Tis not too late to seek a newer world ". On this occasion of his Sixtieth Birthday, we heartily wish him many more happy returns of the same with the hope that his vision and wisdom may well and truly serve the cause of science.

B. S. MADHAVA RAO.

SIR C. V. RAMAN AND CRYSTAL PHYSICS

OPTICAL theory and the physics of crystals are linked together almost inseparably in the history of their development. It is not surprising, therefore, that his love of optics has led Sir C. V. Raman to take an ever-increasing interest in crystal physics, as will be evident from the titles of the papers communicated by him to the Academy during the past decade or two. Many aspects of the subject have received his attention at some time or another. More recently, also, he has considered the fundamental problems of crystal physics from a standpoint which, while it is essentially novel, has proved highly successful in explaining the facts of observation. In these circumstances, it has appeared desirable to include in the present Symposium on Crystal Physics which commemorates his Sixtieth Birthday, a classified list of the papers on the subject which have emerged from his laboratories during the last thirty years. It is of particular interest to trace the development of his ideas and to indicate the fundamental character of the contributions made by him and his school. This will be done in the present survey.

Some of the most beautiful illustrations of optical principles are to be found in the phenomena of crystal optics. Haidinger's and Quetelet's rings in crystalline plates, the iridescence of twinned crystals of potassium chlorate, the optical effects observed with amethystine quartz, the diffraction of light by the laminar boundaries in mica and the haloes observed in the Christiansen experiment with crystal powders are amongst the subjects of this kind investigated during the earliest years of Raman's professoriate by his pupils. The phenomena of conical refraction exhibited by biaxial crystals have also had a special fascination for him. Amongst the discoveries made in this field may be mentioned that of the formation of sharply focussed optical images by plane plates of biaxial crystals. That naphthalene crystals have an extremely large angle of conical refraction and exhibit the effects arising therefrom in a very striking way is another significant contribution. Many studies have also been published of the beautiful phenomena exhibited by the nacreous layer in molluscan shells and the manner in which they are influenced by the size, shape and relative orientation of the platelets of aragonite appearing in its stratifications.

2. THE SCATTERING OF LIGHT IN CRYSTALS

In the latter part of 1921, Raman commenced his studies on the diffusion of light in transparent media. These were systematically pursued

over a period of years until finally they led to the discovery of the effect known by his name. The work of this epoch was of significance for crystal physics in several ways. The first major contribution which emerged at an early stage was the discovery of the phenomenon of the *thermal diffusion of light in crystals.* Raman was led to recognize its existence by the fact that the clearest crystals available to him, *viz.*, a polished sphere of quartz and a large transparent block of ice, both exhibited a blue opalescence when traversed by a concentrated beam of sunlight and that the intensities observed were of the right order of magnitude, both relatively and absolutely. Ice, which has a high compressibility, showed the phenomenon more conspicuously than quartz, in spite of the higher refractive index of the latter. The inference suggested by these facts, *viz.*, that the scattering had its origin in the fluctuations of optical density in the crystal due to the thermal agitation was confirmed by heating a quartz block. The intensity of the opalescence was then found to increase, as was to be expected.

Following these early observations, the work with crystals was laid aside and studies with gases and liquids were energetically pursued, as they offered a larger variety of promising material for quantitative work. In February 1928, Raman switched over from sunlight to the monochromatic radiations provided by the mercury arc for his studies on light scattering. When his pocket spectroscope revealed clearly the appearance of radiations of altered frequency in the light scattered by liquids, he instantly realised the importance of looking for a similar phenomenon in the light scattered by crystals as well as by amorphous solids. Observations with a large block of crystalline ice showed sharp displaced lines in approximately the same positions as those observed with distilled water. This fact and its theoretical significance are clearly brought out in the paper announcing the discovery of the effect. The magnitude of the frequency shifts observed with ice showed that the phenomenon was of a different nature from the thermal diffusion of light in crystals discovered in 1921, and was to be accounted for on the same basis as the corresponding effect observed with water, *viz.*, an exchange of energy between the incident light quanta and the vibrations of the structural units of the substance.

3. Birefringence and Pleochroism in Crystals

Apart from the discovery of the Raman effect, the studies on the scattering of light in gases and liquids carried on during the years 1921 to 1927 opened up several other pathways of research. They threw a vivid light on the nature of the liquid state, showing clearly that it is far from being a random distribution in space of the molecules composing it. This

led Raman to seek a confirmation of his ideas by undertaking with the aid of his collaborators a series of systematic studies on the X-ray diffraction haloes of liquids and glasses. The results obtained in these studies were found to be explicable on the same basis as the facts observed earlier in light-scattering. Of special significance to crystal physics were the determinations of the optical anisotropy of the molecules or ions made possible by measurements of the intensity and depolarisation of light-scattering in fluids. A correlation became evident between the optical anisotropy of molecules in fluids and the birefringence exhibited by the same substances in the crystalline state. This indicated that the birefringence of crystals is determined principally by the optical anisotropy of the molecules or ions and by the manner in which they are orientated with respect to the crystal axes. Thus, from the known optical anisotropy and the observed features of the birefringence, it becomes possible to draw useful conclusions regarding the structure of the crystal. Indications of this kind were found to be particularly useful in cases where the optical anisotropy and the birefringence are both large, *e.g.*, organic crystals of the aromatic class.

The extensive data obtained regarding optical anisotropy also enabled some general conclusions to be drawn regarding the relation between this property and the chemical constitution of the molecule. It emerged that a large optical anisotropy is accompanied by the presence of absorption in the near ultra-violet or visible region of the spectrum. Further, in such cases, the crystals of the substance exhibit a marked pleochroism in which the axis of maximum absorption coincides with that of the largest optical polarisability, though there are some exceptions to this rule.

4. Magnetic Anisotropy of Crystals

Many papers on magnetism and magneto-optics figure in the published output of Raman's school. The early studies on light-scattering, remarkably enough, gave an impetus to work in this field. Magnetic birefringence in liquids owes its origin to the fact that while the magnetic field tends to orientate the molecules, their optical anisotropy results in double refraction. Thus, simultaneous studies on magnetic double refraction and on light-scattering in liquids enable the magnetic anisotropy of the molecules or ions to be evaluated and connected with the magnetic anisotropy of the solid crystal of the same substance. The known magnetic behaviour of the crystalline nitrates and carbonates was successfully explained by Raman and Krishnan in this way. The large magnetic anisotropy of the benzene ring deduced by them in the same fashion proved to be a fundamental discovery, since it led to the recognition of the still larger anisotropy of other

aromatic molecules and opened the way to the interpretation of the magnetic behaviour of crystals of those substances. Indeed, magnetic studies were shown to be a powerful aid to crystal structure analysis by the early work of Bhagavantam with naphthalene and anthracene. So impressed was Raman by the importance of the method that he initiated studies on magnetic birefringence in many liquids in which it had not been previously observed. This work led to the discovery of the weak negative birefringence exhibited by water, the aliphatic hydrocarbons and other liquids. Crystals of substances exhibiting such negative magnetic birefringence show a relation between their magnetic and optical behaviour quite different from that of crystals of substances, *e.g.*, the aromatic series, which show a positive magnetic birefringence in the liquid state.

5. Raman Effect Studies

Raman's discovery of 1928 opened up a vast new field of activity which was naturally taken up by his collaborators with enthusiasm, and many publications dealing with different aspects of the subject emerged from his laboratory. The effect exhibited by crystals was in the foreground of this activity from the beginning in view of its evident importance for an understanding of the theory of solids; indeed, during the last ten years, work with gases and liquids has been completely laid aside in favour of crystals which present both a challenge and an incentive to investigators in the field. They are a challenge since the difficulties of obtaining satisfactory material and of eliminating spurious effects due to parasitic illumination and instrumental defects are great. They are an incentive, since the sharpness of the Raman lines observed with crystals encourages employment of the most powerful instruments capable of revealing the maximum of detail and yielding data with the precision characteristic of spectroscopy. The major aim of the work in recent years has been that of elucidating the physical problems of the solid state, the substances chosen and the studies undertaken being both determined by this aim. Amongst the topics investigated are the following: the influence of temperature on the sharpness, position and intensity of the lines; the changes in the spectra accompanying thermal transitions in the crystal; the change from the solid to the liquid state; the identification of the modes of vibration active in light-scattering; the influence of crystal symmetry and structure on the spectra, and so forth. We cannot here describe either the techniques employed or the results obtained in these researches. It is necessary, however, to mention an important group of investigations designed to elucidate the fundamental problem of the nature of the vibration spectrum of a crystal. Taking for instance, the case of diamond, its Raman spectrum as ordinarily recorded

is a single extremely sharp line with a frequency shift of 1332 cm.$^{-1}$ Obviously, this cannot represent the complete vibration spectrum and there should be other frequencies in it. The task of establishing their existence has been successfully accomplished by the present writer and the results are of very great interest. The results show in a perfectly unambiguous way that the vibration spectrum of diamond consists of a whole series of sharply defined discrete frequencies, of which only the highest is represented by the frequency shift of 1332 cm.$^{-1}$ The remaining frequencies do not appear in the first-order Raman spectrum ordinarily recorded. But with adequate exposures they appear as overtones and combinations in the so-called second-order Raman spectrum. The latter has also been successfully recorded with numerous crystals besides diamond.

6. The Thermal Scattering of Light

We return to the phenomenon discovered by Raman in 1921, namely the thermal diffusion of light in crystals. The thermal agitation which gives rise to it may be identified with stationary elastic vibrations of various modes and frequencies determined by the elastic constants and by the size and shape of the crystal. The diffusion itself would arise from the modulation of the optical wave-motion by the elastic vibrations and should therefore exhibit frequency shifts, while its strength would be determined by the photoelastic properties of the crystal. It would evidently not be easy to determine the distribution of intensity in the resulting spectrum unless, following L. Brillouin, we regard the crystal as of infinite extension. Whether this is always permissible is a question.

The frequency shifts to be expected theoretically are small and therefore not easily determined; lack of perfect monochromatism in the incident radiation and any Tyndall scattering present give rise to serious experimental difficulties. The subject is, nevertheless, of great interest and many studies have been published. Particular success has been achieved in the case of diamond which gives large frequency shifts not requiring interferometric aid for their observation. A perfect elimination of the Tyndall scattering is also possible by the use of the resonance radiation of mercury and a mercury vapour filter. An experimental result of great importance which has been established with this technique is that the elastic vibrations in a crystal are wholly incapable of giving rise to an observable diffusion of light, unless their "wave-lengths" are such as to give a regular Brillouin reflection. The behaviour of the elastic vibrations in the crystal is thus in complete contrast with that of the modes of vibration with discrete frequencies which readily record themselves in the second-order Raman spectrum even when they do not appear in the first order.

7. The Vibration Spectra of Crystals

A fundamental question in the theory of the solid state is the nature of the vibration spectrum of a crystal. The new approach to the solution of this problem made by Raman is based on the idea that since we are concerned with the vibrations of a mechanical system, we have necessarily to consider its "normal modes". Further, the approach to the problem of finding these modes is necessarily different for the "elastic" vibrations in a continuum, and the "atomic" vibrations in a discrete structure. In the former case the vibrational modes and frequencies are determined by the external boundary conditions, while in the latter case, the time-periodic movements in the units of the structure are analogous to the vibrations of a polyatomic molecule and hence the external boundary conditions are wholly irrelevant. Following up this idea in a straightforward way, Raman derived his fundamental proposition that the structure of a crystal having p atoms in each of the cells of its structure has $(24p-3)$ normal modes of vibration, and the same number of discrete frequencies of vibration unless this is reduced by reason of symmetry of the crystal and consequent degeneracy of the modes. This is a result of far-reaching importance which explains in a completely quantitative fashion the experimental results mentioned in the preceding two sections. In particular, the experimental fact that the 'elastic vibrations' of a crystal are wholly inactive in light-scattering (except in the case of a Brillouin reflection), while the structural vibrations are active in the second-order if they are not active in the first-order is a clear indication that they are different in their physical nature. The recognition of such a difference is, in fact, the starting point of the new theoretical approach.

8. The Structure and Properties of Diamond

Diamond is a substance of extraordinary interest to the physicist engaged in the study of crystals, since it exhibits the characteristic properties of the solid state in an exceptional degree. For this reason the investigation of the physical behaviour of diamond has of recent years formed one of the principal activities of Raman's laboratory and many papers have been published describing the results.

The properties of diamond may be broadly divided into two groups. The first group comprises those that do not exhibit significant variations as between different specimens of diamond. This group includes density, hardness, elasticity, thermal expansion, specific heat, thermal conductivity, refractivity, dispersion, photoelasticity, dielectric constant, magnetic susceptibility, Faraday effect, Raman effect, and infra-red absorption of the second

and higher orders. The second group of properties are those which exhibit variations, often of a most striking character, as between different diamonds. Amongst them may be listed infra-red absorption of the first order, absorption spectra in the visible and ultra-violet regions, fluorescence excited by visible and ultra-violet light and by X-rays, phosphorescence, photoconductivity, optical birefringence, intensity and sharpness of the Laue and Bragg X-ray reflections, and dynamic X-ray reflections. If the variations in the properties listed above had been unrelated to each other, the study of the diamond would indeed have been a very perplexing subject. Happily, this is not so, as has been shown by Raman and his collaborators by studies covering all the properties listed above with an extensive collection of material. The results present such striking correlations between the variations of the different properties as to leave no room for doubt that differences are systematic and arise from fundamental differences in crystal structure. This inference receives direct observational support from studies on the crystal morphology of diamond. The situation may be summed up broadly by the statement that the electronic structure of diamond may possess either tetrahedral or octahedral symmetry. Assuming each atom of carbon to possess only tetrahedral symmetry, geometric considerations indicate that there must be two sub-species (positive and negative, respectively) of the tetrahedral type and two sub-species of the octahedral type. The recognition of the existence of these four species of the diamond structure, appearing separately or together in any actual specimen of diamond enables the varied behaviours actually met with to be satisfactorily described and interpreted.

9. Luminescence and Absorption Spectra

The luminescence of diamond, a long-known but neglected phenomenon, has been studied with great thoroughness by Raman and his collaborators with results of exceptional interest. Two distinct types of luminescence based on different electronic transitions are observed, and the same electronic transitions can also appear in absorption. They may be coupled with vibrational transitions in the crystal lattice and as the result, the principal emission or absorption in each case appears accompanied by subsidiary radiations of less and greater frequency respectively. The emission and absorption spectra exhibit mirror-image symmetry with respect to each other about the electronic frequency. The lattice frequencies deduced from the spectra agree with those given by the new crystal dynamics, which was in fact first developed to explain the effects observed in the luminescence spectrum of diamond.

The coupling of electronic with vibrational transitions so clearly manifested in the case of diamond is a general feature in the luminescence spectra of crystals. As a consequence, Raman effect studies are of great assistance in interpreting such spectra. As an illustration, one may cite the case of the fluorescence and absorption of the uranyl salts, as also the cases of alumina and of topaz investigated by the present writer. The lattice frequencies of magnesium oxide calculated on the basis of theory fit very well with those deduced from its luminescence spectra resulting from the presence of a trace of chromic oxide as impurity.

10. Infra-Red Absorption Spectra

All diamonds without exception exhibit an infra-red absorption spectrum of the second order, while the diamonds of the tetrahedral class exhibit also a first order absorption. These spectra have been thoroughly investigated and are explicable in all their details on the basis of the new lattice dynamics. Particularly interesting is the fact that the two weakest second-order Raman lines (2176 cm.$^{-1}$ and 2015 cm.$^{-1}$) are represented in the second-order infra-red absorption by its two most conspicuous peaks, as is to be theoretically expected. A feature which manifests itself conspicuously in the first order infra-red absorption by diamond is that all the nine fundamental modes of vibration of the lattice are active, though in different degrees, and not merely the so-called principal oscillation having the highest frequency. The absorption curves exhibit distinct peaks corresponding to the different modes, but their resolution is far from perfect. These features are explicable as due to the coupling of the different modes with each other due to anharmonicity. Such coupling would necessarily manifest itself even more strongly in the case of strongly infra-red active crystals and offers a basis for an explanation of the features exhibited by their absorption spectra.

11. Thermo-Optic Properties of Crystals

Studies of the effect of temperature on the optical properties of diamond have pointed the way to the development of a successful quantitative theory of the thermo-optic behaviour of crystals. The refractive index of diamond increases instead of diminishing with rise of temperature, this increase becoming more rapid as we approach the violet end of the spectrum. In consequence, the dispersion of diamond is enhanced by rise of temperature even more rapidly than its refractive index. The sharply defined electronic absorption lines in the visible and ultra-violet region exhibited by diamond at low temperatures are observed to drift towards lower frequencies when the temperature is raised. It may therefore be reasonably assumed that the characteristic frequency in the extreme ultra-violet principally responsible for the

dispersion also shifts downwards with rise of temperature. Such a shift would result in an increase of dispersion and refraction which would only be partially be set off by the diminution caused by the thermal expansion. Not only does this idea work successfully in the case of diamond, but it is found to be remarkably successful also in explaining the facts observed with numerous other crystals, both those which are isotropic, *e.g.*, the alkali halides and those which are birefringent, *viz.*, quartz, calcite and aragonite. The basis of the theory, namely the diminution of the characteristic frequencies in the remote ultra-violet with temperature, also finds direct observational support.

12. Photoelastic Properties of Crystals

One of the earliest attempts to develop a quantitative theory of the photo-elastic behaviour of crystals was that made at Raman's suggestion in 1927 by Kedareswar Banerji. The subject has acquired considerable importance in recent years by reason of its relationship to other phenomena, *viz.*, the optical effects arising from mechanical oscillations in a crystal and the thermal diffusion of light. The theory of the diffraction of light in ultrasonic fields originally put forward by Raman and Nath to explain the effects observed in liquids, applies *mutatis mutandis* to the case of a crystal when the relevant piezo-optic constants are introduced in the formulæ. The recent determination of the piezo-optic constants of diamond was, in fact, made with a view to work out the consequences of Brillouin's theory of the thermal scattering of light in it. Measurements with other crystals will no doubt prove of great value in this field of research.

13. Magneto-Optic Behaviour of Crystals

One of the many remarkable properties of diamond is the feebleness of the Faraday effect observed with it when considered in relation to its high dispersive power. The rotation of the plane of polarisation of light produced by a magnetic field is only one-fourth of that to be expected on the basis of the well-known Becquerel formula. The measurements which revealed this fact were made possible by the plates of diamond free from birefringence included in Raman's collection. The explanation for the low value is evidently to be found in the covalent character of the bonding of the atoms of carbon in the crystal with each other. The case of diamond thus clearly indicates that measurement of the "magneto-optic anomaly" exhibited by a crystal offers a method of ascertaining the nature of the electronic states in its atoms or ions. Studies with other crystals have since been pursued with this aim in view.

14. Elastic Properties of Crystals

Methods based on the use of piezo-electrically excited oscillations have opened out new possibilities for the accurate determination of the elastic constants of crystals. The recent work of Bhagavantam and his collaborators at Waltair may be specially mentioned in this connection. The problem naturally arises of seeking to connect these experimentally observed constants with the known crystal structure and if possible to derive them theoretically on the basis of that structure. The first step in any such attempt is evidently the evaluation of the interatomic forces arising from the displacements of the atoms from their positions of equilibrium. One way of finding these forces is to connect them with the frequencies of atomic vibration made accessible to observation by the Raman effect and from these frequencies as actually observed to evaluate the forces. A rigorous method of accomplishing this has been worked out in the case of various crystals. Difficulties arise in the next step, namely that of evaluating the elastic constants from the interatomic forces, but we shall not discuss them here.

15. The Thermal Properties of Crystals

The evaluation of the specific heat of a crystal requires a knowledge of its vibration spectrum. The proposition that this spectrum consists of $(24p-3)$ discrete frequencies places the theory of specific heats on a very simple and intelligible basis. Further, when these frequencies are accessible to direct spectroscopic observation, a comparison between the actual and calculated specific heats becomes possible. It may be remarked that the three excluded degrees of freedom represent the spectrum of elastic vibrations in the crystal. These appear at the very lowest end of the frequency range. Hence in most cases it is a sufficient approximation to regard them as fully excited at the temperature of observation and make the necessary addition to the specific heat; a more exact calculation may, however, be necessary if p be small and if the temperature is very low. Calculations of the specific heat made in this manner for crystals for which the necessary spectroscopic data are available, *e.g.*, diamond, show a satisfactory agreement with the facts.

Another property of a crystal which is intimately related to its vibration spectrum is its thermal expansion. Data regarding the thermal expansion coefficient of crystals are rather meagre. For example, no data were available for diamond above the room temperature. The present writer has developed a new precision method of measuring the coefficient of thermal expansion of crystals and applied it to the case of diamond which, as is well known, has a very small dilatation. Attempts to evaluate the thermal expansion of

diamond and of other crystals theoretically on the basis of the spectroscopic data as in the case of their specific heats have given very encouraging results.

16. X-Ray Studies

The striking developments in X-ray physics which followed in the wake of Laue's great discovery of 1912 were already accomplished facts when Raman commenced his professoriate. Hence, neither X-ray spectroscopy nor crystal structure analysis was ever adopted by him as a part of his regular research programme. Nevertheless, these subjects have interested him greatly, as will be evident from the numerous X-ray studies published from time to time from his laboratory.

In April 1940, Raman and Nilakantan published in an articie in *Current Science* under the title "A new X-ray effect", some strongly exposed Laue photographs obtained with an octahedral cleavage plate of diamond and the X-radiation from a copper target. These photographs showed some remarkable features which they explained as arising from dynamic reflections of the incident X-radiation by the (111) planes of the crystal. They gave reasons for believing that the crystal planes giving these reflections were set in vibration with the same frequency as that observed in the Raman spectrum of diamond and that the excitation was quantum-mechanical as in the case of the Raman effect. The reality of the effect is indisputable and on the basis of the explanation indicated, it is clearly of fundamental importance. Raman and Nilakantan subsequently published further experimental results which confirmed the correctness of the explanation given by them. We shall not here enter further into the subject except to remark that the explanation of this X-ray effect stands in the closest relation to the problem of the nature of the vibration spectrum of a crystal. The same question also enters fundamentally into the theory of the diffraction of X-rays by crystals and of the influence of temperature on the same.

R. S. Krishnan.

BIBLIOGRAPHY OF PAPERS ON CRYSTAL PHYSICS

1918 — 1948

	Subject	No. of titles
1.	Optical phenomena	25
2.	Birefringence	6
3.	Magnetic and magneto-optic properties	30
4.	Photo-elasticity and thermo-optic behaviour ..	11
5.	Thermal agitation, scattering of light and hypersonics	11
6.	Raman spectra	85
7.	Infra-red spectra	7
8.	Luminescence and absorption	26
9.	Lattice dynamics	22
10.	Specific heat and thermal expansion	21
11.	Dynamic reflection of X-rays	30
12.	Crystal structure studies	15
13.	Structure and properties of diamond	31
14.	Miscellaneous	8
	TOTAL ..	328

1. Optical Phenomena

No.	Subject	Author	Journal	Year
1	The colours of the striæ in mica ..	C. V. Raman and P. N. Ghosh	*Nature*	1918, **102**, 205
2	On Haidinger's rings in mica	T. K. Chinmayanandam	*Proc. Roy. Soc.*	1918, A, **95**, 176
3	On the colours of the striæ in mica and the radiation from laminar diffracting boundaries	P. N. Ghosh	*Ibid.*	1919, **96**, 257
4	Some phenomena of laminar diffraction observed with mica	Do.	*Proc. Ind. Assn. Cult. Sci.*	1920, **6**, 51
5	On Quetelet's rings and other allied phenomena	C. V. Raman and G. L. Dutta	*Phil. Mag.*	1921, **42**, 826
6	Conical refraction in biaxial crystals ..	C. V. Raman	*Nature*	1921, **107**, 747
7	Some observations on interference phenomena in non-homogeneous light	N. K. Sethi	*Proc. Ind. Assn. Cult. Sci.*	1921, **7**, 37
8	Quetelet's rings in mica	N. K. Sethi and M. Sogani	*Ibid.*	1922, **7**, 61
9	On a new optical property of biaxial crystals	C. V. Raman and V. S. Thamma	*Phil. Mag.*	1922, **43**, 510
10	Deformation of rings and brushes as observed through a spath hemitrope	B. N. Chackerbutti	*Ibid.*	1922, **43**, 560
11	Colours of chlorate of potash	L. A. Ramdas	*Proc. Ind. Assn. Cult. Sci.*	1923, **8**, 231
12	The optical properties of amethyst quartz	C. V. Raman and K. Banerji	*Trans. Opt. Soc., London*	1925, **26**, 289
13	The effect of dispersion on the interference figures of crystals	C. V. Raman	*Nature*	1924, **113**, 127
14	Diffraction of light by transparent laminæ	C. V. Raman and I. Ramakrishna Rao	*Proc. Phys. Soc.*	1927, **39**, 453
15	Pleochroic haloes in cordierite	C. Mahadevan	*Ind. Jour. Phys.*	1927, **1**, 444
16	Studies in laminar diffraction. Part II. Laminar boundaries in mica	I. R. Rao	*Ibid.*	1928, **2**, 365
17	Pleochroic giant haloes in cordierite ..	M. S. Krishnan and C. Mahadevan	*Ibid.*	1930, **5**, 669

		Mahadevan		
18	Transmission of light through suspensions of powdered crystals	B. Mukhopadhyaya	*Ibid.*	1932, **7**, 307
19	On iridescent shells. Part I. Introductory	C. V. Raman	*Proc. Ind. Acad. Sci.*	1934, **1**, 567
20	On iridescent shells. Part II. Colours of laminar diffraction	Do.	*Ibid.*	1934, **1**, 574
21	On iridescent shells. Part III. Body colours and diffusion haloes	Do.	*Ibid.*	1934, **1**, 859
22	The structure and optical properties of nacre in iridescent shells—Part I	V. S. Rajagopalan	*Ibid.*	1936, **3**, 572
23	Conical refraction in naphthalene crystals	C. V. Raman, V. S. Rajagopalan and T. M. K. Nedungadi	*Ibid.*	1941, **14**, 221
24	Phenomena of conical refraction ..	C. V. Raman	*Curr. Sci.*	1942, **11**, 44
25	Optical images formed by conical refraction	C. V. Raman and T. M. K. Nedungadi	*Nature*	1942, **149**, 552

2. Birefringence

1	The birefringence of crystalline carbonates, nitrates and sulphates	C. V. Raman	*Nature*	1926, **118**, 264
2	Colour and optical anisotropy of organic compounds	Do.	*Ibid.*	1929, **123**, 494
3	Relation between colour and molecular structure	C. V. Raman and S. Bhagavantam	*Ind. Jour. Phys.*	1929, **4**, 57
4	Optical properties of some aromatic crystals	K. L. Narasimhan	*Ibid.*	1931, **6**, 233
5	The dispersion, birefringence and optical activity of quartz	T. Radhakrishnan	*Proc. Ind. Acad. Sci.*	1947, **25**, 260
6	The dispersion formulæ of the alkali halides	Do.	*Ibid.*	1948, **27**, 165

3. Magnetic and Magneto-Optic Properties

1	The magneto-crystalline properties of the Indian braunites	K. Seshagiri Rao	*Proc. Ind. Assoc. Cult. Sci.*	1920, **6**, 87
2	The magnetic anisotropy of crystalline nitrates and carbonates	K. S. Krishnan and C. V. Raman	*Proc. Roy. Soc.*	1927, **115**, 549

No.	Subject	Author	Journal	Year
3	Diamagnetism and crystal structure ..	C. V. Raman	*Nature*	1929, **123**, 945
4	Magnetic behaviour of organic crystals ..	Do.	*Ibid.*	1929, **123**, 605
5	Anomalous diamagnetism	Do.	*Ibid.*	1929, **124**, 412
6	Magnetic birefringence in solutions and its relation to crystal structure and properties	M. Ramanadham	*Ind. Jour. Phys.*	1929, **4**, 109
7	The magnetic anisotropy in naphthalene crystals	S. Bhagavantam	*Proc. Roy. Soc.*	1929, **124**, 545
8	The magnetic and optical properties of benzene ring in aromatic compounds	Do.	*Ibid.*	1929, **126**, 143
9	Anomalous diamagnetism of graphite ..	S. Paramasivan	*Ind. Jour. Phys.*	1929, **4**, 139
10	Magnetic behaviour of some organic crystals	S. Bhagavantam	*Ibid.*	1929, **4**, 1
11	Diamagnetism and molecular structure ..	C. V. Raman	*Proc. Phy. Soc., Lonaon*	1930, **42**, 309
12	Anomalous diamagnetism and crystal structure	V. I. Vaidyanathan	*Ind. Jour. Phys.*	1930, **5**, 559
13	Orientation of the molecules in naphthalene and anthracene crystals	K. Banerji	*Ibid.*	1930, **4**, 557
14	The magnetic anisotropy of naturally occurring substances. Part I. Mother of pearl	P. Nilakantan	*Proc. Ind. Acad. Sci.*	1935, **2**, 621
15	The magnetic anisotropy of naturally occurring substances. Part II. Molluscan shells	Do.	*Ibid.*	1936, **4**, 542
16	Magnetic anisotropy of rhombic sulphur ..	Do.	*Ibid.*	1936, **4**, 419
17	Temperature variation of the magnetic anisotropy of ammonium nitrate	Do.	*Phys. Rev.*	1937, **52**, 383
18	Temperature variation of magnetic anisotropy of organic crystals	Do.	*Nature*	1937, **140**, 29
19	Magnetic anisotropy of naturally occurring substances. Part III. Wood lignin and wood cellulose	Do.	*Proc. Ind. Acad. Sci.*	1938, **7**, 38
20	Magnetic anisotropy and pleochroism of biotite mica	Do.	*Ibid.*	1938, **8**, 39
21	Studies in crystal magnetism	Do.	*Jr. Ind. Inst. Sci.*	1940, **23**, 187
22	Magnetic susceptibility of diamond ..	A. Sigamony	*Proc. Ind. Acad. Sci.*	1944, **19**, 310

22	Magnetic susceptibility of diamond ..	A. Sigamony	*Proc. Ind. Acad. Sci.*	1944, **19**, 310
23	Magnetic susceptibility and anisotropy in carborundum	Do.	*Ibid.*	1944, **19**, 377
24	The magnetic properties of tourmaline and epidote	Do.	*Ibid.*	1944, **20**, 200
25	The magnetic behaviour of iron pyrites ..	Do.	*Ibid.*	1944, **20**, 204
26	The magnetic properties of augite ..	Do.	*Ibid.*	1944, **20**, 261
27	The magnetic behaviour of tektite ..	Do.	*Ibid.*	1944, **20**, 15
28	The Faraday effect in diamond	S. Ramaseshan	*Ibid.*	1946, **24**, 104
29	The magnetic properties of iron pyrites ..	Do.	*Ibid.*	1947, **25**, 201
30	Faraday effect in some cubic crystals ..	Do.	*Ibid.*	1947, **25**, 459

4. Photo-Elasticity and Thermo-Optic Behaviour

1	Theory of photoelasticity	K. Banerji	*Ind. Jour. Phys.*	1927, **2**, 195
2	Photo-elastic constants of diamond ..	G. N. Ramachandran	*Proc. Ind. Acad. Sci.*	1947, **25**, 208
3	Thermo-optic behaviour of solids. I. Diamond	Do.	*Ibid.*	1947, **25**, 266
4	Thermo-optic behaviour of solids. II. Fused quartz	Do.	*Ibid.*	1947, **25**, 280
5	Thermo-optic behaviour of solids. III. Fluorspar	Do.	*Ibid.*	1947, **25**, 286
6	Thermo-optic behaviour of solids. IV. Zinc blende	Do.	*Ibid.*	1947, **25**, 375
7	Thermo-optic behaviour of solids. V. Alkali halides	Do.	*Ibid.*	1947, **25**, 481
8	Birefringence of crystals and its temperature variations. Part I. Calcite and Aragonite	Do.	*Ibid.*	1947, **26**, 77
9	Birefringence of crystals and its temperature variations. Part II. Sodium and potassium nitrates	Do.	*Ibid.*	1947, **26**, 114
10	Temperature variation of the refractive indices of quartz	T. Radhakrishnan	*Ibid.*	1947, **25**, 382
11	Temperature variation of the refractive indices of quartz	Do.	*Ibid.*	1948, **27**, 44

5. Thermal Agitation, Scattering of Light and Hypersonics

No.	Subject	Author	Journal	Year
1	The molecular scattering of light by liquids and solids	C. V. Raman	*Nature*	1921, **108**, 402
2	Smoky quartz	Do.	*Ibid.*	1921, **108**, 81
3	Optical observations of the thermal agitation of the atoms in crystals	Do.	*Ibid.*	1922, **109**, 42
4	Molecular diffraction of light	Do.	Calcutta University Press	1922
5	Thermal opalescence in crystals and colour of ice in glaciers	Do.	*Nature*	1923, **111**, 13
6	The scattering of light by smoky quartz ..	N. K. Sur	*Proc. Ind. Assn. Cult. Sci.*	1923, **8**, 271
7	Doppler effect in light scattering	C. V. Raman	*Nature*	1931, **128**, 636
8	Optical observation of the Debye heat waves in crystals	C. V. Raman and C. S. Venkateswaran	*Ibid.*	1938, **142**, 250
9	The scattering of light in quartz	V. Chandrasekharan	*Proc. Ind. Acad. Sci.*	1947, **25**, 256
10	The scattering of polarised light beams in birefringent solids	Do.	*Ibid.*	1947, **26**, 110
11	Thermal scattering of light by diamond ..	R. S. Krishnan	*Nature*	1947, **159**, 740

6. Raman Spectra

1	A new radiation	C. V. Raman	*Ind. Jour. Phys.*	1928, **2**, 387
2	The Raman effect in crystals	I. Ramakrishna Rao	*Ibid.*	1928, **3**, 123
3	The Raman effect in crystals	K. S. Krishnan	*Nature*	1928, **122**, 477
4	Relation of Raman effect to crystal structure and properties of diamond	S. Bhagavantam	*Ind. Jour. Phys.*	1930, **5**, 169
5	Further studies on the Raman effect of diamond	Do.	*Ibid.*	1930, **5**, 573
6	Raman spectra of crystalline inorganic chlorides	P. Krishnamurthi	*Ibid.*	1930, **5**, 113
7	Raman spectra of inorganic crystals. Part II. Hydroxides, cyanides and sulphocyanides	Do.	*Ibid.*	1930, **5**, 651

8	Raman spectra of crystalline powders ..	Do.	*Nature*	1930, **125**, 463
9	Raman effect, fluorescence and colour of diamonds	S. Bhagavantam	*Ibid.*	1930, **126**, 168
10	Raman spectra of inorganic crystals. Part I. Substances containing XO_3 and XO_4 groups	P. Krishnamurthi	*Ind. Jour. Phys.*	1930, **5**, 633
11	Raman effect in paramagnetic crystals ..	Do.	*Nature*	1930, **126**, 169
12	Raman effect in some crystalline inorganic sulphates; influence of paramagnetism on Raman lines	Do.	*Ind. Jour. Phys.*	1930, **5**, 183
13	Raman effect in metallic halides ..	Do.	*Nature*	1930, **125**, 892
14	Raman spectrum and infra-red absorption of sulphur	Do.	*Ind. Jour. Phys.*	1930, **5**, 105
15	The Raman effect in crystal powders of inorganic nitrates	Do.	*Ibid.*	1930, **5**, 1
16	Raman effect in calcite and aragonite ..	S. Bhagavantam	*Zeit. fur. Krist.*	1931, **77**, 43
17	Raman spectra of some organic crystals and solutions	P. Krishnamurthi	*Ind. Jour. Phys.*	1931, **6**, 309
18	Raman spectra of organic sulphides ..	S. Venkateswaran	*Ibid.*	1931, **6**, 51
19	Raman spectra of inorganic crystals—Part III	P. Krishnamurthi	*Ibid.*	1931, **6**, 7
20	Raman spectra of pinene, thiophene, salol and thymol	S. Venkateswaran and S. Bhagavantam	*Ibid.*	1932, **7**, 585
21	Raman spectra of some metallic halides ..	C. S. Venkateswaran	*Proc. Ind. Acad. Sci.*	1934, **1**, 850
22	Raman spectra of sulphur in solid and liquid states	Do.	*Ibid.*	1934, **1**, 120
23	The Raman spectra of iodic acid and alkaline iodates as solids and as solutions	Do.	*Ibid.*	1935, **2**, 119
24	Raman spectrum of phosphorus ..	Do.	*Ibid.*	1935, **2**, 260
25	Raman spectra of metallic formates and constitution of formic acid	Do.	*Curr. Sci.*	1935, **4**, 736
26	Raman spectra of metallic formates and constitution of formic acid	Do.	*Proc. Ind. Acad. Sci.*	1935, **2**, 615
27	The Raman spectrum of crystalline selenious acid	Do.	*Curr. Sci.*	1936, **4**, 309
28	Raman spectra of selenious acid and its sodium salts	Do.	*Proc. Ind. Acad. Sci.*	1936, **3**, 533

No.	Subject	Author	Journal	Year
29	Raman spectra of sulphur and phosphorus. Part I. Polarisation and molecular structure	C. S. Venkateswaran	*Proc. Ind. Acad. Sci.*	1936, **4**, 345
30	Raman spectra of sulphur and phosphorus. Part II. Lattice oscillations	Do.	*Ibid.*	1936, **4**, 414
31	Raman spectra of orthophosphoric acid and some phosphates	Do.	*Ibid.*	1936, **3**, 25
32	Constitution of phosphorus acid and phosphites	R. Ananthakrishnan	*Nature*	1936, **138**, 803
33	A new technique of complementary filters for photographing Raman spectra of crystal powders	Do.	*Curr. Sci.*	1936, **5**, 131
34	Raman spectra of crystal powders. Part I. Halides and sulphates of ammonium	Do.	*Proc. Ind. Acad. Sci.*	1937, **5**, 76
35	Raman spectra of crystal powders. Part II. Chlorides and sulphates of hydroxylamine and hydrazine	Do.	*Ibid.*	1937, **5**, 87
36	Raman spectra of crystal powders. Part III. Exchange reactions of ammonium chloride and heavy water	Do.	*Ibid.*	1937, **5**, 175
37	Raman spectra of crystal powders. Part IV. Some organic and inorganic substances	Do.	*Ibid.*	1937, **5**, 200
38	Raman spectra of crystal powders. Part V. Inorganic nitrates and water of crystallisation	Do.	*Ibid.*	1937, **5**, 447
39	Note on the intensity of Raman lines in crystals	C. S. Venkateswaran	*Curr. Sci.*	1937, **6**, 92
40	Raman spectra of some inorganic compounds	Do.	*Proc. Ind. Acad. Sci.*	1938, **7**, 144
41	Scattering of light in sodium nitrate crystals	T. M. K. Nedungadi	*Ibid.*	1938, **8**, 397
42	A chart of Raman bands of water in crystals	P. G. N. Nayar	*Ibid.*	1938, **8**, 419
43	Low frequency Raman lines in organic crystals	C. S. Venkateswaran	*Ibid.*	1938, **8**, 448
44	The effect of crystal orientation on the Raman spectrum of sodium nitrate	T. M. K. Nedungadi	*Ibid.*	1939, **10**, 197

45	Effect of temperature on the Raman spectrum of quartz	Do.	*Ibid.*	1940, **11**, 86
46	Raman effect and crystal symmetry ..	B. D. Saxena	*Ibid.*	1940, **11**, 229
47	Raman effect in rochelle salt crystal ..	T. M. K. Nedungadi	*Ibid.*	1940, **11**, 413
48	Analysis of the Raman and infra-red spectrum of α-quartz	B. D. Saxena	*Ibid.*	1940, **12**, 93
49	Raman spectrum of gypsum	Do.	*Ibid.*	1941, **13**, 25
50	Effect of crystal orientation on the Raman spectra of naphthalene and benzophenone	T. M. K. Nedungadi	*Ibid.*	1941, **13**, 161
51	Raman spectra of some crystalline nitrates and sulphates	B. Lakshmana Rao	*Ibid.*	1941, **14**, 48
52	Raman spectrum of potassium tartrate crystal	Do.	*Ibid.*	1941, **14**, 41
53	Studies in the Raman effect in single crystals of potassium nitrate	T. M. K. Nedungadi	*Ibid.*	1941, **14**, 242
54	The effect of crystal orientation on the Raman effect of barytes	T. A. S. Balakrishnan	*Ibid.*	1941, **14**, 257
55	Temperature variation of the Raman frequencies of diamond	P. G. N. Nayar	*Ibid.*	1941, **13**, 284
56	Analysis of the Raman spectrum of single crystals of naphthalene	T. M. K. Nedungadi	*Ibid.*	1942, **15**, 376
57	Raman spectra of crystals excited by mercury resonance radiations	Roopkishore	*Ibid.*	1942, **16**, 36
58	Luminescence, absorption and scattering of light in diamond—Part IV	P. G. N. Nayar	*Ibid.*	1942, **15**, 310
59	Raman effect and change of state of naphthalene	R. Norris	*Ibid.*	1942, **16**, 250
60	Raman spectrum of sulphur under high dispersion	Do.	*Ibid.*	1942, **16**, 287
61	Raman spectra of crystals and their interpretation	R. S. Krishnan	*Ibid.*	1943, **18**, 298
62	The Raman spectrum of diamond ..	Do.	*Ibid.*	1944, **19**, 216
63	Polarisation of Raman scattering and of fluorescence in diamond	A. Mani	*Ibid.*	1944, **20**, 117
64	Scattering of light in crystals	C. V. Raman	*Nature*	1945, **155**, 396
65	Raman spectrum of quartz	R. S. Krishnan	*Ibid.*	1945, **155**, 452

No.	Subject	Author	Journal	Year
66	Raman and infra-red absorption spectra of rock-salt	R. S. Krishnan	*Nature*	1945, **156**, 267
67	Raman spectra of the second order. Part I. Calcite	Do.	*Proc. Ind. Acad. Sci.*	1945, **22**, 182
68	Raman spectra of the second order. Part II. Gypsum	Do.	*Ibid.*	1945, **22**, 274
69	Raman spectra of the second order. Part III. Quartz	Do.	*Ibid.*	1945, **22**, 329
70	Raman spectra of the second order. Part IV. Barytes	Do.	*Ibid.*	1946, **23**, 288
71	Raman effect in rock-salt	Do.	*Nature*	1946, **157**, 623
72	The Raman spectrum of rock-salt ..	Do.	*Proc. Roy. Soc. Lond.*	1946, **187**, 188
73	Second order Raman spectrum of diamond	Do.	*Proc. Ind. Acad. Sci.*	1946, **24**, 25
74	Temperature variation of the Raman frequencies of diamond	Do.	*Ibid.*	1946, **24**, 45
75	Raman spectrum of rock-salt under high resolution	Do.	*Nature*	1947, **159**, 266
76	Second order Raman spectra of crystals ..	Do.	*Ibid.*	1947, **160**, 230
77	Vibration spectra of alkali halides ..	Do.	*Ibid.*	1947, **160**, 711
78	The Raman spectrum of diamond under high resolution	Do.	*Ibid.*	1947, **159**, 60
79	Scattering of light in diamond and its Raman spectrum	Do.	*Proc. Ind. Acad. Sci.*	1947, **26**, 399
80	The Raman spectrum of rock-salt and its interpretation	Do.	*Ibid.*	1947, **26**, 419
81	The Raman spectrum of ammonium chloride and its variations with temperature	Do.	*Ibid.*	1947, **26**, 432
82	Influence of temperature on the Raman spectra of crystals. Part I. Calcite	P. K. Narayanaswamy	*Ibid.*	1947, **26**, 511
83	Influence of temperature on the Raman spectra of crystals. Part II. Quartz	Do.	*Ibid.*	1947, **26**, 521
84	Raman spectra of water, heavy water and ice	Do.	*Ibid.*	1948, **27**, 311
85	Raman spectrum of ammonium bromide and its variations with temperature	R. S. Krishnan	*Ibid.*	1948, **27**, 321

and its variations with temperature

7. Infra-Red Spectra

1	Infra-red spectrum of diamond ..	K. G. Ramanathan	*Nature*	1945, **156**, 23
2	The infra-red absorption spectrum of diamond	Do.	*Proc. Ind. Acad. Sci.*	1946, **24**, 150
3	Infra-red absorption spectrum of diamond	R. S. Krishnan and K. G. Ramanathan	*Nature*	1946, **157**, 45
4	Infra-red absorption spectrum of diamond	Do.	*Ibid.*	1946, **157**, 582
5	A home-made infra-red spectrometer ..	K. G. Ramanathan	*Curr. Sci.*	1946, **15**, 184
6	The infra-red spectrum	C. V. Raman	*Ibid.*	1947, **16**, 359
7	The infra-red absorption spectrum of diamond and its variations	K. G. Ramanathan	*Proc. Ind. Acad. Sci.*	1947, **26**, 469

8. Luminescence and Absorption

1	Cathode luminescence of diamond ..	M. V. John	*Ind. Jour. Phys.*	1931, **6**, 305
2	The fluorescence of ruby, saphire and emerald ..	C. S. Venkateswaran	*Proc. Ind. Acad. Sci.*	1935, **2**, 459
3	Luminescence, absorption and scattering of light in diamonds. Part I. Fluorescence	P. G. N. Nayar	*Ibid.*	1941, **13**, 483
4	Luminescence, absorption and scattering of light in diamonds. Part II. Phosphorescence	Do.	*Ibid.*	1941, **13**, 534
5	Luminescence, absorption and scattering of light in diamonds. Part III. Absorption	Do.	*Ibid.*	1941, **14**, 1
6	Fluorescence, absorption and scattering of light in ruby	A. Mani	*Ibid.*	1942, **15**, 52
7	Lattice and electronic spectrum of diamond	Do.	*Ibid.*	1942, **15**, 293
8	Spectroscopic investigation of the solid and liquid states	C. V. Raman	*Curr. Sci.*	1942, **11**, 225
9	Luminescence spectra and vibrations in crystal lattices	D. D. Pant	*Proc. Ind. Acad. Sci.*	1943, **18**, 309
10	Fluorescence spectrum of uranyl fluoride ..	D. D. Pant and N. D. Sakhwalkar	*Ibid.*	1944, **19**, 135
11	The fluorescence and absorption spectra of diamond in the visible region	A. Mani	*Ibid.*	1944, **19**, 231

No.	Subject	Author	Journal	Year
12	The ultraviolet absorption spectrum of diamond	K. Sunanda Bai	*Proc. Ind. Acad. Sci.*	1944, **19**, 253
13	Excitation curves of luminescence in diamond	A. Mani	*Ibid.*	1945, **21**, 280
14	Some studies in the spectra of single uranyl halides and other uranyl salts	D. D. Pant	*Ibid.*	1945, **22**, 95
15	Analysis of the fluorescence bands of the uranyl salts	Do.	*Ibid.*	1945, **22**, 110
16	The luminescence of diamond excited by X-radiation	G. N. Ramachandran	*Ibid.*	1946, **24**, 81
17	The absorption of ultra-violet radiation by diamond	K. G. Ramanathan	*Ibid.*	1946, **24**, 137
18	The absorption spectrum of diamond in the visible region	Do.	*Ibid.*	1946, **24**, 145
19	Luminescence as "Forbidden" electronic transition in diamond	G. N. Ramachandran and V. Chandrasekharan	*Ibid.*	1946, **24**, 176
20	The thermo-luminescence of diamond ..	V. Chandrasekharan	*Ibid.*	1946, **24**, 187
21	The phosphorescence of diamond ..	Do.	*Ibid.*	1946, **24**, 193
22	The emission and absorption spectra of luminescent diamonds	K. G. Ramanathan	*Ibid.*	1947, **26**, 479
23	The Raman spectrum of alumina and the luminescence and absorption spectra of ruby	R. S. Krishnan	*Nature*	1947, **160**, 26
24	Raman spectrum of alumina and the luminescence of ruby	Do.	*Proc. Ind. Acad. Sci.*	1947, **26**, 450
25	The Raman effect in topaz and its relation to the luminescence spectrum	Do.	*Ibid.*	1947, **26**, 460
26	Fluorescence and phosphorescence of diamond at different temperatures	V. Chandrasekharan	*Ibid.*	1948, **27**, 316

9. Lattice Dynamics

1	The dynamical theory of the diamond lattice—Part I	N. S. Nagendra Nath	*Proc. Ind. Acad. Sci.*	1934, **1**, 333
2	The dynamical theory of the diamond lattice. Part II. The elastic constants of diamond	Do.	*Ibid.*	1934, **1**, 841
3	The dynamical theory of the diamond lattice. Part III. The diamond—graphite transformation	Do.	*Ibid.*	1935, **2**, 143
4	Lattice oscillations in crystals	C. V. Raman and T. M. K. Nedungadi	*Nature*	1939, **143**, 679
5	Vibration spectrum of a crystal lattice ..	C. V. Raman	*Proc. Ind. Acad. Sci.*	1943, **18**, 237
6	Normal vibrations of some typical cubic crystals	E. V. Chelam	*Ibid.*	1943, **18**, 257
7	Modes of atomic vibrations in fourteen Bravais lattices	G. N. Ramachandran	*Ibid.*	1943, **18**, 266
8	The normal vibrations of crystal lattices: Application of group theory	E. V. Chelam	*Ibid.*	1943, **18**, 283
9	Character tables for four cubic crystals ..	Do.	*Ibid.*	1943, **18**, 327
10	Vibrations of a close packed hexagonal lattice	G. N. Ramachandran	*Ibid.*	1943, **18**, 341
11	Fundamentals of crystal physics ..	C. V. Raman	*Curr. Sci.*	1943, **12**, 342
12	The vibration spectra of crystals. Part I. Basic theory	Do.	*Proc. Ind. Acad. Sci.*	1947, **26**, 339
13	The vibration spectra of crystals. Part II. The case of diamond	Do.	*Ibid.*	1947, **26**, 356
14	The vibration spectra of crystals. Part III. Rock-salt	Do.	*Ibid.*	1947, **26**, 370
15	The vibration spectra of crystals. Part IV. Magnesium oxide	Do.	*Ibid.*	1947, **26**, 383
16	The vibration spectra of crystals. Part V. Lithium and sodium fluorides	Do.	*Ibid.*	1947, **26**, 391
17	The vibration spectra of crystals. Part VI. Sylvine	Do.	*Ibid.*	1947, **26**, 396

No.	Subject	Author	Journal	Year
18	Dynamical theory of the vibration spectra of crystals. Part I. Diamond	K. G. Ramanathan	*Proc. Ind. Acad. Sci.*	1947, **26**, 481
19	Dynamical theory of the vibration spectra of crystals. Part II. Rock-salt structure	Do.	*Ibid.*	1947, **26**, 493
20	Dynamical theory of the vibration spectra of crystals. Part III. Cæsium chloride structure	Do.	*Ibid.*	1947, **26**, 500
21	Dynamical theory of the vibration spectra of crystals. Part IV. The metallic crystals	Do.	*Ibid.*	1947, **26**, 507
22	The eigenvibrations of crystal structures	C. V. Raman	*Curr. Sci.*	1948, **17**, 1

10. Specific Heat and Thermal Expansion

1	Specific heat in relation to Raman effect data	S. Paramasivan	*Ind. Jour. Phys.*	1931, **6**, 413
2	The Raman spectrum and the specific heat of crystalline sulphur	R. Norris	*Proc. Ind. Acad. Sci.*	1941, **13**, 291
3	The thermal energy of crystalline solids: Basic theory	C. V. Raman	*Ibid.*	1941, **14**, 459
4	The thermal energy of crystalline solids: White phosphorus	R. Norris	*Ibid.*	1941, **14**, 468
5	The thermal energy of crystalline solids: Diamond	V. B. Anand	*Ibid.*	1941, **14**, 484
6	The thermal energy of crystalline solids: Lithium, tungsten, gold, silicon and grey tin	Bisheshwar Dayal	*Ibid.*	1941, **14**, 473
7	The thermal energy of crystalline solids: Magnesium, zinc and cadmium	Do.	*Ibid.*	1941, **14**, 492
8	The thermal energy of crystalline solids: Alkali halides	C. S. Venkateswaran	*Ibid.*	1941, **14**, 506
9	The thermal energy of crystalline solids: Quartz	R. Norris	*Ibid.*	1941, **14**, 499

10	The evaluation of the specific heat of rock-salt by the new crystal dynamics	Bisheshwar Dayal	*Ibid.*	1944, **19**, 182
11	Specific heat of metals crystallising in the cubic system	Do.	*Ibid.*	1944, **20**, 24
12	Specific heat of alkali halides	Do.	*Ibid.*	1944, **20**, 77
13	Specific heat of metallic silicon	Do.	*Ibid.*	1944, **20**, 87
14	Thermal expansion of diamond	B. D. Saxena	*Ibid.*	1944, **20**, 92
15	Lattice spectrum, specific heat and thermal expansion of lithium and sodium fluorides	Bisheshwar Dayal	*Ibid.*	1944, **20**, 138
16	A theory of the thermal expansion of alkali halides	Do.	*Ibid.*	1944, **20**, 145
17	The thermal expansion of diamond ..	Do.	*Ibid.*	1944, **20**, 187
18	The thermal expansion of metals at low temperatures	Do.	*Ibid.*	1944, **20**, 192
19	The lattice spectrum and specific heat of diamond	Do.	*Ibid.*	1944, **19**, 224
20	The thermal expansion of solids	C. V. Raman	*Curr. Sci.*	1944, **13**, 295
21	Thermal expansion of diamond ..	R. S. Krishnan	*Proc. Ind. Acad. Sci.*	1946, **24**, 33

11. Dynamic Reflection of X-Rays

1	A new X-ray effect	C. V. Raman and P. Nilakantan	*Curr. Sci.*	1940, **9**, 165
2	Specular reflection of X-rays by high frequency sound waves	Do.	*Nature*	1940, **145**, 667
3	Reflection of X-rays with change of frequency. Part I. Theoretical discussions	Do.	*Proc. Ind. Acad. Sci.*	1940, **11**, 379
4	Reflection of X-rays with change of frequency. Part II. The case of diamond	Do.	*Ibid.*	1940, **11**, 389
5	Reflection of X-rays with change of frequency. Part III. The case of sodium nitrate	Do.	*Ibid.*	1940, **11**, 398
6	The quantum theory of X-ray reflection and scattering. Part I. Geometric relations	C. V. Raman and N. S. Nagendra Nath	*Ibid.*	1940, **12**, 83

No.	Subject	Author	Journal	Year
7	Reflections of X-rays with change of frequency. Part IV. The case of rock-salt	C. V. Raman and P. Nilakantan	*Proc. Ind. Acad. Sci.*	1940, **12**, 141
8	The two types of X-ray reflections in crystals	C. V. Raman and N. S. Nagendra Nath	*Ibid.*	1940, **12**, 427
9	Modified reflection of X-rays	C. V. Raman and P. Nilakantan	*Nature*	1940, **146**, 523
10	Classical and quantum reflection of X-rays in crystals	Do.	*Ibid.*	1940, **146**, 686
11	Quantum theory of X-ray reflection: Basic ideas	C. V. Raman	*Proc. Ind. Acad. Sci.*	1941, **14**, 317
12	Quantum theory of X-ray reflection: Mathematical formulation	Do.	*Ibid.*	1941, **14**, 332
13	Quantum theory of X-ray reflection: Experimental confirmation	C. V. Raman and P. Nilakantan	*Ibid.*	1941, **14**, 356
14	A quantum theoretical explanation of the appearance of forbidden X-ray reflections in diamond	P. Rama Pisharoti	*Ibid.*	1941, **14**, 377
15	Low temperature studies of the Raman X-ray reflections in crystals	C. S. Venkateswaran	*Ibid.*	1941, **14**, 387
16	The quantum reflections and the quantum scattering of X-rays by rock-salt	Do.	*Ibid.*	1941, **14**, 395
17	The Raman X-ray reflection in organic crystals: I. Naphthalene	Do.	*Ibid.*	1941, **14**, 402
18	The Raman X-ray reflection in organic crystals: II. Benzophenone	Do.	*Ibid.*	1941, **14**, 409
19	The Raman X-ray reflection in organic crystals: III. Hexamethylene tetramine	Do.	*Ibid.*	1941, **14**, 415
20	The lattice spectrum and the Raman X-ray reflections in rock-salt	Do.	*Ibid.*	1941, **14**, 426
21	The absolute intensity of the Raman X-ray reflections in diamond	P. Rama Pisharoti	*Ibid.*	1941, **14**, 434
22	X-ray reflections of the second kind in metallic crystals	Bisheshwar Dayal	*Ibid.*	1941, **14**, 421

23	On the Raman X-ray reflections in organic crystals: IV. Benzyl	R. V. Subrahmanian	*Ibid.*	1941, **14**, 445
24	Quantum reflection of X-rays in calcite ..	P. Nilakantan and P. G. N. Nayar	*Ibid.*	1941, **14**, 450
25	Classical and quantum reflection of X-rays	C. V. Raman and P. Nilakantan	*Phys. Rev.*	1941, **60**, 63
26	Quantum theory of X-ray reflection ..	C. V. Raman, P. Nilakantan and P. Rama Pisharoti	*Nature*	1941, **147**, 805
27	On the multiple spots and streamers exhibited by the (111) dynamic reflection in diamond	P. Rama Pisharoti and R. V. Subrahmanian	*Proc. Ind. Acad. Sci.*	1941, **14**, 439
28	On the geometry of the quantum reflection of X-rays in diamond	P. Rama Pisharoti	*Ibid.*	1941, **14**, 56
29	Dynamic X-ray reflections in diamond ..	R. S. Krishnan and G. N. Ramachandran	*Nature*	1945, **155**, 234
30	Dynamic X-ray reflections in crystals ..	C. V. Raman	*Curr. Sci.*	1948, **17**, 65

12. Crystal Structure Studies

1	Crystal structure of para-nitro-toluene ..	B. N. Sreenivasiah	*Ind. Jour. Phys.*	1928, **2**, 151
2	X-ray diffraction of crystal powders and liquids in relation to their constitution	P. Krishnamurthi	*Ibid.*	1928, **3**, 225
3	X-ray studies of vitrain and durain and their constituents	C. Mahadevan	*Ibid.*	1929, **4**, 79
4	Structure of some organic crystals ..	S. Bhagavantam	*Proc. Inst. Chem.*	1929, **2**, 15
5	On the Laue-photographs of iridescent crystals of potassium chlorate	S. C. Sirkar	*Ind. Jour. Phys.*	1930, **5**, 337
6	X-ray studies of vitrains	C. Mahadevan	*Ibid.*	1930, **5**, 525
7	Further X-ray studies of carbonaceous and bituminous materials	Do.	*Ibid.*	1930, **4**, 457
8	X-ray diffraction studies in calculi ..	S. Ranganathan	*Ibid.*	1931, **6**, 433
9	X-ray analysis of the structure of diphenyl	J. Dhar	*Ibid.*	1932, **7**, 43
10	X-ray analysis of the structure of iridescent shells—Part I	S. Rama Swamy	*Proc. Ind. Acad. Sci.*	1935, **1**, 871
11	X-ray analysis of the structure of iridescent shells—Part II	Do.	*Ibid.*	1935, **2**, 345

No.	Subject	Author	Journal	Year
12	The structure of thin metallic films ..	S. Rama Swamy	*Proc. Ind. Acad. Sci.*	1936, **4**, 656
13	X-ray studies of wood lignin and wood cellulose	P. Nilakantan	*Ibid.*	1937, **5**, 166
14	X-ray analysis of the structure of a fibrous modification of tourmaline	S. Rama Swamy and K. Y. S. Iyengar	*Ibid.*	1937, **5**, 419
15	New concepts of crystal structure ..	C. V. Raman	*Curr. Sci.*	1946, **15**, 329

13. Structure and Properties of Diamond

1	Physics of the diamond	C. V. Raman	*Curr. Sci.*	1942, **11**, 261
2	The structure and properties of diamond ..	Do.	*Ibid.*	1943, **12**, 33
3	The four forms of diamond	Do.	*Ibid.*	1944, **13**, 145
4	The crystal symmetry and structure of diamond	Do.	*Proc. Ind. Acad. Sci.*	1944, **19**, 189
5	The nature and origin of the luminescence of diamond	Do.	*Ibid.*	1944, **19**, 199
6	Intensity of X-ray reflection by diamond ..	P. S. Hariharan	*Ibid.*	1944, **19**, 261
7	Birefringence patterns in diamond ..	C. V. Raman and G. R. Rendall	*Ibid.*	1944, **19**, 265
8	Luminescence patterns in diamond ..	K. Sunanda Bai	*Ibid.*	1944, **19**, 274
9	X-ray topographs of diamond	G. N. Ramachandran	*Ibid.*	1944, **19**, 280
10	Ultra-violet transparency patterns in diamond	G. R. Rendall	*Ibid.*	1944, **19**, 293
11	Experimental evidence for the four possible structures of diamond	R. S. Krishnan	*Ibid.*	1944, **19**, 298
12	X-ray reflection and the structure of diamond	G. N. Ramachandran	*Ibid.*	1944, **19**, 304
13	The crystal forms of the Panna diamonds ..	S. Ramaseshan	*Ibid.*	1944, **19**, 334
14	Spectroscopic study of luminescence patterns in diamond	A. Mani	*Ibid.*	1944, **20**, 155
15	Fluorescence and absorption patterns in diamond at low temperature	Do.	*Ibid.*	1944, **20**, 323
16	X-ray topographs of diamond	G. N. Ramachandran	*Curr. Sci.*	1944, **13**, 156

17	The angular divergence of the X-ray reflections by diamond	Do.	*Proc. Ind. Acad. Sci.*	1944, **20**, 245
18	The crystal forms of diamond and their significance	C. V. Raman and S. Ramaseshan	*Ibid.*	1946, **24**, 1
19	On the crystal symmetry of diamond and its X-ray reflections	G. N. Ramachandran	*Ibid.*	1946, **24**, 58
20	On the nature and origin of the laminations observed in diamond	Do.	*Ibid.*	1946, **24**, 65
21	X-ray topographs of diamond	Do.	*Ibid.*	1946, **24**, 95
22	The cleavage properties of diamond ..	S. Ramaseshan	*Ibid.*	1946, **24**, 114
23	A theory of the crystal forms of diamond ..	Do.	*Ibid.*	1946, **24**, 122
24	Variation in the absorption of infra-red radiations by diamond	K. G. Ramanathan	*Ibid.*	1946, **24**, 130
25	Local variations in the photo-conductivity of diamond	K. Achyuthan	*Ibid.*	1946, **24**, 162
26	Geometric patterns of fluorescence in diamond	G. R. Rendall	*Ibid.*	1946, **24**, 168
27	Phosphorescence patterns in diamond ..	V. Chandrasekharan	*Ibid.*	1946, **24**, 182
28	Allotropic modifications of diamond ..	C. V. Raman	*Nature*	1945, **156**, 22
29	Crystal structure of diamond	G. N. Ramachandran	*Ibid.*	1945, **156**, 83
30	The diamond and its teachings	C. V. Raman	*Curr. Sci.*	1946, **15**, 205
31	Directional variations in the photoconductivity of diamond	K. Achyuthan	*Proc. Ind. Acad. Sci.*	1948, **27**, 171

14. Miscellaneous

1	The elastic properties of mother of pearl ..	P. S. Srinivasan	*Proc. Ind. Acad. Sci.*	1937, **5**, 463
2	Young's modulus of diamond	P. R. Pisharoti	*Ibid.*	1940, **12**, 208
3	α-β transformation of quartz	C. V Raman and T. M. K. Nedungadi	*Nature*	1940, **145**, 147
4	Crystals and photons	C. V. Raman	*Proc. Ind. Acad. Sci.*	1941, **13**, 1
5	New concepts of the solid state	Do.	*Curr. Sci.*	1942, **11**, 85
6	X-rays, crystals and the infra-red spectrum	Do.	*Ibid.*	1941, **10**, 473
7	The photo-conductivity of diamond—Part I	D. D. Pant	*Proc. Ind. Acad. Sci.*	1944, **19**, 315
8	The photo-conductivity of diamond—Part II	Do.	*Ibid.*	1944, **19**, 325

PREFATORY NOTE TO THE SYMPOSIUM

THE present Symposium published in commemoration of the Sixtieth Birthday of Sir C. V. Raman consists of twenty-nine papers dealing with various aspects of the subject of Crystal Physics. Shortness of time stood in the way of its being made more fully representative and the range of topics dealt with in it more comprehensive. That it has been possible to include a few contributions by distinguished investigators in other countries is due to the great kindness of these authors in responding to the invitation of the Council in spite of the extremely short notice given to them. Professors Forrest F. Cleveland, R. Bowling Barnes, N. F. Mott, Linus Pauling, C. Manneback, Robert Hoftstadter, R. W. G. Wycoff and Geo. Glockler, who were invited to contribute but were unable to send papers, have sent very kind messages conveying their good wishes and felicitations. To them and to all those who have contributed to the Symposium, the Council wish to express their grateful thanks.

THE VIBRATIONS OF AN INFINITE LINEAR LATTICE CONSISTING OF TWO TYPES OF PARTICLES

By N. S. Nagendra Nath and Sanat Kumar Roy
(From the Department of Mathematics, Science College, Patna)

Received September 27, 1948

The vibrations of a finite linear lattice of equal masses were first investigated by Lagrange,[1] assuming the end particles to be at rest and those of an infinite linear lattice by Hamilton.[2] The former work is well quoted in connection with the vibrations of strings and Fourier series, while Hamilton's work has not been properly appreciated.[3]

In this paper the vibrations of an infinite linear lattice consisting of two types of particles have been investigated. We consider a lattice consisting of two types of particles of masses m_1 and m_2 alternating one another at equal distances and in stable equilibrium. At time $t = 0$, one of the particles is given an arbitrary but small displacement a along the lattice and all the others are at rest in their equilibrium configurations. We assume that the forces acting on a particle arise due to changes in the positions of all the particles and are proportional to them. Later in the paper, we shall make certain simplifying assumptions in order to find out the asymptotic nature of the vibrations. We denote the displacements of the particles at the instant of time t by $x_m(t)$ where m is any integer ranging from $-\infty$ to $+\infty$. The initial conditions are given by $x_m(0) = 0$ for all m except $m = 0$, $x_0(0) = a$ and $\dot{x}_m(0) = 0$ for all m.

The equations of motion of the $2r$th and $(2r+1)$th particles are

$$\begin{aligned} -m_1\ddot{x}_{2r} &= B_0 x_{2r} + \sum_{s=1}^{\infty} B_{2s}(x_{2r+2s} + x_{2r-2s}) \\ &\quad + \sum_{s=0}^{\infty} B_{2s+1}(x_{2r+2s+1} + x_{2r-2s-1}), \\ -m_2\ddot{x}_{2r+1} &= C_0 x_{2r+1} + \sum_{s=1}^{\infty} C_{2s}(x_{2r+2s+1} + x_{2r-2s+1}) \\ &\quad + \sum_{s=0}^{\infty} B_{2s+1}(x_{2r+2s+2} + x_{2r-2s}). \end{aligned} \tag{1}$$

We seek solutions of the type

$$x_{2r} = f(\phi)\, e^{i(\omega t - r\phi)},\quad x_{2r+1} = g(\phi)\, e^{i(\omega t - r\phi)} \tag{2}$$

where ω, f and g are functions of the real parameter ϕ.

Substituting (2) in the equations of motion (1) and removing common factors, we get

$$\left[B_0 + 2\sum_1^\infty B_{2s}\cos s\phi - \omega^2 m_1\right] f(\phi) + 2\left[\sum_0^\infty B_{2s+1} e^{\frac{i\phi}{2}} \cos\left(s+\tfrac{1}{2}\right)\phi\right] g(\phi) = 0,$$

$$2\left[\sum_0^\infty B_{2s+1} e^{-\frac{i\phi}{2}} \cos\left(s+\tfrac{1}{2}\right)\phi\right] f(\phi) + \left[C_0 + 2\sum_1^\infty C_{2s}\cos s\phi - \omega^2 m_2\right] g(\phi) = 0.$$

Eliminating $f(\phi)$ and $g(\phi)$ in (3), we find that ω satisfies the equation

$$m_1 m_2 \omega^4 - \omega^2\left[m_1 C_0 + m_2 B_0 + 2\sum_1^\infty (m_1 C_{2s} + m_2 B_{2s})\cos s\phi\right] + \left[C_0 + 2\sum_1^\infty C_{2s}\cos s\phi\right]\left[B_0 + 2\sum_1^\infty B_{2s}\cos s\phi\right] - 4\left[\sum_0^\infty B_{2s+1}\cos\left(s+\tfrac{1}{2}\right)\phi\right]^2 = 0. \quad (4)$$

The equation gives four values of ω for each ϕ, which we shall denote by ω_1, ω_2, $-\omega_1$, $-\omega_2$ and the corresponding values of $f(\phi)$ and $g(\phi)$ will be denoted by f_1, f_2, f_3, f_4 and g_1, g_2, g_3, g_4. The general solutions can be built up by the superposition of the solutions of the type (2) within the range of ϕ between 0 and 2π. Since the period of ω is 2π, there is no use in repeating the values of ω over and over again by assigning to ϕ, values outside the range. The general solutions of (1) can now be written as

$$x_{2r} = \frac{1}{4\pi}\int_0^{2\pi} \{f_1(\phi)\, e^{i\omega_1 t} + f_2(\phi)\, e^{i\omega_2 t} + f_3(\phi)\, e^{-i\omega_1 t} + f_4(\phi)\, e^{-i\omega_2 t}\}\, e^{-ir\phi}\, d\phi,$$

$$x_{2r+1} = \frac{1}{4\pi}\int_0^{2\pi} \{g_1(\phi)\, e^{i\omega_1 t} + g_2(\phi)\, e^{i\omega_2 t} + g_3(\phi)\, e^{-i\omega_1 t} + g_4(\phi)\, e^{-i\omega_2 t}\}\, e^{-ir\phi}\, d\phi. \quad (5)$$

From equations (3), we get

$$f_1(\phi) = \lambda(\phi)\, g_1(\phi),\ f_2(\phi) = \mu(\phi)\, g_2(\phi),\ f_3(\phi) = \lambda(\phi)\, g_3(\phi),\ f_4(\phi) = \mu(\phi)\, g_4(\phi) \quad (6)$$

where

$$\lambda(\phi) = \frac{m_2\omega_1^2 - \left[C_0 + 2\sum_1^\infty C_{2s}\cos s\phi\right]}{2\sum_0^\infty B_{2s+1} e^{-\frac{i\phi}{2}} \cos\left(s+\tfrac{1}{2}\right)\phi} \text{ and}$$

$$\mu(\phi) = \frac{m_2\omega_2^2 - \left[C_0 + 2\sum_1^\infty C_{2s}\cos s\phi\right]}{2\sum_0^\infty B_{2s+1} e^{-\frac{i\phi}{2}} \cos\left(s+\tfrac{1}{2}\right)\phi}.$$

The second equation in (5) can now be written as

$$x_{2r+1} = \frac{1}{4\pi}\int_0^{2\pi}\left\{\frac{f_1(\phi)\,e^{i\omega_1 t} + f_3(\phi)\,e^{-i\omega_1 t}}{\lambda(\phi)} + \frac{f_2(\phi)\,e^{i\omega_2 t} + f_4(\phi)\,e^{-i\omega_2 t}}{\mu(\phi)}\right\} e^{-ir\phi}\,d\phi. \tag{7}$$

The boundary conditions are given by $x_0(0) = a$, $x_m(0) = 0$ for all m except $m = 0$ and $\dot{x}_m(0) = 0$ for all m. Hence from the expressions for x_{2r} and x_{2r+1}, we get

$$\begin{aligned}
&\int_0^{2\pi}(f_1 + f_2 + f_3 + f_4)\,d\phi = 4\pi a,\\
&\int_0^{2\pi}(f_1 + f_2 + f_3 + f_4)\,e^{-ir\phi}\,d\phi = 0, \text{ for all } r \text{ except } r = 0,\\
&\int_0^{2\pi}\left(\frac{f_1 + f_3}{\lambda} + \frac{f_2 + f_4}{\mu}\right) e^{-ir\phi}\,d\phi = 0,\\
&\int_0^{2\pi}\omega_1(f_1 - f_3) + \omega_2(f_2 - f_4)\,e^{-ir\phi}\,d\phi = 0,\\
&\int_0^{2\pi}\left\{\frac{\omega_1}{\lambda}(f_1 - f_3) + \frac{\omega_2}{\mu}(f_2 - f_4)\right\} e^{-ir\phi}\,d\phi = 0,
\end{aligned} \tag{8}$$

the last three equations being true for all integral values of r.

Thus,

$$\begin{aligned}
&f_1 + f_2 + f_3 + f_4 = 2a,\\
&\mu(f_1 + f_3) + \lambda(f_2 + f_4) = 0,\\
&\omega_1(f_1 - f_3) + \omega_2(f_2 - f_4) = 0,\\
&\omega_1\mu(f_1 - f_3) + \omega_2\lambda(f_2 - f_4) = 0.
\end{aligned} \tag{9}$$

From these equations it follows that

$$f_1 = \frac{a\lambda}{\lambda - \mu},\ f_2 = \frac{a\mu}{\mu - \lambda},\ f_3 = f_1,\ f_4 = f_2. \tag{10}$$

The solutions under the specified boundary conditions, can now be written as

$$x_{2r} = \frac{a}{2\pi}\int_0^{2\pi}\frac{m_2\omega_1^2 - \left[C_0 + 2\sum_1^\infty C_{2s}\cos s\phi\right]}{m_2(\omega_1^2 - \omega_2^2)}\,e^{-ir\phi}\cos\omega_1 t\,d\phi$$

$$+ \frac{a}{2\pi}\int_0^{2\pi}\frac{m_2\omega_2^2 - \left[C_0 + 2\sum_1^\infty C_{2s}\cos s\phi\right]}{m_2(\omega_2^2 - \omega_1^2)}\,e^{-is\phi}\cos\omega_2 t\,d\phi,$$

and

$$x_{2r+1} = \frac{a}{\pi} \int_0^{2\pi} \frac{\sum_s^{\infty} B_{2s+1} e^{-\frac{i\phi}{2}} \cos\left(s + \frac{1}{2}\right)\phi}{m_2(\omega_1^2 - \omega_2^2)} (\cos \omega_1 t - \cos \omega_2 t)\, e^{-ir\phi}\, d\phi. \tag{11}$$

We now make the simplifying assumption that the forces acting on a particle arise only due to changes in the neighbouring distances. This case is obtained by putting $B_{2s} = C_{2s} = 0$ for all s, except B_0 and C_0 and all $B_{2s+1} = 0$ except B_1. We shall put $2a = \frac{B_0}{m_1}$, $2b = \frac{C_0}{m_2}$, $am_1 = bm_2 = -B_1$ and $z = e^{i\phi}$, so that ω_1, ω_2, $-\omega_1$ and $-\omega_2$ are now the roots of

$$z\omega^4 - 2z\omega^2(a+b) - ab(z-1)^2 = 0, \tag{12}$$

and the solutions are given by

$$x_{2r} = \frac{a}{2\pi i} \int_C \frac{(\omega_1^2 - 2b)\cos \omega_1 t}{(\omega_1^2 - \omega_2^2)\, z^{r+1}}\, dz + \frac{a}{2\pi i} \int_C \frac{(\omega_2^2 - 2b)\cos \omega_2 t}{(\omega_2^2 - \omega_1^2)\, z^{r+1}}\, dz,$$

and

$$x_{2r+1} = \frac{a}{2\pi i} \int_C \frac{b(1+z)(\cos \omega_2 t - \cos \omega_1 t)}{(\omega_1^2 - \omega_2^2)\, z^{r+2}}\, dz, \tag{13}$$

which can be expressed in the form

$$x_{2r} = \frac{1}{4\pi i} \oint \frac{f(z)\, e^{i\omega t}}{z^{r+1}}\, dz, \quad x_{2r+1} = \frac{1}{4\pi i} \oint \frac{g(z)\, e^{i\omega t}}{z^{r+1}}\, dz, \tag{14}$$

where ω is a four-valued function given by the equation (12) and *the path of the integral is a closed curve on the four-sheeted Riemann surface for* $\omega(z)$.

The Riemann surface for $\omega(z)$ is given by

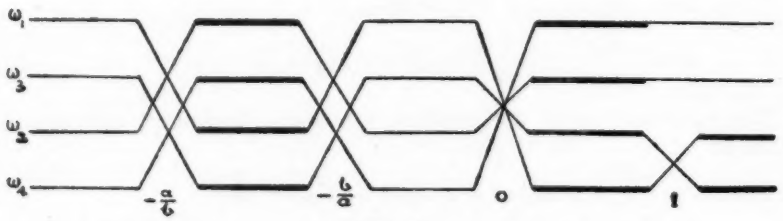

FIG. 1

The thick lines are cuts along which the surfaces are connected for the passage from one plane to the other. $\omega(z)$ is a holomorphic function of z on this four-sheeted surface.

We shall find the asymptotic nature of the solutions by the method of steepest descents. We select the contour of integration in (13) in such a way that it coincides with the paths of the steepest descents.

The equations (13) can be written in the form

$$x_{2r} = \frac{a}{8\pi i} \oint \frac{e^{i\omega_1 t} + e^{-i\omega_1 t} + e^{i\omega_2 t} + e^{-i\omega_2 t}}{z^{r+1}} dz$$

$$+ \frac{a(a-b)}{8\pi i} \oint \frac{e^{i\omega_1 t} + e^{-i\omega_1 t} - e^{i\omega_2 t} - e^{-i\omega_2 t}}{z^{r+1}\sigma} dz,$$

and

$$x_{2r+1} = \frac{a}{8\pi i} \oint \frac{b(1+z)(e^{i\omega_2 t} + e^{-i\omega_2 t} - e^{i\omega_1 t} - e^{-i\omega_1 t})}{z^{r+2}\sigma} dz, \qquad (15)$$

where $2\sigma = \omega_1^2 - \omega_2^2$ and $\omega_1^2 = a + b + \sigma$, $\omega_2^2 = a + b - \sigma$.

The above expressions are the sum of terms of the form

$$P = \oint R(z)\, e^{\omega(z)t}\, dz. \qquad (16)$$

The saddle points are given by $\frac{d\omega}{dz} = 0$. If z_0 be a saddle point then the asymptotic value of P is given by[4]

$$\frac{R(z_0)\, e^{\omega(z_0)t} \sqrt{2\pi}\, e^{i\theta}}{|\, t\omega''(z_0)\,|^{\frac{1}{2}}} \qquad (17)$$

where θ denotes the angle that the path of the steepest descents makes with the real axis and its value is to be found in each case by the usual method.

We shall first assume that $a > b$. The saddle points are given by $\omega_1' = 0$, $\omega_2' = 0$, that is by $z = \pm 1$. At the point $z = 1$, $\omega_1(z)$ has a development in powers of $(z-1) = z'$ of the type $A + Bz'^2 + \ldots$. where z' is small and $B > 0$; therefore, the behaviour of $i\omega_1$ at $z = 1$ is like that of iz'^2. Putting $z' = \xi + i\eta$, we have $i\omega_1(z) = \phi + i\psi = i(\xi^2 - \eta^2) - 2\xi\eta$. Now $\psi = 0$ gives the lines of steepest descents and they are therefore given by $\xi = \pm\eta$, (ξ, η) being the set of rectangular axes at $z = 1$ as origin, the ξ-axis coinciding with the real axis. Also $\phi = -2\xi\eta$ and ϕ has to decrease as we proceed along the lines of steepest descents. ϕ will decrease if both ξ and η be positive or if both of them be negative. Taking the counter-clockwise direction as the path of integration we get $\theta = \frac{1}{4}\pi$. Similarly at $z = -1$ we get $\theta = \frac{3}{4}\pi$. For $i\omega_2(z)$ we get at $z = 1$, $\theta = \frac{3}{4}\pi$ and at $z = -1$, $\theta = \frac{5}{4}\pi$.

After substituting in (17) the values of θ, $\mathrm{R}(z_0)$, etc., we get after some reduction,

$$x_{2r} = a\left(\frac{a}{b}\right)^{\frac{1}{4}}\left(\frac{2}{\pi \mathfrak{I}_1 t}\right)^{\frac{1}{2}} \cos\left(\mathfrak{I}_1 t - \frac{\pi}{4}\right)$$
$$+ (-1)^r a\left\{\frac{|a-b|}{b}\right\}^{\frac{1}{4}}\left(\frac{2}{\pi \mathfrak{I}_2 t}\right)^{\frac{1}{2}} \cos\left(\mathfrak{I}_2 t + \frac{\pi}{4}\right) \qquad (18)$$

where $\mathfrak{I}_1 = \sqrt{2a+2b}$, $\mathfrak{I}_2 = \sqrt{2a}$.

Similarly the asymptotic value of x_{2r+1} is given by

$$x_{2r+1} = -a\left(\frac{b}{a}\right)^{\frac{1}{4}}\left(\frac{2}{\pi \mathfrak{I}_1 t}\right)^{\frac{1}{2}} \cos\left(\mathfrak{I}_1 t - \frac{\pi}{4}\right) \qquad (19)$$

In case $b > a$, the phase $\frac{\pi}{4}$ in the second term of (18) will be changed to $-\frac{\pi}{4}$.

The normal vibrations of the lattice according to Raman are given below:—

FIG. 2

If the lattice at the time $t = 0$ is disturbed as follows

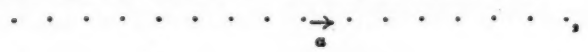

FIG. 3

the amplitudes of the particles for sufficiently large t are asymptotically given by (18) and (19) which show that the solutions tend to a time dependent superposition of normal solutions with frequencies ν_1 and ν_2. If however a particle with mass m_2 had been displaced, the asymptotic nature would have been a time dependent superposition of vibrations with frequencies ν_1 and ν_3. If either both m_1 and m_2 or an arbitrary finite set of particles of the lattice had been disturbed, we can say by the principle of superposition, *that the asymptotic nature of the vibration would tend to a time dependent superposition of the normal vibrations according to Raman.*

If $a = b$, the vibrations with frequencies ν_2 and ν_3 cease to be normal vibrations according to Raman. There is no discontinuity in the result of

the above paragraph as $a \to b$ from that when $a = b$, for the controlling factors in the contributions of oscillations with frequencies ν_2 and ν_3 depend on $| a - b |$. *It may also be noted that when $a = b$, the oscillations ν_2 and ν_3 cease to be saddle point oscillations.* In this case x_{2r} and x_{2r+1} take the form[5] $J_{4r}(\sqrt{2a}t)$ and $J_{4r+2}(\sqrt{2a}t)$ corresponding to Hamilton's solutions.

Summary

The solutions for the displacements of an infinite linear lattice consisting of two types of particles under some initial disturbance have been obtained and their asymptotic nature has been investigated by the method of "steepest descents" which shows that the displacements are asymptotically time dependent superposition of the normal vibrations according to Raman.

. . . . . .

I take this opportunity of recording here my indebtedness and gratitude to my Professor, Sir C. V. Raman, on the occasion of his sixtieth birthday.

N. S. Nagendra Nath.

References

1. Lagrange .. *Mecanique Analytique*, Tome, 1, p. 408.
2. Hamilton .. *Works*, 2, p. 452.
3. Havelock .. *The Propagation of Disturbances in Dispersive Media*, 1914, p. 6.
4. Jeffreys and Jeffreys .. *Methods of Mathematical Physics*, p. 472.
5. ———— .. *Ibid.*, p. 567.

THE VIBRATION SPECTRA OF THE ALKALI HALIDES

By Dr. R. S. Krishnan and P. S. Narayanan

(From the Department of Physics, Indian Institute of Science, Bangalore)

Received November 29, 1948

1. Introduction

The scattering of light in crystals comprises two different phenomena, the thermal scattering and the Raman effect. The former is due to the optical stratifications in the crystal associated with thermally excited stationary vibrations of the elastic type. The latter arises from the excitation of the vibrations of the atoms in a crystal by the radiations traversing it and is closely linked up with its vibration spectrum. Theoretical considerations and facts of observation alike indicate that we are here concerned, not with a coherent reflection as in the case of the thermal scattering, but with an incoherent scattering in which the process involved is the transfer of energy in discrete quanta between the radiation field and the individual volume elements of molecular dimensions in the crystal. This view of the phenomenon is indicated in the first place by the obvious points of similarity between the effects exhibited by crystals and those observed in the Raman scattering by gases and liquids. In the case of ionic or molecular crystals, vibrational frequency shifts appear as sharp lines and have nearly the same values as those observed with the same substance in the fluid state. In fact, the lines are generally sharper in the case of the crystal than in the liquid because of the more precise character of the force-fields in the crystalline medium. Overtones and summations of the fundamental frequencies are also recorded as sharp lines with observable intensities in the well-exposed spectrograms of numerous crystals like calcite, quartz, gypsum, barite, etc. (Krishnan, 1945 *a*, 1946 *a*). This is an indication that the amplitudes of the excited vibrations are not negligibly small in comparison with inter-atomic distances and that in consequence, the optical anharmonicity or lack of proportionality between the atomic displacements and the resulting variations of optical polarisabilities becomes operative. For this to be possible with an oscillator of which the energy is quantised and hence determinate, its dimensions should be of molecular order of magnitude.

In view of the situation stated above, it becomes evident that we are concerned with the evaluation of the normal modes of vibration of the

structural units of which the crystal is composed. This is the problem which has been considered and solved by Sir C. V. Raman (1943, 1947) in two theoretical papers in these *Proceedings*. If there are p atoms in the unit cell of the crystal structure, one might think that there would be only $3p$ normal modes characteristic of the individual unit cells. But this is not actually the case because the influence of the neighbouring units on the oscillation of any particular unit cell has to be taken into consideration. Since the crystal consists of sets of equivalent atoms ordered in such a manner that each atom in a set is geometrically and physically related to its environment in exactly the same way as every other atom of the same set, the oscillations of the atoms in adjacent cells of the structure have to be alike in every respect except that the phases may be either the same or opposite along each axis of the lattice. Combining the three pairs of these alternative possibilities gives eight possibilities and therefore, eight times $3p$ or $24p$ modes of vibration as has been shown by Sir C. V. Raman. In $(3p-3)$ of these modes, equivalent atoms in adjacent cells have the same amplitudes and the same phase of vibration, while in the remaining $21p$ modes, they have the same amplitude but alternately opposite phases in successive cells along one, two, or all three axes of the space lattice. In relation to the entire crystal, the $(24p-3)$ oscillation frequencies are highly degenerate, being the characteristic frequencies of the group of $8p$ atoms in a volume element having twice the linear dimensions and eight times the volume of the lattice cells. The three excluded modes are the simple translations of such a volume element. Thus, if we approach the problem from the atomistic standpoint, the $(24p-3)$ modes are the only ones possible and they describe the vibration spectrum of the structure completely. In any actual case, the number of distinct frequencies would necessarily be less than $(24p-3)$ if the crystal possesses additional elements of symmetry. In the first order Raman effect, only the fundamentals of not more than $(3p-3)$ of these modes are active, while all the $(24p-3)$ modes can appear as overtones and summations in the second order Raman effect, thus yielding highly complex spectra which are necessarily of low intensity.*

A verification of the foregoing ideas is already forthcoming in the case of diamond from the results of a variety of studies on different aspects, namely, light-scattering, infra-red absorption, luminescence, ultra-violet absorption, etc. The considerations mentioned in the last paragraph are

* The basic principles of lattice dynamics have been critically examined by Bhagavantam and Venkatarayudu in their book on *Group Theory and Its Application to Physical Problems*, Bangalore Press, 1948, Chapters X and XI, to which the reader may be referred.

perfectly general and should be applicable to all crystals alike in such simple cases as the alkali halides and to complex ones such as quartz, topaz, organic crystals, etc. Detailed investigations on the Raman spectra of rock-salt, ammonium chloride and ammonium bromide carried out by one of us (R. S. Krishnan, 1945 *b*, 1946 *b*, 1947 *a*, 1948) have clearly established the discrete character of their vibration spectra, thus confirming the correctness of the theoretical ideas presented earlier in this section. The Raman spectrum of potassium bromide has now been studied by us and the results are presented in this paper.

2. Experimental Details

Because of the ionic nature of the binding forces, and the heavy atomic weights of the ions in alkali halides, their vibration spectra are spread over a narrow range and the actual frequencies have low values. The large number of frequency shifts belonging to the second order Raman spectrum therefore appear crowded together. The spectrum exhibiting these frequency shifts is weak and is recorded near the exciting radiation which, unless it is completely eliminated, results with prolonged exposures in recording various spurious effects in its vicinity even with the best of instruments. Further, the fact that the vibration frequencies are low has the consequence that the vibrations will be thermally excited to an appreciable extent, giving rise to a broadening of the lines. If all these factors are taken into consideration, the resulting spectrum could easily be mistaken for a continuous one. In order to find the real nature of the spectrum, it may be necessary to use the highest possible dispersive and resolving powers. In spite of these difficulties, the very first photograph of the Raman spectrum of rock-salt taken by Rasetti with a medium quartz spectrograph showed the presence of a line at 235 $cm.^{-1}$ to the sharpness of which Rasetti drew special attention. Since then, detailed studies of the Raman spectrum of rock-salt under more favourable conditions of dispersion and resolution have not only confirmed Rasetti's observation but also shown the discrete character of the rock-salt spectrum unambiguously.

Potassium bromide has a crystal structure similar to that of rock-salt, but as the ions in the former are heavier, the Raman frequency shifts are smaller and hence less easy to record in a satisfactory manner. Menzies and Skinner (1948 *a*, *b*) who first photographed the spectrum of potassium bromide observed some details in the spectrum. In the present investigation, the authors have made considerable improvements in the experimental technique. By effecting a very perfect elimination of the diffuse continuum of instrumental origin and by using a large quartz spectrograph, the details of the KBr spectrum have been clearly brought out in the photograph.

Three specimens of synthetic potassium bromide were made available to us for the present study by the kindness of Dr. A. C. Menzies to whom the authors' thanks are due. One of them which had a slight yellowish tinge was found to be only partially transparent to the λ 2537 radiation and as such it had to be rejected. The second one was extremely clear and free from any colour. This had the following dimensions ($2'' \times 1\frac{1}{2}'' \times 1''$). Using this specimen and a medium quartz spectrograph with a fine slit (0·025 mm.) an exposure of about 4 hours was sufficient to record all the features of the spectrum. However, longer exposures of the order of 24 hours were given to get intense photographs. The experiment was repeated with a Hilger large quartz spectrograph. Due to prolonged exposure to the rays from the mercury arc, this crystal acquired a distinct colouration and a diminished transparency and the spectrum was, therefore, not recorded with the full intensity hoped for even after an exposure of 15 days. The third specimen ($4'' \times 2'' \times 1\frac{1}{2}''$) which was not as clear as the second one was also found to be partially opaque in thick layers to the λ 2537 radiations. Using this, moderately intense spectrograms were taken with the large quartz spectrograph with a moderate slit width and an exposure of ten days. The negatives were measured with the aid of a Hilger cross slide micrometer.

3. Results

The spectrogram taken with the medium quartz spectrograph having a slit width of 0·025 mm. and an exposure of 24 hours is reproduced together with the microphotometer record of a lighter negative as Figs. 1 (*a*) and (*b*) respectively in the Plate. As is evident from the reproduced photograph, the spectrum of potassium bromide is confined to a region of frequency shifts from 46 cm.$^{-1}$ to about 290 cm.$^{-1}$ It consists of a series of distinct Raman lines with frequency shifts 46 (5), 84 (6), 126 (10), 146 (9), 170 (5), 186 (3), 216 (5), 228 (2), 232 (2), 242 (2) and 287 (1) cm.$^{-1}$ They can be easily distinguished in the photograph. Their positions have been marked in the microphotometer record. The figures given in brackets represent visual estimates of the relative intensities of the lines. Menzies and Skinner (1948 *b*) were able to identify only seven frequency shifts in the spectrogram taken by them. The values agree reasonably well with those reported by them. Our photographs show greater detail than the ones taken by Menzies and Skinner* evidently due to better technique of experimentation and more efficient filtering of the exciting radiation.

* Dr. Menzies informs us that they have recently succeeded in getting good photographs showing as many details as those taken by us.

The most conspicuous feature in the spectrum of potassium bromide is the extreme sharpness of the lines 84, 126, 146, 170 and 216 cm.$^{-1}$ The corresponding anti-Stokes lines are also clearly visible in the spectrogram. The line 126 cm.$^{-1}$ is most intense. The line at 46 cm.$^{-1}$ is also fairly intense and sharp. Unfortunately, it falls adjacent to a ghost line at about 60 cm.$^{-1}$ In spite of this, it can be seen as a separate kink in the microphotometer record. The high frequency shift lines at 242 and 287 cm.$^{-1}$ are rather broad, the latter being less intense and more diffuse having a width of about 50 cm.$^{-1}$ Beyond this broad line the intensity falls off abruptly.

Figs. 2 (*a*) and 2 (*b*) represent photographs enlarged to the same extent of the spectrograms taken with the large and medium quartz spectrographs respectively. In spite of the fact that a fairly wide slit had to be used with the larger instrument to get the spectrograms within a reasonable time of exposure, the details of the bromide spectrum are more clearly seen in

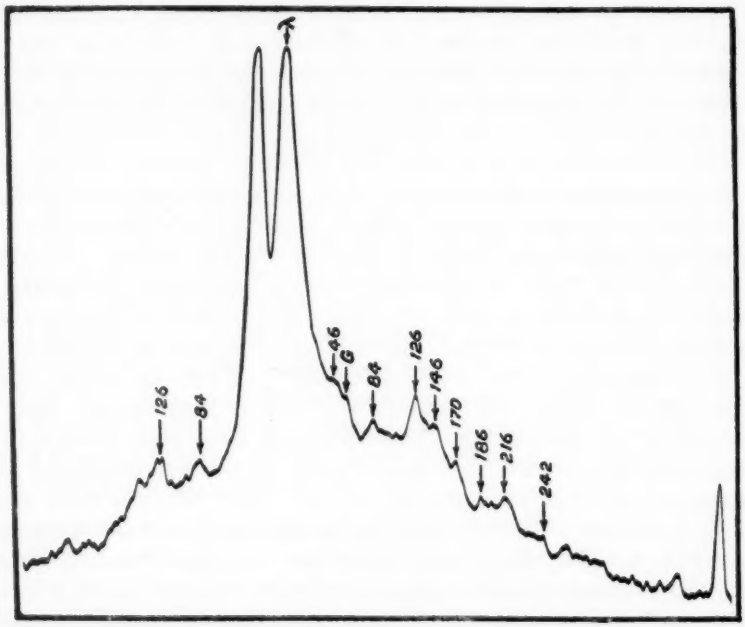

FIG. 3. Microphotometer record of the Raman spectrum of potassium bromide taken with the large quartz spectrograph.

Fig. 2 (*a*), evidently due to the higher dispersion and resolution of the larger spectrograph. The sharpness and discrete character of some of the Raman

lines are also evident from a scrutiny of the microphotometer record of the spectrogram taken with the large quartz spectrograph reproduced in Fig. 3.

The lines 228 and 232 cm.$^{-1}$ appear as a single line with a mean shift of 230 cm.$^{-1}$ in the photograph taken with the medium quartz spectrograph. In the microphotometer record of the spectrogram taken with the larger quartz spectrograph (Fig. 3) the doublet nature could be easily identified. The width of the line at 186 cm.$^{-1}$ is partly due to presence of a mercury line separated from λ 2536·5 radiation by about 184 cm.$^{-1}$

Fig. 2 (*c*) represents the spectrum of rock-salt taken with the large quartz spectrograph and a fine slit and enlarged to the same extent as Fig. 2 (*a*). It is interesting to note that the discrete character of the second-order spectrum is more clearly evident in the case of potassium bromide than in the case of rock-salt. In the case of the latter, only one line at 235 cm.$^{-1}$ stands out very prominently while in the case of the former, no less than five lines, *viz.*, 84, 126, 146, 170 and 216 cm.$^{-1}$ appear conspicuously. In spite of the smaller values of the frequency shifts in potassium bromide, the lines do not appear bunched up as in sodium chloride, but are evenly distributed over the entire spectrum. Photographs of the Raman spectra of NaCl and KBr taken under comparable conditions with the aid of the medium quartz spectrograph suggested that the scattering power of KBr is greater than that of NaCl.

4. Discussion

Crystal structures of the rock-salt type contain two interpenetrating face-centred cubic lattices. The unit cell is a rhombohedron with one metallic ion and one halogen ion contained in it. According to the new lattice dynamics, of the 48 degrees of freedom, 45 will appear as the atomic frequencies. These 45 frequencies would be reduced by degeneracy to 9 modes with distinct frequencies ν_1 to ν_9. The detailed description of these modes are given in Table I. The expressions for the frequencies of these modes as worked out by K. G. Ramanathan (1947) using only four force constants P, P′, T, T′ are also included in the table. P and P′ represent the forces arising from unit displacements respectively of the two types of atoms in the structure from their positions of equilibrium, while T and T′ represent the forces on a given atom due to a unit displacement of a neighbouring atom of the same kind. The undashed quantities refer to the ions of mass m_1 and dashed ones to ions of mass m_2; $P + 8T = P' + 8T'$. The descriptions of the modes given in Table I are determined only by the crystal structure and are independent of the masses of constituent ions and of the nature of the forces in the crystalline medium. If m_1 and m_2 are the masses of the

TABLE I

The Eigenvibrations of the Rock-salt Structure

Descending Sequence of Frequency	Symbol	Degen-	Oscillating unit	Direction of motion	$4\pi^2\nu^2c^2$	Detailed description
I	ν_1	3	Cubic planes	Normal	$\frac{P-8T}{m_1}+\frac{P'+8T'}{m_2}+\frac{16(T+T')}{m_1+m_2}$	K and Br ions moving in the same phase
II	ν_2	6	Cubic planes	Tangential	$\frac{P}{m_1}+\frac{P'}{m_2}+\frac{8(T+T')}{m_1+m_2}$	K and Br ions moving in opposite phases
III	ν_3	3	Two lattices	Arbitrary	$\frac{P+8T}{m_1}+\frac{P'+8T'}{m_2}$	K and Br ions moving in opposite phases
IV	ν_4	4	Octahedral planes	Normal	$\frac{P-8T}{m_1}$	K ions moving and the Br ions at rest
V	ν_5	8	Octahedral planes	Tangential	$\frac{P+4T}{m_1}$	K ions moving and Br ions at rest
VI	ν_6	4	Octahedral planes	Normal	$\frac{P'+8T'}{m_2}$	K ions at rest and Br ions moving
VII	ν_7	8	Octahedral planes	Tangential	$\frac{P'+4T'}{m_2}$	K ions at rest and Br ions moving
VIII	ν_8	3	Cubic planes	Normal	$-\frac{16(T+T')}{m_1+m_2}$	K and Br ions in opposite phases
IX	ν_9	6	Cubic planes	Tangential	$-\frac{8(T+T')}{m_1+m_2}$	K and Br ions in the same phases

lighter and heavier ions respectively and P, P' $\gg$ T, T', Sir C. V. Raman (1947) has shown that the nine eigenvibrations arrange themselves in descending sequence of frequency in the order indicated in Table I. Before considering the case of potassium bromide in detail, it is useful to discuss the general features of the spectra of different alkali halides possessing the rock-salt structure.

Because of the high symmetry of the structure, all the nine modes will be inactive in the first order Raman effect. In the second-order Raman spectrum, the 9 octaves and 36 combinations of the primary vibration frequencies are allowed to appear. In any particular case, only the octaves and a few combinations may be expected to appear in the spectrum with any appreciable intensity. The actual magnitude of the frequency shifts and their distribution in the spectrum will be determined by the absolute and relative values of the masses of the two kinds of ions. As is to be expected, if the ions are of low atomic weight as in LiF, the frequencies will be high and conversely if the ions are heavy the frequencies will be low. If the ratio of the masses of the cation and the anion is large, the frequencies of nine modes will be such that in the resulting second-order spectrum the Raman lines would be more evenly distributed, thus enabling the discrete character of

the spectrum to be exhibited quite clearly. As the ratio of the masses is progressively decreased, the majority of the modes will have frequencies slightly different from one another and the Raman lines appear bunched together over a narrow region of frequency shifts. These conclusions are fully substantiated by the results obtained with KBr and NaCl. As the ratio of the masses of K and Br ions is greater than the ratio of Na and Cl ions, the details of the spectrum are more clearly evident in the case of KBr than in the case of NaCl [see Figs 2 (*a*) and 2 (*c*)]. If the ratio of the masses is nearly unity, *i.e.*, if $m_1 \sim m_2$ as in NaF, KCl and RbBr, the frequencies of some of the pairs of modes become identical, resulting in a perturbation of the vibrational modes. The resulting spectrum will be a complicated one. This aspect of the problem will be discussed in greater detail in a forthcoming paper on the Raman spectrum of potassium chloride.

5. Case of Potassium Bromide

The nine eigenfrequencies of potassium bromide can be calculated to a first approximation with two assumed force constants only. $P = P'$ and $T = T'$. For the alkali halides P is nearly fifty times T. The force constants, for KBr may be expected to be smaller than those for NaCl and KCl (C. V. Raman, 1947). Taking $P = 2{\cdot}2 \times 10^4$ dynes/cm. and $T = -0{\cdot}034 \times 10^4$ dynes/cm., the frequencies have been evaluated and the values are given in Table II.

Table II

Eigenfrequencies of KBr

Mode	$4\pi^2\nu^2c^2$	Calculated frequency cm.$^{-1}$	Observed frequency cm.$^{-1}$
ν_1	$\frac{P-8T}{\mu}+\frac{32T}{m_1+m_2}$	121	121
ν_2	$\frac{P}{\mu}+\frac{16T}{m_1+m_2}$	117	116
ν_3	$\frac{P+8T}{\mu}$	112	114
ν_4	$\frac{P-8T}{m_1}$	104	108
ν_5	$\frac{P+4T}{m_1}$	95	93
ν_6	$\frac{P-8T}{m_2}$	73	73
ν_7	$\frac{P+4T}{m_2}$	67	63
ν_9	$-32T/(m_1+m_2)$	40	42
ν_8	$-16T/(m_1+m_2)$	28	23

As already indicated above, the nine eigenvibrations are inactive in the Raman effect to a first approximation. The frequency shifts recorded in the spectrum should therefore be identified as the octaves and some of the combinations of the eigenvibrations. The octaves are generally more intense than the combinations. Taking this as well as the relationships between ν_4 and ν_6, ν_5 and ν_7 and ν_8 and ν_9 (see Table I), into consideration, the observed frequency shifts 242, 232, 228, 216, 186, 146, 126, 84 and 46 cm.$^{-1}$ have been assigned as octaves of ν_1, ν_2, ν_3, ν_4, ν_5, ν_6, ν_7, ν_8 and ν_9. The observed values for the eigenfrequencies are entered in the last column of Table II. The agreement between the observed and calculated frequencies is satisfactory. The line at 170 cm.$^{-1}$ may be identified as a combination of ν_4 and ν_7. The diffuse and faint band at 287 cm.$^{-1}$ may belong to the third-order spectrum.

The modes ν_4 and ν_5 represent oscillations of the K ions only lying in the octahedral planes, while modes ν_6 and ν_7 represent similar oscillations of the Br ions only. In the normal modes, ν_4 and ν_6, six ions of one kind simultaneously approach or recede from an ion of the other kind, while in the tangential modes, *viz.*, ν_5 and ν_7, two ions of one kind approach, two recede and two others remain at the same distance. Hence the changes of polarisability should be much larger in the normal modes ν_4 and ν_6 than in the tangential modes ν_5 and ν_7. It follows, therefore, that ν_4 and ν_6 should show much stronger activity in the second-order Raman effect than ν_5 and ν_7 respectively. Experimentally it is found that octave of ν_4 (216 cm.$^{-1}$) is more intense than the octave of ν_5 (186 cm.$^{-1}$), while the octave of ν_6 (146 cm.$^{-1}$) is less intense than that of ν_7 (126 cm.$^{-1}$). The abnormally high intensity of the 126 cm.$^{-1}$ line may be attributed to the fact that the combination of ν_4 and ν_9 falls roughly on the octave of ν_7. Since the refractivity of the Br ions is very much larger than that of the K ions, the octaves of modes ν_6 and ν_7 may be expected to appear with greater intensity than the octaves of the corresponding modes ν_4 and ν_5. Indeed, the octaves of ν_6 and ν_7, *viz.*, 146 and 126 cm.$^{-1}$, would be the most intense lines in the spectrum. This is what is actually observed. See Fig. 1.

In modes ν_1, ν_2 and ν_3, the movements of the K and Br ions are similar, the two Br ions on each side of a K ion along the cube axis respectively approaching and receding from it, while the two K ions on each side of a Br ion behave similarly with respect to the latter. Each pair of neighbouring K and Br ions at the phase of their nearest approach would have polarisability greater than the value averaged over the whole period, thus giving rise to scattered radiations of double frequency. Therefore, modes ν_1, ν_2

and ν_3 would be active more or less to the same extent and their octaves would have nearly the same intensity. This conclusion is also supported by facts.

6. The Infra-Red Absorption Spectrum

The infra-red absorption spectrum of thin films of potassium bromide has been investigated by Barnes (1932). The principal absorption peak was located at $88{\cdot}3 \pm 0{\cdot}5\,\mu$ (113 wavenumbers). Besides this, the existence of one other subsidiary maximum at about $82\,\mu$ (122 wavenumbers) has been established.

Since the two interpenetrating lattices in the structure of potassium bromide consist of dissimilar particles, their oscillation against each other, *viz.*, mode ν_3 in Table I is necessarily active in infra-red absorption. The frequency of the principal infra-red absorption maximum agrees very well with the calculated value for ν_3 (see Table II). In all the other eight eigenvibrations, the phase of the motion is reversed at each successive layer, and hence if they are regarded as independent normal vibrations of the structure they should be inactive in respect of infra-red absorption. But, as has been shown by Sir C. V. Raman, owing to the anharmonicity and the finite amplitudes of oscillation, there would be sufficient coupling between the different modes to make some of the fundamentals or combinations having frequencies near about the frequency of ν_3 active in infra-red absorption. This would explain the broad character of the principal infra-red absorption maximum at $88{\cdot}3\,\mu$ ($113\,\text{cm.}^{-1}$) and also the appearance of a subsidiary infra-red maximum at about $82\,\mu$ ($122\,\text{cm.}^{-1}$) corresponding to the intense Raman line at $126\,\text{cm.}^{-1}$

7. Summary

The physical basis for the derivation of the result that any crystal has only $24p-3$ normal modes of atomic vibration, p being the number of non-equivalent atoms in the unit cell, has been briefly reviewed. The difficulties connected with the successful recording and interpretation of the spectra of the alkali halides have been pointed out. The Raman spectrum of potassium bromide excited by $\lambda\,2536{\cdot}5$ radiation has been recorded, using both moderate and high dispersion spectrographs. It exhibits a series of sharp Raman lines, eleven of which could be easily identified. The five most intense lines which stand out prominently in the spectrum on account of their extreme sharpness have frequency shifts 84, 126, 146, 170 and $216\,\text{cm.}^{-1}$ The numerical evaluation of the nine eigenfrequencies for KBr on the basis of the new lattice dynamics leads to results in good agreement with observational data. Their activities in light-scattering and infra-red absorption

are also discussed. The vibrations which are most active in Raman effect are those in which the Br ions lying in the octahedral layers alone move. This result is in general agreement with the observed facts.

References

1. Barnes, R. B. .. *Zeits. fur Physik*, 1932, **75**, 723.
2. Krishnan, R. S. .. *Proc. Ind. Acad. Sci.*, A, 1945*a*, **22**, 182, 274 and 329.
   ——— .. *Nature*, 1945*b*, **156**, 267.
   ——— .. *Proc. Ind. Acad. Sci.*, A, 1946*a*, **23**, 288.
   ——— .. *Nature*, 1946*b*, **157**, 623.
   ——— .. *Proc. Roy. Soc.*, A, 1946*b*, **187**, 188.
   ——— .. *Nature*, 1947*a*, **159**, 266.
   ——— .. *Proc. Ind. Acad. Sci.*, A, 1947*a*, **26**, 419, 432; 1948, **27**, 321.
3. Menzies, A. C., and Skinner, J. *Proc. Phys. Soc.*, 1948*a*, **60**, 498.
   ——— .. *Journ. de Physique et le Radium*, 1948*b*, **9**, 93.
4. Raman, C. V. .. *Proc. Ind. Acad. Sci.*, A, 1943, **18**, 237; 1947, **26**, 339, 370 and 396.
5. Ramanathan, K. G. .. *Ibid.*, 1947, **26**, 493.

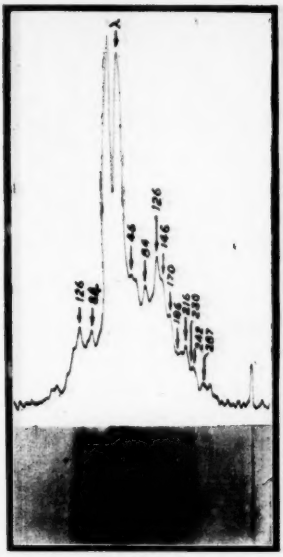

FIG. 1. The Raman spectrum of potassium bromide taken with the medium quartz spectrograph and its microphotometer record.

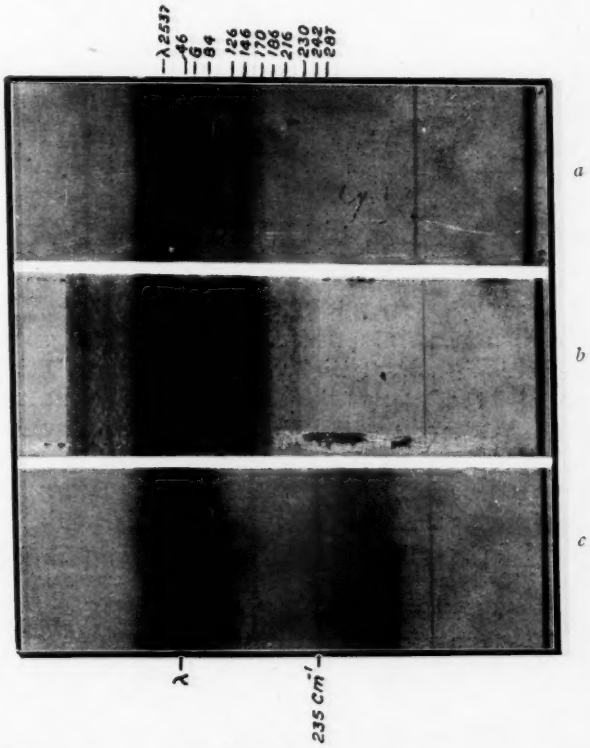

FIG. 2. (*a*) The Raman spectrum of KBr taken with the large quartz spectrograph.
(*b*) The Raman spectrum of KBr taken with the medium quartz spectrograph and enlarged to the same extent as (*a*).
(*c*) The Raman spectrum of NaCl taken with the large spectrograph.

THE THEORY OF THE VIBRATIONS AND THE RAMAN SPECTRUM OF THE DIAMOND LATTICE

By Dr. R. S. Krishnan

(From the Department of Physics, Indian Institute of Science, Bangalore)

Received November 24, 1948

Several investigations by the author on the scattering of light in diamond and on its Raman spectrum have already been reported in earlier publications (Krishnan, 1944, 1945, 1946, 1947 *a*, *b*, *c*). The frequency shifts observed in diamond are of three kinds:—(*a*) the Brillouin shifts in the vicinity of the exciting radiation less intense than (*b*), the first-order frequency shift of 1332 cm.$^{-1}$, but both are recorded with short exposures, while (*c*) the second-order spectrum requires much heavier exposures. Under the high resolution provided by the Hilger E1 quartz spectrograph, the second-order Raman spectrum which is confined to the region of frequency shifts 2665·4 cm.$^{-1}$ and 2015 cm.$^{-1}$ exhibits a set of sharply defined and discrete lines. These results together with those obtained by Ramanathan (1947) by the method of infra-red absorption have been fully and satisfactorily explained on the basis of the new lattice dynamics.

A paper by Helen M. J. Smith (1948), a student of Born, with the same title as the present one has appeared in a recent number of the *Transactions of the Royal Society*, in which she has attempted to work out theoretically the vibration spectrum of the diamond lattice on the basis of the Born theory and to derive its second-order Raman spectrum. She has claimed to have satisfactorily explained the facts reported by the present writer. It is the purpose of this paper to point out that the above claim is not justified.

On the basis of the cyclic postulate, Helen Smith has calculated the second-order vibration spectrum of the diamond lattice. It is a continuous one with 13 branches as shown in the accompanying Fig. 1. From the vibration spectrum she has calculated the intensity distribution in the second-order Raman spectrum involving some arbitrary assumptions. The theoretical curve is reproduced in Fig. 2 *a*.

(1) *The form of the curve.*—In order to fit the theoretical curve with the experimental one, the author arbitrarily assumes that the factors A (*jj*) must be zero for the branches 4, 5, 7, 8, 9, 11, 12 and 13 (see Fig. 1). This is sufficient to show the artificial character of the procedure adopted by Smith in deriving the theoretical curve.

(2) *The extent of the spectrum in the region of high frequency shifts.*— The theoretical curve extends over a region of frequency shifts 1700 to 2700 cm.$^{-1}$, *i.e.*, 1000 wavenumbers. The observed second-order spectrum, on the other hand, is restricted to a region of frequency shifts 2176 cm.$^{-1}$ to 2665 cm.$^{-1}$ Below 2176 cm.$^{-1}$ there is only one faint line at 2015 cm.$^{-1}$ but no continuum of even 1/10th intensity of the 2176 cm.$^{-1}$ line. The extension of the spectrum up to about 1700 cm.$^{-1}$ on the shorter wavelength side, of the type and of comparable intensity as suggested by the theory does not find experimental support.

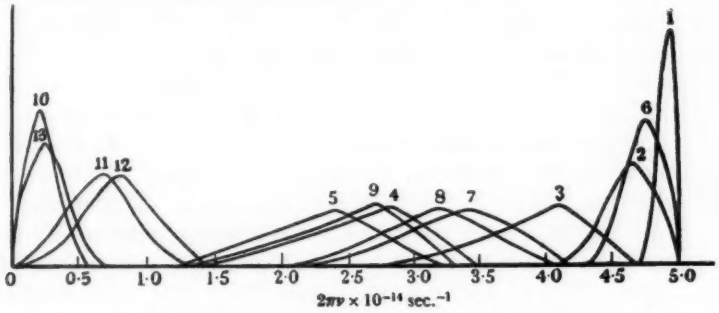

FIG. 1. Frequency density functions $Z^{jj}(\omega)$ taken from Smith's paper.

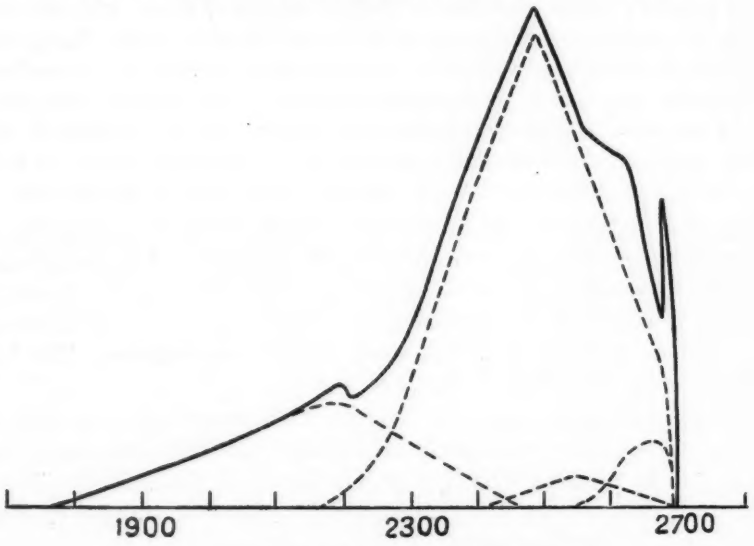

FIG. 2 *a*. The theoretical intensity distribution curve.

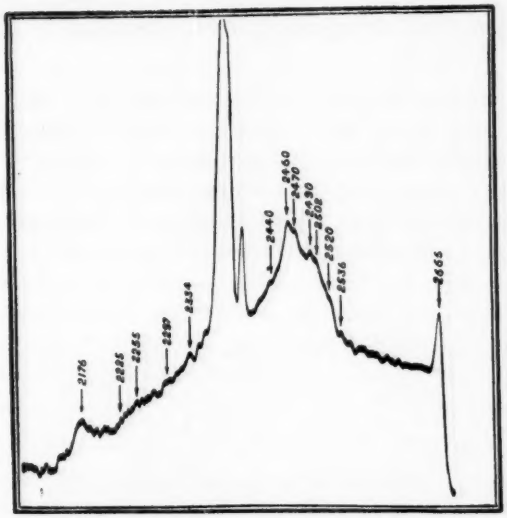

FIG. 2 *b*. Microphotometer record of the second-order Raman spectrum of diamond taken with large quartz spectrograph.

(3) *The number of lines or peaks.*—The theoretical curve exhibits four maxima, as is to be expected by the superposition of the four branches (1), (2), (3) and (6). Any further refinement in the theoretical calculations cannot give rise to more than four maxima in the region under consideration. The microphotometer record of the observed spectrum shows no less than 12 kinks, each one of them representing a sharply defined line. That these kinks are not due to random fluctuations in intensity as Smith would like to call them, will be obvious to anybody who examines the spectrograms taken under high dispersion and resolution. Even a lightly exposed spectrogram reproduced in Fig. 3 exhibits at least four extremely sharp lines adjacent to the most intense line at 2460 cm.$^{-1}$ The theoretical curve has, instead, only one maximum in this region.

(4) *The high frequency cut-off of the spectrum.*—In the intensity distribution curve calculated on the basis of the Born theory, the peak with the maximum frequency shift, *i.e.*, 2664 cm.$^{-1}$ does not coincide with the end of the spectrum, whereas in the experimental curve the line at 2665·4 cm.$^{-1}$ represents the upper limit of the spectrum. This line is the octave of the fundamental mode of oscillation of the diamond lattice having the highest frequency shift, namely 1332 cm.$^{-1}$ As is to be expected, the octave appears as a sharp line and stands out from the rest of the spectrum. The sharp

peak at 2664 cm.$^{-1}$ of the theoretical curve, on the other hand, appears to have been manufactured by giving suitable intensities to the branches (1) and (6).

(5) *Region of low frequency shifts.*—According to the calculations of Smith, the branch (10) (see Fig. 1) has an intensity comparable to that of the high frequency branches and a maximum at 106 cm.$^{-1}$ She says that this low frequency band is not observed experimentally as it may be covered by the incident mercury line. Heavily exposed spectrograms taken with efficient filtering of the exciting radiation do not exhibit any low frequency shift line even faintly, much less a band of the type predicted by the Born theory, other than the Brillouin components. Spectrograms reproduced on page 230 of *Nature* (1947, **160**) and on Plate X of the *Proceedings of the Indian Academy of Sciences* (1947, **26**) will bear testimony to the above statement.

From what has been said above, it is clear that the theoretical intensity curve for the second-order Raman spectrum of diamond is wholly artificial and bears no resemblance whatsoever to the facts. Any theory which wants to hold on its own should be capable of explaining the existence of at least the five sharp intense lines (see Fig. 3), appearing in the second-order spectrum of diamond, not to say anything about the rest. The Born theory as worked out by Smith for the case of diamond, however, is unable to explain them.

In conclusion, the author feels it necessary to refer to some points concerning the theoretical paper by Helen Smith. The experimental results mentioned above were first published in two notes in the correspondence columns of *Nature* in the January 11th and August 16th (1947) issues. In the first note on the " Raman spectrum of diamond under high dispersion ", the spectrograms taken with the large quartz spectrograph and exhibiting the true nature of the Raman spectrum of diamond unambiguously were reproduced. Anyone familiar with the elements of spectroscopy would unhesitatingly admit that the characteristic feature of the spectrum as revealed by the reproduced photographs is the appearance of a whole series of sharply defined Raman lines clearly resolved from one another, a fact which does not find any explanation whatsoever on the Born theory. In the second note on the " Second-order Raman spectra of crystals ", it was clearly pointed out that in spectrograms heavily exposed under the most perfect experimental conditions, there is not a trace of any scattered radiations having frequency shifts (other than the Brillouin doublets) less than 1332 cm.$^{-1}$ The two notes mentioned were published long before Prof. Born

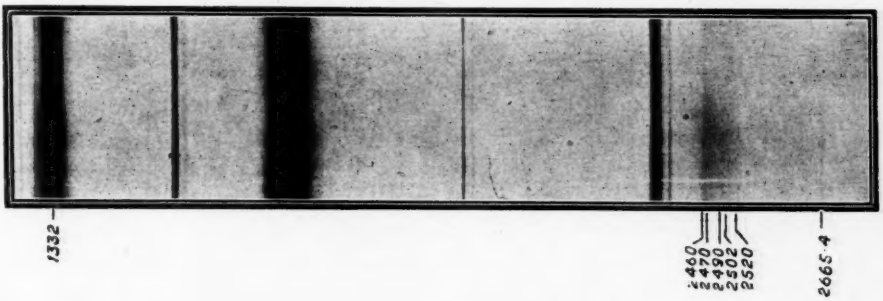

FIG. 3. Lightly exposed photograph of the Raman spectrum of diamond taken with the large quartz spectrograph

communicated the manuscript of Smith's paper to the Royal Society. No reference to them, however, is made in Helen Smith's paper as published.

The detailed paper giving the latest results and a full theoretical discussion appeared in the December (1947) issue of the *Proceedings of the Indian Academy of Sciences*, which would have been received by Prof. Born in the normal course in January or February, 1948. Moreover, the author understands that when Prof. Born presented Smith's theoretical intensity distribution curve during the Bordeaux meeting in April, 1948, he was appraised of the latest experimental results and slides exhibiting them were shown. This took place long before Smith's paper was actually published in the *Transactions of the Royal Society*. It is therefore extremely surprising to find no reference to the author's detailed publication and no attempt to correct the wholly misleading and erroneous statements concerning the experimental facts appearing in Helen Smith's paper.

SUMMARY

The observed features of the Raman spectrum of diamond have briefly been summarised and compared with the theoretical conclusions arrived at by Helen Smith on the basis of Born's postulate of the cyclic lattice. In every respect and especially as regards the form, the extent, the number and sharpness of the lines, the spectrum in the low frequency shift region, etc., the theoretical intensity distribution curve is found to differ widely from what has been observed experimentally. It has been shown that the Born theory as worked out by Smith for the case of diamond is unable to explain the characteristic features of the second-order spectrum of diamond.

REFERENCES

1. Helen M. J. Smith .. *Trans. Roy. Soc.* A, 1948, **241**, 105.
2. Krishnan, R. S. .. *Proc. Ind. Acad. Sci.* A, 1944, **19**, 216.
.. *Nature*, 1945, **155**, 171.
.. *Proc. Ind. Acad. Sci.*, A, 1946, **24**, 25.
.. *Nature*, 1947 *a*, **159**, 60.
.. *Ibid.*, 1947 *b*, **160**, 230.
.. *Proc. Ind. Acad. Sci.* A, 1947 *c*, **26**, 399.
3. Ramanathan, K. G. .. *Ibid.*, 1947, **26**, 469.

SOME NEW TECHNIQUES IN X-RAY DIFFRACTION

By Professor I. Fankuchen

(Polytechnic Institute of Brooklyn, 85, Livingston Street, Brooklyn, N. Y.)

Received December 8, 1948

X-Ray diffraction since the original experiment of von Laue has done much —but it has yet much to do. It is a respected branch of science but it depends for much of its future development on the production of new tools to collect the necessary experimental data, the acquiring of new skills in their use and the development of new arts in the interpretation of the data. We have to-day cameras which permit of the determination of lattice constants to one part in fifty thousand, single crystal cameras which photograph the reciprocal lattice, Geiger counter units which automatically record powder diffraction data and computing machines which take much of the toil from the computation of Fourier series and the determination of crystal structures. What shall we plan now?

A part of the program in our X-ray laboratory is devoted to the development of new instruments. In this brief paper, the program is outlined. Some of the ideas will doubtlessly prove bad—others may prove useful but if they suggest new approaches, then this rather speculative paper will have been justified.

A. Micro Camera Techniques

X-ray scattering gives information concerning the structure of the volume of specimen irradiated by the X-ray beam. The usual techniques employ X-ray beams of the order of a millimetre in cross-section, and so any structural information derived from the study of scattered radiation will be an average of a volume of the order of a cubic millimetre. Many research workers are concerned with structure differentiation on a smaller scale—for this reason the biologist uses the microscope. It has occurred to many workers[1, 2] that the use of finer beams would permit the systematic exploration of specimens by X-ray diffraction on a microscopic scale. The use of fine glass capillaries to define such beams has permitted the construction and use of transmission-cameras using beams as small as 10 microns in cross section. The design[3] of these cameras permits mounting the specimen in the X-ray beam under an optical microscope so that one knows exactly what part of the specimen is in the X-ray beam. The applications of such an instrument are wide.

Thus the biologist can often differentiate structures under the microscope but be unable to identify them. This is particularly true in pathological tissues and yet many biological structures can give distinctive X-ray diagrams. Micro camera techniques seem an answer to this problem.

One need not stop here. A back reflection micro camera has been constructed* and is now being tested. It is hoped to use this instrument in the study of single grains in metals and of intergranular material.

Many biological tissues give significant scattering at very small angles. A small angle micro camera may prove helpful in such studies.

It is usually necessary to have single crystal X-ray data to work out complete structure determination. One can work with very small crystals to-day; crystals as small as 1/20 mm. in the largest direction have been successfully used. This appears to be a lower limit to what can be done with conventional slit systems as the air scattering of the comparatively large X-ray beams approaches the crystal scattering in magnitude. A single crystal micro camera should make possible studies of very much smaller single crystals.

B. Spectrometers

(Automatic Recorders of Powder Diffraction Data)

There are available commercially to-day two somewhat similar (in principle) spectrometers.[5, 4] These use a focussing principle and depend for their resolution on the fine slits (or X-ray focal spots) employed. In theory one can get as high resolution as one wants by narrowing the slits and by obeying very accurately the focussing conditions but in practice it does not work out so easily.

Again many workers have suggested the use of plane crystals[6] and bent crystals[7] for achieving adequate resolving power. The writer suggests that a spectrometer of high resolving power could be constructed using essentially a double plane crystal spectrometer with a scatterer between the crystals. The first crystal could have incident on it at the Bragg angle for the characteristic K radiation a very broad beam of X-rays from a large area focal spot. This incident beam could be slightly collimated by a gross Soller slit arrangement so that the Kβ is not reflected. The broad reflected monochromatic beam would then be incident on a plane surface of a powder

---

* The back reflection microcamera was constructed by J. Singer,
(*a*) of the M. W. Kellogg Co., Jersey City, N. J.
(*a*) Present address: The Franklin Institute of the State of Philadelphia, Phila., 3 Pa.

specimen set up on an axis of rotation (as in the present spectrometers). Rotating on an arm about the same axis but at twice the angular velocity would be the second plane crystal set to make the Bragg angle for the radiation used with scatttered beams travelling in the direction of the arm. A *wide* window Geiger counter tube mounted on the same arm would be set to receive the radiation reflected by this second crystal. This instrument would have no limiting slits, the angles over which the single crystals used reflect X-rays would in effect be the factors deciding its potential resolving power.

One sometimes wishes to detect and study crystalline impurities in a crystalline matrix. Often the faint lines of the impurity are lost in the more intense pattern of the matrix. A similar problem exists in infra-red work where the lines of a solute are swamped in the pattern of a solvent. The balanced split beam infra-red spectrometer has been of great help and its success suggests that a similar instrument could be constructed for X-ray work. We are attempting to construct such an instrument. The X-ray beam emergent from one window of a tube is split by a horizontal diaphragm. The split beams then enter a similarly bifurcated conventional spectrometer[4] and the reflected beams are received by two Geiger tubes in one glass envelope. The outputs are balanced and the difference is fed into a recorder. Acceptable balancing has not as yet been achieved.

C. Low Temperature Cameras

Recently we have had occasion to study the structure of cyclooctatetræne.[8] This substance is liquid at room temperatures and X-ray studies, both powder and single crystal, had to be done at below room temperatures. A literature search revealed a dearth of work in this field. Apparently, a few workers had, at one time or another, wanted to study with X-rays, materials not solid at room temperatures and had devised comparatively primitive techniques for doing the job in question. We did the same sort of thing for cyclooctatetræne but because of our experiences realized that a systematic development of low temperature cameras is necessary. Only then can the vast number of simple but important compounds which are crystalline only at low temperatures be properly investigated. We are therefore experimenting with three types of low temperature cameras, namely, single crystal, powder and spectrometer type cameras.

Many rather involved types of cameras have been tried but interestingly enough, for each type, the latest model has been the simplest to construct, the easiest to use and has given the best results. It is already evident that here there is a vast important field waiting to be explored.

These few examples of proposed new X-ray techniques are of course only illustrative of what is needed. X-ray scattering gives evidence of structure and structure is fundamental to so many fields of inquiry which X-rays have not as yet touched. An extensive instrumental development is clearly called for.

Sir C. V. Raman himself in much of his work has given us beautiful new tools to work with, tools which have extended the horizons in many diverse fields of science. This paper is contributed as a tribute to a true prophet of science.

References

1. O. Kratky and H. Mark .. *Fortshritte auf dem Gebiete der Hochpolymeren* (J. Springer, Berlin, 1938).
2. I. Fankuchen and H. Mark .. *Journal of Applied Physics*, 1944, **15**, 364.
3. F. G. Chesley .. *Rev. Scientific Instruments*, 1947, **18**, 422.
4. North American Philips Company, New York, City.
5. General Electric X-Ray Corporation, Milwaukee, Wis.
6. Fankuchen, I. and M. Jellinek — *Phys. Rev.*, 1945, 67, 201.
7. A. Guinier (Unpublished work).
8. H. Kaufman, I. Fankuchen and H. Mark — *Nature*, Jan. 1948, **161**, 165.

THE DYNAMIC X-RAY REFLECTIONS IN CARBON SILICIDE

By Dr. C. S. Venkateswaran

(From the Department of Physics, Indian Institute of Science, Bangalore, and the University College, Trivandrum)

Received November 1, 1948

1. Introduction

Though it has been known for a long time that well-exposed Laue photographs show additional streaks or spots which are not explicable as regular reflections from the crystal planes, the theoretical significance of the phenomenon was first clearly elucidated in the publications of Sir C. V. Raman on the subject in *Current Science* (1940), and *Proceedings of the Indian Academy of Sciences* (1940, 1941). The analysis of the experimental facts observed with diamond (Raman and Nilakantan, 1940–41) revealed three important features of the phenomenon, namely, (1) that it is intimately connected with the dynamics of the crystal, (2) that it is accompanied by a change of frequency, and (3) that it is essentially in the nature of reflections of X-rays by dynamic stratifications in the medium. Further studies of the subject showed that the frequencies of vibration operative in the production of the additional reflections are those of the monochromatic eigenvibrations of the crystal structure excited by the incident X-rays. Besides such reflections, the theoretical treatment also predicts diffuse maxima due to the scattering by the elastic vibrations of the crystal having the largest amplitude. An intensive study of the problem which was stimulated by these publications has led to a clarification of the fundamental ideas regarding the physical nature of these reflections and the vibration spectrum of the crystal lattice.

While it has been conceded by all theorists and experimenters working in the field that the three basic ideas outlined by Raman are essentially valid, there exists some difference of opinion regarding the frequency (or wavelength) region, which is responsible for the observed X-ray effects. According to Born (1941) and his school, the effective wavelengths giving rise to the spot are only the longest in the elastic vibrational spectrum of the crystal. This conclusion is a direct consequence of the hypothesis of Debye, and Born and Karman that the vibrations of a crystal lattice are *non-degenerate* (or single) and distributed over a wide range of frequency. Following Ott

(1935), Born (1942) has also shown that the effect of the type visualised by Raman's theory is theoretically possible, but he *believes* that the intensity of such modified Raman reflections will be extremely small, as the probability of such transitions taking place is not great.

The defect in the argument of Born consists in his assumption that the vibrations in the higher part of the frequency range—the so-called optical series—are non-degenerate in the same manner as the elastic vibrations. By his analysis of the problem which is supported by the experimental spectroscopic facts, Sir C. V. Raman (1943, 1947) has shown that the units of the vibration pattern in crystals are supercells having twice the linear dimensions and therefore eight times the volume of the static units of the crystal structure. The vibrations of the supercell are closely analogous to those of a poly-atomic molecule with the appropriate symmetries, but with this important difference that the atoms in the unit cell are not isolated from the rest of the crystal. There are $(24p-3)$ eigen-vibrations for such a super-cell, where p is the number of atoms in the unit cell. Each of the eigen-vibrations of the super-cell is truly monochromatic and N-fold degenerate, if N is the number of the supercells contained in the crystal. This degeneracy is further increased by virtue of the symmetry of the crystal and is a maximum for cubic crystals. Born's assumption that the lattice vibrations of high frequency are non-degenerate is thus physically untenable, and his objection against the modified X-ray reflections caused by them being sufficiently intense for observation has therefore no theoretical justification. On the other hand, on account of the very high degeneracy of these vibrations one should expect the Raman X-ray reflections caused by them to appear with appreciable intensity. In the above description, a small residue of three degrees of freedom of translation for every supercell appears on ultimate analysis as elastic vibrations having a frequency distribution of the type envisaged by Debye. These elastic waves could be treated as thermal waves which come under the treatment of Faxen (1923) and Waller (1923). The refinement of the latter's theory by Born and Sarginson (1941) leads to a modified expression for the intensity of thermal scattering, and its distribution in terms of the elastic constants of the crystal.

The Raman X-ray reflections are characterised principally by their sharpness and a temperature effect on intensity depending on the eigen-frequency of the lattice vibration but not on the angle of mis-setting of the crystal. The thermal scattering, on the other hand, is characterised by a weak diffuse maximum and a temperature effect whose magnitude depends on the characteristic temperature and on the difference between the glancing angle and the correct Bragg angle of the crystal. In the vast majority of

crystals studied, *e.g.*, rock-salt, sylvine, metals, organic crystals, etc., the modified X-ray reflections due to eigen-vibrations and elastic vibrations are superposed, and it is not easy to differentiate them by their experimentally observed features. In the case of diamond, however, the thermal scattering is so weak and the Raman reflections are so pronounced that a study of this crystal has enabled Raman and Nilakantan (1940) to prove all the characteristics of the phenomenon uniquely. Born (1942) and Lonsdale (1942), however, have attempted to explain the specific results of diamond on the plea that "it is not a normal crystal" or "that a strain which is cubic in symmetry is inherent in the majority of diamonds". In an article in *Nature*, Sir C. V. Raman (1942) has shown that such hypotheses are devoid of justification.

In the present investigation the author has studied the dynamic X-ray reflections by carbon silicide (carborundum) which has a structure similar to that of diamond and the results are discussed in relation to the current theories of the phenomenon.

2. Crystal Structure and Lattice Spectrum of Carborundum

The crystal structure of carborundum has been extensively studied by Ott (1925, 1926). He has discovered four different types, three of which are hexagonal and one is cubic. Sommerfeld (1928) has given a fifth one which is also hexagonal. In the present investigation the author has made use of a thin plate of a natural crystal which is bluish-green in transmitted light. The Laue pattern taken with X-rays normal to the plate shows that it belongs to type II, hexagonal (Fig. 1 *a*). The Bravais elementary cell of this type contains six molecules of SiC. Atoms of one kind are bound to those of the other tetrahedrally. The smallest Si–C distance is 1·9 A.U. and those of the other tetrahedrally. The smallest Si-C distance is 1·9 A.U. and the binding between the atoms is non-polar. The axial lengths of the unit cell are $a = 3{\cdot}095$, $b = 5{\cdot}38$ and $c = 15{\cdot}17$ A.U., where c-axis is perpendicular to the cleavage plane. The structure thus bears a close resemblance to the diamond lattice. According to Schaefer and Thomas (1923) this type of carborundum shows only one strong sharp infra-red reflection at 12 μ (830 cm.$^{-1}$). This obviously corresponds to an oscillation of silicon against carbon atoms.

3. Specular Character of the Dynamic Reflections

The X-ray generator used in the present investigation was a demountable Coolidge tube with a Mo-anticathode and operated at 45 kilo-volts and a fairly steady milliampereage of 20 m.A. The crystal was mounted with its

(0001) plane vertical. A narrow beam of X-rays limited by a system of lead slits is let fall on the crystal normally to this plane. The film was placed at a distance of 43·5 mm. from the crystal. Figs. 1 *a* and *b* in the accompanying plate illustrate the Laue pattern obtained after an exposure of one hour; Fig. 1 *a* was taken with a wide circular beam and Fig. 1 *b* with a fine slit. It will be seen that all the six spots arising by reflection from $(\bar{2}021)$ planes are accompanied by sharp circular modified spots. The extreme sharpness of the latter may be seen from Fig. 1 *b*. As the white radiation in the source was pronounced, the radial streaks are fairly prominent. Much more satisfactory photographs are obtained using a narrow linear slit. Figs. 2 *a–g* are taken with a linear slit for various settings of the crystal.

The outstanding feature in all these photographs is that the dynamic reflection is as sharp as the Laue reflection itself for a range of 4° on either side of the Bragg setting. The intensity of the spot falls off rapidly as the crystal is turned away and almost completely disappears for an angle of $2\frac{1}{2}°$ from the latter position. Unlike diamond, however, the modified spot remains more or less in a stationary position for the whole range. Table I gives the measurements of the angular distances of the Laue (θ_i) and the Raman reflections (θ_m) and the lattice spacing d of $(20\bar{2}\bar{1})$ planes calculated according to Raman-Nath (1940) formula both for k_α and k_β radiations of the source. It will be seen that the spacing has nearly a constant value for both the rays and agrees well with the theoretical data.

TABLE I

Carborundum

$20\bar{2}\bar{1}$ reflections $d = 2{\cdot}68$ Å

$M_o k_\alpha = 0{\cdot}708$ Å; $k_\beta = 0{\cdot}620$ Å

$2\theta_i$	$2\theta_m$		d in Å	
	k_α	k_β	k_α	k_β
19° 33′	15° 10′	13° 7′	2·68	2·72
17° 38′	15° 25′	13° 24′	2·64	2·66
16° 24′	15° 10′	13° 7′	2·68	2·72
15° 10′	15° 10′	13° 7′	2·68	2·72
11° 36′	15° 25′	13° 24′	2·64	2·66
8° 30′	15° 10′	13° 7′	2·68	2·72
7°	15° 10′	13° 7′	2·68	2·72
			Mean d = 2·69Å	

Another interesting feature of the circular spots (Fig. 1 *a*) which is worth mentioning is the fact that the intensity distribution is *annular with a minimum at its centre*. In order to see whether this is the result of each of the spots being a composite of six others situated hexagonally, the experiment was repeated with a fine aperture lead slit (Fig. 1 *b*); but it was not possible to resolve them any further. In the case of linear slits, however, it was observed that each modified line is accompanied on either side by faint close companions (see Fig. 2). It is possible that each of the spots has a fine structure due to the co-existence of six ' phase waves ' similar to three waves in diamond (Pisharoti, 1941).

4. Influence of High and Low Temperatures

While the geometric character of the modified spot and the rapid fall of intensity with the rotation of the crystal indicate that we are dealing with a modified reflection, investigations of the relative intensities of these reflections at temperatures varying from $-180°$ C. to 600° C. have yielded decisive results in favour of the Raman's theory. For low temperature work, the technique of high vacuum low-temperature X-ray spectroscopy described in a previous paper (Venkateswaran, 1941) was employed. A linear slit was made use of, instead of a circular one and the relative intensities were determined by varying the time of exposure at the room temperature till its intensity is equal to that at the low or high temperature as judged visually. For high temperatures, the crystal was mounted in a copper block which is heated by a heating coil. The temperature of the crystal was determined by means of a calibrated thermocouple. The crystal was set at different angles and the intensities at various temperatures compared for each setting with that at the room temperature. The results of measurements are given in Tables II and III. Typical photographs taken at 600° C., 300° C., room temperature 30° C. and the liquid-air temperature $-180°$ C. for the same time of exposure are given in Figs. 3 and 4 (Plate).

Table II

Low Temperatures

$2\theta_i$	$2\theta_m$	2ϵ	λ in A.U.	$I_{30°}/I_{-180°}$
11° 15′	15° 10′	3° 55′	89	1
11° 54′	,,	3° 16′	94	1
15° 48′	,,	0° 38′	512	1·1
16° 29′	,,	1° 19′	307	1·05
16° 48′	,,	1° 38′	192	1·05
17° 48′	,,	2° 38′	118	1
19° 5′	,,	3° 55′	89	1

TABLE III

High Temperatures

$2\theta_i$	$2\theta_m$	2ϵ	λ in A.U.	$\frac{I_{30}}{I_{300}}$	$\frac{I_{80}}{I_{600}}$
17° 18′	15° 20′	1° 58′	154	1	1·1
17° 46′	15° 10′	2° 36′	118	1·2	1·2
20° 19′	15° 25′	4° 54′	63	1·2	1·4

According to Raman's formula, the intensity of dynamic reflection is proportional to $\frac{e^{h\nu^*/k\nu T}+1}{e^{h\nu^*/kT}-1}$, where ν^* is the frequency of the lattice vibration and T is the absolute temperature. If we assume that $\nu^* = 830\,\text{cm.}^{-1}$ given by the infra-red absorption for carborundum (*loc. cit.*), there should not be any pronounced variation of the intensity of the spot for the range of temperature used. The relative intensity between the different temperatures should also be independent of the angular distance ϵ between the Laue spot and the appropriate Bragg position θ_m. These predictions of the theory are fully supported by the experimental facts. It should, however, be mentioned that due to the diminution of the lattice spacing at low temperatures there is a slight increase in the intensity of the spot compared with that at the room temperature. A similar error prevents an accurate estimate of the intensities at the higher temperatures as well.

If on the other hand, we treat the spot as a diffuse scattering of X-rays by the solid elastic waves, according to Born (1942) the maximum intensity at the Bragg position is proportional to $Te^{-T/T0}$, where

$$T_0 = \frac{mk\theta^2}{3h^2} \cdot \frac{a^2}{h_1^2 + h_2^2 + h_3^2}.$$

(T, absolute temperature, m, atomic mass in grams, a, lattice constant in cm., θ, Debye temperature, k, and h, Boltzman and Planck constants, h_1, h_2 and h_3 are the Miller indices of the nearest Bragg reflection.) The characteristic temperature θ for SiC is estimated roughly from the specific heat data and is about 1750. This gives for the $(20\bar{2}1)$ plane a value for $T_0 \simeq 10^5$. Hence for the temperatures used, the intensity of the diffuse scattering at the Bragg position is nearly proportional to the absolute temperature T. The wavelength λ of the elastic wave effective at each setting of the crystal is calculated according to the approximate relation $\lambda = \frac{d}{\sin \epsilon}$ and given in column 4 of Tables II and III. The thermal theory of diffuse

scattering thus leads us to expect that the intensity at the liquid-air temperature should be one-third and those at 300° C. and 600° C. to be respectively twice and thrice at the room temperature. These relative intensities should also show a dependence on the wavelength of the wave corresponding to the angle of setting of the crystal. Both these conclusions drawn from Born's theory are not supported by the results of the present investigation.

5. Conclusion

The main results of the present investigation of the non-Laue spots in the diffraction of X-rays by carborundum may be stated as follows:

1. The modified spots show a hexagonal pattern similar to the Laue spots and are closely related to the internal structure of the crystal.

2. They are sharp for an angular range of nearly 4° on either side of the correct Bragg setting.

3. They are fairly intense near the Bragg position; but the intensity falls off rapidly as the crystal is rotated away from this position.

4. The spots obtained with a circular beam of X-rays have an annular distribution of intensity.

5. The intensity of the modified spot is nearly independent of temperature for all orientations of the crystal.

These results for carborundum are exact parallels to those for diamond. As has been remarked by Sir C. V. Raman (1948) in a recent note in *Nature*, the very fact that the modified spots have a regular geometric pattern bearing an observable relationship to the structure of the crystal is itself a sufficient indication of the connection between them and the eigen-vibrations of the super-cell. The characteristics of the spots enumerated above follow as a necessary consequence of such an origin for these spots.

The above experimental work was carried out in the Physics Laboratory of the Indian Institute of Science, Bangalore, and I desire to place on record my heartfelt gratitude to Sir C. V. Raman for his kind suggestions and inspiring interest in the work.

Summary

Raman's theory of dynamical X-ray reflections and the thermal theory of diffuse X-ray scattering are critically reviewed. An investigation of the extra-spots in X-ray diffraction by the {2021} planes of a hexagonal type of carborundum crystal shows that the spots are sharp and their intensity is nearly independent of temperature for a wide range from — 180° C. to 600° C. and for different orientations of the crystal. It has been shown that they

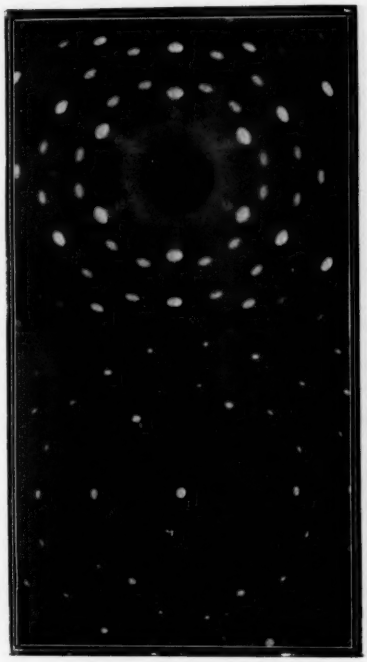

FIG. 1. Carborundum—Laue Photographs
(*a*) Broad Slit. (*b*) Fine Slit

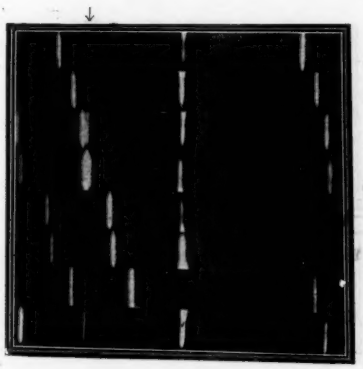

FIG. 2. Carborundum—Orientation Studies

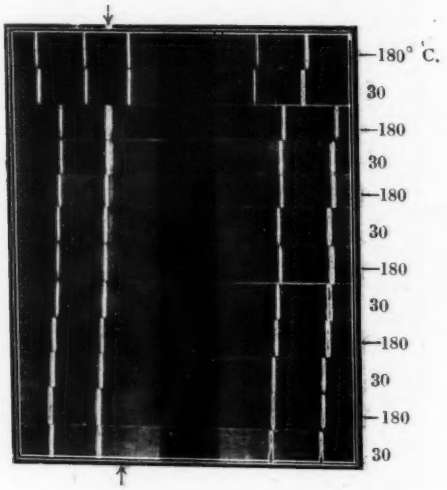

FIG. 3. Carborundum. Low Temperature Studies

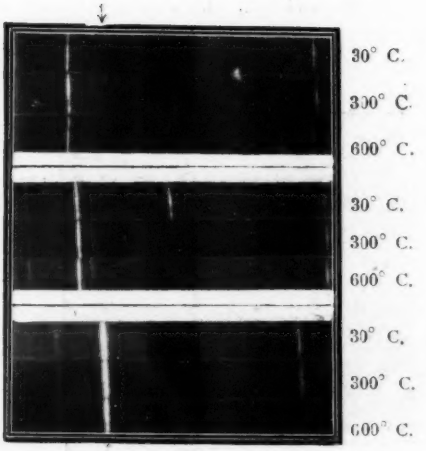

FIG. 4. Carborundum. High Temperature Studies

can be explained as due to the coherent modified reflections of X-rays by the eigen-vibrations of the crystal lattice having a frequency of 830 cm.$^{-1}$ which is observed in the infra-red absorption as well and that the diffuse thermal scattering due to the long elastic waves is not responsible for their appearance.

References

Born	..	*Proc. Phys. Soc.*, 1942, **54**, 362.
—— and Lonsdale	..	*Nature*, 1942, **150**, 490.
—— and Sarginson	..	*Proc. Roy. Soc.*, A, 1941, **179**, 69.
Faxen	..	*Zeits. f. Physik*, 1923, **17**, 266.
Lonsdale	..	*Proc. Roy. Soc.*, A, 1942, **179**, 315.
——	..	*Proc. Phys. Soc.*, 1942, **54**, 314.
Ott, H.	..	*Ann. Phys. Lpz.*, 1935, **23**, 169.
——	..	*Zeit. f. Krist.*, 1925, **61**, 515 ; 62, 201 ; 1926, **63**, 1.
Pisharoti	..	*Proc. Ind. Acad. Sci.*, A, 1941, **14**, 439.
Raman, C. V.	..	*Nature*, 1942, **150**, 366.
——	..	*Ibid.*, 1948, **162**, 23.
——	..	*Proc. Ind. Acad. Sci.*, A, 1943, Sept. Number ; 1947, **26**, 339.
—— and Nilakantan, P.	..	*Current Science*, 1940, **9**, 165.
——	..	*Proc. Ind. Acad. Sci.*, A, 1940, **11**, 379; **12**, 83; 1941, **14**, 356.
—— and Nagendra Nath	..	*Ibid.*, 1940, **12**, 427.
Schaefer and Thomas	..	*Zeit. f. Phys.*, 1923, **12**, 330.
Sommerfeld, A.	..	*Zeit. f. Krist.*, 1928, 208.
Venkateswaran	..	*Proc. Ind. Acad. Sci.* A, 1941, **14**, 387.
Waller	..	*Zeit. f. Physik*, 1923, **17**, 398.

FOURIER ASPECTS OF IMPLICATION THEORY

By M. J. Buerger

(Massachusetts Institute of Technology, Cambridge, Massachusetts, U.S.A.)

Received November 28, 1948

Introduction

It is well known that the electron density of the structure of a crystal at a selection of points with co-ordinates xyz can be determined from the collection of diffraction spectra produced by a crystal, with the aid of the relation

$$\rho(xyz) = \frac{1}{V} \sum_h \sum_k \sum_l F_{hkl}\, e^{2\pi i (hx+ky+lz)} \tag{1}$$

The difficulty with the practical application of this relation is that the diffraction coefficients F_{hkl} are not simple magnitudes, but rather are complex quantities involving both magnitude and phase components. Although the magnitudes of the F's can be determined by experiment, to date there has been no experimental method developed for the determination of their phases. One vehicle for supplying some of these phases or their equivalents is *implication theory*. This has been discussed previously[1] from a group theoretical approach, an approach which has not met with favour in some quarters. In the present communication, a Fourier approach to implication theory is given.

Fourier Development of the Implication Function

In implication theory, use is made of the Patterson function[2]

$$P(uvw) = \frac{1}{V^2} \sum_h \sum_k \sum_l F^2_{hkl}\, e^{2\pi i (hu+kv+lw)} \tag{2}$$

This function has peaks at positions uvw corresponding to locations of all pairs of atoms in (1), such that

$$\begin{aligned} u &= x_2 - x_1 \\ v &= y_2 - y_1 \\ w &= z_2 - z_1, \end{aligned} \tag{3}$$

where the 2's and 1's refer to the two atoms of the pair.

Now, if the crystal has symmetry, there are symmetry relations among the co-ordinates of equivalent atoms, that is, among some of the x's, y's, and

z's of (3). These relations for the operation of a symmetry element parallel to Z are listed in Table I. For these axes, w assumes the limited and characteristic values of 0, $\frac{1}{2}$, $\frac{1}{3}$, $\frac{1}{4}$, or $\frac{1}{6}$ only, corresponding with screw operations with translation components 0, $\frac{1}{2}c$, $\frac{1}{3}c$, $\frac{1}{4}c$, or $\frac{1}{6}c$, respectively. For such values of w, characteristic of an operation allowed by the symmetry of the crystal, the designation w_c will be adopted.

If these characteristic values of w_c are substituted into (2), it takes the following, simpler two-dimensional form:

$$P(uvw_c) = \frac{1}{V^2} \sum_h \sum_k C_{hk} e^{2\pi i (hu+kv)}, \tag{4}$$

where values of the Fourier coefficients, fixed for each value of hk, are of the form

$$C_{hk} = \sum_l F^2_{hkl} e^{2\pi i l w}. \tag{5}$$

This can be compared with the two-dimensional projection of (1) on the plane (001):

$$\rho(xy) = \frac{1}{A} \sum_h \sum_k F_{hk0} e^{2\pi i (hx+ky)} \tag{6}$$

$$P(uvw_c) = \frac{1}{V^2} \sum_h \sum_k C_{hk} e^{2\pi i (hu+kv)} \tag{4}$$

These two functions have very similar form. Furthermore, for every peak on (6) there is a corresponding peak on (4), only these peaks are differently placed. In the first case, the peak is at xy, while in the second it is at uv. The question arises, is it possible to refer (4) to different axes such that for each peak on (6), the corresponding peak on (4) has the same co-ordinates, xy? If this can be done, then (4) will perform the same function for the crystal structure analyst as (6).

Now, this transformation can indeed be effected, and in the following way: New axes, $\vec{a}'$ and $\vec{b}'$, are required to replace the old axes, $\vec{a}$ and $\vec{b}$. Furthermore, the fractional co-ordinates, x' and y', along these axes must be equal to u and v. In short, the requirements of the transformation are

$$x'\vec{a}' + y'\vec{b}' = u\vec{a} + v\vec{b}. \tag{7}$$

Table I, column 3, provides the specific values of u and v for the various symmetries. To make clear the use of (7) in finding the required transformation, consider the following specific examples:

For $n = 2$, Table I, column 3, shows that (7) must have the following specific form:

$$x'\vec{a'} + y'\vec{b'} = 2x\vec{a} + 2y\vec{b}. \tag{8}$$

Now, to solve for $\vec{a'}$, let $x' = 1$ and $y' = 0$. Since the purpose of this transformation is that $x' = x\,(=1)$ and that $y' = y\,(=0)$, (8) takes the particular form

$$\vec{a'} = 2\vec{a}. \tag{9}$$

To solve for b', let $x' = x = 0$, and $y' = y = 1$. Then the particular form of (8) is

$$\vec{b'} = 2\vec{b} \tag{10}$$

Assembling the information from (9) and (10), the required transformation for $n = 2$ is evidently

$$\begin{aligned} \vec{a'} &= 2\vec{a} \\ \vec{b'} &= 2\vec{b}. \end{aligned} \tag{11}$$

For $n = 3$ (to take another example), Table I, column 3, shows that (7) assumes the specific form

$$x'\vec{a'} = y'\vec{b'} = (x + y)\,\vec{a} + (-x + 2y)\,\vec{b}. \tag{12}$$

To solve for $\vec{a'}$, assume, as before, that $x' = x = 1$, $y' = y = 0$. The particular form of (11) then is

$$\vec{a'} = \vec{a} - \vec{b}. \tag{13}$$

To solve for $\vec{b'}$, next consider $x' = x = 0$, $y' = y = 1$. Then (12) becomes

$$\vec{b'} = \vec{a} + 2\vec{b}, \tag{14}$$

and the entire transformation for $n = 3$ is

$$\begin{aligned} \vec{a'} &= \vec{a} - \vec{b} \\ \vec{b'} &= \vec{a} + 2\vec{b}. \end{aligned} \tag{15}$$

The transformations for these and other symmetries are listed in column 4 of Table I. Now, if an axial transformation is performed on (8), a transformation of indices, $hk \rightarrow h'k'$ also occurs simultaneously. The index transformations are listed in column 5 of Table I.

TABLE I

Symmetry operation. $(n)^p$ indicates the p^{th} power of the operation	Point produced by operation from point at xyz	Patterson uvw for operation	Axial transformation a' b'	Index transformation h' k'
2	$\bar{x}$ $\bar{y}$ z	$2x$ $2y$ 0	$2a$ $2b$	$2h$ $2k$
2_1	$\bar{x}$ $\bar{y}$ $z+\frac{1}{2}$	$2x$ $2y$ $\frac{1}{2}$		
3	$\bar{y}$ $x-y$ z	$x+y$ $-x+2y$ 0	$a-b$ $a+2b$	$h-k$ $h+2k$
3_1	$\bar{y}$ $x-y$ $z+\frac{1}{3}$	$x+y$ $-x+2y$ $\frac{1}{3}$		
3_2	$\bar{y}$ $x-y$ $z-\frac{1}{3}$	$x+y$ $-x+2y$ $-\frac{1}{3}$		
$(\bar{3})^4 = 3$	$\bar{y}$ $x-y$ z	$x+y$ $-x+2y$ 0		
4	$\bar{y}$ x z	$x+y$ $-x+y$ 0	$a-b$ $a+b$	$h-k$ $h+k$
4_1	$\bar{y}$ x $z+\frac{1}{4}$	$x+y$ $-x+y$ $\frac{1}{4}$		
4_2	$\bar{y}$ x $z+\frac{1}{2}$	$x+y$ $-x+y$ $\frac{1}{2}$		
4_3	$\bar{y}$ x $z-\frac{1}{4}$	$x+y$ $-x+y$ $-\frac{1}{4}$		
$(\bar{4})^2 = 2$	$\bar{x}$ $\bar{y}$ z	$2x$ $2y$ 0	$2a$ $2b$	$2h$ $2k$
6	$x-y$ x z	y $-x+y$ 0	$-b$ $a+b$ (equivalent to: a b)	$-k$ $h+k$ (equivalent to h k)
6_1	$x-y$ x $z+\frac{1}{6}$	y $-x+y$ $\frac{1}{6}$		
6_2	$x-y$ x $z+\frac{1}{3}$	y $-x+y$ $\frac{1}{3}$		
6_3	$x-y$ x $z+\frac{1}{2}$	y $-x+y$ $\frac{1}{2}$		
6_4	$x-y$ x $z-\frac{1}{3}$	y $-x+y$ $-\frac{1}{3}$		
6_5	$x-y$ x $z-\frac{1}{6}$	y $-x+y$ $-\frac{1}{6}$		
$(\bar{6})^2 = 3$	$\bar{y}$ $x-y$ z	$x+y$ $-x+2y$ 0	$a-b$ $a+2b$	$h-k$ $h+2k$

Since the transformed series (8) has a peak at co-ordinates xy for every peak on (6) at xy, one can infer atom locations from the transformed series. It is therefore called the *implication function.* Let n be the order of the symmetry axis ($n = 2$, 3, 4, or 6), then the symbol $I_n(xyw_c)$ is used to indicate the transformed series $P(uvw_c)$. Thus, if the operation of transformation is represented by ϕ,

$$I_n(xyw_c) = \phi P(uvw_c) \tag{16}$$

Applying this transformation to (4), it compares with (6) as follows:

(6)
$$\rho(xy) = \frac{1}{A} \sum_h \sum_k F_{hk0}\, e^{2\pi i(hx+ky)} \tag{17}$$

$$I_n(xyw_c) = \frac{1}{V^2} \sum_{h'} \sum_{k'} C_{k'k'}\, e^{2\pi i(h'x+k'y)} \tag{18}$$

The practical value of (18) can be briefly summarized as follows: It is impossible to make use of (17) directly because the phases of the F's are not

known. However, (8) has peaks at the same places, yet does not require a knowledge of the phases of the F's, since the Fourier coefficients, namely, the C's in this case, depend only on F^2's, according to (5). Thus, function (18) may be used as a practical substitute for (17).

Implication Ambiguities

Unfortunately (18) not only provides peaks at the same locations as (17) but it also contains certain additional peaks as well. These unwanted peaks fall into two classes:

Additional peaks of one variety are known as *satellites*. These arise as a consequence of higher powers of symmetry operations than the first having w_c the same as the first power. Since satellites are dependent on the characteristic symmetry operations, their co-ordinates bear simple geometrical relations to the desired peaks. They can therefore be identified as satellites on this basis.

The other variety of additional peaks are called ambiguities. These arise as a consequence of the transformation of axes which converted (4) into (18). An important feature of this transformation is that h is transformed into h' and k into k'. The transformations occur modulo M, where M has the value of 4, 3, 2, or 1. It follows that all possible values of h' and k' do not occur. Indeed only a fraction, $f = \frac{1}{M}$, of all possible combinations of h' and k' arise. This fraction varies with the order of the symmetry operation of the implication. Let n be the order of axial symmetry. Then the symmetry operation has an angular component $\alpha = \frac{2\pi}{n}$. The fraction of the possible $h'k'$ combinations which are made available through the transformation are then as follows:

n	M	f
2	4	$\frac{1}{4}$
3	3	$\frac{1}{3}$
4	2	$\frac{1}{2}$
6	1	1

The significance of this is that each $h'k'$ combination corresponds to a Fourier coefficient. If only a fraction, f, of the $h'k'$'s are available, only that fraction of the Fourier coefficients are available for forming the implication function (8).

Now, a Fourier series with only a fraction of the coefficients available produces a picture composed of M overlapping images of the crystal structure.

The images are displaced from one another by a translation interval related to the true translations of the crystal by the same transformation which transformed the *hk*'s into *h'k'* 's. In other words, this implies that the implication cell is a submultiple of the true crystal cell. The submultiple aspect is responsible for the overlapping images.

This feature can also be appreciated by reference to reciprocal space as follows: Each available Fourier coefficient corresponds with a point on the reciprocal lattice. A missing coefficient corresponds with a reciprocal lattice point of weight zero, namely a missing point. Thus the reciprocal lattice of the implication has a larger cell than the crystal, and so the direct lattice of the implication must have a smaller cell than the crystal.

Thus, the implication contains a map of the crystal structure plus M–1 ghosts of the structure. To wipe out the ghosts, M times as many Fourier coefficients would have to be available.

Resolution of the Ambiguities

It is possible to choose between the M possible locations of atoms by the following considerations: In the first place, the ambiguity factor for one symmetrical set of atoms alone has no meaning because it presents no problem. For, any one of the M locations could be chosen arbitrarily as the location of the one atom, and the remaining ones would be known to be ghosts.

The ambiguity factor is only important when there are two or more atoms. The location of the first atom, say A, can then be arbitrarily chosen at one of its M locations on the implication. However, the location of the second atom, B, cannot be determined from the implication without ambiguity. Fortunately, both the three-dimensional Patterson function $P(uvw)$ and its two-dimensional projection, $P(uv)$ contain criteria for distinguishing between the several allowed locations of B, for they both contain peaks for interatomic vectors from A to B, at the co-ordinates

$$uv = (x_B - x_A)(y_B - y_A) \tag{19}$$

The implication function contains M peaks for B, namely $x_{B1}\, y_{B1}$, $x_{B2}\, y_{B2}, \cdots$, $x_{BM}\, y_{BM}$. But only one of these values appear in (19) for the Patterson function, and, therefore, with its aid all but one can be eliminated from the implication as ghosts. This elimination method has been successfully used in the writer's laboratory.

To make this elimination, either a three-dimensional Patterson function, or a two-dimensional Patterson function must be computed. The use of the three-dimensional function for this purpose is not only elegant, but

it eliminates many possibilities of overlap of peaks, which might otherwise occur in the two-dimensional function, but the labour of computation is great. For many crystal structure purposes, the two-dimensional Patterson function supplies sufficient information for elimination of ghosts, and its computation is much less tedious.

Note that an ambiguity exists for every kind of atom in the crystal except the first atom, designated A above. Therefore, if the crystal is composed of R symmetrically different kinds of atoms, the implication contains $(M-1)(R-1)$ incorrect atom locations. To remove these requires the finding of $R-1$ peaks due to unsymmetrical interactions in the Patterson function.

Ambiguities in Phase Determination

Since (18) has all the peaks contained in (17), plus some additional satellitic peaks, plus some peaks representing ambiguities, it should be possible to find relations between the Fourier coefficients $C_{h'k'}$ and F_{hk0} of these two distributions. The method of finding these relations has been discussed in another place.[3,4] In effect, these relations provide the means of determining the unknown phases of the Fourier coefficients F_{hk0}, provided that the crystal has some kind of axial symmetry.

One of the remarkable features brought out by such relations is that the imaginary component of the phase can be found in the one crystallographic case where it occurs, namely where $n = 3$ (the method fails if $w_c = 0$). To appreciate this, recast (17) and (18) into forms which decompose them into real and imaginary components, *i.e.*, $F = A + iB$, and $e^{i\phi} = \cos\phi + i \sin\phi$. They then become

$$(17): \quad \rho(xy) = \frac{1}{A} \sum_h \sum_k A_{hk0} \cos 2\pi (hx + ky) + B_{hk0} \sin 2\pi (hx + ky) \tag{20}$$

$$(18): \quad \mathrm{I}_n(xyw_c) = \frac{1}{V^2} \sum_{h'} \sum_{k'} C_{\mathrm{A}.h'k'} \cos 2\pi (h'x + k'y) + C_{\mathrm{B},h'k'} \sin 2\pi (h'x + k'y). \tag{21}$$

The value of $C_{\mathrm{B},h'k'}$, and its reduction for the case of $n = 3$, is as follows:

$$C_{\mathrm{B},h'k'} = \sum_l F^2_{h'k'l} \sin 2\pi \frac{l}{w_c} = \frac{\sqrt{3}}{2} \left(\sum_{l=3n+1} F^2_{h'k'l} - \sum_{l=3n-1} F^2_{h'k'l} \right). \tag{22}$$

Unfortunately, (21) becomes zero either for $w_c = 0$ (which occurs for axes of pure three-fold rotation) or when the space group contains symmetry operations of both the first and second sorts, *i.e.*, when it contains both right and left-handed three-fold screws. In other cases, namely, when the space

group contains only three-fold screws of one sense, (21) does not vanish, and then provides the imaginary component of the Fourier coefficients.

Another method of limiting the phases of the F_{hk}'s has been provided by Harker and Casper[5] in the form of inequalities connecting F_{hk}'s with certain $F^2_{h'k'}$'s. These inequalities also involve the same transformed $h'k'$'s as the ones discussed above. Therefore, both the inequalities and the relations discussed above in this section suffer from providing only a fraction of the Fourier coefficients required for the complete electron density summation. They therefore both suffer from the ambiguities discussed above.

Literature

1. M. J. Buerger .. "The interpretation of Harker syntheses," *J. Appl. Phys.*, 1946, **17**, 579–95.
2. A. L. Patterson .. "A direct method for the determination of the components of interatomic distances in crystals," *Zeit. f. Krist.*, 1935, **A 90**, 517–42.
3. M. J. Buerger .. "Phase determination with the aid of implication theory," *Phys. Rev.*, 1948, **73**, 927–28.
4. ———— .. "Some relations between the F's and F^2's of X-ray diffraction theory," *Proc. Nat. Acad. Sci.* (*U.S.A.*), 1948, **34**, 277–85.
5. D. Harker and J. S. Kasper "Phases of Fourier coefficients directly from crystal diffraction data," *J. Chem. Phys.*, 1947, **15**, 882–84.

A SIMPLIFIED TREATMENT OF THE DIFFRACTION OF X-RAYS FROM PERTURBED LATTICES

By Andrew D. Booth

(Electronic Computor Project, Birkbeck College, University of London)

Received November 2, 1948

Introduction

In this paper it is proposed to present an account of the diffraction of X-rays from perturbed lattices. Certain simplifying assumptions will be made which render the mathematics tractable and, at the same time, are not so much at variance with the true physical picture as to cause violent disagreement with observation.

It should be understood that no attempt is made to decide between the various theories of the basic causes of lattice perturbation; the present treatment is sufficiently general to cover all of these, and forms a means of directly linking any conception of the state of a crystal lattice with the X-ray pattern which it would produce.

2. Basic Assumptions

It is proposed to treat two general kinds of lattice perturbation.

(1) Periodic.

(2) Random.

The former case will be simplified by the following assumption. If a certain cell be chosen as origin the perturbation of any other cell is a periodic function of its position and the perturbation displacements of all the atoms in that particular cell are equal. This is equivalent to treating the cell contents as rigid units.

For the case of random displacements it will be assumed that all cells are in their correct positions but that a particular atom in each cell is displaced from its mean position in such a way that no phase relationship obtains between the displacements of the same atom in different cells.

3. The Case of Periodic Disturbance

Classical X-ray crystallography shows that the most general form of the structure factor of an X-ray reflection is given by (1):

$$\left.\begin{aligned} \mathrm{F}^2(h,k,l) &= \mathrm{A}^2 + \mathrm{B}^2 \\ \mathrm{A} &= \Sigma_r f_r \cos\theta_r \\ \mathrm{B} &= \Sigma_r f_r \sin\theta_r \\ \theta_r &= 2\pi\left(h\frac{x_r}{a} + k\frac{y_r}{b} + l\frac{z_r}{c}\right) \end{aligned}\right\} \quad (1)$$

where (h, k, l) are the indices of the plane giving rise to reflection, f_r is the atomic scattering factor of the rth atom in the unit cell (x_r, y_r, z_r) are the co-ordinates of the rth atom and (a, b, c) are the repeat units of the cell.

If now the whole crystal lattice is perturbed in such a manner as to repeat on a superlattice of axes (Ma, Nb, Rc), instead of Bragg reflections occurring only for integral values of (h, k, l) in (1) a new set of reflections will occur in what are effectively fractional values of (h, k, l) as referred to the primitive lattice (a, b, c).

These new reflections can be assigned indices:

$$\left.\begin{aligned} \mathrm{H} &= h + \frac{\mu}{\mathrm{M}} \\ \mathrm{K} &= k + \frac{\nu}{\mathrm{N}} \\ \mathrm{L} &= l + \frac{\rho}{\mathrm{R}} \end{aligned}\right\} \quad (2)$$

where (μ, ν, ρ) are integers which take up all values less than M, N and R respectively.

The perturbation function is defined by:—

$$\left.\begin{aligned} &\Delta_a(\alpha, \beta, \gamma) \\ &\Delta_b(\alpha, \beta, \gamma) \\ &\Delta_c(\alpha, \beta, \gamma) \end{aligned}\right\} \quad (3)$$

such that *all* x co-ordinates in the unit cell located at $(\alpha a, \beta b, \gamma c)$ are displaced by the same amount $\Delta_a(\alpha, \beta, \gamma)$ are similarly for y and z.

Introducing the above notations into equation (1) it is seen that:

$$\mathrm{A}(\mathrm{H}, \mathrm{K}, \mathrm{L}) = \Sigma_r f_r \sum_{\alpha=0}^{\mathrm{M}-1} \sum_{\beta=0}^{\mathrm{N}-1} \sum_{\gamma=0}^{\mathrm{R}-1} \cos\left[\Theta_r + 2\pi\left\{\frac{\mathrm{H}}{a}(a\alpha + \Delta_a) + \frac{\mathrm{K}}{b}(b\beta + \Delta_b) + \frac{h}{c}(c\gamma + \Delta_c)\right\}\right] \quad (4)$$

where Θ_r is the value of θ_r under the substitution $h = \mathrm{H}$, etc.

After some manipulation (4) reduces to:

$$\mathrm{A}(\mathrm{H}, \mathrm{K}, \mathrm{L}) = \sigma_c \Sigma_r f_r \cos \Theta_r - \sigma_s \Sigma_r f_r \sin \Theta_r$$

and similarly

$$\mathrm{B}(\mathrm{H}, \mathrm{K}, \mathrm{L}) = \sigma_s \Sigma_r f_r \cos \Theta_r + \sigma_c \Sigma_r f_r \sin \Theta_r \tag{5}$$

where

$$\left.\begin{aligned} \sigma_c &= \sum_{\alpha=0}^{M-1} \sum_{\beta=0}^{N-1} \sum_{\gamma=0}^{R-1} \cos 2\pi \left[\left(\frac{\mu\alpha}{\mathrm{M}} + \frac{\nu\beta}{\mathrm{N}} + \frac{\rho\gamma}{\mathrm{R}}\right) + \left(\frac{\mathrm{H}\Delta_a}{a} + \frac{\mathrm{K}\Delta_b}{b} + \frac{\mathrm{L}\Delta_c}{c}\right)\right] \\ \sigma_s &= \sum_{\alpha=0}^{M-1} \sum_{\beta=0}^{N-1} \sum_{\gamma=0}^{R-1} \sin 2\pi \left[\left(\frac{\mu\alpha}{\mathrm{M}} + \frac{\nu\beta}{\mathrm{N}} + \frac{\rho\gamma}{\mathrm{R}}\right) + \left(\frac{\mathrm{H}\Delta_a}{a} + \frac{\mathrm{K}\Delta_b}{b} + \frac{\mathrm{L}\Delta_c}{c}\right)\right] \end{aligned}\right\} \tag{6}$$

From (1) and (5) the interesting fact emerges that:

$$\mathrm{F}^2(\mathrm{H}, \mathrm{K}, \mathrm{L})_{(\text{superlattice})} = (\sigma_c^2 + \sigma_s^2)\, \mathrm{F}^2(\mathrm{H}, \mathrm{K}, \mathrm{L})_{(\text{primitive lattice})} \tag{7}$$

which means that the intensity of any superlattice reflection contains as a factor the F^2 value from the primitive lattice considered as being generated by a plane of *fractional indices*.

This result is important as it establishes the validity of phase angle determination methods[2] based on the vanishing of non-Bragg reflections.

In all of the foregoing treatment the perturbation of the lattice has been considered as a static one. Since, however, the frequency of any lattice vibration is very small compared with that of the incident X-ray beam, this assumption will not affect the results. The intensity recorded in a photographic plate will be the time integral of reflections from the lattice. Thus, assuming that the Δ_a, Δ_b, Δ_c are functions of time, the actual recorded intensity is given by:

$$\begin{aligned} \mathrm{I}_{\mathrm{HKL}} &= \mathrm{GF}^2(\mathrm{H}, \mathrm{K}, \mathrm{L})_{\text{superlattice}} \\ &= \mathrm{GF}^2(\mathrm{H}, \mathrm{K}, \mathrm{L})_{\text{primitive lattice}} \times \int_0^{\mathrm{T}} (\sigma_c^2 + \sigma_s^2)\, dt, \end{aligned} \tag{8}$$

where G is the usual constant involving Lorentz and Polarisation Factors.

Of course, the assumption that the lattice perturbation has wavelengths (Ma, Nb, Rc) can also be generalised but a result of the form of (8) will always obtain, the difference being that, instead of discrete fractional reflections being observed, a continuous background of intensity will be generated due to non-resolution, and this will vanish where F^2 (primitive lattice) is zero.

4. The Case of Random Disturbances

The case of a stationary lattice in which a single atom in each unit cell is executing thermal vibrations will now be considered. It will be assumed that there is no phase relationship between the vibrations of atoms in different cells.

It is easily shown that,[1] if a monochromatic beam of X-rays is incident on the contents of a unit cell, the diffracted beam is given by:

$$\mathscr{A} = \mathrm{A} \sum_{r=1}^{\mathrm{N}} f_r \cos\left[2\pi\left(\frac{t}{\tau} - \frac{x}{\lambda}\right) + \theta_r\right] \tag{9}$$

where
$$\theta_r = 2\pi\left(h\frac{x_r}{a} + k\frac{y_r}{b} + \rho\frac{z_r}{c}\right)^* \tag{10}$$

and A is the amplitude of the incident radiation.

Suppose now that the co-ordinates of the sth atom are not exactly (x_s, y_s, z_s) but differ by small quantities

$$\Delta_a^s,\ \Delta_b^s,\ \Delta_c^s. \tag{11}$$

These quantities will vary randomly from cell to cell and, in general, with time.

Substituting from (11) in (9) and (10), neglecting squares and higher powers of the Δ^s and expanding gives:

$$\mathscr{A} = \mathrm{A}\,|\,\mathrm{F}(h, k, l)\,|\cos\left[2\pi\left(\frac{t}{\tau} - \frac{x}{\lambda}\right) + \alpha\right]$$
$$- 2\pi\,\mathrm{A} f_s\left(\frac{h}{a}\Delta_a^s + \frac{k}{b}\Delta_b^s + \frac{l}{c}\Delta_c^s\right)\sin\left[2\pi\left(\frac{t}{\tau} - \frac{x}{\lambda}\right) + \theta_s\right] \tag{12}$$

Now, when all the unit cells of the crystal are considered, the total diffracted intensity is given by:

$$\mathscr{A}_{\mathrm{T}} = \Sigma\mathscr{A} = \mathrm{A}\,|\,\mathrm{F}(h, k, l)\,|\sum_{0}^{\mathrm{P}}\sum_{0}^{\mathrm{Q}}\sum_{0}^{\mathrm{R}}\cos\left[2\pi\left(\frac{t}{\tau} - \frac{x}{\lambda} + \phi\frac{(p, q, r)}{\lambda}\right) + \alpha\right]$$
$$- 2\pi\,\mathrm{A} f_s\sum_{0}^{\mathrm{P}}\sum_{0}^{\mathrm{Q}}\sum_{0}^{\mathrm{R}}\left(\frac{h}{a}\Delta_a^{ps} + \frac{k}{b}\Delta_b^{qs} + \frac{l}{c}\Delta_c^{rs}\right)$$
$$\times \sin\left[2\pi\left(\frac{t}{\tau} - \frac{x}{\lambda} + \frac{\phi}{\lambda}\right) + \theta_s\right] \tag{13}$$

where (P, Q, R) are the numbers of unit cells in each axial direction, and
$\phi(p, q, r) = pa(\cos\alpha + \cos\alpha') + qb(\cos\beta + \cos\beta') + rc(\cos\gamma + \cos\gamma')$ (14)
$(\alpha, \alpha';\ \beta, \beta';\ \gamma, \gamma')$ being the angles which the incident and diffracted

* (h, k, l) are no longer necessarily integral.

directions make with the cell axes. (h, k, l) are now so chosen that the plane makes equal angles with these directions.

When the first summation is effected (13) becomes:—

$$\mathscr{A}_T = A \mid F(h,k,l) \mid \frac{\sin PL}{\sin L} \cdot \frac{\sin QM}{\sin M} \cdot \frac{\sin RN}{\sin N}$$
$$- 2\pi A f_s \sum_0^P \sum^Q \sum^R \left(\frac{h}{a} \Delta_a^{ps} + \frac{k}{b} \Delta_b^{qs} + \frac{l}{c} \Delta_c^{rs}\right)$$
$$\times \sin\left[2\pi\left(\frac{t}{\tau} - \frac{x}{\lambda} + \frac{\phi}{\lambda}\right) + \theta_s\right] \qquad (15)$$

where:—

$$\left.\begin{aligned} L &= \frac{\pi}{\lambda} a(\cos\alpha + \cos\alpha') \\ M &= \frac{\pi}{\lambda} b(\cos\beta + \cos\beta') \\ N &= \frac{\pi}{\lambda} c(\cos\gamma + \cos\gamma') \end{aligned}\right\} \qquad (16)$$

In the Laue-Bragg positions; $L = h\pi$, $M = k\pi$, $N = l\pi$ so that the first term is dominant. When these conditions are *not* satisfied, however, this term is of the order $A \mid F(h, k, l) \mid$.

Next, since there is *no* phase relationship between the Δ's in adjacent cells means displacements $\bar{\Delta}$ can be introduced giving:—

$$\sum_0^P \sum^Q \sum^R \left(\frac{h}{a} \Delta_a^{ps} + \frac{k}{b} \Delta_b^{qs} + \frac{l}{c} \Delta_c^{rs}\right) \sin\left[2\pi\frac{t}{\tau} - \frac{x}{\lambda} + \frac{\phi}{\lambda}\right) + \theta_s\right]$$
$$= \left(\frac{h}{a} \bar{\Delta}_a^s + \frac{k}{b} \bar{\Delta}_b^s + \frac{l}{c} \bar{\Delta}_c^s\right) \sqrt{\sum_0^P \sum^Q \sum^R \sin^2\left[2\pi\left(\frac{t}{\tau} - \frac{x}{\lambda} + \frac{\phi}{\lambda}\right) + \theta_s\right]} \qquad (17)$$
$$\doteq \left(\frac{h}{a} \bar{\Delta}_a^s + \frac{k}{b} \bar{\Delta}_b^s + \frac{l}{c} \bar{\Delta}_c^s\right) \sqrt{\frac{PQR}{2}}, \qquad (18)$$

where the mean value of $\sin^2 x$ has been used.

This term is consequently much larger than the Laue-Bragg term at *non* lattice points and so *between* lattice points the intensity of X-ray diffraction is given by:—

$$I = 2\pi^2 f_s^2 \left(\frac{h}{a} \bar{\Delta}_a^s + \frac{k}{b} \bar{\Delta}_b^s + \frac{l}{c} \bar{\Delta}_c^s\right)^2 P.Q.R.\ A^2 \qquad (19)$$

or, substituting for A and P.Q.R.

$$\frac{I}{I_0} = \frac{2\pi^2 e^4}{m^2 c^4} f_s^2 \frac{(1+\cos^2 2\theta)}{2} \left(\frac{h}{a} \bar{\Delta}_b^s + \frac{k}{b} \bar{\Delta}_a^s + \frac{l}{c} \bar{\Delta}_c^s\right)^2 N\delta V, \qquad (20)$$

where N is the number of unit cells per unit volume and δV is the volume of the reflecting crystal.

This is to be compared with the value:—

$$\frac{I}{I_0} = \frac{e^4}{m^2c^4} |F|^2 \frac{1+\cos^2 2\theta}{2} N^2 \delta V^2 \tag{21}$$

which obtains at the Laue-Bragg positions.

If there is more than one *independently* vibrating atom in the unit cell, (20) is replaced by:—

$$\frac{I}{I_0} = \frac{2\pi^2 e^4 (1+\cos^2 2\theta)}{m^2c^4 \quad 2} \left[\sum_s f_s^2 \left(\frac{h}{a}\overline{\Delta_a}^s + \frac{k}{b}\overline{\Delta_b}^s + \frac{l}{c}\overline{\Delta_c}^s\right)\right] N\delta V \tag{22}$$

Should pairs of atoms be *associated* in vibration this formula is no longer valid and must be replaced by:—

$$\frac{I}{I_0} = \frac{2\pi^2 e^4 (1+\cos^2 2\theta)}{m^2c^4 \quad 2} \left[2\sum_{st} f_s^2 \left(\frac{h}{a}\overline{\Delta_a}^s + \frac{k}{b}\overline{\Delta_b}^s + \frac{l}{c}\overline{\Delta_c}^s\right)^2 \times \sin^2\left(\frac{\theta_s - \theta_t}{2}\right)\right] N\delta V \tag{23}$$

where the summation extends over all *pairs* of vibrating atoms.

Some deductions can be made from the foregoing equations. From (20) it is seen that the diffuse intensity will be greatest when (h, k, l) is *normal* to the direction of vibration and it will be zero for any plane parallel to this direction.

Again, from (22), if just two similar atoms are vibrating in different parts of the structure the diffuse scatter is greatest for planes normal to the line whose direction cosines are:—

$$(\lambda + \lambda'), (\mu + \mu'), (\nu + \nu')$$

where (λ, μ, ν), (λ', μ', ν') are the direction cosines of the vibration directions of the two atoms. Here again there is a zero of intensity, this time for planes parallel to the plane containing the two vibration directions.

In the case of more than two independently vibrating atoms there will be, in general, no zero and the iso-intensity surfaces will be ellipsoids.

Using (23), and considering only one *pair* of vibrating atoms it is seen that the state of affairs is much more complex. For planes normal to the vibration direction the intensity is periodic and decays due to the variation in the atomic scattering factor f.

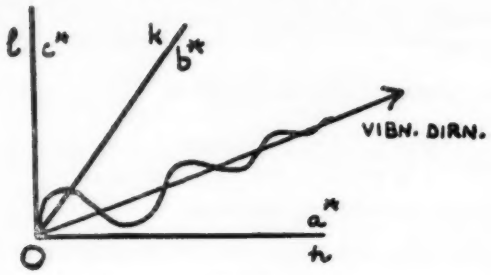

FIG. 1

When symmetry of the space group is added the variation is even more involved but in general the symmetry of the pattern follows that of the lattice.

5. CONCLUSION

The preceding treatment is to some extent naïve but has the virtue of extreme simplicity. When compared with the results of experiment, the agreement is quite good from the qualitative point of view. It is not worth attempting the evaluation of, for example, the summations for the σ_s and σ_c of (6) or the integrals of (8) until more is known regarding the detailed causes of lattice perturbation. When this knowledge is available there are several methods of handling summations of the types considered which can be applied to specific cases.

REFERENCES

1. Booth, A. D. .. "Fourier Technique in X-Ray Organic Structure Analyses," *C.U.P.*, 1948.

2. ———— .. *Nature*, 1946, **158**, 380.

RECHERCHES SUR LES CRISTAUX DANS LE SPECTRE INFRAROUGE

PAR JEAN LECOMTE

Directeur de Recherches au Centre National de la Recherche Scientifique
(Laboratoire des Recherches physiques à la Sorbonne)

Received November 20, 1948

LE Laboratoire des Recherches physiques à la Sorbonne ne s'est pas spécialisé dans l'étude des spectres infrarouges des cristaux, ayant surtout consacré une partie de son activité à la mesure de l'absorption et de la réflexion, dans l'infrarouge, par des composés organiques ou minéraux, ainsi qu'à la détermination consécutive des structures moléculaires. Néanmoins, nous avons eu l'occasion de diriger plusieurs recherches concernant le comportement des cristaux dans l'infrarouge, et aussi d'y participer personnellement. Par suite, nous semble-t-il intéressant de donner ici une synthèse rapide des résultats obtenus.

Nous passerons successivement en revue:

I.—L'absorption des cristaux dans le proche infrarouge (en lumière naturelle ou polarisée,;

II.—Les spectres infrarouges des poudres cristallines;

III.—La détermination des indices de réfraction des cristaux par une méthode interférentielle (infrarouge moyen);

IV.—La pyroélectricité des cristaux et son application à la détection des radiations infrarouges.

* * * *

I.—L'absorption des cristaux dans le proche infrarouge (en lumière naturelle ou polarisée).—On peut examiner les cristaux, dans l'infrarouge, soit par réflexion, soit par transmission. La première méthode a donné lieu, on le sait, à la célèbre méthode des rayons restants. Mais il existe souvent, pour un cristal, des domaines étendus, dans lesquels les pouvoirs réflecteurs restent faibles, et même, pour certains minéraux, les variations de ces pouvoirs réflecteurs, dans tout le spectre, demeurent fort réduites. C'est ce qui a conduit à passer à l'examen par transmission. Jusqu'ici, au Laboratoire des Recherches physiques, à la Sorbonne, on n'a étudié les lames cristallines, d'une manière systématique, que dans le proche infrarouge. Nous rappellerons que, dans cette région, les recherches restent relativement peu nombreuses. Parmi elles, celles de Coblentz[1] représentent vraiment le travail le plus complet, quoique un peu ancien. Dans les recherches plus récentes

se placent celles de Lyon et Kinsey[2], Passerini,[3] Matossi et Bronder,[4] Plyler,[5] van Arkel et Fritzius,[6] Ellis[7] &.... Mais la technique prend surtout son intérêt, lorsque l'on recourt à des radiations polarisées. Parmi les travaux, dont certains remontent déjà à la fin du siècle dernier, nous citerons ceux de Koenigsberger[8] Merrit,[8] Carvallo,[9] Goens,[10] Reinkober,[11] et, dans de plus récents, ceux de Ellis et Bath,[12] Valasek[13] &....

Dans l'ensemble, il existe relativement peu de recherches sur le spectre d'absorption des cristaux dans le proche infrarouge.

Mlle J. Louisfert, en utilisant un spectrographe à prisme de verre (flint extra-dense) et, comme polariseur un prisme de Foucault, a mesuré, entre 0,8 et 2,5 μ, l'absorption de 12 cristaux hydratés: une série de silicates, dont 4 zéolites (analcime, mésotype, heulandite, apophyllite), la topaze, la muscovite, le béryl, une série de sulfates (gypse, $SO_4Cd,8/3\ H_2O$, SO_4Zn, $7\ H_2O$, $SO_4Cu,5\ H_2O$).[14] Avec chacun d'eux, on a déterminé des courbes de transmission, pour des orientation bien définies du plan de polarisation par rapport aux axes cristallographiques. Il apparaît, dans chaque cas, une dizaine de bandes d'absorption, dont quelques unes se présentent comme très fortes. *Les variations en position de ces maxima, avec la rotation du plan de polarisation des radiations incidentes, restent généralement peu importantes, alors que l'intensité des bandes d'absorption varie souvent beaucoup, au point même d'arriver à la disparition de certaines d'entre elles.* (Dans les Fig. 1 et 2, chaque courbe correspond à une position différente du polariseur.

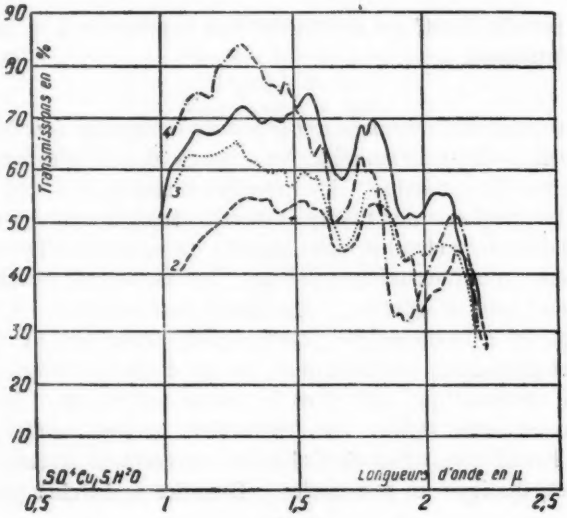

FIG. 1

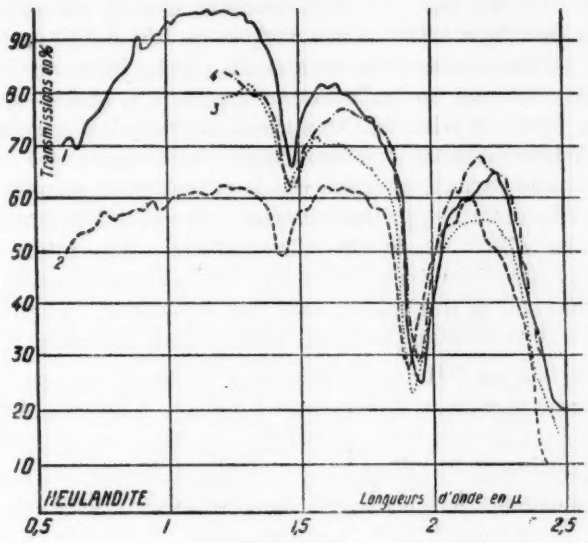

FIG. 2

Ce travail a eu pour objet: 1°) en étudiant la position des bandes d'absorption, d'un cristal à un autre, de préciser la maière dont l'eau se trouve liée dans ces minéraux, et 2°) d'essayer d'utiliser les variations en intensité des bandes pour orienter les molécules dans l'édifice cristallin. Nous développerons un peu ces deux points de vue.

La plupart des bandes d'absorption qui, ont été mesurées par Mlle J. Louisfert dans le proche infrarouge, proviennent de la présence de l'eau dans les cristaux. D'après les études d'autres auteurs, on sait que les maxima d'absorption de l'eau liquide, dans cette région, se déplacent vers de plus courtes longuers d'onde, quand l'eau prend l'état de vapeur. D'une manière plus précise, les vibrations de valence symétrique et antisymétrique de la molécule H O H, considérée comme angulaire (Fig. 3), pour l'état liquide, se placent à 2,90 μ (ν_1) et 2,79 μ (ν_3), et, pour l'état de vapeur,

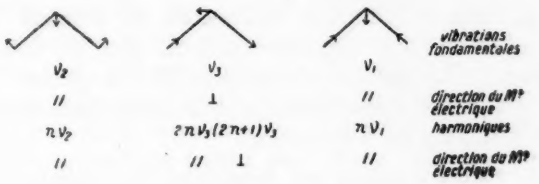

FIG. 3

á 2,76 μ (ν_1) et 2,66 μ (ν_3). De cette manière, dans le changement d'état, se déplacent de 1,55 à 1,38 μ, d'une part, et de 1,95 à 1,87 μ, d'autre part, des bandes particulièrement importantes du proche infrarouge, qui correspondent respectivement aux vibrations: 2 ν_1 ou 2 ν_3 ou $\nu_1 + \nu_3$, et $\nu_1 + \nu_2$ ou $\nu_2 + \nu_3$. Dans les cristaux, les maxima d'absorption mesurés se placent entre les nombres extrêmes, correspondant à l'eau liquide et à l'eau à l'état de vapeur, ce qui permet, inversement, de connaître la manière dont l'éau est liée dans la molécule, en accord avec des recherches antérieures, par exemple, celles d'Ellis et de ses collaborateurs. La même conclusion s'applique aux vibrations des groupements OH, contenus dans les molécules, avec la différence qu'il n'existe, dans ces conditions, qu'une vibration fondamentale caractéristique, avec ses harmoniques successifs.

Ainsi, les liaisons OH avec le reste de la molécule sont peu prononcées pour la topaze et la muscovite (maximum à 1,40 μ). L'eau se présente comme sensiblement libre dans le béryl (maximum à 1,40 μ), un peu plus liée dans l'analcime (maximum à 1,42 μ) et le mésotype (maximum à 1,43 μ), la heulandite (maximum à 1,45 μ), très liée, par contre, dans les sulfates de cadmium et de zinc (maximum á 1,48 μ). Pour le sulfate de cuivre, à 5 molécules d'eau, les deux maxima à 1,37 et 1,46 μ indiquent la présence de deux espèces d'eau, conformément aux conclusions bien connues des chimistes. Le cas du gypse présente une complication plus grande en raison du nombre plus important des bandes observées.

Dans la fig. 3, sont représentés les trois modes de vibration d'une molécule triatomique angulaire comme H_2O. Le moment électrique vibre parallèlement à l'axe binaire dans les vibrations symétriques ν_1 et ν_2, et perpendiculairement pour la vibration antisymétrique ν_3. En ce qui concerne tous les harmoniques, pairs ou impairs des vibrations ν_1 et ν_2, le moment électrique continue à vibrer parallèlement à l'axe binaire de la molécule; mais, pour la vibration ν_3, les harmoniques pairs possèdent un moment électrique parallèle à l'axe, et les harmoniques impairs un moment électrique perpendiculaire á l'axe. L'intensité d'une bande d'absorption infrarouge est liée, on le sait, à la variation du moment électrique: si celle-ci reste nulle, la vibration correspondente est inactive dans l'absorption. En particulier, si, dans la vibration considérée, le moment électrique ne possède pas de composante perpendiculaire au plan de polarisation de la lumière, la bande correspondante manquera dans le spectre. Au contraire, elle prendra une intensité maximum, si le moment électrique est lui-même perpendiculaire au plan de polarisation.

Mlle J. Louisfert a utilisé ces remarques pour essayer d'orienter les molécules d'eau dans les cristaux, au moyen des variations qu'elle a

observées dans les spectres d'absorption. On sait que les rayons X ne donnent pas facilement l'emplacement des atomes d'hydrogène, et l'infrarouge prend ainsi une grande importance pour contribuer à l'étude de la structure cristalline. La difficulté réside en ce que les vibrations de valence ν_1 et ν_3, étant fort voisines, il est souvent difficile de savoir, dans l'attribution des modes de vibration aux bandes observées, s'ils 'agit de $2\nu_1$ ou de $2\nu_3$, ou encore de $\nu_1 + \nu_3$. Néanmoins, cette méthode a donné d'intéressants résultats, en particulier pour le gypse, la heulandite &....

Yeou Ta a repris, sur un cristal d'iodoforme (CHI_3),[15] les expériences d'Ellis et Bath[12] sur le pléochroisme des cristaux dans l'infrarouge, avec l'application aux modes de vibration de la liaison carbone-hydrogène. Opérant d'abord en lumière naturelle, il a montré que la bande d'absorption à 17·175 Å n'apparaissait pas lorsque la lamelle se trouvait placée perpendiculairement au faisceau incident, et qu'elle réapparaissait en inclinant légèrement le cristal. Par contre, les bandes à 14·610, 19·705, et 24·780 Å ne présentaient pas de changement notable dans les mêmes expériences. On admet que la bande à 17·175 Å correspond au premier harmonique de la vibration C–H. Ce qui précède montre qu'elle s'effectue dans la direction de la liaison C–H, et que celle-ci est bien orientée suivant l'axe du cristal. En effet, seulement lorsque la lamelle se trouve inclinée par rapport au faisceau, le vecteur électrique possède une composante parallèle à l'axe du cristal, condition nécessaire à l'apparition de la bande due à la vibration C–H. Des expériences en lumière polarisée, avec des lamelles inclinées sur le faisceau, confirment ces résultats.

Ces conclusons analogues ont été obtenues par le même auteur[16] avec la brucite, $Mg(OH)_2$, en étudiant une bande vers 1,4 μ, qui correspond au premier harmonique de la vibration O–H. Cette liaison doit être parallèle à l'axe sénaire du cristal, qui se présente comme perpendiculaire au plan de clivage, car, comme précédemment avec le cristal d'iodoforme, la bande disparaît lorsque la lame reçoit le faisceau sous l'incidence normale. En collaboration avec Cl. Duval et R. Freymann,[17] nous avons confirmé ces résultats en les étendant à la vibration de déformation du groupement OH. Sous l'incidence normale, une lamelle relativement épaisse de brucite (0,7 mm.) ne présentait aucun maximum d'absorption, alors qu'une mince couche (inférieure à 0,01 mm.) d'oxyde de magnésium hydraté ou de brucite en poudre donnait lieu à de forts maxima respectivement vers 1467 et 1487 $cm.^{-1}$ Dans cette dernière expérience, la poudre présente des axes moléculaires orientés au hasard par rapport à la direction du faisceau incident, de sorte que la variation du moment électrique, au cours de la

vibration OH, devient statistiquement différente de zéro: ce qui conduit à une absorption sélective.

II. Les spectres infrarouges des poudres cristallines.—Depuis 1938, nous avons développé, d'une manière systématique, au Laboratoire des Recherches physiques à la Sorbonne, les études sur les composés organiques ou minéraux à l'état pulvérulent. La méthode apparaît comme absolument générale, car plus de mille substances, appartenant à des types moléculaires les plus divers, ont été ainsi examinées. On obtient, avec une mince couche de poudre finement broyée, un spectre aussi net que s'il s'agissait de substances liquides ou gazeuses, ou de lamelles solides. Il faut seulement que la longueur d'onde des radiations utilisées se présente comme suffisamment grande pour que la diffusion ne joue qu'un rôle restreint. Avec de nombreux collaborateurs, nous avons exploré le domaine de 6 à 20 ν, et M. Parodi[18] a montré que la méthode donnait d'excellents résultats vers de plus grandes longueurs d'onde (80 μ environ). Avec cette technique, tout en ne disposant que d'une quantité de matière très réduite, on peut étudier une foule de substances, dont l'examen aurait été pratiquement impossible, en raison de leur insolubilité dans tous les solvants utilisables, de leur décomposition au cours de la fusion, ou bien de l'existence de points de fusion élevés. De plus, on est certain d'étudier les composés dans l'état exact où ils se trouvent, sans avoir à craindre une modification. Cette circonstance se montre particulièrement précieuse pour l'étude de substances possédant plusieurs degrés d'hydratation.

Avec divers collaborateurs, nous avons transposé cette technique au cas des cristaux, mais les résultats n'ont pas encore été publiés. Lorsque l'on étudie la transmission d'une poudre cristalline, on peut supposer qu'une bonne partie des vibrations du réseau n'apparaîtra pas dans les spectres, en particulier par suite de l'arrangement incohérent des particules. Mais on peut obtenir, exactement comme nous l'avons vu pour la brucite, des renseignements sur la nature des groupements chimiques contenus dans les molécules examinées. Comme l'on pouvait s'y attendre, le gypse et l'anhydrite en poudre reproduisent les maxima d'absorption caractéristiques de SO_4. Mais, si nous examinons des ortho-silicates tels que la willemite (SiO_4Zn_2), le zircon (SiO_4Zr) ou l'orangite (SiO_4Th), et la forsterite (SiO_4Mg_2), la structure d'une région d'opacité vers 11 μ, attribuable à la présence de SiO_4 se présente comme différente. Avec le premier minéral, on note trois maxima distincts (10,31 10,94 et 11,56 μ), dont le deuxième est beaucoup plus intense que les autres, alors que les trois silicates restants ne donnent qu'une bande large, plus ou moins déplacée. Avec la phénacite (SiO_4Gl_2),

on retrouve bien trois maxima, comme dans la willemite, mais considérablement déplacés vers de plus courtes longueurs d'onde (9,63 10,09 10,62 μ). L'interprétation est à chercher dans une structure différente du groupement SiO_4. S'il possède une structure tétraédrique régulière, il ne doit donner naissance, dans cette région qu'à une seule bande forte et étroite. Mais s'il se trouve déformé, dans le cristal, par les molécules avcisinantes, ou par des liaisons dont ne fait pas mention la formule chimique, la vibration triplement dégénérée se décompose en deux ou trois bandes distinctes, ou bien l'absorption s'étend sur un large domaine En collaboration avec Cl. Duval, nous avons étudié une cinquantaine d'orthophosphates et nous avons montré que, suivant l'aspect du spectre, on pouvait en déduire la symétrie du groupement PO_4 dans les composés étudiés. Avec la vivianite (PO_4Fe_3, 8 H_2O) ou l'autunite ($PO_4)_2$ ($UO_2)_2Ca$, 8 H_2O, le spectre comprend, entre 6 et 15 μ, beaucoup plus de bandes que n'en comporte une symétrie tétraédrale pour le groupement PO_4.

Ces quelques exemplees montrent que, *lorsque l'on ne possède pas une lamelle de dimensions suffisantes pour obtenir un spectre d'absorption infrarouge, la méthode des poudres permet néanmoins de caractériser les groupements contenus dans les molécules considérées comme isolées.*

III. La détermination des indices de réfraction des cristaux par une méthode interférentielle (infrarouge moyen).—Il est très important, pour mettre au point les propriétés des cristaux dans l'infrarouge, de connaître leur dispersion dans ce domaine. Malheureusement, dès que l'on dépasse des longueurs d'onde de quelques μ, l'absorption devient si grande qu'il n'est plus possible de recourir à la méthode classique du prisme. D'ailleurs, celle-ci nécessiterait des échantillons de taille très supérieure à ceux que l'on peut se procurer. Aussi, Mme J. Ramadier-Delbès a-t-elle abordé ce problème par une méthode interférentielle.[19]

On commence par tailler une lamelle cristalline très mince (quelques centièmes de mm.), ayant, par exemple, 5 mm. de coté. Cette opération présente des difficultés, qui sont accrues par la nécessité d'orienter convenablement la lamelle par rapport aux axes cristallographiques. On produit un dépot métallique, opaque sur l'une des faces et semi-transparent sur l'autre. On enregistre, au moyen d'un spectrographe à miroirs et à prisme de sel gemme, avec une pile thermoélectrique comme détecteur, les franges d'interférences produites entre les radiations réfléchies par la surface supérieure du cristal (semi-métallisée), et celles qui sont renvoyées par la métallisation opaque de la surface inférieure, après avoir traversé deux fois l'épaisseur *e* du cristal (Fig. 4).

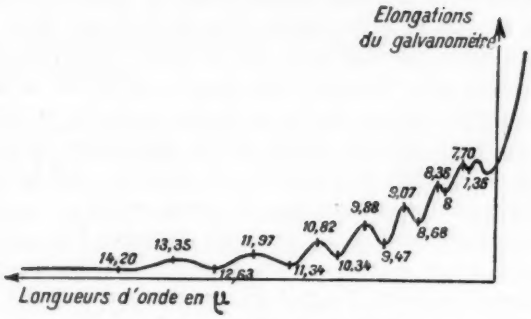

FIG. 4. Interférences d'une lame mince de fluorine $z = 2\,e \cos r = 68,6\,\mu$.

Si l'on désigne par n l'indice de réfraction du cristal pour la longueur d'onde λ, r l'angle de réfraction, les minima d'interférences apparaîtront aux positions données par la relation:

$$2\,n\,e \cos.\,r = k\lambda.$$

On détermine $Z = 2\,e$ cos. r par des mesures effectuées dans le visible, en comptant le nombre des cannelures noires entre deux longueurs d'onde connues, ce qui permet de calculer n, si l'on connait k, ordre d'interférence. D'une frange à la suivante, dans le visible comme dans l'infrarouge, k varie bien d'un nombre entier; mais il ne représente pas nécessairement un nombre entier, en raison du changement de phase, produit pur la réflexion sur la surface métallisée de la lamelle.

Mme J. Ramadier-Delbès est en train d'appliquer avec succès cette méthode à la fluorine, où elle a pu prolonger au delà de 14 μ la connaissance des indices qui s'arrêtait vers 9 μ. Pour la calcite, entre 8 et 14 μ, l'indice de réfraction varie entre 6 et 2. D'autres cristaux sont à l'étude, et donneront certainement des résultats intéressants, puisque la dispersion anomale représente un phénoméne relativement rare dans le spectre visible, mais très fréquent dans le spectre infrarouge.

Cette méthode avait déjà été ' appliquée à la calcite par Taylor et Rideal[20]; mais avec une précision bien moindre, qui tenait à ce que ces auteurs observaient des franges par transmission, avec des lamelles non métallisées, et surtout parcequ'ils éliminaient l'ordre d'interférence entre deux équations du type précédemment indiqué, donnant la position des franges noires, en supposant l'indice de réfraction du cristal constant dans l'intervalle de longueur d'onde considéré.

IV. La pyroélectricité des cristaux et son application à la détection des radiations infrarouges.—Lorsque l'on fait tomber, sur un cristal pyroélectrique, des radiations qui sont absorbées par lui, il s'échauffe et se polarise suivant son axe électrique. YeouTa[21] a taillé des lamelles de tourmaline en forme de lames à faces parallèles, perpendiculaires à l'axe, rectangulaires ou en forme de disque. Les radiations arrivent ainsi que l'indique la Fig. 5,

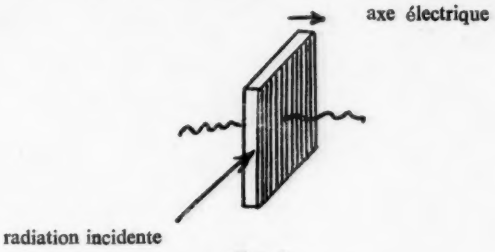

FIG. 5

et les faces terminales sont recouvertes d'un dep^{o}t métallique servant d'électrode. L'effet pyroélectrique reste toujours très petit, mais,si l'on décelait une charge de 10^{-15} coulombs/cm^2, on pourrait mesurer une variation de température du cristal d'un millionième de degré centigrade. L'auteur s'est assuré que l'effet produit par l'éclairement est essentiellement dû à l'infrarouge. Comme, d'autre part, une partie au moins de l'effet est modulable, il en résulte que le cristal pyroélectrique peut servir de détecteur dans la partie infrarouge du spectre (la limite d'utilisation n'étant pas encore précisée). Il serait possible de perfectionner la méthode, en prenant un cristal possédant une constante pyroélectrique plus élevée que la tourmaline, et une constante diélectrique plus petite: en fait, Yeou Ta a trouvé que l'acide tartrique droit se montrait quatre ou cinq fois plus sensible que la tourmaline.

* * * *

Ce qui précède montre que l'étude des cristaux, dans le spectre infrarouge, si elle n'a pas constitué un des objectifs principaux au Laboratoire des Recherches physiques à la Sorbonne, a néanmoins conduit à des résultats intéressants. Il nous est malheureusement impossible, dans le cadre de cet article, de résumer un important travail, éxécuté sous notre direction par M. Parodi:[18] Recherches dans l'infrarouge lointain par la méthode des rayons restants. On trouvera dans cette thèse un ensemble de résultats théoriques et expérimentaux, qui intéresse directement les cristaux, et qu'il est nécessaire de consulter dans le texte original.

BIBLIOGRAPHIE

1. W. W. Coblentz .. *Investigations of infrared spectra.* Publ. Carnegie Inst. N° 35, 65 *et.* 97 Washington (D.C.), 1905 à 1907.
2. W. Lyon et E. Kinsey .. *Phys. Rev.*, 1942, t. **61**, 482–89.
3. L. Passerini .. *Gaz. Chem. Ital.*, 1935, t. **65**, 534–42.
4. F. Matossi et O. Bronder .. *Z. für Phys.*, 1938, t. **111**, 1–17.
5. E. K. Plyler .. *Phys. Rev*, 1926, t. **28**, 284–91.
6. A. E. van Arkel et C. P. Fritzius .. *Recueil Trav. Chim. Pays Bas*, 1931, t. **50**, 1035–45.
7. J. W. Ellis .. *Phys. Rev.*, 1931, t. **38**, 693–98.
8. J. Koenigsberger .. *Ann. der Phys.*, 1897, t. **61**, 687–704.
8. bis. E. Merrit .. *Ibid.*, 1895, t. **56**, 49–64.
9. E. Carvallo .. *C. R. Acad. Sci*, 1895, t. **120**, 415–16.
10. E. Goens .. *Z. für Phys.* 1921, t. **5**, 12–28.
11. O. Reinkober .. *Ann. der Phys.*, 1911, t. **34**, 343–72.
12. J. W. Ellis, *et.* J. Bath .. *J. Chem. Phys.*, 1938, t. **6**, 221–22 ; 1939, t. 7, 862–68.
13. J. Valaseck .. *Phys. Rev.*, 1934, t. **45**, 654.
14. J. Louisfert .. *Diplôme d'Etudes supérieures, Paris*, 1946; *C. R. Acad. Sci.*, 1946, t. **222**, 1092–94 ; 1947, t. **224**, 109–111 ; *J. de Phys.*, 1947, t. 7, 21–28 et 46–55; *J. Chim. Phys.*, 1948, t **45**, 44–46.
15. Yeou Ta. .. *C. R. Acad. Sc.*, 1939, t. **209**, 990–92.
16. ———— .. *Ibid.*, 1940, t. **211**, 467–68.
17. Cl. Duval, R. Freymann et J. Lecomte .. *Bull. Soc. Chim.*, France, 1941, t. **8**, 713–24.
18. M. Parodi .. Thèse Paris, 1938 ; *Collection actualités scientifiques et industrielles*, N° 757, Paris Hermann, 1939 ; *C. R. Acad Sci.*, 1937, t. **204**, 1111–12 ; et 1636–37 ; 1937, t. **205**, 607–8 ; 906–9, et 1224–26 ; 1938, t. **206**, 1717–19 ; 1939, t. **208**, 334–35 ; 1940, t. **211**, 545–46 ; *Bull. Soc. fr. Physique*, 1938, N° **420**, 92–93, & ..
19. J. Ramadier–Delbès .. *J. de Phys.*, 1948, t. **9**, 179.
20. A. M. Taylor et E. K. Rideal .. *Phil. Mag.*, 1927, t. **4**, 682–88.
21. Yeou Ta. .. *C. R. Acad. Sc.*, 1938, t. **207**, 1042–44.

LES OSCILLATIONS EXTERNES DU RESEAU CRISTALLIN DE LA CALCITE

PAR ALFRED KASTLER

(Laboratoire de Physique de l'Ecole Normale Supérieure, Faculté des Sciences de l'Université de Paris)

Received November 20, 1948

Summary.—The normal modes of vibration of the unit cell of crystals built up by complex units (molecules or complex ions) may be classified into internal modes of vibration of these units and into external or lattice oscillations where these units move like rigid bodies towards the lattice. These external vibrations are generally subdivided into translatory modes and rotatory modes of oscillation. This subdivision is not a rigorous one: the translatory motions and the rotatory motions are ideal forms of motion, but the real oscillations of the lattice must be considered as couplings of these two ideal modes. These couplings, determined by the symmetry of the lattice forces, are only possible between motions of the unit cell belonging to the same class of symmetry. The example of calcite is considered to illustrate these coupling effects and to count the number of different low frequency oscillations active in the Raman Spectrum of the crystal and in its infrared absorption spectrum.

Le spectre Raman d'un cristal de calcite CO_3Ca, a été étudié par plusieurs auteurs qui ont déterminé les caractères de polarisation des différentes raies en fonction de l'orientation du cristal et de l'état de polarisation de la lumière incidente.[1] Des mono-cristaux de nitrate de sodium NO_3Na qui ont la même structure cristalline que la calcite, ont été également étudiés et ont donné des résultats analogues en ce qui concerne le nombre, la fréquence et la polarisation des raies.[2] En dehors des raies qui sont dues aux vibrations internes de l'ion complexe CO_3 (ou NO_3) et qu'on retrouve, avec des fréquences peu différentes, dans tous les carbonates ou nitrates à l'état solide, fondu ou dissous, les cristaux de calcite et de nitrate de sodium présentent chacun deux raies Raman de faible fréquence (156 $cm.^{-1}$ et 283 $cm.^{-1}$ pour la calcite, 100 $cm.^{-1}$ et 189 $cm.^{-1}$ pour le nitrate de sodium). Ces raies de faible fréquence sont caractéristiques du réseau cristallin et disparaissent lorsque l'arrangement du réseau est détruit par fusion ou dissolution du cristal. Elles sont très sensibles à une variation de température: un échauffement du cristal les rend plus diffuses et les rapproche de la raie

excitatrice.[3] Leurs fréquences sont du même ordre de grandeur que les fréquences d'absorption de ces cristaux observés dans l'infrarouge lointain[4] et qu'on attribue à des vibrations de translation des cations par rapport aux anions.

Dans une note parue en 1939, C. V. Raman et T. M. K. Nedungadi[5] ont montré que la polarisation caractéristique des deux raies Raman de basse fréquence du nitrate de sodium suggère leur attribution à des mouvements de pivotement (oscillations de rotation) des anions NO_3 dans le réseau. A cause de la forte anisotropie optique de ces ions leurs changements d'orientation dans le réseau doivent en effet se manifester fortement dans le spectre de diffusion.

A. Kastler et A. Rousset[6] ont montré que les deux raies Raman de basse fréquence de la calcite ont la même origine.

Mais par suite de la symétrie ternaire des anions complexes et de leur entourage cristallin, les mouvements de pivotement de ces anions, autour d'un axe de leur plan doivent être dégénérés et la théorie ne prévoyait qu'une seule fréquence de pivotement, alors que l'expérience fournit deux raies Raman ayant les caractères de raies de pivotement. Dans une note récente deux auteurs italiens L. Giulotto et G. Olivelli[7] ont donné la clef du mystère: ils ont montré que la disposition des ions dans le réseau et la symétrie des forces qui s'exercent entre proches voisins entraînent un couplage entre oscillations de translation et oscillations de rotation, et que ce couplage est responsable de l'apparition de deux raies Raman. L'auteur du présent article a montré[8] que les modes de mouvement désignés par ' oscillations de translation ' et ' oscillations de rotation ' ne sont en général que des types idéaux, et que les oscillations fondamentales réelles sont presque toujours des superpositions de ces deux types, oscillations au cours desquelles chaque centre matériel décrit une trajectoire qui est en général de forme hélicoïdale. Il se propose ici d'illustrer ce fait par l'exemple de la calcite en envisageant les diverses oscillations externes de ce type de réseau.

La maille élémentaire de la calcite contient deux anions complexes CO_3 et deux cations Ca, alignés le long de l'axe optique du cristal (Fig. 1). Le long de cet axe les cations alternent régulièrement avec les anions. Ces derniers sont plans et ont la symétrie d'un triangle équilatéral qui est perpendiculaire à l'axe optique du cristal. Les deux anions de la maille élémentaire ont leurs sommets opposés (staggered configuration). Chaque maille élémentaire contient donc quatre éléments constitutifs distincts (deux anions CO_3 que nous distinguerons par les lettres A et B et deux cathions Ca que

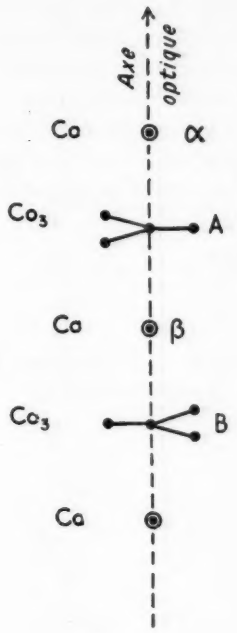

FIG. 1

nous distinguerons par les lettres α et β). Chacun de ces éléments constitutifs forme, par sa répétition dans chaque maille un réseau simple d'éléments congruents. L'examen d'un modèle cristallin montre que ces éléments constitutifs sont disposés en couches perpendiculaires à l'axe optique du cristal. La Fig. 2 donne une coupe d'ensemble du réseau par un plan de symétrie normal à un axe binaire du réseau (plan de section principale d'un spath calcaire). Les petits cercles représentent des cations Ca situés dans le plan de coupe; les petites croix correspondent chacune à deux cations, l'un en avant, l'autre en arrière du plan de coupe, et formant avec les cations voisins situés dans le plan de coupe un pavage de triangles équilatéraux dans un plan perpendiculaire à l'axe optique du cristal. Les deux orientations opposées des anions CO_3 sont indiquées sur la figure (en réalité, les axes binaires de ces anions ne sont pas dans le plan de coupe, mais à 30° de celui-ci). La coupe fait voir la disposition des éléments congruents en couches successives A, α, B, β, etc..... Chaque anion a comme plus proches voisins six cations Ca, dont trois sont disposés en un triangle équilatéral au dessus de l'anion, les trois autres en un triangle équilatéral, d'orientation

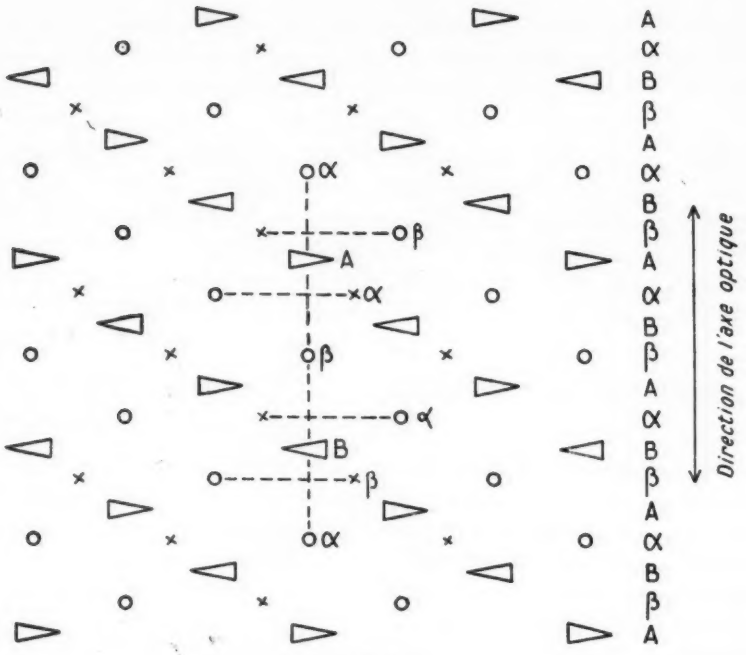

FIG. 2

opposée au-dessous de l'anion. L'orientation de ces triangles est la même autour des anions de type A et des anions de type B, mais la parité des couches est différente. Un anion A a au-dessus de lui un triangle de Ca β, au-dessous de lui un triangle de Ca α. L'inverse a lieu pour un anion B.

A l'état d'équilibre chaque atome d'oxygène d'un anion CO_3 se trouve à égale distance de ceux cathions Ca, appartenant aux couches voisines de part et d'autre. Il est naturel d'admettre, avec les auteurs italiens, que des forces s'exercent entre les cathions et les atomes d'oxygene des anions. Nous ignorons le sens de ces forces, nous admettrons, pour fixer les idées, qu'elles sont attractives. A l'état d'équilibre ces forces se compensent. Elles interviennent lorsque les ions se déplacent, et nous allons voir qu'elles entrainent une interdépendance entre les oscillations de translation et les oscillations de rotation des ions.

Jean Cabannes[9] a dénombré et classé les divers types d'oscillations fondamentales de la maille de calcite: Suivant leurs caractères de symétrie ces oscillations peuvent se classer en oscillations symétriques par rapport à l'axe ternaire (symbole A) et oscillations dégénérées par rapport à cet axe

(symbole E). Chaque cation Ca est un centre de symétrie du réseau indéfini, et les oscillations peuvent aussi se classer en oscillations symétriques par rapport à ce centre (suffixe *g*) ou antisymétrique par rapport à lui (suffixe *u*). Enfin, il est commode (mais comme nous verrons non essentiel de distinguer des mouvements de translation et des mouvements de pivotement. On peut ainsi distinguer dix types de mouvement qui se classent en cinq classes de symétrie distinctes A_{2g}, E_g, A_{1u}, A_{2u}, E_u. La Fig. 3 montre ces

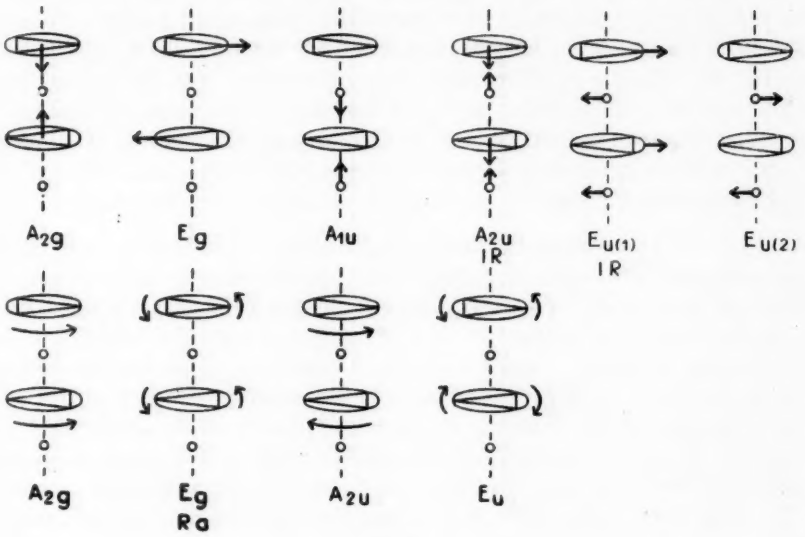

FIG. 3

formes de mouvements des éléments de la maille. Remarquons que les deux mouvements de translation $E_u(1)$ (translation mutuelle des cations et des anions) et $E_u(2)$ (translation mutuelle des cathions α et des cations β) appartiennent à la même classe de symétrie et que le chiffre ajouté entre parenthèse a uniquement pour but de les distinguer. Rappelons que les mouvements symétriques par rapport au centre (*g*) sont toujours inactifs en absorption infrarouge alors que les mouvements antisymétriques par rapport à ce centre (*u*) ne peuvent pas apparaître en effet Raman. Les oscillations de translation A_{2u} et $E_u(1)$ sont actives en infrarouge, le moment électrique de la première étant parallèle à l'axe, le moment électrique de la seconde perpendiculaire à l'axe. Les oscillations de translation A_{1u} et $E_u(2)$ ainsi que les oscillations antisymétriques de pivotement ne produisent pas de moment électrique et ne se manifestent pas dans le spectre infrarouge.

Le mouvement de pivotement E_g doit apparaître fortement dans la diffusion; l'oscillation de torsion A_{2g} des ions CO_3 autour de l'axe ternaire ne peut se manifester que faiblement dans l'effet Raman, et à la condition d'admettre que le mouvement de torsion déforme l'ellipsoide de polarisabilité des ions CO_3 ce qui n'est pas impossible. Mais la déformation ne peut être que du second ordre et ne peut pas se manifester sur la fréquence fondamentale. Des considérations de symétrie montrent que les mouvements de translation A_{2g} et E_g ne peuvent pas se manifester en diffusion sur la fréquence fondamentale. Les figures 4 à 9 illustrent les effets de couplage entre les mouvements de translation et de rotation de même classe de symétrie. Chaque figure représente au milieu un ion CO_3 (à gauche l'ion A, à droite l'ion B) et autour de lui les six ions Ca qui sont ses plus proches voisins, l'ensemble étant projeté sur un plan perpendiculaire à l'axe optique. Les cercles noirs (signe +) représentent des ions Ca au-dessus de l'ion CO_3, les cercles clairs (signe −) des ions Ca au-dessous de l'ion CO_3.

La Fig. 4 montre que la torsion A_{2g} des ions CO_3 autour de l'axe ternaire entraîne une translation A_{2g} de ces ions parallèlement à l'axe optique. En effet, la rotation de l'ion CO_3 de type A éloigne les atomes d'oxygène de cet ion des ions Ca au-dessus et le rapproche des ions Ca au-dessous dont l'attraction l'emporte (signes −). En tournant dans le sens des aiguilles de la montre, l'ion CO_3 de type A se trouve donc poussé vers le bas, alors que l'ion CO_3 de type B (figure de droite) se trouve sollicité vers le haut. La rotation A_{2g} et la translation A_{2g} se couplent donc et leur couplage engendre deux oscillations réelles de forme hélicoïdale et de fréquences distinctes. Ces oscillations sont inactives en absorption infrarouge et en diffusion.

La Fig. 5 montre que la translation E_g de l'ion CO_3 perpendiculairement à l'axe optique entraîne un pivotement de cet ion autour de l'axe de translation par suite de la dissymétrie des forces attractives produite par la translation. Mais les mouvements de translation et de pivotement qui se couplent ainsi sont tous les deux de la classe E_g et ne se manifestent pas en absorption infrarouge. Ce couplage explique l'apparition des deux raies Raman de faible fréquence, et l'intensité relative de ces deux raies permet d'evaluer la part que prend le pivotement à chacune de ces deux oscillations.

La Fig. 6 illustre le couplage entre l'oscillation de torsion A_{2u} et l'oscillation de translation parallèle à l'axe optique de même classe de symétrie. La torsion des deux ions CO_3 de la maille, en sens inverse, entraîne, en effet, des forces d'attraction qui s'exercent sur les deux ions CO_3 dans le même sens (vers le bas dans le cas de la figure). Ce couplage crée deux fréquences d'absorption infrarouges, le vecteur électrique absorbé étant parallèle à l'axe

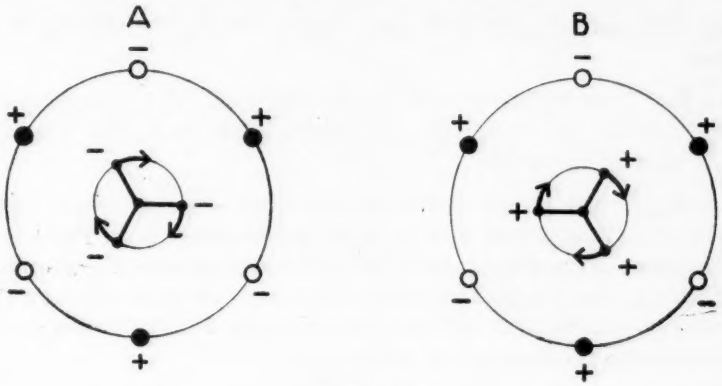

FIG. 4

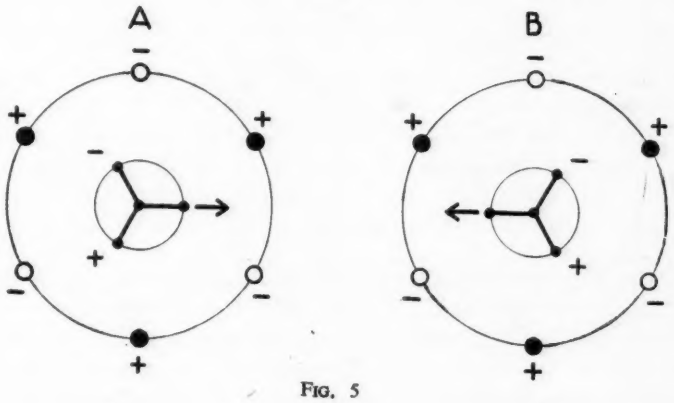

FIG. 5

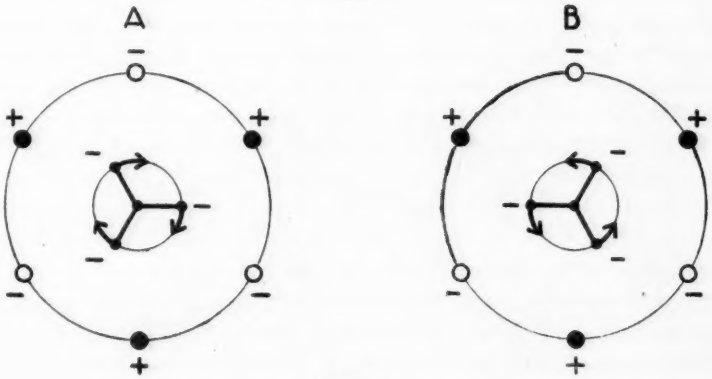

FIG. 6

optique (106 cm.$^{-1}$ et 357 cm.$^{-1}$ pour CO_3Ca, 71 cm.$^{-1}$ et 217 cm.$^{-1}$ pour NO_3Na).

La Fig. 7 montre que l'oscillation de translation $E_u(1)$, perpendiculaire à l'axe, entraîne un pivotement antisymétrique des deux ions CO_3 autour de leurs axes de translation.

La Fig. 8 montre que l'oscillation mutuelle des deux réseaux partiels Ca (α) et Ca (β) se couple avec ce même pivotement; et la Fig. 9 illustre l'effet inverse: le pivotement antisymétrique des deux ions CO_3 A et B de la maille écarte l'ion Ca, qui se trouve entre eux, de l'axe ternaire. Dans l'hypothèse de forces attractives cet ion a tendance à se rapprocher de l'arête du dièdre formé par les deux ions CO_3.

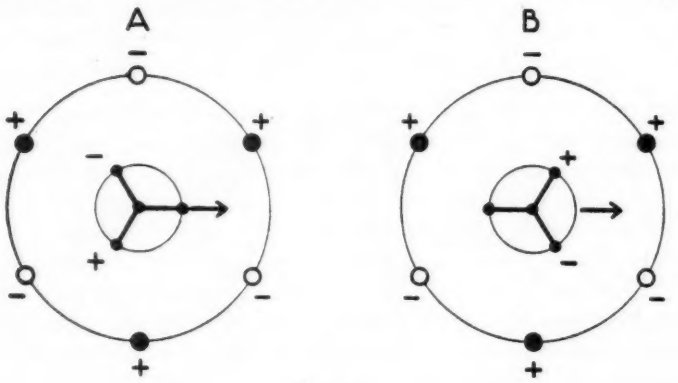

FIG. 7.

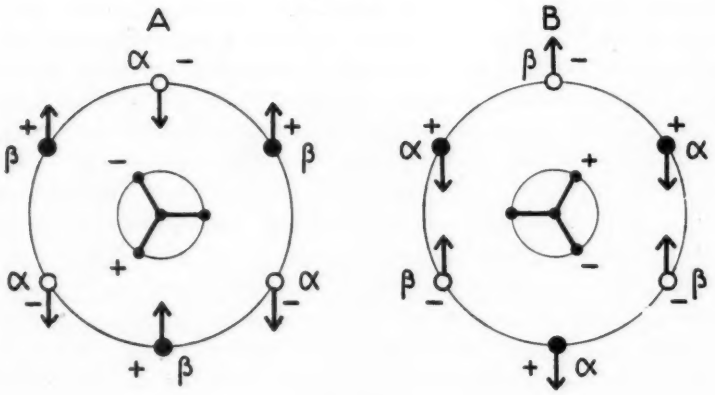

FIG. 8

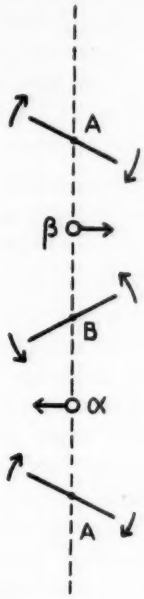

FIG. 9

Le fait que le pivotement E_u est couplé d'une part avec la translation $E_u(1)$ et d'autre part avec la translation $E_u(2)$ montre que ces deux translations sont couplées ensemble et ne peuvent s'effectuer séparément (remarquons que les mouvements de translation $E_u(1)$ et $E_u(2)$ qui se couplent ainsi s'effectuent à angle droit l'une de l'autre). Nous avons donc à faire ici à un couplage triple, et nous prèvoyons trois oscillations réelles de classe E_u formées chacune des trois composantes idéales de cette classe. La participation de la translation $E_u(1)$ confère à ces trois oscillations l'activité infrarouge; la mesure de l'intensité relative des bandes d'absorption infrarouges permettra d'évaluer la participation de la composante $E_u(1)$ à chacune de ces oscillations. Pour la calcite, ces oscillations correspondent aux fréquences d'absorption 106 cm.$^{-1}$, 182 cm.$^{-1}$, 330 cm.$^{-1}$, pour NO_3Na aux fréquences 71 cm.$^{-1}$, 133 cm.$^{-1}$, 217 cm.$^{-1}$

Les considérations précédentes montrent que si la subdivision des oscillations externes en oscillations de translation (cisaillement) et en oscillations de rotation (pivotements) est commode, elle ne peut correspondre qu'à des mouvements idéaux limites. Les oscillations réelles sont constituées par des couplages entre ces formes idéales. La seule subdivision rigoureuse des

oscillations fondamentales d'une maille est celle en classes de différentes symétrie, et il convient de remarquer que seuls des formes idéales de même classe de symétrie peuvent se combiner ensemble. Lorsqu'une classe de symétrie ne contient qu'un seul mode idéal de mouvement celui-ci apparaît à l'état pur comme oscillation réelle. C'est le cas de l'oscillation de translation A_{1g} de la calcite.

Des considérations analogues peuvent s'appliquer à d'autres types de cristaux, au type ' aragonite ' par exemple, et permettront de rendre compte du nombre de fréquences actives observées en spectrographie Raman et en spectrographie infrarouge, et de leurs caractères de polarisation.

Sur l'effet Raman des monocristaux en lumière polarisée nous possédons actuellement des données nombreuses qui s'enrichissent constamment par les travaux de plusieurs équipes. Mais sur les spectres d'absorption et de réflexion de ces cristaux dans l'infrarouge lointain nous ne disposons que de données anciennes, incomplètes et peu précises. Il serait très désirable que ces études infrarouges soient reprises en lumière polarisée et avec une grande dispersion. La connaissance précise des fréquences des oscillations externes des réseaux cristallins et des intensités des raies d'absorption et de diffusion qui leur correspondent nous fournira des données intéressantes pour aborder le calcul des forces de liaison qui s'exercent entre les éléments constitutifs des réseaux cristallins.

Nous avons envisagé, jusqu' à présent, uniquement des couplages entre oscillations principales de fréquences finies (branches optiques). Mais il est facile de montrer qu'il doit y avoir aussi certains couplages entre les translations des centres de gravité de la branche acoustique et les mouvements de pivotement.

Considérons, comme exemple simple (Fig. 10), un réseau linéaire de molécules planes, dont les plans sont perpendiculaires au plan de la figure,

FIG. 10

et qui sont inclinées alternativement des deux cotés de la verticale. Il est évident qu'une compression longitudinale va redresser les plans moléculaires alors qu'une dilatation va les aplatir (mouvement d'accordéon). Une onde de compression-dilatation produira des effets analogues dans des cristaux réelles à trois dimensions formées de molécules planes d'orientation diverses

(c'est le cas des cristaux de substances aromatiques). Les ondes thermo-élastiques de basse fréquence des cristaux provoqueront donc des changements d'orientation des éléments constitutifs anisotropes, et ceux-ci se manifesteront par une dépolarisation appréciable des composantes Brillouin de la raie Rayleigh.

Bibliographie

1. Cl. Schaefer, F. Matossi, H. Aderhold .. *Zeitschr. f. Physik*, 1930, **65**, 289 et 319.
   J. Cabannes *et* Mlle D. Osborne .. *C. R. Acad. Sci., Paris*, 1931, **193**, 156 *et* 1410.
   Mlle Osborne .. *thèse Montpellier*, 1931.
   H. Michalke .. *Zeitschr. f. Physik*, 1938, **108**, 748.
   Mlle L. Couture .. *Annales de Physique*, 1947, **2**, 5 (p. 21).
2. J. Cabannes et E. Canals .. *C.R. Acad. Sci., Paris*, 1931, **193**, 289.
   T. M. K. Nedungadi .. *Proc. Ind. Acad. Sci.*, A, 1939, **10**, 197.
   B. S. R. Rao .. *Ibid.*, 1944, **19**, 93.
3. T. Kopcewicz .. *Journal de Physique*, 1937, **8**, 6.
   P. K. Narayanaswamy .. *Proc. Ind. Acad. Sci.*, A, 1946, **26**, 511.
   T. M. K. Nedungadi .. *Ibid.*, 1938, **8**, 397.
   Mme C. Vassas-Dubuisson .. *Journal de Physique*, 1948, **9**, 91.
4. Th. Liebisch u. H. Rubens .. *Sitzungsber. Akad. zu, Berlin*, 1919, **12**, 198.
   Cl. Schaefer, C. Bormuth, F. Matossi .. *Zeitsch. f. Physik*, 1926, **39**, 648.
5. C. V. Raman, a. T. M. K. Nedungadi .. *Nature*, 1939, **143**, 679.
6. A. Kastler, et A. Rousset .. *Journal de Physique*, 1941, **2**, 49 (p. 56).
7. L. Giulotto a. S. Olivelli .. *Journal of Chemical Physics*, 1948, **16**, 555.
8. A. Kastler .. *C.R. Acad. Sci., Paris*, 1948, **227**, 102, **4**.
9. J. Cabannes .. *Revue Scientifique*, 1942, p. 407.

THE FARADAY EFFECT AND MAGNETO-OPTIC ANOMALY OF SOME CUBIC CRYSTALS

By S. Ramaseshan

(From the Department of Physics, Indian Institute of Science, Bangalore)

Received November 20, 1948

(Communicated by Prof. R. S. Krishnan, F.A.SC.)

The magnitude of the Faraday rotation in most transparent substances is expressible by a formula of the Becquerel type, *viz.*,

$$V = \gamma (e/2mc^2) \lambda dn/d\lambda$$

where V is the Verdet constant, e and m are the electronic charge and mass respectively, c the velocity of light, λ the wavelength and n the refractive index. γ is a multiplying factor (called the magneto-optic anomaly) which is approximately constant throughout the visible and the ultra-violet regions, provided the contribution made to the dispersive power by the infra-red absorption bands is eliminated from the formula. Becquerel (1897) arrived at his original formula, in which the factor γ had a value of unity, purely from classical considerations. Van Vleck (1932) has considered the derivation of the Becquerel formula from quantum mechanical ideas and arrives at a conclusion that the value of γ depends on the state of the electrons of an atom and it need not necessarily have a value equal to one. He also found that for atoms and ions in which the electrons have an inert gas configuration (*viz.*, when the outer electrons are in the s state), the value of γ must be equal to unity, *i.e.*, the anomaly disappears. Surprisingly enough, (as has been remarked by Darwin and Watson (1927), such crystals like NaCl and KCl which are reputed to be of the ionic type have a value of γ of about 0·8. This decrease in γ must obviously be due to the distortion of the electron atmospheres of the atoms due to the crystal structure. The value of γ may be therefore tentatively assumed to be an indication of the departure of the binding from the true ionic type. A study of the magneto-optic rotation and anomaly in crystals would throw considerable light on the nature of the binding in the crystalline state. Accordingly the present writer made some measurements in diamond, zinc blende, and other crystals (Ramaseshan, 1946, 1947). The present work was undertaken with a view to get more accurate data in the case of the crystals already investigated and to extend the studies to other crystals. The Faraday

rotation measurements were made in a series of cubic crystals (NaCl, KCl, KBr, KI, NH_4Cl, NH_4Br, $NaClO_3$, $KAl(SO_4)_2\,12\,H_2O$ and $NH_4Al(SO_4)_2\,12\,H_2O$ and the magneto-optic anomaly has been calculated in each case. To get a clearer insight into the meaning of the magneto-optic anomaly, the Verdet constant and γ for concentrated solutions of these crystals in water have also been determined and the results are reported in this paper.

2. Experimental Methods

For measurements of the Faraday effect, a polarimeter made by Franz Schmidt and Haench and Co., Berlin, was used. The analyser was mounted on a divided circle that could read upto 0·01°. The polarimeter was fitted with a Lippich double field polariser in which the half shadow angle could be varied from 0° to 20°. When this angle was between 3° and 4° most accurate and satisfactory results were obtained. With clear transparent crystals or solutions repeated settings of the match-point do not vary by more than 0·02°. While taking measurements, the usual precautions that are necessary to eliminate instrumental errors were taken. Each value given in the tables is a mean of ten settings. The sources of light used in these visual measurements were a sodium lamp with a light yellow filter for λ 5893 and a mercury point-o-lite lamp with suitable filters for isolating λ 5461 λ 4358.

On account of the low sensitivity of the eye to the region below λ 4358, visual observations could not be extended below this wavelength. Instead a spectrographic method was resorted to. With the same polarimeter arrangement as mentioned above, the light coming out of the analyser was focussed by means of an achromatic lens on the widened slit of a Hilger baby quartz spectrograph. A series of photographs was taken with different settings of the analyser. Each line in the spectrum being an image of the half shade, the match-point for different wavelengths could be easily determined. It was found that with a half shadow angle of 6° and with a point-o-lite mercury lamp running at 2·4 amps. as the source, an exposure of 30 seconds was sufficient to record the spectral line at the match-point when it is least intense. The analyser was rotated by 0·05° between successive photographs and the match point could be placed within 0·05° to 0·10°; and as the magnetic rotation was usually above 10° the accuracy obtained was quite satisfactory. The extinction positions for the wavelengths λ 5780, λ 5461, λ 4358, λ 4046 and λ 3665 were determined for each crystal without the magnetic field and with the magnetic field on and reversed. The values obtained for the first three wavelengths did not differ by more than $\frac{1}{2}$ to 1% from the values obtained by visual measurements.

These measurements could not be extended beyond λ 3665, since the absorption of the film of canada balsam in the double field polariser became considerable below this wavelength. It is proposed to extend these studies to the far ultraviolet (at least upto λ 2537) by using ultra-violet polarising prisms.

The magnet used in these experiments was of the Rutherford type fitted with special pole-pieces. With currents upto 6 amps. the magnet could be run continuously for an hour without much heating. The refractive indices of the crystals and solutions were measured with a Pulfrich refractometer. The measurements were always made at room temperature ($25 \pm 1°$ C.).

3. Materials Studied

The crystals whose Verdet constants are to be measured by the above method must be absolutely free from birefringence, since irregular birefringence induced by residual strain would make it impossible to match the two halves of the double field polariser. Further, magnetic rotation as measured by the usual method is known to diminish in the presence of a small amount of birefringence. Therefore, great care was taken to see that only isotropic crystals were chosen for these measurements. A piece of rock-salt about 2 cm. × 2 cm. × 0·8 cm. was cleaved from a larger specimen. The potassium chloride, sodium chlorate, potassium alum and ammonium alum were grown by the method of slow evaporation from saturated solutions. Crystals of ammonium chloride and bromide were grown from saturated solutions in which urea was introduced as an impurity catalyst. Refractive index measurements show that the urea present in the crystals obtained in this way could not be more than 1%. A large crystal of potassium bromide 7·5 cm. × 6·10 cm. × 3·05 cm. in size was used. Although the crystal was full of irregular birefringence there was a small region 3 mm. × 3 mm. where the light was always extinguished when observed between crossed nicols. The surfaces of all the crystals were polished with rouge and putty powder so that the half-shade could be seen through them very clearly.

The solutions were prepared from the purest chemicals manufactured by either Kahlbaum or Merck. In the measurement of the Faraday rotations in solutions, the same glass cell was used for all the solutions.

4. Results

Tables I to IX give the values of the Verdet constant determined for different wavelengths for crystals of NaCl, KCl, KBr, KI, NH_4Cl, NH_4Br, $NaClO_3$, $KAl(SO_4)_2\,12H_2O$ and $NH_4Al(SO_4)_2\,12H_2O$. The thickness of the crystal used, the magnetic field and the specific gravity of the crystal are

TABLE I

Magneto-optic data for NaCl crystal

Thickness 2·231 cm. Magnetic field 8450 oersteds
Specific gravity 2·163

Wavelength in Angstroms	2ρ Magnetic rotation in degrees	V Verdet constant in min./cm. oersted		$\gamma\%$
		Author	Mayer & Landau	
5893	21·68	0·0345	0·0328	89·0
5780	23·06	0·0367	..	89·8
5461	25·76	0·0410	0·0390	90·1
4358	43·00	0·0685	0·0655	88·0
4046	50·80	0·0809	0·0775	89·0
3665	69·70	0·111	0·106	90·0

TABLE II

Magneto-optic data for KCl crystal

Thickness 0·965 cm. Magnetic field 9780 oersteds.
Specific gravity 1·988

λ	2ρ	V		$\gamma\%$
		Author	Mayer	
5893	8·64	0·0275	0·0267	82·1
5780	9·08	0·0289	..	82·1
5461	10·32	0·0328	0·0316	82·2
4358	17·30	0·0551	0·0534	82·7
4046	21·40	0·0680	..	83·1
3665	27·40	0·0870	..	83·2

TABLE III

Magneto-optic data for KBr crystal

Magnetic field 3540 oersteds Specific gravity 2·75

λ	2ρ		V	$\gamma\%$
	Thickness 6·10 cm.	Thickness 3·05 cm.		
5893	30·60	15·40	0·0425	78·5
5461	36·00	18·10	0·0500	79·5
4358	60·4	30·15	0·0840	78·2
4046	..	38·00	0·106	79·4
3665	..	48·20	0·134	79·1

TABLE IV

Magneto-optic data for KI crystal

Thickness 1·070 cm. Magnetic field 8450 oersteds

Specific gravity 3·13

λ	2ρ	V	γ%
5893	21·10	0·070	78·2
5461	25·00	0·083	78·9
4358	45·50	0·151	78·3

TABLE V

Magneto-optic data for NH_4Cl crystal

Thickness 0·900 cm. Magnetic field 9780 oersteds

Specific gravity 1·529

λ	2ρ	V	γ%
5893	10·62	0·0362	71·9
5461	12·61	0·0430	72·7
4358	21·68	0·0739	72·9

TABLE VI

Magneto-optic data for NH_4Br crystal

Thickness 0·746 cm. Magnetic field 9780 oersteds

Specific gravity 2·325

λ	2ρ	V	γ%
5893	12·28	0·0504	69·0
5461	14·61	0·0601	69·8
4358	25·29	0·1040	69·5

TABLE VII

Magneto-optic data for $NaClO_3$ crystal

Thickness 2·054 cm. Magnetic field 8·50 oersteds
Specific gravity 2·490

λ	2ρ	V		γ%
		Author	Voigt	
5893	4·68	0·0081	..	31·0
5780	5·02	0·0087	0·0088	31·2
5461	6·08	0·0105	0·0106	31·5
4358	9·40	0·0163	..	31·2
4046	11·60	0·0201	..	32·0
3665	15·80	0·0272	..	33·0

TABLE VIII

Magneto-optic data for potassium alum

Thickness 0·931 cm. Magnetic field 9940 oersteds
Specific gravity 1·76

λ	2ρ	V	γ%
5893	3·82	0·0124	53·3
5780	4·01	0·0130	54·2
5461	4·44	0·0144	55·1
4358	6·78	0·0220	55·5

TABLE IX

Magneto-optic data for ammonium alum

Thickness 0·895 cm. Magnetic field 9940 oersteds
Specific gravity 1·64

λ	2ρ	V	γ%
5893	3·79	0·0128	54·3
5780	3·97	0·0134	54·7
5461	4·48	0·0151	55·2
4358	6·87	0·0232	55·4

also given at the top of each table. The values of the Verdet constant determined by other authors (Mayer, 1909; Landau, 1908; Voigt, 1908) have also been included in the tables. The refractive index data are not given

here as they correspond to the values determined by previous workers (Soret, 1884; Haase, 1927; Ramaseshan, 1947). The last column in each table gives the value of γ, the magneto-optic anomaly, expressed as a percentage. Table X gives the natural and magnetic rotations in $NaClO_3$

TABLE X

Natural and magnetic rotations in $NaClO_3$

Thickness of the crystal 2·054

λ	ρ (natural) in degrees/cm.	$\rho \times 10^4$ in degrees/cm. oersted	$\frac{\rho_n}{\rho_m} \times 10^{-4}$
5893	31·4	1·35	23·3
5780	33·2	1·45	23·0
5461	37·0	1·75	21·1
4358	59·2	2·71	21·9
4046	68·2	3·35	20·4
3665	86·0	4·53	18·9

crystal as also the ratio of the two for different wave-lengths. Table XI gives the concentration, specific gravity, Verdet constant and the magneto-

TABLE XI

Magneto-optic data for solutions

Magnetic field 8450 oersteds $\lambda = 5461$ A

Thickness of the column 1·767 cm.

Substance	No. of gms. in 100 gms. water	Sp. Gr.	2ρ	V	γ%
Water ..	..	1·00	7·71	0·0155	76·3
KCl ..	21·2	1·114	9·12	0·0183	79·1
KBr ..	48·78	1·288	11·30	0·0227	85·4
KI ..	88·10	1·476	17·08	0·0343	85·4
NaCl ..	24·12	1·136	9·72	0·0195	79·4
NH_4Cl ..	27·20	1·061	9·98	0·0200	78·8
NH_4Br ..	75·08	1·297	13·68	0·0275	83·2
$NaClO_3$ ..	106·3	1·442	8·61	0·0173	72·9
$KAl(SO_4)_2\,12H_2O$ ..	12·68	1·051	7·86	0·0158	75·5

optic anomaly for all the solutions that were studied and Table XII gives their dispersion data.

TABLE XII

Dispersion data for solutions

Substance	n_{5893}	n_{5461}	n_{4358}	$\frac{\lambda}{\Delta\rho}\frac{dn}{}$(5461)
Water ..	1·33239	1·33381	1·33940	2011
KCl ..	1·35594	1·35756	1·36411	2294
KBr ..	1·37771	1·37957	1·38764	2634
KI ..	1·41660	1·41941	1·43159	3979
NaCl ..	1·36462	1·36634	1·37335	2435
NH_4Cl ..	1·37230	1·37408	1·38138	2520
NH_4Br ..	1·40915	1·41146	1·42127	3271
$NaClO_3$ ..	1·38739	1·38905	1·39593	2351
$KAl(SO_4)_2 12H_2O$	1·34304	1·34447	1·35036	2048

5. DISCUSSION OF RESULTS

The tabulated results reveal many interesting features. For instance, one notices that the modified Becquerel formula is very nearly obeyed by all the crystals in the wavelength region between λ 5893 and λ 3665 and the values of γ for each crystal is approximately constant in this region of the spectrum. It is significant that in the case of crystals, γ (NaCl) $>$ γ (KCl) and γ (KCl) $>$ γ (KBr) $>$ γ (KI) and similarly γ (NH_4Cl) $>$ γ (NH_4Br). If it is assumed that the reduction in the value of γ is an indication of the distortion of the electron atmospheres of the ions in the crystal, then heavier ions distort the electron atmospheres more than the lighter ones. The low value of γ for $NaClO_3$ and the alums is probably due to the fact that the covalent linkages in ClO_3 and SO_4 ions produce a very great distortion in the electron atmospheres of the atoms. The comparatively lower values of γ for NH_4Cl and NH_4Br may also be due to the covalent nature of the N–H bond.

Table XIII gives the γ values for the different crystals and solutions.

TABLE XIII

Magneto-optic anomaly in crystals and solutions

Substance	Concentration No gm./100 gm. solution	γ (solution)%	γ (crystal)%
Water ..	100·0	76·3	..
NaCl ..	19·4	79·4	89
KCl ..	17·5	79·1	82
KBr ..	32·8	85·4	79
KI ..	46·8	85·4	78
NH_4Cl ..	21·4	78·8	72
NH_4Br ..	42·9	83·2	69
$NaClO_3$ ..	51·5	72·9	32
$KAl(SO_4)_2 12H_2O$	11·3	75·5	54

Excepting in the case of $NaClO_3$ and potassium alum (the two crystals having very low γ values), the γ for the solutions is always greater than that for water. Of special significance is the fact that γ values for KBr, KI, NH_4Cl and NH_4Br solutions are greater than the corresponding values for the crystals. This indicates that the γ for the ions in solution is greater than that for the ions in the crystal. Tentative calculations show that γ for the ions in solution is between 95% and 100%, *i.e.*, they approach the value suggested by Van Vleck for free ions with inert gas configurations. These calculations and conclusions are purely tentative, as the effects of the ions in solution on the dispersive power of water have not been taken into consideration.

The results obtained with $NaClO_3$ solution are very striking. While the γ in the crystal is only 33%, the γ for a 50% solution shoots upto 72%, *i.e.*, only 4% less than that for water. In fact, if the γ value for the ions in solution were the same as that for the ions in the crystal, then γ for a 50% solution should be of the order of 50%. On the other hand, if the γ for Na ion is assumed to be 100%, then approximate calculations show that γ for ClO_3 ion is of the order of 50 or 60%. The low value of 33% obtained in the $NaClO_3$ crystal is most probably due to partial covalent forces that come into play in the crystal.

In conclusion, the author wishes to thank Prof. Sir C. V. Raman and Prof. R. S. Krishnan for the keen interest they took in these investigations.

Summary

Using a Lippich double field polarimeter together with a spectrograph, the Faraday rotation for crystals of NaCl, KCl, KBr, KI, NH_4Cl, NH_4Br, $NaClO_3$, $KAl(SO_4)_2\,12\,H_2O$ and $NH_4Al(SO_4)_2\,12\,H_2O$ have been measured for the wavelengths, λ 5893, λ 5780, λ 5461, λ 4358, λ 4046 and λ 3665. The magnetic rotation for concentrated solutions of these crystals in water were also measured. The magneto-optic anomaly for the crystals and solutions has been calculated from the measurements of the dispersion values. It is found that in the case of crystals, $\gamma(NaCl) > \gamma(KCl) > \gamma(KBr) > \gamma(KI)$ and $\gamma(NH_4Cl) > \gamma(NH_4Br)$. The γ for the solutions except in the case of $NaClO_3$ and the alums is always greater than that for water. The γ values for the ions in solution are higher than those for the ions in the crystal. The presence of covalent bonds tends to diminish the value of γ [$\gamma(NaClO_3$ crystal) = 33% and γ(Alum) = 52%]. The γ value for a 50% solution of $NaClO_3$ is 72%.

References

Becquerel, H. .. *Comptes Rendus*, 1897, **125**, 679.

Darwin and Watson .. *Proc. Roy. Soc.*, London, **A**, 1927, **114**, 474.

Haase .. *Zeit. f. Kryst*, 1927, **65**, 509.

Landau, S. .. *Phys. Z. S.*, 1908, **9**, 417.

Mayer, V. .. *Ann. d. Phys.* (4), 1909, **30**, 622.

Ramaseshan .. *Proc. Ind. Acad. Sc.*, A, 1946, **24**, 104.

Soret .. *Arch. Sc. Phys.* (3), 1884, **12**, 554.

Van Vleck .. *Theory of Electric and Magnetic Susceptibility, Oxford*, 1932, 367.

Voigt .. *Phys. Z. S.*, 1908, **9**, 589.

THEORETICAL EVALUATION OF THE ACOUSTIC WAVE-VELOCITIES IN DIAMOND

By K. G. Ramanathan

(From the Department of Physics, Indian Institute of Science, Bangalore)

Received November 30, 1948

(Communicated by Prof. R. S. Krishnan, F.A.SC.)

1. Introduction

Studies on the scattering of light in crystals yield data of two distinct types which may enable us to evaluate the acoustic wave-velocities in the solid. In the first place, we observe in the scattered light small spectral shifts, which, following L. Brillouin, have been interpreted as Doppler shifts of frequency arising in the reflection of the incident light waves by sound waves of thermal origin. This interpretation, however, ignores the possible influence of the presence of an external boundary in the crystal on the types of stationary elastic vibrations. It has been suggested (Raman, 1948) that the discrepancies noticed between the facts as actually observed and those theoretically expected according to the assumptions of Brillouin (Krishnan, 1947), are to be explained in this manner. The second method available for the evaluation of the acoustic wave-velocities in the crystal is purely theoretical. It is based on the knowledge of the forces acting between the various constituent atoms, the latter being themselves found out from the Raman effect data. A method has been recently worked out (Ramanathan, 1947) which enables these forces to be evaluated from the observed frequencies of the normal modes of vibration of the crystal. Using the force-constants thus evaluated, one may proceed to calculate the frequencies of stationary elastic vibrations of different types and of various wavelengths. When the latter are sufficiently large, the product of the frequency of the vibration and its wavelength reaches a constant value which is the acoustic wave-velocity in the crystal for the particular direction. We shall proceed to find out the acoustic wave-velocities in diamond in different directions using the procedure indicated and compare the same with the experimentally determined sound-velocities.

2. Description of the Method

We shall here consider the three principal directions, *viz.*, cubic, dodecahedral and octahedral, and calculate the velocities of transverse and longitudinal stationary vibrations along these in diamond. In the cubic and dodecahedral directions, the carbon atoms in this crystal are arranged in

equidistant layers spaced at intervals of 0·89 A.U. and 1·259 A.U. respectively. However, the spacing of the layers of atoms perpendicular to any octahedral direction is alternately greater and smaller, the distance between any two equivalent layers being 2·055 A.U. In the two former cases, the nodal planes must necessarily be located in a plane of atoms along the cubic and dodecahedral directions respectively. Consequently, only such vibrations are possible whose wavelengths are even multiples of the lattice spacing d. Further, if the displacements of the atoms in any plane are assumed to vary harmonically with its distance from the nodal plane, it is found that the equations of motion of all the atoms in the entire crystal are simultaneously satisfied, showing thereby that these are possible modes of elastic vibration in the crystal. This result is found to be valid whether the displacements of the planes of atoms are transverse or longitudinal.

Considering now the cube directions, only two distinct types of vibrations are possible, one longitudinal and one transverse. Along any dodecahedral direction however, three distinct types of vibration are possible, in one of which the planes move normal to themselves while in the other two, they move tangentially with respect to themselves, the direction of motion being along a cube axis or along another dodecahedral direction.

In the case of the octahedral planes, if we assume any two nearly-spaced layers to move always with the same phase and further if the displacements of the double-layers (nearly-spaced layers) are supposed to vary harmonically from any nodal plane which is also another double-layer, then, the equations of motion of all the atoms in the crystal are simultaneously satisfied. There will be two kinds of such vibrations, one longitudinal and the other transverse. Here again, as in the cubic case, there is only one distinct transverse vibration.

Let us suppose that the planes of rest are separated by n oscillating planes which vibrate with their phases opposite on either side of a nodal plane. Then, if d denotes the lattice spacing, the wavelength of the stationary vibration is $\lambda = 2d(n+1)$. The phases and amplitudes of motion of all the atoms in a particular plane will be the same, while, it will be different for atoms in different planes. The displacement ξ_k of any atom in plane k at an instant of time t is given by $\xi_k = \xi \sin \frac{\pi k}{n+1}$, where ξ is the displacement at the antinode. The equation of motion of any atom in plane k is

$$m \frac{d^2\xi_k}{dt^2} = a\xi_k + b(\xi_{k-1} + \xi_{k+1}) + c(\xi_{-2} + \xi_{k+2}) + d(\xi_{k-3} + \xi_{k+3}) + \ldots\ldots(1)$$

where m is the mass of the carbon atom, a represents the sum of the forces

acting on the atom under consideration due to the displacements of all the atoms in the kth layer, b the sum of the forces acting on the atom due to the displacements of all the atoms in the $(k-1)$ st or $(k+1)$ st layer (these two will be equal), c the sum of the forces on the atom due to the displacements of atoms in $(k-2)$ nd or $(k+2)$ nd layer, etc. There will be n equations of motion corresponding to $k = 1, 2, 3, \ldots . n$. All the n equations become identical on eliminating ξ_k and expressing them in terms of ξ, the equation obtained being

$$m\frac{d^2\xi}{dt^2} = \Big(a + 2b\cos\frac{\pi}{n+1} + 2c\cos\frac{2\pi}{n+1} + 2d\cos\frac{3\pi}{n+1} + \ldots\ldots\Big)\xi \qquad (2)$$

Or, if ν_n, v_n and λ_n represent respectively the frequency of vibration of the atoms, velocity and wavelength of the stationary elastic vibration, then

$$4\pi^2 m\nu_n^2 = \frac{4\pi^2 m v_n^2}{\lambda_n^2} =$$

$$a + 2b\cos\frac{\pi}{n+1} + 2c\cos\frac{2\pi}{n+1} + 2d\cos\frac{3\pi}{n+1} + \ldots . \qquad (3)$$

3. Evaluation of the Constants

In formula (3), when n becomes large and tends to be infinite, the frequency ν_n tends to be zero and the expression on the right-hand side also tends to be zero. Also, the value of the expression $(a + 2b + 2c + 2d + \ldots .)$ which represents a translation of the crystal, is zero. Therefore, an accurate evaluation of the limiting value of the velocity will involve a knowledge of the exact values of the constants a, b, c, d and the other constants representing the series.

In a recent paper already referred to (Ramanathan, 1947), expressions for the frequencies of the nine normal modes of vibration of diamond, were derived in terms of eight force-constants P, Q, R, S, U, W, Σ and Ω, which take account of the influence on each carbon atom of the 28 nearest of its neighbours. A description of these constants and the method of arriving at them by applying the principles of symmetry, are described in the above paper. Also, numerical values for the constants are given there, calculated from the known spectroscopic data.

The constants a, b, c, d, etc., of formula (3) represent, as have been defined already, *the sum of the forces* due to the displacements of *all the atoms* in the plane or planes which they represent. An exact evaluation of these will therefore require also a knowledge of the forces of interaction

between atoms in distant planes as well as distant atoms in neighbouring planes. But, at present, since we have no knowledge of these distant forces of interaction, we shall have to be satisfied with those which we know, *viz.*, P, Q, R, S, U, W, Σ and Ω and evaluate *a*, *b*, *c*, etc., in terms of these. It must be remarked here that the distant forces are not likely to play any sensible part in determining the frequencies of the eigenvibrations of the crystal, because, in these the phases of vibration go on alternating at each successive equivalent layer and so there will be a tendency for these forces to cancel out each other. On the other hand, in the case of elastic vibrations of large wavelengths, there will be mass movements of atoms in a very large number of neighbouring planes all moving in the same direction, and therefore, the distant forces of interaction, though of small magnitude, work together and may be expected to have an appreciable effect on the frequency of vibration.

The constants *a*, *b*, *c*, etc., calculated from P, Q, R, etc., satisfy the condition that a translation involves no energy ($a + 2b + 2c +$ etc. $= 0$) because the latter have been made to satisfy this condition in the paper referred to already.

4. Results

I. Cubic Planes: Longitudinal.

The values of the constants can be easily written down from an examination of a model of diamond.

$a = P + 4S = 7{\cdot}33 \times 10^5$ dynes per cm.
$b = 2Q + 4\Sigma = -3{\cdot}018 \times 10^5$,,
$c = 4U = -0{\cdot}525 \times 10^5$,,
$d = 2\Sigma = -0{\cdot}12 \times 10^5$,,

The value of the velocity increases gradually as we consider vibrations of larger and larger wavelengths and finally reaches a constant value (v_{lim}) which, in this case, is 15900 metres per second.

II. Cubic Planes: Transverse.

$a = P + 4U = 6{\cdot}826 \times 10^5$ dynes per cm.
$b = 2Q + 4\Sigma = -3{\cdot}018 \times 10^5$,,
$c = 2S + 2U = -0{\cdot}272 \times 10^5$,,
$d = 2\Sigma = -0{\cdot}12 \times 10^5$,,

$v_{lim} = 14300$ metres per second.

III. Dodecahedral Planes: Longitudinal.

$a = (P+2Q-2R+2U-2W+2\Sigma-2\Omega) = 6{\cdot}122 \times 10^5$ dynes per cm.
$b = (Q + R + 2S + 2U + 3\Sigma + 3\Omega) = -2{\cdot}685 \times 10^5$,,
$c = (U + W + 2\Sigma - 2\Omega) = -0{\cdot}375 \times 10^5$,,

The limiting velocity = 18300 metres per sec.

IV. Dodecahedral Planes: Transverse along cube axis.

$a = (P + 2Q + 2S + 2\Sigma) = 4{\cdot}44 \times 10^5$ dynes per cm.
$b = (Q + 4U + 3\Sigma) = -2{\cdot}094 \times 10^5$,,
$c = (S + 2\Sigma) = -0{\cdot}125 \times 10^5$,,
$v_{lim} = 14300$ metres per sec.

V. Dodecahedral Planes: Transverse along dodecahedral axis.

$a = (P+2Q+2R+2U+2W+2\Sigma+2\Omega) = 2{\cdot}254 \times 10^5$ dynes per cm.
$b = (Q - R + 2S + 2U + 3\Sigma - 3\Omega) = -1{\cdot}00 \times 10^5$,,
$c = (U - W + 2\Sigma + 2\Omega) = -0{\cdot}127 \times 10^5$,,
$v_{lim} = 10900$ metres per sec.

VI. Octahedral: Longitudinal.

$a = (P + 3Q - 2R + 2S + 4U - 4W + 3\Sigma + 6\Omega) = 4{\cdot}668 \times 10^5$ dynes per cm.
$b = \frac{1}{2}(Q + 2R + 2S + 4U + 4W + 9\Sigma - 6\Omega) = -2{\cdot}333 \times 10^5$,,
$v_{lim} = 22300$ metres per sec.

VII. Octahedral: Transverse.

$a = (P + 3Q + R + 2S + 4U + 2W + 3\Sigma - 3\Omega) = 1{\cdot}365 \times 10^5$ dynes per cm.
$b = \frac{1}{2}(Q - R + 2S + 4U - 2W + 9\Sigma + 3\Omega) = -0{\cdot}683 \times 10^5$,,
$v_{lim} = 12100$ metres per sec.

The classical theory of elasticity leads to expressions for the velocities of propagation of longitudinal and transverse waves in a cubic crystal in terms of its three elastic constants C_{11}, C_{12} and C_{44}, and ρ its density. The expressions in the case of the cubic, dodecahedral and octahedral directions are $v = \sqrt{\chi/\rho}$ where χ is the quantity shown in the last column.

Cubic	Longitudinal	C_{11}
Cubic	Transverse	C_{44}
Dodecahedral	Longitudinal	$\frac{1}{2}(C_{11} + C_{12} + 2C_{44})$
Dodecahedral	Transverse	C_{44}
Dodecahedral	Transverse	$\frac{1}{2}(C_{11} - C_{12})$
Octahedral	Longitudinal	$\frac{1}{3}(C_{11} + 2C_{12} + 4C_{44})$.
Octahedral	Transverse	$\frac{1}{3}(C_{11} - C_{12} + C_{44})$.

Theory thus shows that there are two transverse velocities possible for any dodecahedral direction and that one of them is the same as the transverse

velocity along a cube direction. It is gratifying to note that the above calculations lead to two different transverse velocities for any dodecahedral direction, and that one of them in which the direction of motion is along a cube axis is the same as the velocity of transverse vibrations along a cube direction. That this agreement is not accidental is shown by the fact that in spite of the two formulæ being different, the phase-wavelengths of the vibrations also being different, the limiting velocities come out to be the same.

The Table below reproduces the velocities of acoustic waves calculated above together with those calculated from the elastic constants of diamond determined experimentally by Bhagavantam and Bhimasenachar (1946). It will be seen that in the case of the longitudinal vibrations the agreement is best for the cubic planes, the calculated value being only about 3% lower than the experimental. For the dodecahedral planes the value obtained is about 4% higher than the value calculated from experimental data, while for the octahedral planes it is about 25% higher. It was already explained in an earlier section that the distant interactions have to be considered to make accurate calculations of the velocity. As will be seen from the calculations above, we have considered in the cubic case, the interaction of three planes on either side of the one under consideration, while in the dodecahedral case we were obliged to consider only two. In the octahedral case, only one set of double-layers on either side of the double-layer under consideration is taken account of. It is probable that a consideration of the influence of some more layers of atoms might yield better results in the latter two cases.

Acoustic wave-velocities in diamond

Oscillating planes	Direction of oscillation	Velocity from force-constants	Velocity from elastic-constants
		metres per sec.	metres per sec.
(100)	[100]	15900	16400
"	[001] or [010]	14300	10800
(110)	[110]	18300	17700
"	[001]	14300	10800
"	[1$\bar{1}$0]	10900	8900
(111)	[111]	22300	17700
"	[01$\bar{1}$]	12100	9500

The agreement in the case of all the transverse modes is much worse, the discrepancy being nearly 25 to 30% in all the cases. This should also

be not surprising in view of the remarks about distant interactions already made in a previous section and in view of the fact that the interaction between any two atoms is large when the displacement in question involves a change in the distance between the interacting atoms and small when it does not involve a change in the distance. Therefore, a transverse vibration is likely to be much more influenced by the interaction of distant atoms in the plane under consideration and in neighbouring planes, than a longitudinal vibration. On the other hand, a longitudinal vibration will be more and more influenced than the transverse by the more and more distant planes.

It can be seen that the velocities calculated from the interatomic force-constants lead to nearly the correct value for C_{11}, too high a value for C_{44} and too low a value for C_{12}.

In conclusion, the author wishes to express his grateful thanks to Prof. Sir C. V. Raman, with whom he had many useful discussions.

Summary

A dynamical method has been described for evaluating the acoustic wave-velocities in different directions in a crystal, from the interatomic force-constants. The method, applied to the case of diamond, yields two transverse velocities for the dodecahedral directions, one of them coming out to be the same as the transverse velocity in a cubic direction. These facts are in full accordance with theoretical expectations.

References

1. Bhagavantam, S., and Bhimasenachar, J. B. .. *Proc. Roy. Soc.*, A, 1946, **187**, 381.
2. Krishnan, R. S. .. *Proc. Ind. Acad. Sci.*, A, 1947, **26**, 399.
3. Raman, C. V. .. *Curr. Sci.*, 1948, **17**, 65.
4. Ramanathan, K. G. .. *Proc. Ind. Acad. Sci.*, A, 1947, **26**, 481.

THE PHOTOELASTIC PROPERTIES OF IONIC CRYSTALS

By Elias Burstein and Paul L. Smith
(Crystal Section, Naval Research Laboratory, Washington, D.C.)

Received November 16, 1948

Abstract.—Recent photoelastic data are used to obtain values of the change in refractive index with density for a series of cubic crystals. These experimental values are found to be smaller than those calculated from either the Lorentz-Lorenz or the Drude equations. The difference between the experimental and calculated values results from a decrease in the molar polarizability with increase in density. In MgO the change in polarizability is relatively large and the refractive index actually decreases with increase in density while the other crystals show an increase. The decrease in molar polarizability with density as measured by the strain-polarizability, λ_0, can be correlated with the amount of homopolar binding and ion overlap in the crystal. It is suggested that an increase in density increases the amount of homopolar binding and ion overlap. Further information about the dynamic changes in polarizability during vibration of the ions can be obtained from the change in refractive index with temperature at constant density and from Raman spectra.

Introduction

As part of a fundamental investigation of the relation between the properties of non-metallic crystals and their atomic structure, a detailed study is being carried out of the photoelastic, thermo-optic and infrared properties of crystals. During Sir C. V. Raman's visit to the United States the authors had several stimulating discussions with him about this work, which was then in progress, and it is with pleasure that they present the results of some of these investigations as a contribution to this special issue dedicated to him.

Although it is not possible as yet to calculate from fundamental considerations either classically or quantum mechanically the effect of interaction between the atoms in a solid on their polarizabilities, one can obtain considerable information about these interactions from data on the change of refractive index with density $dn/d\rho$ (Mueller, 1935; Burstein and Smith, 1948*a*). The $dn/d\rho$ cannot be measured directly but can be calculated from photoelastic constants. Such data yield information about the change in the average polarizability of the atoms with change in equilibrium interatomic distance resulting from a homogeneous deformation.

Background

When an electric field at optical frequencies is applied at the boundaries of an ionic crystal dipole moments are induced in the ions. The effective field at the interior of the dielectric which is acting to polarize the ions is given by

$$\mathbf{E}' = \mathbf{E} - \frac{4\pi}{3}\mathbf{P} + \mathbf{E}_L + \mathbf{E}_C, \tag{1}$$

where E is the applied electric field; P is the polarization of the medium; $\frac{4\pi}{3}\mathbf{P} - \mathbf{E}_L$ is the Lorentz-Lorenz field contributed by the surrounding dipoles; and $\mathbf{E}_C$ is the Coulomb field contributed by the surrounding ions acting on the displaced charge.

The polarization of the medium is related to the applied electric field by the relation

$$\mathbf{P} = \frac{\epsilon - 1}{4\pi}\mathbf{E}, \tag{2}$$

where ϵ is the dielectric constant at the frequencies of the applied field.

The dipole moment μ_i induced in an ion of type i is given, to a first approximation, by the linear equation

$$\mu_i = \alpha_i \mathbf{E}', \tag{3}$$

where α_i is the polarizability of the i type ion. The μ_i's, E and P are vectors while the α_i's and ϵ are second-order tensors.*

The polarization of the medium can also be defined in terms of the dipole moments induced in the ions by the effective field

$$\mathbf{P} = \Sigma N_{Vi}\mu_i = \rho\Sigma N_{Gi}\mu_i, \tag{4}$$

where N_{Vi} is the number of i type atoms per unit volume; ρ is the density and N_{Gi} is the number of atoms per gram.

In cubic crystals the $\mathbf{E}_L$ and $\mathbf{E}_c$ contributions are zero to a first approximation. The effective field for such crystals is given by

$$\mathbf{E}' = \mathbf{E} - \frac{4\pi}{3}\mathbf{P} \tag{5}$$

and the induced moment is given by

$$\mu_i = \alpha_i\left(\mathbf{E} - \frac{4\pi}{3}\mathbf{P}\right). \tag{6}$$

* Only the real part of the polarizability will be considered here since the discussion will be limited to frequencies for which the crystal is transparent.

By combining equations, one obtains the well-known Lorentz-Lorenz equation for the molar polarizability or refractivity of a cubic crystal in terms of the refractive index, n_0,

$$V_M \left(\frac{n_0^2 - 1}{n_0^2 - 2}\right) = \frac{4\pi}{3} N_A \Sigma N_{Mi} \alpha_i = R, \tag{7}$$

where V_M is the molar volume, n_0 is the refractive index, N_{Mi} is the number of i type ions per molecule, and N_A is the Avogadro number.

E_L and E_c do contribute to the effective field in crystals which do not have cubic symmetry and their magnitudes will in general be different along the three principal axes of the crystal. This is also true for deformed cubic crystals where the cubic symmetry of the lattice is destroyed. The magnitude of the L–L and Coulomb fields will depend on the magnitude and type of deformation. The change in refractive index resulting from an elastic deformation will, therefore, depend on the magnitude of these fields and on the change in density.

Photoelastic Theory

In developing his theory of photoelasticity Banerjee (1927) took into account the L–L field resulting from the deformation of the cubic symmetry, but neglected the Coulomb field. Following Fajans and Joos (1924) who showed that the polarizabilities of the ions are smaller in the crystal than in the independent gaseous state, Banerjee considered that a further decrease in volume decreased the polarizability still further. He therefore included in his calculations the change in polarizability of the ions with strain but neglected to treat the polarizability as a second-order tensor. In another theoretical treatment Herzfeld and Lee (1933) took into account the Coulomb field as well as the L–L field in the deformed crystal but neglected the change in the polarizability of ions with strain. All three factors; the L–L field, the Coulomb field and the change in polarizability of the ions with strain were properly considered by Mueller (1935) who was able to explain qualitatively the magnitudes and signs of the photoelastic effects of the few crystals whose constants were known at that time. His theory does not permit quantitative predictions of the photoelastic properties since it requires empirical values of the optical strengths and polarizabilities, which are available for only a few crystals and the strain-polarizability constants of the ions which are not available. Mueller's theory is, however, useful for determining the change in polarizability of the ions with strain since there is no way as yet for calculating the strain polarizability constants from fundamental considerations. Given the optical strengths and polarizabilities of the ions one can calculate the L–L and Coulomb contributions by means

of this theory. The strain polarizability constants can then be calculated from these contributions and the photo elastic constants.

For the changes in refractive index caused by hydrostatic pressure the theory is considerably simplified since the cubic symmetry of the crystal is maintained and E_L and E_c remain zero. Therefore, one need only consider the changes in the polarizability of the ions with interatomic distance and the change in density. Following Mueller, the change in molar polarizability with strain (homogeneous displacement of the ions) is represented by a set of phenomenological strain polarizability constants λ defined by the relation

$$\mathbf{R} = \mathbf{R}_0(1 + \lambda S), \tag{8}$$

where $\mathbf{R}_0$ is the molar polarizability for the undeformed crystal; $\mathbf{R}$ is the molar polarizability of the deformed crystal and S is the strain. For the higher symmetry cubic crystals there are only three constants λ_{11}, λ_{12}, and λ_{44}, analogous to the strain optical constants p_{11}, p_{12}, and p_{44}. The change in molar polarizability due to a hydrostatic deformation $d\mathrm{V}/\mathrm{V}_M$ is determined by

$$\mathbf{R} = \mathbf{R}_0\left(1 + \lambda_0 \frac{d\mathrm{V}}{\mathrm{V}_M}\right) = \mathbf{R}_0\left(1 - \lambda_0 \frac{d\rho}{\rho}\right) \tag{9}$$

where
$$\lambda_0 = (\lambda_{11} + 2\lambda_{12})/3 \tag{10}$$

The change in refractive index due to a change in density results from a change in the number of ions per unit volume and a change in the polarizability of the ions and is given by

$$\frac{dn}{d\rho} = \left(\frac{\partial n}{\partial \rho}\right)_{\mathrm{R}} + \left(\frac{\partial n}{\partial \mathbf{R}}\right)_{\rho} \frac{d\mathbf{R}}{d\rho}. \tag{11}$$

The change in refractive index with change in density calculated from the L–L equation gives the first term in equation (11), since, in deriving the L–L equation, the polarizability of the ions was assumed to be constant and independent of the density. The total change in refractive index with density can be written as

$$\frac{dn}{d\rho} = (1 - \lambda_0)\frac{(n_0^2 + 2)(n_0^2 - 1)}{6n_0\rho} = (1 - \lambda_0)\left(\frac{\partial n}{\partial \rho}\right)_{\mathrm{R}}. \tag{12}$$

The experimental value of $dn/d\rho$ can be calculated from the photoelastic constants p_{11} and p_{12} (Pockels, 1906) by means of the relation

$$\frac{dn}{d\rho} = \frac{n_0^3(p_{11} + 2p_{12})}{6\rho} \tag{13}$$

Values of λ_0 can therefore be calculated from the experimental values of $dn/d\rho$ and the $(\partial n/\partial \rho)$ calculated from the L–L equation.

Using these relations, Mueller calculated the λ_0 for NaCl, CaF_2 and KCl.* Within the accuracy of the data, these crystals were found to have the same λ_0 value (approximately 0·5). On the basis of these results Mueller assumed that other crystals would have similar λ_0 values. Calculations based on recent photoelastic data (Burstein and Smith, 1948) show, however, that λ_0 varies considerably from crystal to crystal and that Mueller's assumption concerning the strain polarizability contribution to the photoelastic constants must also be modified to take into account structure effects.

Experimental Data

The available data on $dn/d\rho$ calculated from photoelastic data by means of equation (13), $(\partial n/\partial\rho)_R$ calculated from the L–L equation, and λ_0 calculated from these quantities by means of equation (12) are given in Table I. Data for diamond which is completely homopolar are also included.

Table I

Crystal	n_D	$\rho\left(\frac{dn}{d\rho}\right)_{obs.}$	L—L Equation			Drude Equation		
			$\rho\left(\frac{\partial n}{\partial\rho}\right)_{calc.}$	λ_0	$\frac{\Delta R‡}{R}$	$\rho\left(\frac{\partial n}{\partial\rho}\right)_{calc.}$	λ_0	$\frac{\Delta R‡}{R}$
LiF ..	1·392	0·1	·44	~·7	·16	·34	~·7	−·12
NaCl ..	1·544	0·24	·66	·63	·15	·45	·47	−·26
KCl ..	1·490	0·23	·58	·61	·05	·41	·44	−·29
KBr ..	1·559	0·35	·68	·48	·02	·46	·24	−·38
KI ..	1·667	0·44	·85	·48	·02	·53	·19	−·45
MgO ..	1·736	−·4	·97	~1·4	·76	·52	~1·8	·41
CaF_2 ..	1·434	·25	·50	·50	·02	·37	·32	−·31
Diamond*	2·417	1·24	2·62	·53	..	1·00	·24	..
K-alum†	1·456	·50	·53	·06	..	·38	·31	..

* Ramachandran (1947 *a*), Burstein and Smith (1948 *b*)

† Bhagavantam and Suryanaryana (1947)

‡ The R_f values used to calculate $\frac{\Delta R}{R}$ are taken from Pauling (1927).

The experimental values of $dn/d\rho$ are in every case smaller than the values of $(\partial n/\partial\rho)_R$ calculated from the L–L equation. In MgO an increase in density actually decreases the refractive index; the contribution from the decrease in polarizability of the ions is greater than the contribution from the change in the number of ions per unit volume. MgO is unique in this respect. Of the alkali halides studied thus far, LiF has the largest change in polarizability of the ions with change in density. Diamond, which is completely homopolar, and CaF_2 have λ_0 values which are about the same

* The $dn/d\rho$ for KCl was estimated from dn/dT data.

as those of the alkali halides, while K-alum has the smallest λ_0 of the cubic crystals studied thus far.

Discussion

A physical picture of the significance of λ_0 can be obtained by comparing the molar polarizability of the ions in the gaseous state R_g with that of the ions in the undeformed crystals R_s. The difference in these quantities as measured by $\frac{\Delta R}{R_{AV.}} = \frac{R_g - R_s}{R_{AV.}}$ is also given in Table I. The ΔR corresponds to the overall change in molar polarizability of the ions in going from the independent gaseous state to the solid state and is a measure of the amount of overlapping of the ions in the unstressed solid. The λ_0 then represents the further change in polarizability as the density of the solid is changed. That is, it corresponds to the slope of the relative molar polarizability *vs.* density curve for the solid at a given temperature. This curve is given schematically in Fig. 1 for ionic crystals. The R and λ_0 values are indicated on the curve for crystals in which (*a*) the interaction between the ions is small (ionic bonding, ΔR small and $\lambda_0 < 1$), (*b*) the interaction is appreciable (intermediate ionic and homopolar bonding, ΔR large and $\lambda_0 > 1$) and (*c*) the interaction is complete (homopolar bonding, ΔR large and $\lambda_0 < 1$).

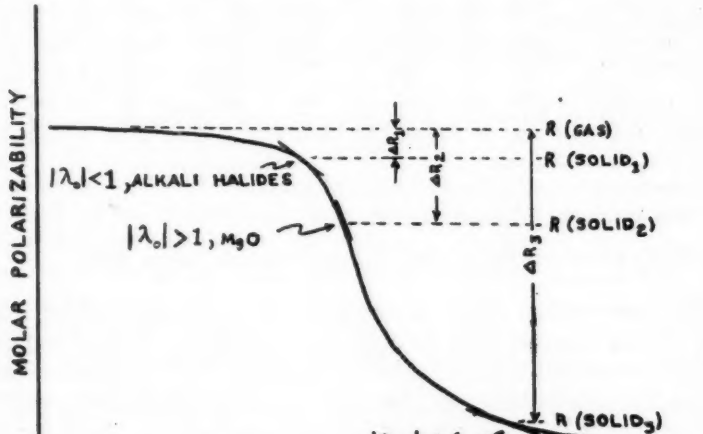

Fig. 1

Fajans and Joos (1924) attributed the change in the polarizability of the ions in going from the gaseous state to the solid state and the non-addivity

of the polarizabilities of the ions in solids to Coulomb deformations of the ions by its neighbours. This was indicated by the fact that ions with small radii and large charge produced the largest effects. Mueller (1935), however, has suggested that since a change in molar polarizability is found in homopolar solids, changes in polarizability are due to changes in the energy levels and transition probabilities of the optical electrons.

The new λ_0 data suggest further that the change in polarizability with interatomic distance in ionic crystals is due primarily to a change in the amount of ion overlapping and, therefore, to a change in the relative amount of ionic and homopolar bonding (non-central force interactions between the ions). The magnitude of these changes will, therefore, depend on the amount of overlapping and homopolar bonding already present in the unstressed crystal, which accounts for the large variation in λ_0 from crystal to crystal.

In addition to the change in polarizability due to a change in the character of the bonding, there is also a contribution due to the tightening of shared electrons in homopolar crystals, as shown by the data for diamond and by the calculation on the change in polarizability of the hydrogen molecule with change in interatomic distance (Wang, 1930).

In crystals which contain radicals the interatomic distances within the radicals are not appreciably altered when the crystal is deformed by an external stress. Since the major contribution to R comes from these groups, changes in R with density will be small. This is apparently the explanation for the small λ_0 in K-alum, where the contribution to R comes mainly from the $SO_4^=$ and H_2O groups.

That λ_0 can be correlated with the extent of ion overlapping and homopolar bonding in polar crystals is shown by the data in Table II where they are tabulated for a number of NaCl-type crystals together with other properties known to be associated with homopolar bonding, such as the deviations of the elastic constants from Cauchy relations and the coefficient of expansion. The deviations from the Cauchy relation are a measure of the non-central forces resulting from ion overlapping and homopolar bonding (Löwdin, 1947). Although this does not always show up, as in diamond where the Cauchy relations appear to hold, they are of value when comparing different NaCl-type crystals with one another. Thus we find that the deviation from the Cauchy relations is considerable in both MgO and LiF. Additional evidence for the existence of appreciable overlapping between the ions and homopolar bonding in MgO is found in the calculations of the electron distribution about ions from X-ray scattering data (Wollan, 1930)

and X-ray emission band data (O'Brian and Skinner, 1940). Since homopolar bonding in ionic crystals increases the attractive force between the ions and therefore the lattice energy, there will also be a rough correlation between homopolar bonding and such properties as thermal expansion, Debye temperature and melting point. These are also given in Table II.

TABLE II

Crystal	λ_0	C_{44}/C_{12}	$\gamma \times 10^4$	θ°k	Tm.p.°k
LiF ..	·7	1·4	10·2	..	1140
NaCl ..	·63	·9	12·0	280	1070
KCl ..	·61	1·0	11·4	230	1050
KBr ..	·48	1·1	12·0	180	1000
KI ..	·48	1·0	13·5	130	955
MgO ..	1·4	1·8	3·9	770	3070

λ_0 = strain polarizability constant for hydrostatic pressure;
C_{44}/C_{12} = ratio of elastic constants (the Cauchy relations are $C_{44}/C_{12} = 1$);
γ = cubical coefficient of expansion;
θ = Debye temperature;
$T_{m.p.}$ = melting point.

It has been shown from quantum mechanical considerations that the L–L equation is valid only for solids in which the atoms are arranged in a lattice with cubic symmetry and can be treated as harmonic oscillators. Classically this condition is satisfied by point-like ions. It is apparent that as a result of ion overlapping and homopolar binding this condition is not satisfied for the alkali halides. The effective field acting to polarize the ions will not be given simply by equation (5) but will contain additional terms which depend on the amount of ion overlapping and homopolar binding and which will vary from crystal to crystal.* Attempts to derive expressions for the refractive index which take such terms into account lead to expressions which are intermediate between the L–L and the Drude equations. The Drude equation, in which the L–L field is neglected, can be written in the form

$$V_M(n_0^2 - 1) = 4\pi N_A \Sigma N_{Mi} \alpha_i = 3R_D. \qquad (14)$$

The λ_0 and $\Delta R/R$ values calculated from $dn/d\rho$ and $(\partial n/\partial \rho)_R$ by means of the Drude equation which represents one limiting case are also given in Table I for comparison with those obtained from the L–L equation as the

* The concept of individual ion polarizabilities loses its meaning in crystals with homopolar bonding. One should use a polarizability of the crystal per unit cell rather than per ion.

other extreme. The magnitude and sign of λ_0 calculated from the two equations show the same trend. It appears therefore that, although the form of the refractive index equation may influence the magnitude of λ_0 it is still a useful measure of the change in polarizability with density. On the other hand, the values of $\frac{\Delta R}{R}$ calculated from the two equations are quite different. The Drude equation leads to relatively large negative values of $\frac{\Delta R}{R}$ while the L–L equation leads to positive values.* Since λ_0 is positive for the crystals considered here one would expect the $\Delta R/R$ to be positive. This indicates that the proper form of the refractive index equation may be closer to the L–L equation than to the Drude equation.

Concluding Remarks

Numerous attempts have been made to fit the data for the refractive index of crystals at different wavelengths into dispersion formulæ. By adjusting arbitrary constants it has been possible to get the different types of dispersion equations into good agreement with the data (Ramachandran, 1947). Since however, the physical validity of the form of the equation cannot be verified, no attempt will be made to discuss the significance of λ_0 in terms of a detailed dispersion equation. Instead, the changes in polarizability resulting from changes in density will be discussed qualitatively in term of the factors which determine the magnitude of the polarizability. For purposes of discussion one need only assume that the combined polarizability of the positive and negative ions can be represented by an equation of the form

$$a = C \Sigma \frac{f_{0k}}{\nu_{0k}^2 - \nu_k^2}, \tag{15}$$

where ν_{0k} is a dispersion frequency of the crystal and f_{0k} is the corresponding optical strength or transition probability.† This is based on the use of a refractive index equation in which the local field is taken into account. Neglecting the effect of a change in the local field on the calculated λ_0 the decrease in the polarizability of an ion with density can result from a change in either ν_{0k} or f_{0k}. In order to distinguish between the two effects it is necessary to study the change in $dn/d\rho$ with frequency of the applied field.

* λ_0 is less affected than is $\Delta R/R$ by the form of the equation since it represents the slope of the change in R while $\Delta R/R$ depends on the magnitude of R.

† The dispersion frequency corresponds to the absorption frequency of the ions in the absence of the L-L field. The experimentally observed absorption frequency (*i.e.*, when the L-L field is present) is given by

$$\nu_{rk} = \nu_{0k} - \frac{4\pi}{3} \frac{Ne^2 f_k}{m}$$

Obviously if the effect is primarily one of wavelength shift the magnitude of $dn/d\rho$ will depend on the relative position of the dispersion frequencies and the frequency at which the measurements are made. Since the dispersion frequencies for the various crystals are different this may account in part for the variation in the observed values of λ_0.

Although there are no data for the shift in the absorption bands or for changes in the transition probabilities with a change in density, data are available for such changes caused by temperature. Fesefeld (1930) has made a detailed study of the absorption of KI and RbBr in the near ultraviolet as a function of temperature. As the temperature is increased the bands are found to shift toward longer wavelengths and their intensities are decreased. The wavelength shifts for KI calculated from dn/dT data are in agreement with the observed values (Ramachandran, 1947 *b*).

The polarizability of an ion is a function of the instantaneous configuration of the surrounding ions. Since the ions vibrate relative to one another as a result of thermal energy, the polarizability, which is a non-linear function of the interatomic distance will vary periodically in time. The polarizability defined by equation (3) is the time average of the instantaneous values. Its magnitude depends on the non-linear variation of the polarizability with interatomic distance as well as on the value of the instantaneous polarizability of the ions at the equilibrium interatomic distance. The strain polarizability constant λ_0 is a measure of the change in the average polarizability of the ions with change in equilibrium distance.

Information about the instantaneous changes in polarizability of the ions in a crystal during vibration can also be obtained from data on the change in refractive index with temperature at constant density, $(\partial n/\partial \mathrm{T})_\rho$, which is a measure of the change in polarizability of the ions with temperature at constant equilibrium distance and is determined by the change in magnitude of the non-linear terms corresponding to the change in amplitude of vibration of the ions with change in temperature.* Values of $(\partial n/\partial \mathrm{T})_\rho$ cannot be obtained directly but can be calculated by combining data on the total change in refractive index with temperature, dn/dT, with data on $dn/d\rho$ and thermal expansion.

Still further information about the linear and quadratic changes in polarizability which take place during vibration can be obtained from data on Raman spectra intensities. For crystals with NaCl structure, only second-

* In his papers on thermo-optic properties of solids, Ramachandran (1947 *b*) does not separate the effect of density and the effect of temperature on the polarizability.

order Raman spectra are observed since the optical vibrations are symmetrical and the linear changes in polarizability are zero. Measurements on NaCl show that the zero order spectra are quite weak (Krishnan, 1947). Measurements of the intensity of the second-order Raman spectra of MgO and LiF would be of particular value for correlation with λ_0 data.

The investigation of the photoelastic and thermo-optic properties of crystals and their dependence on temperature is being continued at this laboratory, and is being supplemented by a study of Raman and infrared spectra.

The authors wish to acknowledge the assistance of Mrs. Bertha W. Henvis in making many of the calculations used in this paper.

References

1. Banerjee, K. .. *Ind. J. Phys.*, 1927, **2**, 195.
2. Bhagavantam, S., and Suryanarayana, S. .. *Proc. Ind. Acad. Sci.*, A, 1947, **26**, 97.
3. Burstein, E. and Smith, P. L. *Phys. Rev.*, *a*, 1948, **74**, 229; *b*, 1948, **74**, Dec. 15 issue.
4. Fajans, K., and Joos, G. .. *Zeit. f. Physik.*, 1924, **23**, 1.
5. Fesefeld, H. .. *Ibid.*, 1930, **64**, 623.
6. Herzfeld, K. F., and Wolf, K. L... *Ann. d. Phys.*, 1925, **78**, 35.
7. Krishnan, R. S. .. *Proc. Ind. Acad. Sci.*, A, 1947, **26**, 419.
8. Löwdin, P. .. *Diss., Upsala, Sweden, Arkiv f. Mat. Ast. o. Fys.*, 1947, **39**, A, 1.
9. Mueller, H. .. *Phys. Rev.*, 1935, **47**, 947.
10. O'Bryan, H. M., and Skinner, H. W. B. *Proc. Roy. Soc.*, A, 1940, **176**, 229.
11. Pockels, F. .. *Lehrbuch der. Kristalloptik*, 1906, *Leipzig*.
12. Ramachandran, G. N. .. *Proc. Ind. Acad. Sci.*, A, *a*, 1947, **25**, 208; *b*, 1947, **25**, 481.
13. Wollan, E. O. .. *Phys. Rev.*, 1930, **35**, 1019.
14. Wang, S. C. .. *Phys. Zeit.*, 1928, **26**, 663.

THE INFRARED PROPERTIES OF MAGNESIUM OXIDE AND THEIR INTERPRETATION

By Elias Burstein, John J. Oberly
(Crystal Section, Naval Research Laboratory, Washington, D.C.)
AND
Earle K. Plyler
(National Bureau of Standards, Washington, D.C.)

Received November 16, 1948

Abstract.—New determinations of the infrared absorption and reflection curves of magnesium oxide show that these curves do not differ in form from those of other NaCl-type crystals. Detailed comparison of MgO with LiF, NaF, NaCl, and KCl, for which accurate data are available, reveals a correlation between the amount of coupling of vibrational modes and the amount of homopolar bonding and ionic overlapping. It is suggested that the coupling is primarily associated with the change in polarizability of the ions during vibration rather than with anharmonic vibrations as proposed by existing theories.

Introduction

The infrared properties of ionic crystals depend on the vibration of the ions relative to one another and thereby on the interaction between these ions. Photoelastic studies (Burstein and Smith, 1948 *a*, *b*) show that an increase in density decreases the refractive index of magnesium oxide as a result of a relatively large decrease in the polarizability of the ions. The alkali halides, on the other hand, exhibit an increase in refractive index and a correspondingly smaller decrease in the ionic polarizabilities when the density is increased. The large change in ionic polarizability in MgO can be attributed to the considerable overlapping of the ions and to the partially homopolar character of their bonding. There is less overlapping of ions in the alkali halides and the bonding is correspondingly more ionic. This is borne out by other evidence for partially homopolar bonding in MgO such as the large deviation of its elastic constants from the Cauchy relations (Durand, 1936). The infrared properties of MgO were therefore investigated in order to see whether they could also be correlated with the overlapping and the partially homopolar bonding of the ions.

Data in the literature on the infrared properties of MgO are incomplete and contradictory. Tolksdorf (1928), studying the transmission of thin

films of powdered MgO held between plates of sodium chloride, observed absorption bands at 3·85, 7·65 and 14·2 microns. Strong (1931), using reststrahlen, found that a fumed layer of MgO showed strong absorption in the neighbourhood of 23 μ and that a cleavage plate of MgO showed 80 per cent. reflection at this wavelength. Fock (1934), measuring the transmission of MgO fumed onto nitrocellulose films, found a strong absorption maximum at 17·3 μ with minor maxima at 14·9 and 25 μ.

A more detailed study was then made by Barnes, Brattain and Seitz (1935) (hereafter referred to as B–B–S) of the transmission of thin cleavage plates of MgO, as well as thin films of MgO evaporated under vacuum onto nitrocellulose and layers of MgO fumed onto plates of NaCl. Using a NaCl prism spectrometer, they observed a large number of narrow, weak absorption bands starting at 6 μ. They also obtained a reflection curve for a cleavage plate which showed two sharp reflection peaks at 14·8 and 15·3 μ.

In attempting to explain the complex secondary structure observed by B–B–S in the transmission curves of MgO, Seitz pointed out in the theoretical section of the paper that, since the elastic constants of MgO exhibited considerable deviation from the Cauchy relations, its properties could not be completely calculated from a model using central force interactions between the ions. He, therefore, used a more general potential function and treated the crystal as a three-dimensional, quantum mechanical system of interacting particles. The results of these calculations indicated that the crystal should exhibit a complex absorption spectrum. It was not possible, however, to obtain any correlation of the theory with the experimental data since the position of the fundamental absorption band was not known and since data on the numerous secondary bands were incomplete because of temperature broadening and the low resolving power of the spectrometer employed by Barnes and Brattain.

From the B–B–S data on single crystals it appears that the infrared properties of MgO differ considerably from those of the alkali halides which also have NaCl structures. For example, their MgO reflection curve as reproduced in Fig. 1 contains two adjacent, sharp peaks, whereas curves for the alkali halides show one broad major peak and a narrower minor peak at shorter wavelengths. In addition, their MgO transmission curves (Fig. 2) show considerably more secondary structure than those of the alkali halides in the corresponding wavelength regions.

Examination of the transmission curves obtained by B–B–S showed that the curves for the various thicknesses differed among themselves in the position and appearance of the secondary bands in a manner that did not

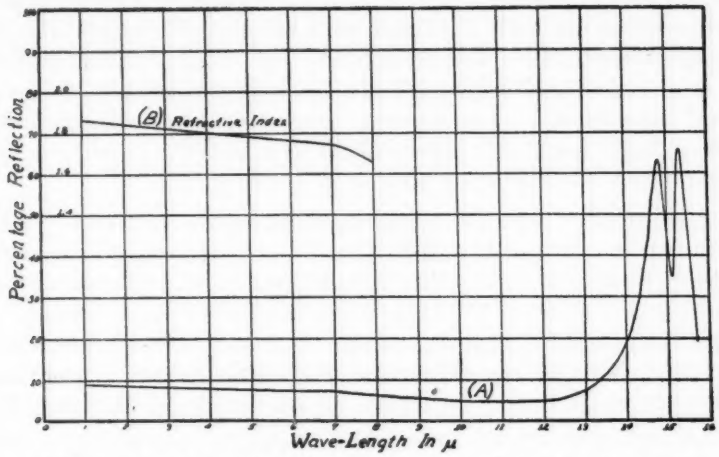

FIG. 1. (A) Reflection of a crystal of MgO ; relative to a silver mirror Barnes, (Brattain and Seitz, 1935).

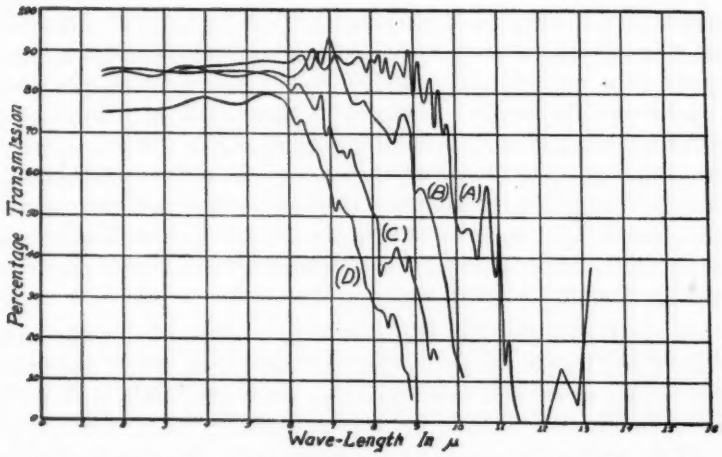

FIG. 2. Transmission of cleaved plates of MgO ; (*a*) 0.12 mm., (*b*) 0.47 mm., (*c*) 1.75 mm., (*d*) 3.05 mm. (Barnes, Brattain and Seitz, 1935).

seem attributable to a thickness factor as suggested by B–B–S. In view of the uncertainty concerning the validity of the B–B–S data and the considerable differences found between MgO and other NaCl-type crystals, it was decided to repeat the measurements and to extend them to longer wavelengths by means of KBr and TlBr–I prisms. Data on the transmission

and reflection of cleavage plates of MgO have been obtained at room temperature and the measurements are now being extended to thin films and low temperatures.

Experimental Procedure and Results

The infrared transmission and reflection measurements were made with Perkin-Elmer spectrometers employing NaCl, KBr, and TlBr–I (Plyler, 1948) prisms and appropriate shutters and reflection filters to minimize errors due to scattered light. Continuous records of the data as a function of wavelength were obtained by means of electronic amplifiers and recorders.

A simple modification of the pre-slit optical system (Fig. 3) was employed for reflection measurements. The image of a globar source is focused

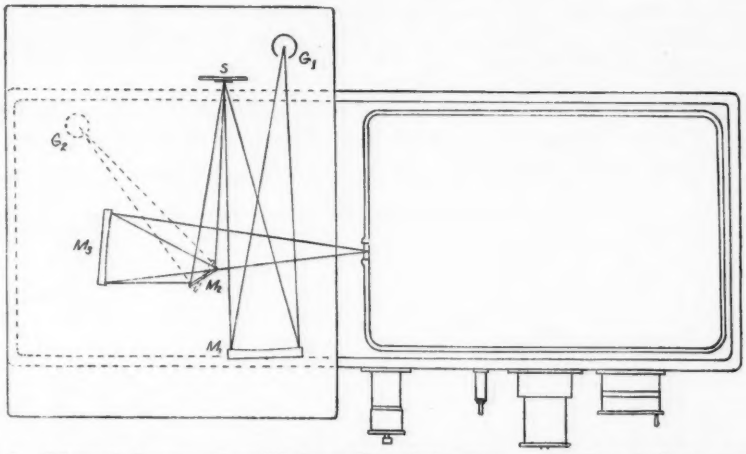

Fig. 3. Schematic layout of modified pre-slit optical system. Full lines indicate new light path for reflection measurements. The components are : G_1 and G_2, globar sources ; M_1 and M_2, concave mirrors ; M_3, plane mirror ; S, sliding holder for sample and reference mirror.

at the reflection sample holder at an angle of incidence of 10°. The reflection sample or the aluminum comparison mirror thus acts as a virtual source which is then focused on the entrance slit. Small samples can be used by locating them at a focus in this manner. Either the sample or the aluminum reference mirror can be moved into the beam by means of a simple slide mechanism. The new components (a globar source, concave mirror and sample holder) are mounted on a plate with appropriate cutouts so that it can be put into position without disturbing the original source, plane mirror, and concave mirror that are supplied with the instrument.

This enables the instrument to be used for either transmission or reflection measurements. In order to change from one type of measurement to the other, it is only necessary to switch the power to the appropriate globar and to rotate the plane mirror (or reflection filter) M_2. The reflection components are also useful for transmission measurements, especially when two reflection filters are required to minimize scattering errors. For this purpose a second reflection filter is placed in the reflection sample holder.

Transmission measurements were made on a series of MgO plates with thicknesses ranging from 0·09 to 9·0 mm. which were cleaved from a number of crystals obtained from The Norton Company, Worcester, Mass, U.S.A. Relative spectral reflection curves were obtained by comparing the reflection from freshly cleaved surfaces of MgO with that from an aluminum mirror. In all cases there was very good agreement between the data obtained with a given sample by the Naval Research Laboratory and the National Bureau of Standards.

Transmission curves of cleavage plates of different thicknesses (0·09 to 9 mm.) at room temperature are given in Fig. 4. Absorption bands are found at 8·3, 10·18, and 11·82 μ and there are indications of very weak

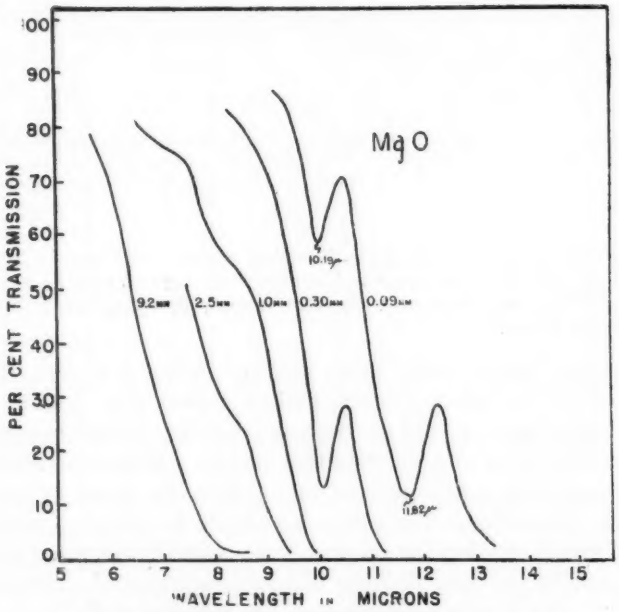

FIG. 4. Transmission of five cleavage plates of MgO.

bands at shorter wavelengths. The absorption bands are broad and not at all like the fine structure observed by B–B–S.

The possibility that these bands may be due to impurities was checked by calculating the absorption coefficient $\left(k = -\frac{1}{d} ln \frac{I}{I_0}\right)$ from the transmission data for plates cleaved from several original crystals. The values of the coefficient for the different samples were found to agree with one another within the experimental error. On the other hand, large differences in ultraviolet transmission were observed for the different samples in the region of 2,000 to 3,000 Å, indicating that there were considerable differences in impurity content. It is reasonable to conclude from the agreement in the infrared absorption coefficient for the different samples that the bands in the infrared are not due to impurities but to MgO itself.

The reflection curve of a freshly cleaved surface of MgO relative to aluminum is given in Fig. 5. The reflection increases rapidly beyond 13 μ,

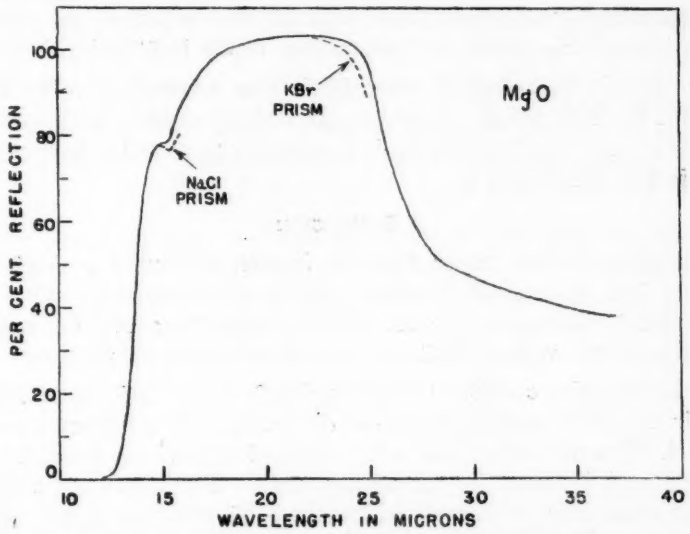

FIG. 5. Reflection curve of MgO cleavage surface relative to an aluminum mirror.

levels off briefly at about 15 μ and rises again at 16 μ until a peak is reached at approximately 22 μ after which the curve falls off rapidly beyond 24 μ. Data obtained with the NaCl prism in the region of 15·5 μ show a slight dip of a few percent. which is not found when using the KBr prism. This dip can be attributed to the lack of complete correction for scattering since the NaCl prism begins to absorb strongly in this region. Similarly the data

obtained with the KBr prism show lower values above 23 μ than the data obtained with the TlBr–I prism because the scattering error is magnified by the decreased transmission of the KBr prism. Scattering errors do not become appreciable in the TlBr–I prism until a wavelength of 35 μ is reached.

The numerous, narrow secondary bands in the data obtained by B–B–S could be due to errors likely to occur in their point-by-point method of measurement in which the sample was alternately moved into and out of the beam, and could also be due to interference bands. The present data are less subject to these errors because the continuous method of recording data is more reliable and the large angular aperture of the Perkin-Elmer spectrometer reduces the chance of obtaining interference bands. The absence of fine structure was confirmed by measurements made with a large recording infrared spectrometer of much higher resolving power.*

The double reflection peak found by B–B–S in the region of 15 μ appears to be due to errors resulting from scattered light which are appreciable in the region of the CO_2 absorption band at 14·97 μ and in the wavelength region beyond 15 μ where the transmission of the NaCl prism is low.

As seen in the reflection curve, MgO is an excellent reflection filter for use with the KBr prism. However, since single crystals with large cross-sections are not readily available, it is necessary to place the filter at a focus point in the optical system.

Discussion

According to the present data, the infrared properties of MgO do not differ in form from those of other sodium chloride-type crystals. Nevertheless definite differences become apparent when the absorption and reflection curves of the various NaCl-type crystals are compared with one another.

The absorption coefficient curves for MgO and for LiF and NaF (Hohls, 1937) in the short wavelength region of their absorption spectra are given in Fig. 6. Two well-defined secondary absorption peaks are found for MgO; only one peak is found for the other crystals. The absorption coefficients have the same order of magnitude, but the MgO peaks are more prominent and broader. The 11·82 μ peak in MgO also shows additional structure.

The reflection curves of MgO, and of LiF, NaF, NaCl and KCl for which accurate data are available (Hohls, 1937), are plotted on a logarithmic wavelength scale in Fig. 7. The major reflection peak is highest in MgO. The

* The authors are indebted to Dr. D. C. Smith and Mr. R. A. Saunders of the Chemistry Division of the Naval Research Laboratory for making these measurements on their large prism spectrometer.

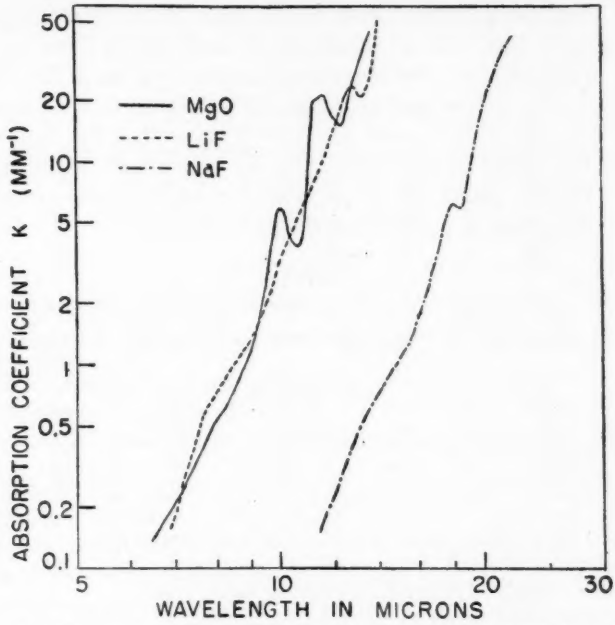

FIG. 6. Absorption coefficients of MgO and of LiF and NaF (Hohls, 1937).

$$k = -\frac{1}{d} \text{ en } \frac{1}{10}$$

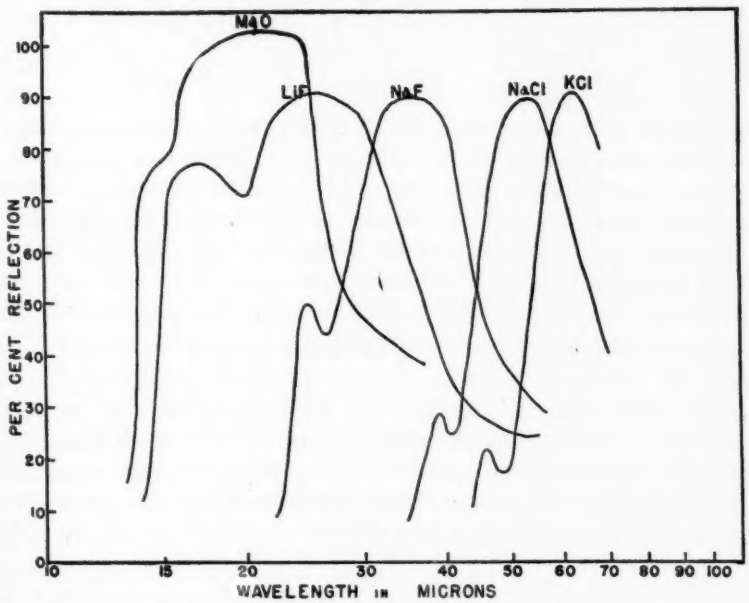

FIG. 7. Reflection of MgO and of some alkali halide crystals (Hohls, 1937) relative to an aluminum mirror.

fractional band width (width/peak wavelength) of the MgO major peak is probably smaller than that of LiF, but it is much larger than the values for the other alkali halides; the same relationship is present for the ratio of the heights of the minor and major peaks (minor peak/major peak). The values of these quantities given in Table I show that the fractional band widths and the height ratios decrease in the order LiF, MgO, NaF, NaCl and KCl. The two peaks are not separated in MgO as they are in the other crystals, so its values are less accurate than the others.

TABLE I

Crystal	Fructional Band Width	Height Ratio	Major Peak Wavelength μ	Minor Peak Wavelength μ
MgO ..	~·43	~·7	~22	~16
LiF ..	·46	·85	26	17
NaF ..	·34	·56	36	25
NaCl ..	·28	·32	53	39
KCl ..	·18	·25	63	46

Fractional band width = width of major peak in microns at 0·8 of peak height / wavelength of peak;

Height ratio = height of minor peak/height of major peak.

Without going into a detailed mechanism of infrared absorption, one can conclude from the broad reflection curve, the secondary bands in the absorption spectrum and the high auxiliary reflection peak of MgO that there is considerable coupling between the modes of vibration of its ions. This coupling is apparently more extensive in MgO and LiF than in the other crystals and decreases in the order NaF, NaCl and KCl.

A similar trend is found in these crystals for homopolar bonding and ion overlapping (Burstein and Smith, 1948 *b*). Therefore, it appears that the extent of coupling between modes of vibration can be correlated with these quantities. The relative amount of homopolar bonding in these crystals is shown in Table II by values of the strain polarizability λ_0 (change in molar polarizability with density) and the deviation of the elastic constants from the Cauchy relation. Data for NaF are not yet available.

Existing classical and quantum mechanical treatments of the coupling between the modes of vibration in crystals (Born and Blackman, 1933; Blackman, 1933; Barnes, Brattain, and Seitz, 1935; Raman, 1947) have attributed the secondary bands in the absorption spectra of ionic crystals to the anharmonic vibration terms (cubic and higher order terms in the potential function). These terms were introduced phenomenologically into

TABLE II

Crystal	λ_0	$\left\lvert \frac{C_{44}}{C_{12}} - 1 \right\rvert$	$\alpha \times 10^5$	θ °K.	$\sqrt{\mu^2}$ Å.
MgO ..	1·4	0·4	13	770	..
LiF ..	·7	0·3	34	..	..
NaF ..	..	..	36	440	·18
NaCl ..	·6	0·1	40	280	·24
KCl ..	·6	0·0	38	230	·26

λ_0 = strain polarizability (change in molar polarizability with density);

$\left\lvert C_{44}/C_{12} - 1 \right\rvert$ = deviation of the elastic constants from the Cauchy relation at room temperature;

α = linear temperature coefficient of expansion;

θ = Debye temperature;

$\sqrt{\mu^2}$ = root mean square of vibration amplitude of ions at 293° K. (Lonsdale, 1948).

the potential energy equation with arbitrary constants since there was no way to calculate them from fundamental considerations. Because of this, there have been no attempts to calculate the intensities and widths of the fundamental and secondary absorption bands from theory. At best it was only possible to show that the existence of secondary bands was not contradictory to the theory, and it was necessary to adjust constants in fitting the theory to the experiment.

According to these theories the coupling between vibrational modes is determined by the magnitude of the anharmonic vibration terms which can be estimated approximately from available data on the temperature coefficient of expansion. This coefficient is directly related to the amplitude of vibration of the ions and thus to the anharmonicity of the vibrations. Values for the coefficient of expansion, the root mean square amplitude of vibration of the ions, and also the Debye temperature for the crystals under consideration are given in Table II. The data shows that those crystals with the larger amount of coupling between vibrations are those with the smaller coefficients of expansion, smaller vibration amplitudes, and the higher Debye temperatures. One can conclude that the anharmonic terms contribute only slightly to the coupling between vibrations at room temperature.

It should be noted that the width of the reflection curves cannot be explained by temperature broadening alone since this broadening would be greater for those crystals with large vibration amplitudes and lower Debye temperatures. The width of the reflection curve is actually greater for the crystals with lower vibration amplitude and higher Debye temperature. The

broad reflection peaks for MgO and LiF can only be attributed to the existence of a number of absorption bands, rather than to temperature broadening. Nevertheless, temperature broadening can partly explain the difference in character of the secondary bands found in the different crystals and the relatively large reflection peak observed in MgO. This is shown, for example, by the increase in height of the major reflection peak in LiF to 100 per cent. when the temperature is lowered to 87° K. (Korth, 1932).

Since the extent of coupling between the modes of vibration in ionic crystals can be correlated with the extent of homopolar bonding, the change in the polarizability with its accompanying change in the charge of the ions during vibration may be one of the important factors in the coupling mechanism (Burstein and Smith, 1948, *b*). That this is plausible can be readily seen from a consideration of the electric moment which determines the transition probabilities for the infrared-active vibrations.

The electric moment in a diatomic ionic crystal can be represented classically by an expression of the form

$$\mathbf{M} = qr,$$

where r is the instantaneous distance between the positive and negative ions and q is the instantaneous charge of the ions. In NaCl-type crystals where the vibrations are symmetrical, only quadratic changes in the polarizabilities manifest themselves. The periodic variations in the polarizabilities of the ions during vibration will, therefore, contain the frequency components $2\omega_1$, $2\omega_2$, $(\omega_1 \pm \omega_2), \ldots$, where ω_1, ω_2, ..., are the frequencies of both active and inactive vibrations. Since the charge of the ions is related to the amount of homopolar bonding and consequently to the polarizability, the charge will also vary periodically at those frequencies.*

Assuming harmonic vibrations, the electric moment is given by an equation of the form

$$\mathbf{M} = q_0 [r_1 \sin \omega_1 t + r_2 \sin \omega_2 t + \ldots.] + r_0 [q_1 \sin 2\omega_1 t + q_{12} \sin (\omega_1 \pm \omega_2) t + q_2 \sin 2\omega_2 t]$$

where r_0, q_0 are the equilibrium distance and the corresponding charge of the ions; r_1, r_2, etc., are displacement amplitudes; and q_1, q_2, q_{12}, etc., are the charge amplitudes.

---

* Owing to overlapping and homopolar bonding, there is some sharing of valence electrons and hence the average charge of the ions is not given simply by the valence. This has been demonstrated by calculations of electron distribution around the ions based on X-ray scattering data (Wollan, 1930). The change in charge with interatomic distance has also been used to explain the large dielectric constants of the heavy-metal halides (Eucken and Büchner, 1934).

Since the electric moment determines the transition probability and the intensity of absorption, the terms in the first bracket correspond to fundamental absorption bands due to active vibrations. The terms in the second bracket correspond to overtone bands, as well as sum and difference bands of both active and inactive vibrations. These are all included under secondary bands. A given vibration need not be infrared active in order to appear active in the sum and difference bands.

According to this equation the intensities of the secondary bands will depend on the magnitudes of the quadratic changes in the polarizability of the ions which take place during vibration. Data on the magnitude of these quantities is not available, but it seems reasonable to expect that crystals which exhibit relatively large changes in the average polarizability with change in average interatomic distance under homogeneous deformation will also have relatively large quadratic changes. An investigation of the intensities of the second-order Raman scattering of MgO and other NaCl-type crystals would yield the magnitude of these quantities more directly.

Although the electric moments and transition probabilities can be obtained more exactly from quantum mechanical considerations, the classical treatment employed here can be used qualitatively to describe the coupling mechanism. The major modification to the classical results introduced by quantum mechanics is the fact that the sum and difference bands have different intensities. The terms in the electric moment corresponding to the difference bands will contain a Boltzmann factor and will decrease rapidly in magnitude with decrease in temperature. This effect is analogous to that found for the intensities of the Stokes and anti-Stokes lines in Raman spectra. In addition, the vibration and charge amplitudes will be replaced by quantities which depend essentially on the differences of these amplitudes in the two states between which the transition is taking place. The effect of temperature on the summation bands will depend on the way these quantities change with temperature. The overlapping of the ions and the homopolar bonding increase as the temperature is decreased, so the overtone and summation terms in the electric moment and the corresponding absorption bands should persist even at low temperatures.

A similar equation for the electric moment can be written by including anharmonic vibrations and neglecting the change in charge of the ions. The two equations will be exactly alike in form. However, the physical interpretation of the terms involving the overtone and the sum and difference frequencies will be different. There is no way of distinguishing between the two equations from infrared data alone. This can only be done by correlating the infrared data with that obtained from other measurements.

After establishing the significance of the various terms in the equation, it should then be possible to estimate their magnitude and to make predictions concerning the relative intensities of the absorption bands in different crystals and their dependence on temperature. A complete theory will, of course, include anharmonic vibration terms which are especially important at higher temperatures.*

The suggestions concerning the role played by the strain polarizability in the coupling between vibrations do not depend on the particular mechanism of vibration which leads to infrared absorption. Additional information concerning the dynamic changes in polarizability with change in interatomic distance is needed before it will be possible to calculate exactly the intensities of the fundamental and secondary bands and their wavelengths. Nevertheless it should be possible to estimate the relative intensities of the absorption bands and to predict the effect of temperature. These aspects of the problem will be treated in a later paper which will also give a more detailed discussion of the concepts which have only been qualitatively presented here.

The authors wish to acknowledge Sir C. V. Raman's stimulating interest in this investigation and the valuable discussions they have had with him.

References

Barnes, B. B., Brattain, R., and Seitz, F. .. *Phys. Rev.*, 1935, **48**, 582.

Blackman, M. .. *Z. Physik*, 1933, **86**, 421.

Born, M. .. *Rev. Mod. Phys.*, 1945, **17**, 245.

——— and Blackman, M. .. *Z. Physik*, 1933, **82**, 551.

Burstein, E., and Smith, P. L. .. (*a*) *Phys. Rev.*, 1948, **74**, 229.

.. (*b*) *Proc. Ind. Acad. Sci.*, A, 1948, **28**, 377.

Durand, M. A. .. *Phys. Rev.*, 1936, **50**, 449.

Eucken, A., and Büchner, A. .. *Z. Physik. Chem.*, B, 1934, **27**, 321.

Fock, J. .. *Z. Physik.* 1934, **90**, 44.

Hohls, H. W. .. *Ann. d. Physik*, 1937, **29**, 433.

Korth, K. .. *Gött. Nachr.*, 1932, 576.

Lonsdale, K. .. *Acta Crystallographica*, 1948, **1**, 142.

Plyler, E. K. .. *J. Res. Nat. Bur. Stand.*, 1948, **41**, 125.

Raman, C. V. .. *Proc. Ind. Acad. Sci.*, A, 1947, **26**, 339.

Strong, J. .. *Z. Phys. Rev.*, 1931, **37**, 1565.

Tolksdorf, S. .. *Z. Physik. Chem.*, 1928, **132**, 161.

Wollan, E. O. .. *Phys. Rev.*, 1930, **35**, 1019.

* M. Born (1945) has recently suggested that the secondary bands can be explained quantum mechanically by second-order terms in the electric moment and that anharmonic vibration is not needed.

SPECTRES DE RAMAN DU CHLORURE ET DU BROMURE D'AMMONIUM

PAR LUCIENNE COUTURE ET JEAN-PAUL MATHIEU
(*Laboratoire des Recherches Physiques, Sorbonne, Paris*)

Received November 20, 1948

1. INTRODUCTION

LE chlorure, le bromure et l'iodure d'ammonium se présentent sous plusieurs formes cristallines, dont les domaines d'existence sont séparés par des températures de transition. On a étudié de nombreuses propriétés physiques de ces composés: dilatation,[1] chaleur spécifique,[2] constante diélectrique,[3] piézoélectricité,[4] réfringence,[4] diffraction des rayons X,[5] et des électrons,[6] spectre d'absorption infrarouge,[7] et spectre de Raman.[8]

L'ensemble des propriétés de ces cristaux n'est pas encore expliqué de façon entièrement satisfaisante par les structures que l'on a pu imaginer pour eux. En particulier, une des questions qui demeurent les plus incertaines est celle de la symétrie et des degrés de liberté que l'on doit attribuer aux ions NH_4^+. Il nous a paru que la théorie de la polarisation des raies de Raman dans les cristaux cubiques, que nous avons développée récemment,[9] pourrait aider à aborder le problème précédent. Aussi, avons nous entrepris des recherches sur le spectre de Raman de monocristaux de chlorure, de bromure et d'iodure d'ammonium. Nous indiquerons et discuterons seulement ici les résultats relatifs aux spectres de ces deux premiers composés, à la température ordinaire.

Rappelons d'abord brièvement que les oscillations fondamentales d'un cristal cubique actives dans l'effet Raman se divisent en trois types, d'après leur symétrie par rapport aux axes ternaires et binaires du groupe du tétraèdre (la considération des éléments de symétrie des autres groupes du système cubique ne modifie pas ce classement). On distingue: les oscillations A, simples et totalement symétriques; les oscillations E, doublement dégénérées par rapport aux axes ternaires; les oscillations F, triplement dégénérées. Pour les vibrations simples, le facteur de dépolarisation ρ est toujours égal à 0, quelle que soit l'orientation du cristal; mais ρ varie, selon les cas, pour les vibrations doubles entre 0 et 3; pour les vibrations triples, entre $\frac{1}{2}$ et 2.

2. Resultats experimentaux

Le tableau I contient les résultats des mesures faites à 20°–25° C, exprimés au moyen des notations suivantes. Pour les intensités, I indique une raie forte, *m* une raie moyenne, *f* une raie faible. Pour l'aspect, *s* désigne une raie fine, *d* une raie diffuse, *b* une bande.

Tableau I

Chlorure d'ammonium				Bromure d'ammonium			
$\Delta\nu$ en cm.$^{-1}$	Type	Intensité	Aspect	$\Delta\nu$ en cm.$^{-1}$	Type	Intensité	Aspect
88	E	6, 3	*d*	56	E	I	*s*
				130	?	*m*	*d*
143	F	10	*d*	136	F	I	*d*
170	F	9, 5	*d*	147	F	I	*d*
197	F	..	*d*	172–182–209	?	*m*	*b*
				1370	?	*tf*	*s*
1403	F	3, 8	*s*	1400	F	I	*s*
1428	F	0, 7	*s*	1422	F	*f*	*d*
1444	F	0, 4	*s*	1687	E	TI	*s*
1711	E	9, 0	*s*	1710	F	*m*	*d*
1771	F	3, 3	*b*	1955	F	I	*b*
1995	F	3, 5	*b*	2804	F	I	*d*
2818	F	12	*d*	3035	F	TI	*d*
3042	A(+F)	51	*d*	3055	A	TI	*d*
3133	F	20	*d*	3126	F	TI	*d* (double?)
				3282–3318	F	*m*	*b*

De plus le spectre du bromure d'ammonium contient un certain nombre de raies très faibles dont nous n'avons pas pu déterminer le type et dont nous indiquons seulement la fréquence et l'aspect.

Tableau II

$\Delta\nu$ en cm.$^{-1}$	258	312	345–472	596–680	997	1018	1032	1071–1130	1160
Aspect ..	*d*	*d*	*b*	*b*	*s*	*s*	*s*	*b*	*s*

3. Discussion des Résultats

L'analyse des cristaux par les rayons X[5] montre avec certitude qu'à la température ordinaire les atomes N et Cl (ou Br) sont disposés comme les atomes Cs et Cl dans les cristaux subiques de chlorure de césium (groupe O_h^1—Pm 3m, symétrie propre de N et de Cl ou de Br: O_h-4/m $\bar{3}$ 2/m; Z = 1). Mais l'étude aux rayons X ne permet pas de déterminer la place des quatre atomes H qui entourent chaque atome N.

Spectre de basse fréquence.—Nous discuterons d'abord les relations qui existent entre la symétrie possible des ions NH_4^+ et le spectre de Raman de basse fréquence que l'on prévoit en considérant ces ions comme rigides et susceptibles d'effectuer des déplacements. Ceux-ci donnent naissance soit à des oscillations de translation, soit à des oscillations de rotation ou librations.

Dans tout ce qui suit nous admettrons que tous les ions NH_4^+ du cristal ne forment qu'une famille, au point de vue de la symétrie. On parviendrait à plus de possibilités que nous n'en considérerons, en renonçant à cette supposition; mais nous verrons que l'on peut la justifier, en étudiant les spectres de haute fréquence.

L'hypothèse la plus simple consiste à supposer que les ions NH_4^+ ont la forme de tétraèdres réguliers et une orientation bien déterminée. Leur symétrie propre est alors celle du goupe T_d; elle est compatible avec l'holoédrie du cristal (groupe O_h^5), en admettant que la maille est double, ou avec son hémiédrie (groupe T_d^1). Ces deux possibilités correspondent respectivement aux dispositions désignées sous le nom de " antiparallèle " et "parallèle" par Menzies et Mills.[10] Aucune libration des ions NH_4^+ n'est active dans ce cas, car leur ellipsoïde de polarisabilité est une sphère.

On peut également supposer que les ions NH_4^+ n'ont pas une forme tétraédrique régulière et que l'un des atomes H se distingue par la formation d'une liaison particulièrement forte avec l'atome d'halogène. Cette hypothèse qui est compatible avec les propriétés chimiques des halogénures d'ammonium, conduit à attribuer à l'ion NH_4^+ la symétrie C_{3v} ou C_3, selon l'orientation occupée par les trois atomes d'hydrogène identiques autour de l'axe privilégié N-H-Cl. Pour trouver la symétrie cubique du cristal, il faut alors admettre que la maille est multiple et contient Z ions NH_4^+. Selon que les axes ternaires des divers ions sont parallèles ou antiparallèles, la symétrie C_{3v} correspond pour l'ensemble du cristal au groupe T_d^3 ($Z = 4$) ou O_h^1 ($Z = 8$), la symétrie C_3 au groupe T_d^4 ($Z = 8$) ou bien à l'un des groupes O^1 ($Z = 8$), T_h^1 ou T_h^6 ($Z = 8$). Dans tous ces cas, les librations des ions autour d'axes perpendiculaires à l'axe ternaire sont seules actives, car l'ellipsoïde de réfractivité est de révolution.

Mais l'existence d'ions NH_4^+ occupant des positions moyennes fixes, autour desquelles ils effectuent des vibrations ou des librations, à la température ordinaire, a été mise en doute par Pauling,[11] qui a supposé que la température de transformation correspond au passage des librations à la rotation libre des ions. Cette conception conduit à attribuer aux ions NH_4^+ une symétrie propre qui dépend de la manière dont on conçoit cette rotation. Dans l'idée de Pauling, il s'agit d'une rotation autour d'axes

quelconques, donc isotrope en moyenne; cela entraine pour les ions NH_4^+, considérés comme un tout, soit la symétrie O_h et pour le cristal le groupe O_h^1; soit la symétrie O et pour le cristal les groupes O^3 ($Z = 1$) ou O_h^6 ($Z = 2$).

L'hypothèse de la rotation libre a été critiquée par Frenkel,[12] qui la remplace par la conception suivante: les molécules ou les ions effectueraient des librations au-dessus du point de transition comme au-dessous; mais tandis qu'à basse température les librations se feraient autour d'axes d'orientation bien définie dans la maille, à température élevée elles se produiraient autour d'axes orientés au hasard, comme dans un liquide. Dans ce cas, les calculs relatifs aux raies de libration devraient être conduits comme dans un liquide; leur facteur de dépolarisation devrait avoir une valeur égale à 6/7, quelle que soit l'orientation du cristal, ce qui est en contradiction avec les faits expérimentaux.

Toutefois, la rotation des ions NH_4^+ ne peut pas être nécessairement isotrope. Pour interpréter les variations thermiques de la constante diélectrique des halogénures d'ammonium, Bauer[3] a fait l'hypothèse d'une rotation des ions NH_4^+ autour d'un de leurs axes ternaires, c'est-à-dire de la direction d'une des liaisons N–H. Cette direction est ainsi privilégiée et l'on retrouve pour l'ion la symétrie C_{3v} ou C_3 discutée plus haut au point de vue statique.

Le tableau III rassemble les diverses possibilités envisagées pour la symétrie des ions NH_4^+ et des cristaux de chlorure et de bromure d'ammonium, ainsi que le dénombrement des raies de Raman de basse fréquence qui peuvent provenir des oscillations fondamentales de translation ou des librations; ces dernières ne se manifestent que si les ions NH_4^+ ne sont pas en rotation isotrope.

TABLEAU III

Symétrie de NH_4^+	Symétrie du cristal	Z	Translations	Librations
O_h ..	O_h^1	1	0	0
O ..	O^3	1	$1F_2$	0
	O_h^6	2	$1F_{2g}$	0
T_d ..	T_d^1	1	$1F_2$	0
	O_h^5	2	$1F_{2g}$	0
C_{3v} ..	T_d^3	4	$1A_1$, $1E$, $4F_2$	$1E$, $1F_2$
	O_h^1	8	$1A_{1g}$, $1E_g$, $2F_{2g}$	$1E_g$, $1F_{2g}$
C_{3M} ..	O^1	8	$1A_1$, $2E$, $4F_2$	$2E$, $2F_2$
	T_d^4	8	$1A_1$, $2E$, $6F_2$	$2E$, $2F_2$
	T_h^1 o T_h^6	8	$1A_g$, $1E_g$, $3F_g$	$1E_g$, $2F_g$

Cela posé, la comparaison des prévisions contenues dans le tableau III avec les résultats expérimentaux montre que l'hypothèse d'une symétrie C_{3v} ou C_3 pour les ions NH_4^+ est seule compatible avec le nombre des raies de basse fréquence contenu dans le spectre de Raman, sans que ce nombre ou le type des raies permette de faire un choix plus précis entre les divers groupes possibles pour le cristal. Mais on peut invoquer des arguments tirés de l'étude d'autres phénomènes.

La disparition de la piézoélectricité du chlorure d'ammonium au dessus de $-30°$ [4] et son absence dans le bromure sont peu compatibles avec l'un des groupes de symétrie T, O ou T_d pour le cristal.

La recherche du pouvoir rotatoire nous a montré que la rotation n'atteint pas 1' par mm pour le chlorure et O, 1' par mm pour le bromure, dans les échantillons que nous avons examinés; ce résultat rend improbable que les cristaux appartiennent à l'un des groupes T ou O. Enfin les figures de corrosion par l'eau, que nous avons faites sur le chlorure, ne révèlent aucune hémiédrie.

Cet ensemble de raisons laisse à penser que les cristaux de chlorure et de bromure d'ammonium appartiennent vraisemblablement au groupe holoèdre du système cubique, à la température ordinaire. Ce serait donc pour le cristal la symétrie O_h (ou T_h) et pour les ions NH_4^+ la symétrie C_{3v} (ou C_3) qui seraient les plus vraisemblables.

Lawson[2] a indiqué que les mesures de la chaleur spécifique C_v du chlorure d'ammonium au voisinage du point de transition demande une contribution de 6 cal. mol/degré pour les mouvements des ions NH_4^+, et il a signalé que ce résultat s'accorde avec l'hypothèse de Frenkel, mais non avec celle de Pauling, qui n'en donne que trois. L'hypothèse de Bauer fournit 5 cal. mol/degré, ce qui est beaucoup plus proche du résultat de Lawson.

Spectre de haute fréquence.—Il doit être dû essentiellement au oscillations internes des ions NH_4^+. On sait que le spectre de Raman des halogénures d'ammonium en solution contient quatre raies, ce qui correspond bien aux quatre fréquences fondamentales actives d'un édifice pentatomique en forme de tétraèdre régulier. Par suite, en attribuant la symétrie T_d à l' ion NH_4^+ contenu dans la maille d'un cristal du groupe O_h^5, on ne parviendra pas à rendre compte du grand nombre de raies qui apparaissent au dessus de 1000 cm^{-1} dans le spectre du chlorure et du bromure d'ammonium.

D'autre part, la symétrie O_h ou O des ions NH_4^+ ne se conçoit que statistiquement, dans l'hypothèse d'une rotation libre autour d'axes pouvant prendre avec une égale probabilité toutes les orientations possibles. Or

dans ce cas, le facteur de dépolarisation devrait avoir la même valeur que celui des raies de l'ion en solution, soit O ou 6/7 selon le type d'oscillation, au lieu des valeurs calculées pour un cristal cubique[9] et variables avec l'orientation. Ce résultat est en contradiction avec les résultats de nos mesures. Pour la même raison, l'hypothèse de Frenkel ne s'accorde pas avec les faits, pour le spectre de haute fréquence comme pour celui de basse fréquence.

Reste à examiner les conséquences de la symétrie C_{3v} ou C_3 pour les ions NH_4^+. C'est le couplage des oscillations fondamentales des ions contenus dans la maille qui fournit le nombre et les types des raies du spectre.[9] Ce couplage se fait sans difficultés si l'on admet que les ions occupent des positions moyennes bien définies; si, au contraire, ils tournent autour de leur axe ternaire, la définition du couplage devient plus délicate; elle conduit au même résultat que dans la première hypothèse, seulement lorsque les rotations des ions ont lieu d'une façon totalement symétrique et que l'on néglige l'interaction de la rotation et de la vibration. Il est possible de faire bien d'autres hypothèses: nous ne les développerons pas ici. Dans ces conditions, on parvient au tableau suivant, que permet de comparer les prévisions théoriques aux données de l'expérience. Nous y avons fait figurer les raies les plus intenses en caractères italiques.

TABLEAU IV

		ν_4	ν_2	ν_1	ν_3
Théorie	Ion NH_4^+ Vibr.				
	Ion NH_4^+ $\Delta\nu$	1397	1685	3033	3134
	Ion NH_4^+ Type T_d	F	E	A	F
	Ion NH_4^+ C_{3v}	A_1 | E	E	A_1	A_1 | E
	Cristal T_d^3	A_1 F_2 | E F_2	E F_2	A_1 F_2	A_1 F_2 | E F_2
	Cristal O_h^1	A_{1g} F_{2g} | E_g F_{2g}	E_g F_{2g}	A_{1g} F_{2g}	A_{1g} F_{2g} | E_g F_{2g}
	Ion NH_4^+ C_3	A_1 | E	E	A_1	A_1 | E
	Cristal O^1 ou T_d^4	A_1 F_2 | 2E $2F_2$	2E $2F_2$	A_1 F_2	A_1 F_2 | 2E $2F_2$
	Cristal T_h^1 ou T_h^6	A_g F_g | E_g $2F_g$	E_g $2F_g$	A_g F_g	A_g F_g | E_g $2F_g$
Expérience	$ClNH_4$ $\Delta\nu$	*1403* 1428 1444	*1711* 1771 1995	*3042*	*2818*	*3133*
	$ClNH_4$ Types	F F F	E F F	A(+F)	F	F
	$BrNH_4$ $\Delta\nu$	1370 *1400* 1422	*1687* 1710 1955	*3035* *3055*	*2804*	*3126*
	$BrNH_4$ Types	F F F	E F F	F A	F	F

On voit aussitôt que le nombre des raies observées ne s'accorde ni avec la symétrie T_d de l'ion NH_4^+ (on s'attendrait à trouver quatre raies fines), ni avec l'hypothèse de Pauling ou celle de Frenkel, qui laissent prévoir quatre raies floues, dont trois polarisées à 6/7.

L'oscillation totalement symétrique ν_1 de l'ion NH_4^+ doit donner naissance, dans toutes les hypothèses envisagées, à une raie de type A et une de

type F. Dans le chlorure, l'étude de la polarisation de la raie 3042 cm.$^{-1}$ montre qu'elle est formée de deux composantes; celles-ci se séparent nettement dans le bromure en 3035 et 3055 cm.$^{-1}$, qui ont les types prévus. En l'absence de mesures de polarisation, Krishnan[8] n'a pu les distinguer à la température ordinaire; il trouve bien deux raies (3037 et 3078 cm.$^{-1}$) á 173° K, mais l'explication de l'origine de ce doublet par une résonance de Fermi est inacceptable, puisque les deux raies n'ont pas le même type. La raie F (3035 cm.$^{-1}$) devrait avoir une intensité nulle si l'ion NH_4^+ gardait dans le cristal la symétrie T_d; or, elle apparait nettement dans le spectre du chlorure et fortement dans celui du bromure: c'est là une preuve très nette de l'abaissement de symétrie de l'ion NH_4^+.

Si l'attribution que nous avons faite est correcte, en plaçant les bandes 1995 (chlorure) et 1955 (bromure) dans l'ensemble des oscillations dérivées de la fréquence ν_2 de l'ion libre, les résultats expérimentaux semblent s'accorder mieux avec la symétrie T_h du cristal qu'avec la symétrie O_h; mais on ne peut considérer cette preuve comme décisive.

Il est peu probable que les raies 2818 cm.$^{-1}$ (chlorure) ou 2804 cm.$^{-1}$ (bromure), plus fortes que les raies 1403 cm.$^{-1}$ ou 1400 cm.$^{-1}$ des mêmes spectres, soient les harmoniques de ces raies. Nous les avons classées dans l'ensemble ν_3. En supposant, en effet, que la cessation de dégénérescence de ν_3 provienne de la diminution de la force d'une liaison N–H, on peut montrer, en adoptant le système des forces de valence[13] que la fréquence de l'une des deux oscillations dérivées dans un ion ne change pas et que celle de l'autre doit diminuer.

L'aspect des raies du spectre de haute fréquence varie beaucoup de l'une à l'autre. Les raies de type E dérivées de l'oscillation ν_2 sont fortes et fines; le fait qu'elles sont toujours uniques est en faveur de l'existence d'une seule famille d'ions NH_4^+ dans les cristaux étudiés. Les raies correspondant aux oscillations de valence ν_1 et ν_3 sont toutes diffuses, même la raie totalement symétrique bien isolée 3055; cela semble indiquer une variation au cours du temps du champ qui entoure l'ion.

Dans aucun cas, nous n'avons aperçu de structure fine des raies d'oscillation internes. Une telle structure a été mise en évidence par Beck[7] pour les bandes d'absorption infrarouges correspondant à la fréquence ν_2; si elle est réelle, on peut encore se demander si elle correspond à une structure de rotation ou à des bandes de combinaison vibration + librations.

Remarquons que la concordance excellente entre les fréquences des raies de Raman et des bandes d'absorption infrarouges relatives aux oscillations internes[7] est en faveur de la symétrie C_{3v} ou C_3 des ions NH_4^+, ces deux

groupes finis étant les seuls dont les oscillations fondamentales soient actives à la fois en absorption et en diffusion.

4. Conclusions

L'étude de la polarisation du spectre de Raman des monocristaux cubiques de chlorure et de bromure d'ammonium, dans diverses orientations, permet d'attribuer les principales raies de ces spectres à des types d'oscillations bien déterminés.

L'interprétation du spectre de basse fréquence se fait de façon satisfaisante sans invoquer les oscillations du second ordre. Elle conduit, de même que l'étude du spectre de Raman de haute fréquence et la comparaison avec le spectre infrarouge, à écarter la forme tétraédrique régulière pour les ions NH_4^+, ainsi que les conceptions de Pauling et de Frenkel sur l'état de mouvement de ces ions au-dessus de la température de transition.

L'ensemble des résultats expérimentaux conduit à adopter une maille cristalline multiple, et rend probable la symétrie O_h ou T_h pour les cristaux, C_{3v} ou C_3 pour les ions NH_4^+. Ce dernier résultat peut s'accorder avec une rotation ou une libration anisotrope des ions NH_4^+.

Bibliographie

1. F. Simon et Bergmann .. *Z. Phys. Chemie*, 1930, **B 8**, 255.
   P. Dinichert .. *Helvetica Physica Acta*, 1939, **15**, 462.
   J. Weigle et H. Saini .. *Ibid.*, 1936, **9**, 515.
2. F. Simon, Cl. V. Simson et M. Ruhemann .. *Z. Phys. Chemie*, 1927, **129**, 339.
   A. W. Lawson .. *Phys. Rev.*, 1940, **57**, 417.
3. R. Guillien .. *Comptes Rendus Ac. Sc. Poris*, 1939, **208**, 1561.
   E. Bauer .. *Cahiers de Physique*, n°21, 1943, 7.
4. A. Hettich .. *Z. Phys. Chemie*, 1934, **168**, 353.
5. R. W. G. Wyckoff .. *American Journ. of Science*, 1922, **53**, 177 et **54**, 1922, 469.
   ———, et A. H. Armstrong .. *Zeit. Kristall*, 1930, **72**, 318.
   J. Weigle, et H. Saini .. *loc. cit.*
6. W. E. Laschkarew, et I. D. Usyskin .. *Zeit. für. Phys.*, 1933, **85**, 618.
7. O. Reinkober .. *Ibid.*, 1921, **5**, 192.
   R. Pohlman .. *Ibid.*, 1932, **79**, 394.
   C. Beck .. *J. Chem. Physics*, 1944, **12**, 71.
   Voir R. S. Krishnan .. *Proc. Ind. Acad. Sci.*, 1947, **26 A**, 432; *et* 1948, **27 A**, 321.
   L. Couture, et J. P. Mathieu *Comptes Rendus Ac. Sc. Paris*, 1948, **226**, 1261.
9. ——— .. *Ibid.*, 1947, **224**, 902 et 1217.
   et. Annales de Physique, 1948, **3**, 521.
10. A. C. Menzies, et H. R. Mills *Proc. Roy. Soc.*, 1935, **148 A**, 407.
11. L. Pauling .. *Phys. Rev.*, 1930, **36**, 430.
12. J. Frenkel .. *Acta Physico Chimica, U.S.S.R.*, 1935, **3**, 23.
13. F. Kohlrausch .. *Der Smekal Raman Effekt, Springer*, Berlin, II, 1937 72.

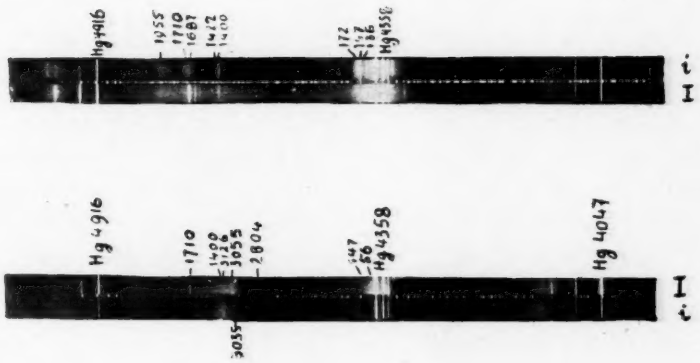

Bromure d'ammonium orienté selon les faces du cube

THE INFLUENCE OF OPTICAL ACTIVITY ON LIGHT-SCATTERING IN QUARTZ

By V. Chandrasekharan

(From the Department of Physics, Indian Institute of Science, Bangalore)

Received November 30, 1948

(Communicated by Prof. R. S. Krishnan, F.A.SC.)

1. Introduction

In a previous paper, the present writer (1947) has shown how the large rotatory power of quartz in the ultraviolet manifests itself in transverse light-scattering. A plane-polarised beam of intense λ 2537 radiation of a water-cooled magnet-controlled mercury arc traverses a perfectly clear and transparent sphere of quartz along the optic axis. A photograph of its track taken in a direction transverse to it exhibits marked fluctuations in intensity along its length. The effect is obviously due to the incident light vector being alternately parallel and perpendicular to the direction of observation and to the strong polarisation of genuine thermal scattering. In a similar effect observed earlier by Lord Rayleigh (1919) in smoky quartz, the strong Tyndall scattering of visible light by the inclusions present was utilised.

In the present investigation, the light scattered by transparent quartz is analysed spectroscopically and the banding for the individual Rayleigh and the more intense Raman lines recorded separately. Also by the use of a mercury vapour filter placed in the path of the scattered light, the Tyndall scattering of λ 2537 radiation due to inclusions in the crystal is suppressed efficiently and the genuine Brillouin components are recorded. The obliteration of the bands when the incident light traverses a sphere of clear quartz at small angles to the optic axis is also recorded and an explanation given.

2. Experimental Technique

A transparent and practically colourless regular hexagonal crystal of quartz 4 cm. long, kindly lent by Prof. R. S. Krishnan, is employed for the purpose of the experiment. Two ends of it are cut normal to the optic axis. These ends and the sides are all ground and polished. As the crystal contained a few visible inclusions, the best portion is chosen.

The crystal is mounted with its optic axis vertical and one of the hexagonal sides facing the spectrograph. A sealed Z-type horizontal quartz

mercury arc is water-cooled and magnet-controlled to give intense λ 2537 radiation. A rectangular aperture of 1 cm. × 0·5 cm. in front of the arc limits the beam. The light from it is condensed by a quartz lens of focal length 9 cm. for λ 2537 and aperture 4 cm. on one of the end surfaces of the crystal so that the beam traverses vertically along the optic axis. A large double-image prism next to the quartz lens served to polarise the beam, one of the images being screened off at the surface of the crystal. The vertical track of the beam in the crystal is focussed on the slit of a Hilger intermediate quartz spectrograph by a quartz lens. As the lens is not achromatic, its position is adjusted to give the best focus for λ 2537 radiation. With a slit width of 0·14 mm., the spectrum is photographed on a Selochrome plate giving an exposure of the order of 50 hours. A mercury vapour filter is employed in the path of the scattered light to absorb efficiently the Tyndall scattering of λ 2537 radiation and thus, record only the Brillouin components due to it.

3. Results and Discussion

A reproduction from the previous paper is given in Fig. 1 *b*, Plate VII, for comparison and shows clearly the bands in a perfectly clear and transparent sphere of quartz traversed by intense λ 2537 radiation. Owing to its high intrinsic intensity and the operation of λ^{-4} law, only the scattering of λ 2537 radiation is recorded even though no filter is employed in the incident light. Both its Rayleigh and Raman scattering would contribute to the intensity and as is well known, in a clear specimen of quartz, the latter makes as much as one fourth the contribution (Landsberg, 1927; Bhagavantam and Venkateswarulu, 1944). The pictures taken in the present investigation using a spectrograph are reproduced in Figs. 1 (*b*) and 1 (*c*). The complete spectrum [see Fig. 1 (*c*)] shows clearly the variation in the band width for different mercury arc lines. A major portion of their intensity recorded on the plate has its origin in the Tyndall scattering by the few inclusions present in the crystal. This is supported by the non-appearance of the intense 466 $cm.^{-1}$ Raman line (the absolute intensity of which is about 1/5 the intensity of the genuine Rayleigh scattering) excited by any mercury line other than λ 2537. On the other hand, as the λ 2537 radiation has been completely suppressed by the mercury vapour filter, what is observed in its place is the banding due to the Brillouin components arising from thermal scattering.

Fig. 1 (*a*) is a high enlargement of the portion between λ 2537 and the triplet λ 2654. It shows clearly the bands for the Brillouin components of λ 2537 and the two symmetric Raman lines 207 and 466 $cm.^{-1}$ excited by it,

while the strong line 128 cm.$^{-1}$ and the weaker 800 (doublet) and 1159 cm.$^{-1}$ lines belonging to the degenerate class E, sub-groups E_1, E_2 and E_3 respectively, show no trace of the banding. It is clear from the work of Saxena (1940) and more recently of Krishnan (1945) that the Raman spectrum of quartz consists in the main of 12 first order lines including two doublets. Of these four lines 207, 357, 466 and 1082 cm.$^{-1}$ lines belong to the symmetric class A which are always completely polarised and should, therefore, show the bands. The rest belong to the degenerate class E divided into three sub-groups depending on their depolarisation values and orientation effects. However, in all sub-groups, as a result of degeneracy the two directions perpendicular to the optic axis are equivalent. This has an important consequence that when light is incident along the optic axis, the scattered intensity would be the same whether the light vector is along or perpendicular to the direction of observation (*vide* Table V of p. 109 of Saxena's paper). This prediction has been beautifully confirmed in the case of quartz for the first time in the present work; the more intense degenerate lines 128, 800 (doublet) and 1159 cm.$^{-1}$ lines showing no trace of the banding. The large optical activity of quartz along the optic axis has been a disturbing factor when it is required to study the effect of polarising an incident beam travelling along that direction. Hence, for such directions, studies have been confined till now to the use of incident unpolarised light. The present arrangement described enables one to make polarisation and intensity measurements using polarised light traversing along the optic axis, and the disturbing factor, namely the optical activity itself is made use of for the purpose. It is interesting to note that some of the degenerate lines, *e.g.*, 800 cm.$^{-1}$ line (E_2 sub-group) and 1159 cm.$^{-1}$ line (E_3 sub-group), have depolarisation values of ∞ and 0 respectively and still show no banding as expected.

The band width for λ 2537 and for the two 207 and 466 cm.$^{-1}$ Raman lines was measured with a glass scale reading to tenths of a millimetre and the reduction produced by the condensing lens and by the spectrograph for λ 2537 along the length of the slit was determined. From this, the actual width, which corresponds to a rotation of 180° of the plane of polarisation of the incident light, was calculated and hence, the rotation per millimetre for λ 2537 deduced. The calculated rotation of 148°·5 per mm. agrees well with the correct value of 148°·6 per mm. It is particularly interesting to note that the band widths of the Raman lines and the exciting line are identical [see Fig. 1 (*a*)]. A Rayleigh line of the same frequency as the 466 cm.$^{-1}$ line excited by λ 2537 would have shown about $\frac{1}{7}$ of a band less in 7 bands and this would have been shown up clearly.

4. Directions inclined to the Optic Axis

As a plane-polarised light beam advances inside a birefringent solid, it undergoes a periodic cycle of changes in its state of polarisation. Hence, its track made visible by the scattered light would exhibit striking fluctuations in intensity along its length. These bright and dark bands have been observed and photographed by the author (1947) using synthetic organic glasses with permanent strains and hence, behaving like very feebly birefringent solids. Now it follows that in a solid showing both optical activity and birefringence, the effect should also be observable. As is well known, quartz has both optical activity and birefringence for directions inclined to the optic axis.

For such directions, the theory of propagation of light in quartz has been dealt with by several workers (Briot, 1863; Gouy, 1885 and Wiener; *vide* Pockel, 1906). Along such directions, two similar elliptically polarised waves but with opposite sense of rotation and lying crossed to each other (*i.e.*, the major axis of one falls on the minor axis of the other) travel unchanged. The axes of the ellipses coincide with the principal planes. Pockels has shown in his book a simple though approximate way of arriving at the ratio of the axes of the vibration ellipses which propagate unchanged and the path difference between the two waves per unit length. If ρ is the rotatory power per unit length along any direction and δ_0 is the path difference due to birefringence alone (if $\rho = 0$), then the actual path difference per unit path between the two elliptic waves is given by

$$\delta = \sqrt{\delta_0^2 + (2\rho)^2}$$

and the ratio of the axis χ is given by

$$\chi = \tan \beta \text{ where } \tan \beta = \frac{2\rho}{\delta_0}$$

or

$$\chi^2 = \frac{\delta - \delta_0}{\delta + \delta_0}.$$

Bruhat (1935) has determined recently the rotatory power of quartz for directions parallel and perpendicular to the optic axis for different wavelengths.

For $\lambda 2537$ $r_1 = -86°$ per mm. perpendicular to the optic axis

$r_3 = 149°$ per mm. parallel to the optic axis

$$\rho = r_1 \sin^2 \phi + r_3 \cos^2 \phi$$

where ϕ is the inclination of the ray with the optic axis. The two refractive indices for $\lambda 2537$ are

$$n_\epsilon = 1 \cdot 60930, \qquad n_\omega = 1 \cdot 59830$$

For different values of ϕ the rotation and the path retardation per unit length are given in Table I.

TABLE I

ϕ in degrees	ρ' in degrees/mm.	ρ/π per mm.	$\delta_0/2\pi$ per mm.	$\delta/2\pi$ per mm.	$2\pi/\delta$ in mms.	χ
0	149·0	0·8278	0	0·8278	1·208	1
1	148·93	0·8276	0·01315	0·8277	1·208	0·9784
2	148·7	0·8264	0·05229	0·8281	1·208	0·9387
3	148·4	0·8244	0·1174	0·8327	1·201	0·8677
4	147·9	0·8218	0·2091	0·8480	1·179	0·7774
5	147·2	0·8177	0·3264	0·8804	1·135	0·6775
6	146·4	0·8130	0·4687	0·9383	1·066	0·5778
7	145·5	0·8084	0·6377	1·0296	0·9716	0·4848
7·86	144·6	0·8032	0·8032	1·1359	0·8805	0·4142
8	144·4	0·8019	0·8318	1·1554	0·8655	0·4035
9	143·2	0·7954	1·049	1·3165	0·7498	0·3363
10	141·9	0·7885	1·294	1·5153	0·6601	0·2806
11	140·5	0·7806	1·562	1·7462	0·5726	0·2360
12	138·8	0·7706	1·855	2·0172	0·4958	0·2043
13	137·1	0·7617	2·172	2·3045	0·4340	0·1713
14	135·2	0·7513	2·512	2·6219	0·3814	0·1463
15	133·3	0·7407	2·874	2·9679	0·3369	0·1268
20	131·5	0·6752	5·020	5·0652	0·1974	0·0670
30	90·2	0·5009	10·73	10·7417	0·0931	0·0233
52·69	0	0	27·22	27·22	0·0367	0
90	−86	0·4778	43·37	43·3726	0·0231	0·0055

$2\pi/\delta$ for any value of ϕ gives the periodic distance after which the incident polarised beam proceeding along that direction returns to its original state of polarisation after undergoing a cycle of changes. It is seen, however, from the table that this length changes but little up to 3°. Hence, when light goes along the optic axis convergence angles of the order of 6° can be used, and the bands in transverse light-scattering would still be clear. On the other hand, at say 8° to the optic axis, when the periodic length is appreciably different, it changes so rapidly with the angle that unless the beam is strictly parallel, the rays going at different angles obliterate the banding. These conclusions have been verified in the observations made with the sphere of quartz. The arrangement used has already been described in the earlier paper.

Fig. (2), Plate VII, shows the bands clearly when a fairly wide beam travels exactly along the optic axis. At 4° to the optic axis the bands are still clear and of the same width and are reproduced in Fig. 2 (*b*). At the edge of the track away from the optic axis the banding is just obliterated. At 8° to the optic axis the series of pictures, Figs. 2 (*c*), (*d*) and (*e*) show the effect of narrowing the beam. With a wide beam [Fig. 2 (*c*)] some rays

are going very near the optic axis and hence, show the banding while on the other side the bands are obliterated. When the beam is strictly limited, the bands have been completely obliterated. At 10° [Fig. 2 (*e*)] the bands have disappeared even with a fairly wide beam. The maximum convergence of the incident light used is about 8° to 10° while the minimum used is about 2°.

It should be recalled that in a purely optically active solid the banding would be equally clear in any azimuth transverse to the beam. On the other hand, in a birefringent solid without optical activity, the banding would be marked only when both the direction of the incident light vector and that of observation are inclined at 45° to the principal planes. When either direction coincides with the principal plane the banding would disappear. Hence, for directions away from the optic axis, the sphere of quartz is rotated so that the bands would be most marked and yet the banding vanished at 10°. The value of χ in the last column of Table I gives a measure of the azimuth effect if strictly parallel light is used.

It is interesting to note that in the visible say at λ 4358, the ratio of the rotatory power to birefringence of quartz is half that for the ultra-violet λ 2537. Hence, to get equal clarity of the banding, the square of the convergence angles used should be only half as large in the visible compared to the ultra-violet. This result has also been verified (no photograph is reproduced).

In the previous paper, it was reported that the sphere of quartz used was a left-handed one. Between crossed polaroids, the observation recorded that the rings of any particular colour appear to expand indicates actually that the sphere is a right-handed one (Cady, 1946).

In conclusion, the author wishes to thank Prof. Sir C. V. Raman and Prof. R. S. Krishnan for their keen interest in the work and for the useful discussions he had with them.

5. Summary

A vertical plane-polarised beam of intense λ 2537 mercury radiation travels along the optic axis of a crystal of quartz and the light vector is alternately parallel and perpendicular to the direction of observation transverse to the beam. A spectral analysis of the scattered light, using a mercury vapour filter to absorb the λ 2537 line, yields bands of fluctuating intensity along the length of the slit for the Brillouin components and for the two symmetric 207 and 466 cm.$^{-1}$ Raman lines. On the other hand, the degenerate lines 128,800 (doublet) and 1159 cm.$^{-1}$ lines belonging to the different

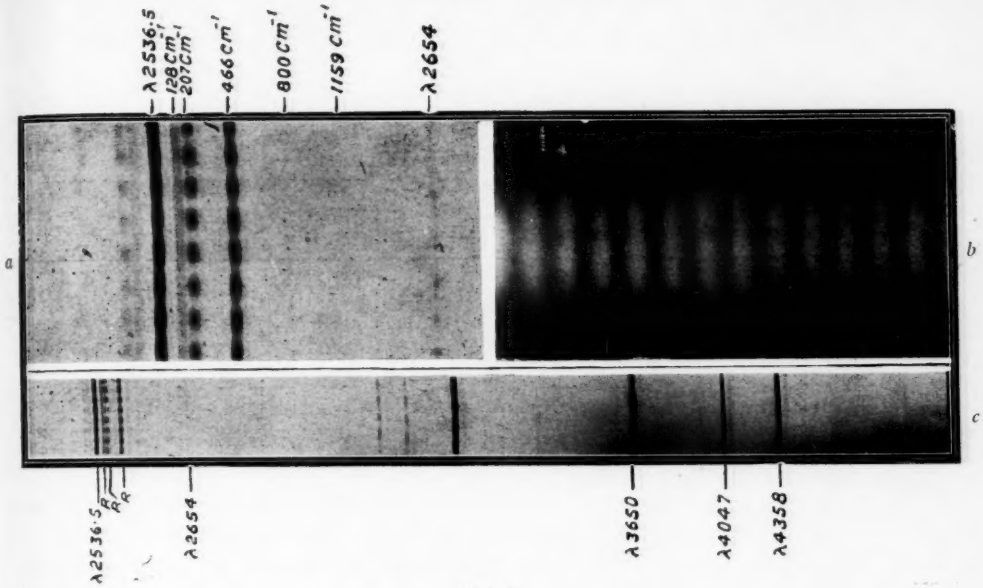

FIG. 1

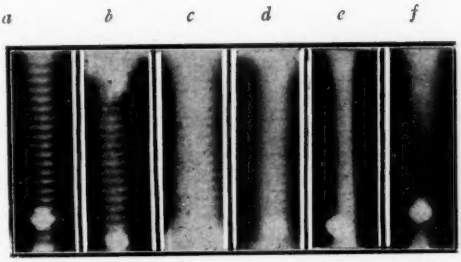

FIG. 2

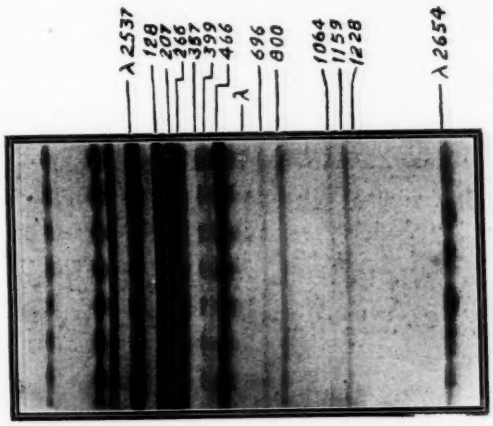

FIG. 3

subgroups are of uniform intensity irrespective of their depolarisation values. This result, which is in complete conformity with theory, verifies for the first time the selection rules for polarised light travelling along the optic axis of quartz—the optical activity itself, usually a disturbing factor, being made use of for the purpose. That the band widths of the Raman lines and that of the exciting line are identical is interesting. The variation in band width of some intense mercury lines, recorded due to inclusions present in the crystal used, shows clearly the rapid increase in the rotatory power of quartz in the ultraviolet.

The obliteration of the banding when the incident light travels at small angles to the optic axis of a clear and transparent sphere of quartz is recorded and a theoretical explanation is given.

Note added in Proof.—Since sending the paper for publication, the author has obtained an intense spectrogram of the scattering in quartz, giving an exposure of the order of 7 days and using a slit width of 0·08 mm. An enlargement of the same is reproduced in Fig. 3, Plate VII. It shows clearly all the principal Raman lines of quartz except 1082 cm.$^{-1}$ line. Of these, three lines (207, 357 and 460 cm.$^{-1}$) belonging to Class A exhibit the banding, while the rest—128, 266, 399, 696, 800, 1063, 1159 and 1228 cm.$^{-1}$ lines—are of uniform intensity. The 266 cm.$^{-1}$ line appears to have a trace of banding, but it is due only to the halation produced by the bands of the intense adjacent 207 cm.$^{-1}$ line. The 1082 cm.$^{-1}$ Raman line, coming under the symmetric Class A, has zero intensity for the particular direction of excitation used in the present investigation (Saxena, 1940) and hence, is not recorded.

References

1. Pockels .. *Lehrbuch der Kristalloptik*, 1906, 309–13.
2. Strutt, R. J. .. *Proc. Roy. Soc.*, 1919, **95**, 476.
3. Landsberg .. *Zeit. f. Phy.*, 1927, **43**, 773; **45**, 442.
4. Bruhat .. *J. Phy. Radium*, 1935, **6**, 12.
5. Saxena .. *Proc. Ind. Acad. Sci.*, A, 1940, **12**, 93.
6. Bhagavantam, S., and Venkateswarulu, K. .. *Ibid.*, 1944, **19**, 108.
7. Krishnan, R. S. .. *Ibid.*, 1945, **22**, 329.
8. Chandrasekharan, V. .. *Ibid.*, 1947, **25**, 256; **26**, 110.
9. Cady .. *Piezoelectricity*, 1946, 418.

Description of Plate

Fig. 1 *b*. Scattering of a clear sphere of quartz traversed by plane-polarised λ 2537 along optic axis.

Fig. 1 *c*. Spectrum of scattering of quartz traversed by plane polarised light along the optic axis.

Fig. 1 *a*. Enlargement of Fig. 1 *c* showing the portion between λ 2537 and λ 2654.

Fig. 2 *a*. Same as 1 *b*.

Fig. 2 *b*. Incident light inclined at 4° to the optic axis.

„ 2 *c,d,e* Incident light inclined at 8° to the optic axis for three different angles of convergence of the beam.

Fig. 2 *f*. Incident light inclined at 10° to optic axis. Fairly wide beam.

Fig. 3. Same as Fig. 1 *a*. Intense picture.

THE α-β TRANSFORMATION IN QUARTZ

By P. K. Narayanaswamy

(From the Department of Physics, Indian Institute of Science, Bangalore)

Received November 30, 1948

(Communicated by Prof. R. S. Krishnan, F.A.SC.)

It is well known that quartz undergoes a sudden polymorphic transition at 575° C. from the lower or α- to the high or β-modification, when many of its physical properties undergo a remarkable reversible change. Jay (1933), for example, has shown that the coefficient of thermal expansion as measured both perpendicular and parallel to the optic axis increases anomalously above 200° C. and becomes infinite at about 575° C. The piezo-electric activity of the crystal also falls rapidly as the critical temperature is approached and disappears altogether at the transition point (Pitt and McKinely, 1936). A rapid decrease has also been reported in the measured Young's modulus of the crystal at and preceding 575° C. (Perrier and Mandrot, 1923). The most important change accompanying the transformation is perhaps the increase in symmetry of the crystal, for while α-quartz is trigonal, β-quartz has been shown to possess hexagonal symmetry. This increased symmetry should manifest itself in the Raman spectrum of β-quartz by causing notable variations, especially the disappearance of some of the lines from the spectrum of α-quartz. It is therefore of great interest to investigate the Raman spectrum of quartz just below and above the α-β transition temperature, as it would throw some light on the nature of the transformation.

Although many investigations have been made by various authors on the Raman spectrum of quartz and its variations with temperature (for a review, see Narayanaswamy, 1947) the spectrum of β-quartz has not been obtained so far. This is mainly due to the well-known behaviour of quartz on heating to about 575° C. when the crystal breaks up invariably into fragments in spite of the usual experimental precautions. Nedungadi (1940) was able to record the spectra at temperatures up to 510° C. above which he found that the crystal fell to pieces. The same difficulty was also experienced by the present author in the course of earlier studies (Narayanaswamy, 1947). The difficulties have been overcome now by the use of thin plates as suggested by Sir C. V. Raman to whom the author's thanks are due, and the Raman spectrum of quartz at temperatures above 575° C. has been successfully photographed and the results are given in this paper. The breaking was evidently due to the use of thick specimens in earlier investigations.

2. Experimental Details

Using a thin crystal plate about 1 cm. × 1 cm. × 2 mm. and increasing the temperature gradually, it was found that the transition temperature could be safely exceeded without damage to the crystal. The specimen was mounted inside a specially designed heater which was cylindrical in shape. To ensure uniform heating, the heating coil was wound both at the top and bottom portions of the hollow cylinder leaving a gap in the middle. In this gap, two holes were made to serve as windows for illumination and observation. The temperature of the heater was measured by means of a nichrome-constantan thermocouple in conjunction with a calibrated millivoltmeter. The heating current was drawn directly from the mains through a series of resistances.

The intense λ 2537 resonance radiation of the mercury arc was used for exciting the spectra, employing the Hilger E3 medium quartz spectrograph. Since the crystal used was necessarily thin, exposures of the order of 10–12 hours were found to be necessary to obtain reasonably intense spectrograms with a slit width of 0·04 mm.

3. Results

In continuation of the previous work by the author on quartz, the Raman spectrum was photographed at 470° C. and 550° C. below the transi-

Table I. *Variations in frequency shift and width of the Raman lines in quartz at different temperatures*

α-quartz						β-quartz	
27° C. room temperature		470° C.		550° C.		660° C.	
Position cm.$^{-1}$	Width cm.$^{-1}$	Position cm.$^{-1}$	Width cm.$^{-1}$	Position cm.$^{-1}$	Width cm.$^{-1}$	Position cm.$^{-1}$	Width cm.$^{-1}$
128	8·5	106	30	101	36	97	37
207	18·0	170	~ 75	120–200		..	
265	3·5	253	9	251	14	250	15
357	3·0	351	12	350	14	..	
395	3·5	396	17	396	18	395	17
403	3·5						
466	12·0	456	37	454	45	452·5	50
695	6·0	686	12	686	14	~ 686	14
795	4·0	796	19	794	22	792	20
805	4·0						
1064	5·0	1074	12	1072	14	~ 1060	
1083	5·0						
1160		1155	14	1154	19	~ 1154	20
1228	5·0	1224	14	1223		..	

tion point, and at 660° C. above it. Typical spectrograms taken at these temperatures are reproduced on Fig. 1 in plate along with the spectrum of

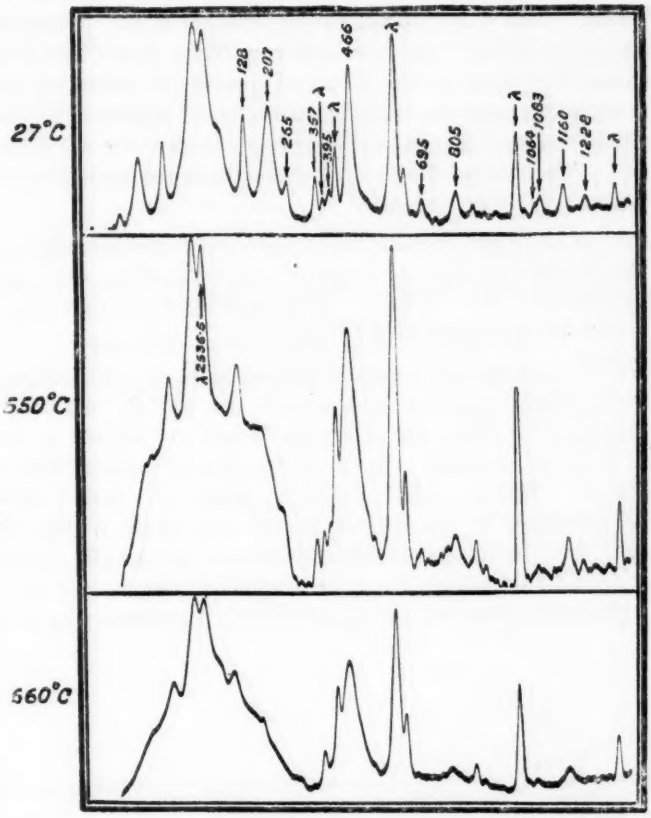

Fig. 2. α—β Transformation in quartz. Microphotometer records of the Raman spectrum of quartz at various temperatures.

quartz at room temperature. The microphotometer records of the spectra at room temperature, 550° C. and 660° C. are shown in Fig. 2. The measured frequency shifts are put down in Table I.

The most important feature noticed in the Raman spectrum above the transition temperature is the decrease in the number of frequency shifts. There are no lines corresponding to 207, 357 and 1228 cm.$^{-1}$, although they are present just below that temperature. According to Saxena's (1940) analysis, α-quartz has four frequencies coming under the symmetric class

and 8 under the degenerate class. He had identified the lines 207, 357, 466 and 1083 cm.$^{-1}$ under the symmetric class. Two of these oscillations, *viz.*, 207 and 357 cm.$^{-1}$ are definitely absent in the spectrum of β-quartz. Regarding the 1083 cm.$^{-1}$ line it is difficult to say whether it has disappeared or merged with the 1063 cm.$^{-1}$ line, but it is very likely it has also faded out. The anomalous behaviour of the 207 cm.$^{-1}$ line which broadens out enormously with rising temperature, drew the attention of Raman and Nedungadi (1940) who suggested that this has a special importance in the α-β transformation in quartz. The disappearance of the line above the transition temperature fully supports their suggestion.

Seven out of the eight lines coming under the degenerate class are also present in the Raman spectrum of β-quartz. Because of the extreme feebleness of the eighth line, *viz.*, 1228 cm.$^{-1}$, it is most probable that it has failed to appear within the exposures given.

Upto 550° C., a progressive shift in the position and broadening of the lines, though to different extents, is observed. At 660° C., after the transition, even though all the lines are extremely broad and shifted in position, the variation is not of the same order as it should have been if there was no structural change. This is clearly shown in Figs. 3, 4 and 5 where the temperature dependence of the frequency shift and width of the 128, 466 and 1160 cm.$^{-1}$ lines in the range 200–700° C. are graphically represented. The vertical dotted line shows the λ or transition temperature of 575° C. The curve in thick line represents the variation with temperature up to 550° C.

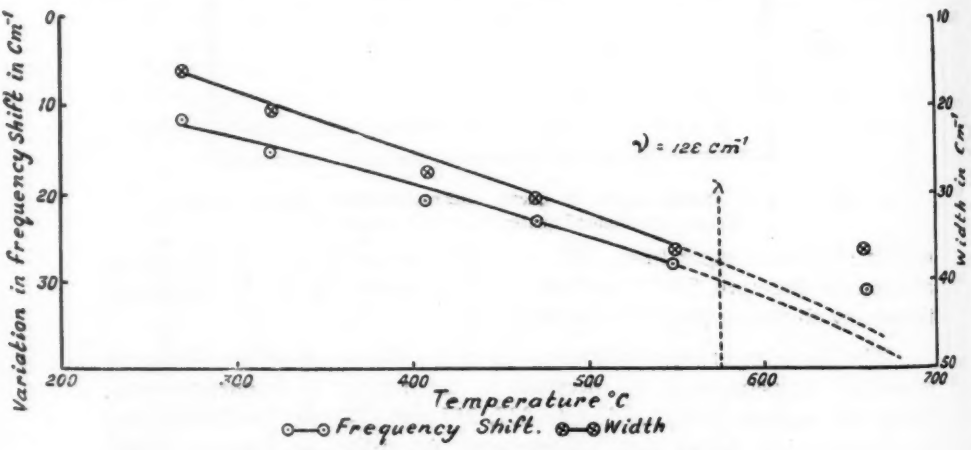

FIG. 3. Temperature dependence of the 128 line.

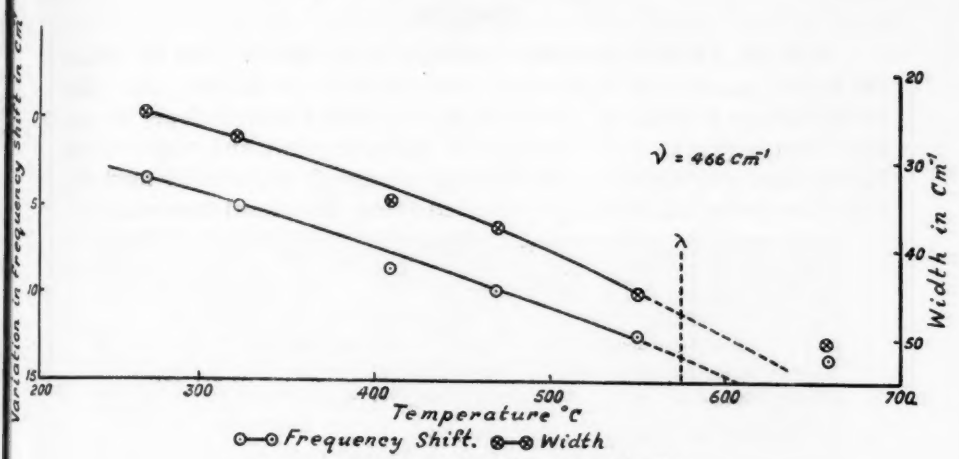

FIG. 4. Temperature dependence of the 466 line.

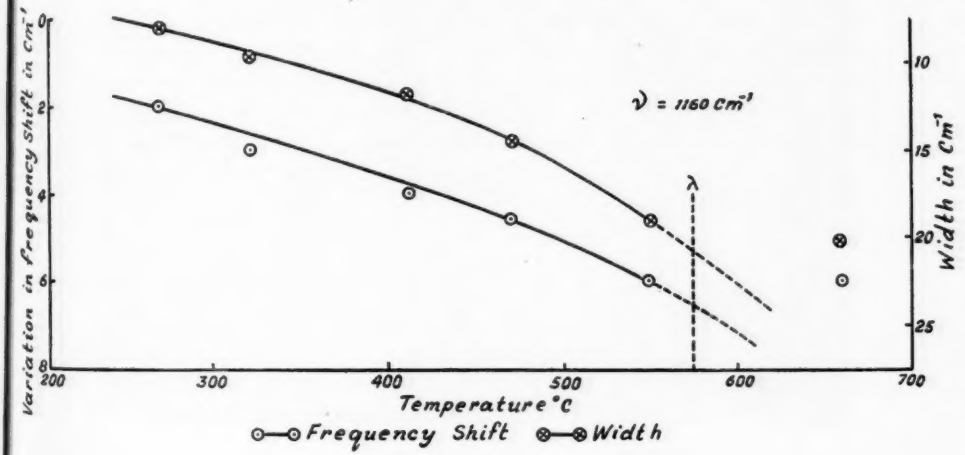

FIG. 5. Temperature dependence of the 1160 line.

The dotted extrapolation shows the variation to be expected beyond that temperature if there was no change in crystal structure. The points outside the curves on the right represent the actually observed variations at 660° C. after the transition.

In conclusion, the author wishes to express his heartfelt thanks to Prof. R. S. Krishnan for his keen interest and guidance in the course of this investigation.

Summary

With the λ 2536·5 resonance radiation of the mercury arc as exciter, the Raman spectrum of β-quartz has been recorded for the first time. Due to the increased symmetry, the spectrum of β-quartz exhibits fewer Raman lines than α-quartz. The variations in frequency shift and width of the Raman lines after the α-β transition point are also found to differ markedly from the corresponding changes observed below the critical temperature.

References

1. Jay .. *Proc. Roy. Soc.* (*Lond.*), 1933, **142 A**, 237.
2. Pitt and McKinely .. *Canadian Journal of Science*, 1936, **14**, 57.
3. Perrier and Mandrot .. *Compt. Rend.*, 1923, **175**, 622.
4. Narayanaswamy, P. K. .. *Proc. Ind. Acad. Sci.*, A, 1947, **25**, 521.
5. Nedungadi, T. M. K. .. *Ibid.*, 1940, **11**, 86.
6. Saxena, B. D. .. *Ibid.*, 1940, **12**, 93.
7. Raman, Sir C. V., and Nedungadi, T. M. K. *Nature*, 1940, **145**, 147.

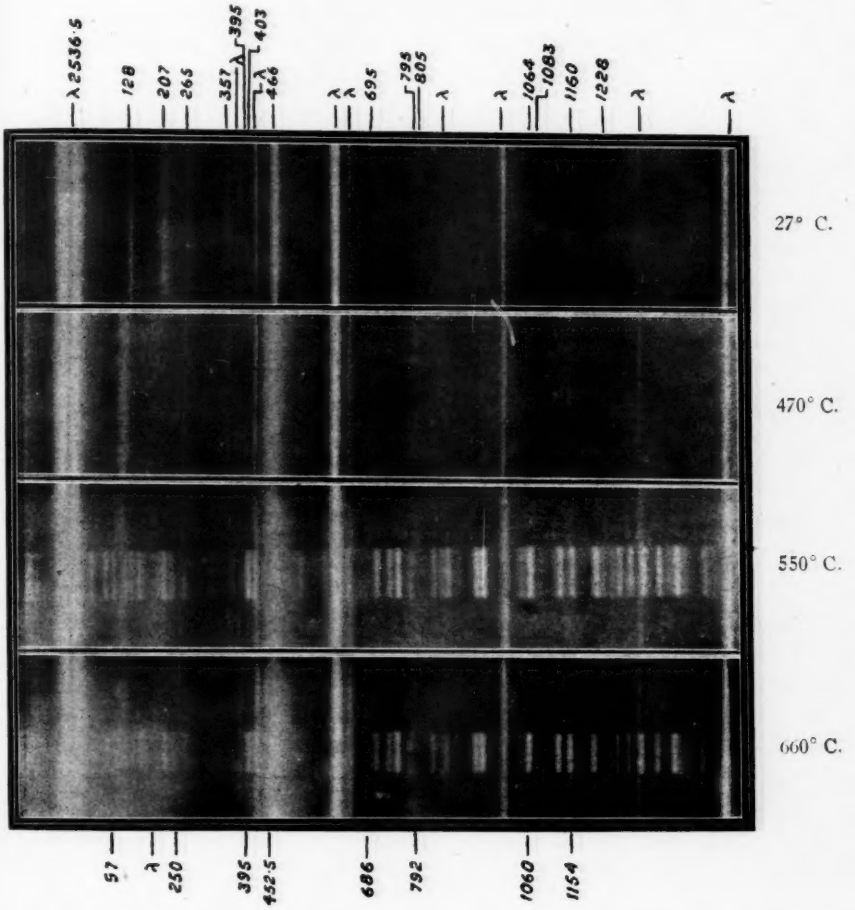

FIG. 1. α-β transformation in quartz. Raman spectrum at different temperatures

A NEW METHOD OF CALCULATING THE PIEZO-ELECTRIC CONSTANTS OF α-QUARTZ*

By Bishambhar Dayal Saksena and Krishna Gopal Srivastava
(Department of Physics, University of Allahabad, Allahabad, India)

Received November 8, 1948

Abstract.—A method of calculating the piezo-electric constants of α-quartz is described which consists in determining the electric moment developed by changes of bond-lengths and bond-angles on strain. Considering three atoms P, Q, R, of which P and R are silicon atoms and Q an oxygen atom or *vice-versa*, the electric moment developed on strain may be resolved into moments in the plane PQR and moments perpendicular to this plane. Resolving these moments along the axes of the crystal and summing up for all the forty-two planes in the unit cell, we get the piezo-electric equations and constants of the crystal. The electric moment in the plane is equivalent to the moment produced by the change of bond-length along the direction of the bonds before strain, while for the moment normal to the plane we take the average value, *i.e.*, half the value of the moment normal to the plane when the displacements of the atoms are wholly normal to the plane. The method gives good agreement with the observed values.

Introduction

The two piezo-electric constants of α-quartz may be calculated on Born's theory (1924). But the results obtained only give the right order of magnitude. In this paper a new method has been developed for calculating the piezo-electric constants of α-quartz which directly takes into account the structure of the crystal as revealed by X-rays and also enables us to obtain from the crystal structure the two equations which connect the electric moment developed on strain with the components of the strain. These equations are:—

$$\begin{aligned} p_x &= \epsilon_{11}(u_{xx} - u_{yy}) + \epsilon_{41}\, u_{yz} \\ p_y &= -\epsilon_{41}\, u_{xz} - \epsilon_{11}\, u_{xy} \\ p_z &= 0 \end{aligned} \qquad (1\cdot1)$$

where p_x, p_y, p_z are the components of the electric moment developed on strain, u_{xx}, u_{xy}, etc., the components of strain and ϵ_{11}, ϵ_{41} the piezo-electric coefficients.

* A report of this work has appeared in *Nature*, 1948, **161**, 203.

As quartz is a crystal with covalent bindings, the calculations have been made on the supposition that the electric moment developed on strain by a change of length of Si-O bond is $ke\Delta r$ and that produced by a change of angle between two Si-O bonds is $ker\Delta\phi$, where Δr and $\Delta\phi$ represent the change of bond-length and bond-angle on strain and ke represents the charge on an atom where 'k' is a constant whose value is in the neighbourhood of unity. We have first found the moments in the plane of the Si-O bonds and perpendicular to these planes and then resolved them along the axes of the crystal. By summing up for all such planes in the unit cell, we get the piezo-electric coefficients. The above method of approach is more intimately connected with the structure of the crystal. The calculation brings out an interesting result that the changes in bond-length contribute very largely to the longitudinal coefficient ϵ_{11} and nothing to the transverse coefficient ϵ_{41}, which arises entirely from a change of bond angles. The results obtained in this investigation show an agreement with the observed values. Even if we take k as 1, the discrepancy is small, the calculated values for $k = 1$ being $\epsilon_{11} = 6{\cdot}7 \times 10^4$ and $\epsilon_{41} = 1{\cdot}64 \times 10^4$. The best values of these coefficients according to Cady are $5{\cdot}1 \times 10^4 (\epsilon_{11})$ and $1{\cdot}23 \times 10^4 (\epsilon_{41})$.

2. The Structure of α-Quartz

The structure of quartz was first worked out by Bragg and Gibbs (1925, 1926). Each silicon atom appears surrounded by four oxygen atoms and each oxygen atom has two silicon atoms as neighbours. The projection of silicon and oxygen atoms in the basal plane is as shown in Fig. 1. The unit cell in α-quartz is hexagonal and each cell contains six oxygen and three silicon atoms as each silicon atoms is shared between two cells. Using hexagonal axes, the position of nine atoms in the unit cell for right-handed quartz are given as:—

Silicons (in order 1, 3, 5) $\rightarrow (u, 0, 0), (0, u, \frac{1}{3}), (\bar{u}, \bar{u}, \frac{2}{3})$.

Oxygens (in order 7, 8, 9, 10, 11, 12) $\rightarrow (\bar{x}, y, z), (y, x, \bar{z} - \frac{1}{3}),$

$(\bar{y}, x - y, \frac{1}{3} - z), (\bar{x}, y - x, z - \frac{1}{3}), (y - x, \bar{x}, -\frac{1}{3} - z), (x - y, \bar{y}, z)$.

From the X-ray data of Gibb's the author (1944) has calculated

$$u = {\cdot}46a,\ x = {\cdot}438a,\ y = {\cdot}287a,\ z = {\cdot}1168c.$$

In Fig. 1 we notice triangular groups of silicon atoms. The triangles are all similar in β-quartz but rotate in opposite senses when the crystal cools to α-quartz. From his X-ray investigations Gibbs found that at room temperature they are rotated by nearly 8° from the positions occupied by them in β-quartz. According to Bragg and Gibbs piezo-electricity arises

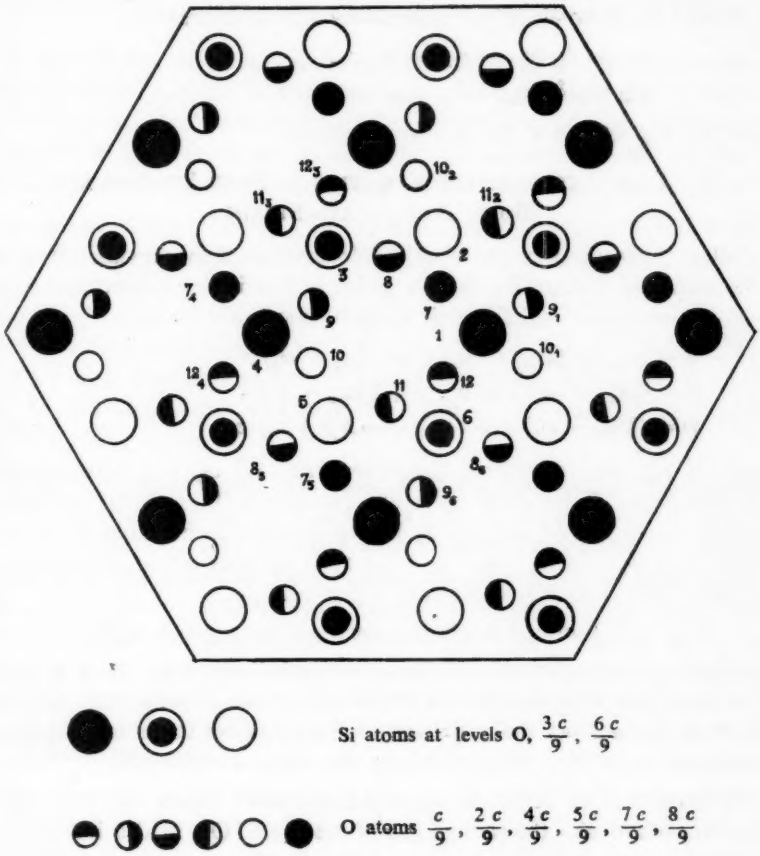

FIG 1

from a distortion of these triangular units on strain. Gibbs obtained a value of the piezo-electric modules δ_{11} by calculating the relative shifts of the centres of gravity of silicon and oxygen units for a pressure of one dyne and multiplying its component parallel to the electric axes by the charge density $4ne$, where n is the number of silicon atoms per c.c. The value of the piezo-electric modulus calculated in this way is 30×10^{-8} which is nearly five times the experimental value. Gibbs has not calculated δ_{41} nor does his method show how the equations (1·1) can be derived from the

structure of the crystal. It is to be noted that the piezo-electric moduli δ are related to piezo-electric constants by the relations:—

$$\epsilon_{11} = \delta_{11}(c_{11} - c_{12}) + \delta_{41} c_{14}$$
$$\epsilon_{41} = 2\delta_{11} c_{14} + \delta_{41} c_{44}, \qquad (2\cdot1)$$

where c_{11}, c_{12}, etc., are the elastic constants.

3. Calculation of the Variation of Bond Lengths and Bond Angles on Strain

Let us now consider the elastic deformation of the crystal. If x, y, z be the rectangular coordinates of a point before it is deformed and $x + u$, $y + v$, $z + w$ after it is deformed, we have (see Love)

$$u = xu_{xx} + (\tfrac{1}{2}u_{xy} - \omega_z)\, y + (\tfrac{1}{2}u_{xz} + \omega_y)\, z$$
$$v = (\tfrac{1}{2}u_{xy} + \omega_z)\, x + u_{yy}\cdot y + (\tfrac{1}{2}u_{yz} - \omega_x)\, z$$
$$w = (\tfrac{1}{2}u_{xz} - \omega_y)\, x + (\tfrac{1}{2}u_{yz} + \omega_x)\, y + u_{zz}\cdot z \qquad (3\cdot1)$$

where u_{xy}, u_{yy}, etc., are strain components and ω_x, ω_y, ω_z are the rotations about the axes. If however there are two points 'P' and 'Q', having co-ordinates x_1, y_1, z_1 and x_2, y_2, z_2 before strain which change to $x_1 + u_1$, $y_1 + v_1$, $z_1 + w_1$ and $x_2 + u_2$, $y_2 + v_2$, $z_2 + w_2$ after strain, the change in the length of the line PQ after strain is given by:—

$$r(l^2 u_{xx}^2 + m^2 u_{yy}^2 + n^2 u_{zz}^2 + lm\, u_{xy} + mn\, u_{yz} + ln\, u_{xz}) \qquad (3\cdot2)$$

where l, m, n are the direction cosines of a line before strain. Thus we notice that although the direction cosines of a line after strain contain the unknown coefficients ω_x, ω_y, ω_z, the extension of the line after strain is independent of them and is entirely determined by the strain coefficients.

Similarly if P, Q, R be the three points before strain which change to P_1, Q_1, R_1 after strain, the change $\Delta\alpha$ of the angle PQR is also independent of the rotation coefficients ω_x, ω_y, ω_z. For if $PQ = r_1$, $QR = r_2$, $PR = r_3$ and $\angle PQR = \alpha$ we have

$$r_3^2 = r_1^2 + r_2^2 - 2r_1 r_2 \cos\alpha$$

and by differentiating this we obtain

$$r_3 \Delta r_3 = r_1 \Delta r_1 + r_2 \Delta r_2 - (r_1 \Delta r_2 + r_2 \Delta r_1)\cos\alpha + r_1 r_2 \sin\alpha\cdot\Delta\alpha \qquad (3\cdot3)$$

Since Δr_1, Δr_2, Δr_3 are independent of ω_x, ω_y, ω_z; $\Delta\alpha$ is also independent of them. It is therefore apparent that in a more general elastic deformation the change in the length of a line and change in the angle between two lines can be completely determined without knowing the rotation components ω_x, ω_y, ω_z; but the same is not true for the direction cosines of a given line.

4. Calculation of the Piezo-Electric Moment in the Plane of Bonds and Perpendicular to this Plane

In any elastic deformation the displacement of positive and negative charges produces a static electric moment. As quartz is a crystal with covalent bonds, we need consider only close neighbours, *i.e.*, only those silicon and oxygen atoms which are in close neighbourhood and are bonded to each other may be expected to contribute effectively to the electric moment.

A change of the length Δr in the direction of the bond would produce a moment $ke\Delta r$ in that direction where ke is the sharing of charge represented by the bond. In each unit cell there are just twelve positive and twelve negative charges and also twelve Si-O bonds. Therefore if all the bonds were equivalent, each bond will have the same value of k and if the crystal be ionic k will be unity. But since the crystal belongs to the point group D_3, six Si-O bonds will have one value k_1 and another six will have a different value k_2.

As the direction cosines of a bond after strain are not known, it is not possible to resolve the moments along the axis of the crystal. We therefore consider a plane formed by three atoms P, Q, R of which P and R are silicon atoms and Q an oxygen or *vice-versa* so that PQ and QR represent Si-O bonds. Any displacement of these atoms can be resolved into displacement in the plane PQR and displacement perpendicular to the plane. An electric moment will therefore be produced by the displacements in the plane PQR and by those perpendicular to the plane; the total moment being a vector sum of these two moments. These moments can be resolved along the axes of the crystal.

The moments in the plane are due to extensions and contractions along the directions of the bonds before strain. This may be proved easily. The result of the strain is to alter the lengths PQ and QR and the bond angle PQR. If $e\Delta r_1$ and $e\Delta r_2$ represent the moments along PQ and QR, then the resultant moment is

$$e^2(\Delta r_1^2 + \Delta r_2^2 + 2\Delta r_1 . \Delta r_2 . \cos\alpha),$$

where α is the angle PQR. If α is changed into $\alpha + \Delta\alpha$, then the resultant moment will be $e^2(\Delta r_1^2 + \Delta r_2^2 + 2\Delta r_1 . \Delta r_2 . \cos\alpha - 2 . \Delta r_1 . \Delta r_2 . \sin\alpha . \Delta\alpha)$. Now according to (3·2) both Δr_1 and Δr_2 can be expressed in terms of u_{xx} and u_{yy} which are small quantities of the first order whose squares may be neglected. According to (3.3), $\Delta\alpha$ can be expressed in terms of the strain components u_{xx}, u_{yy}, etc. Therefore the last term in the above expression being a small quantity of the third order can be neglected in

comparison to the other terms which are of the second order. Hence the moment in the plane PQR is given by terms $ke\Delta r$ along the direction of the bonds PQ and QR before strain.

The moments perpendicular to the plane of bonds may be found from the changes in the angle PQR. In one extreme case the entire change in the angle PQR will be produced by displacements of atoms normal to the plane PQR, and the change of angle in the plane of the bonds PQR will be zero. In this case the moment normal to the plane will be maximum. In the other extreme case the displacements will be wholly in the plane PQR, the moment normal to the plane being zero. In any particular case, the moment perpendicular to the plane of the bonds will lie between these two values. Since the angle change is small and since in finding out the electric moment of the unit cell, the contributions of a large number of planes have to be considered we may take the average value, *i.e.*, half the value of the maximum moment, as the value of the moment normal to the plane.

The moments perpendicular to the plane may be found in the following manner. Suppose the co-ordinates of the atoms P, Q, R are (x_1, y_1, z_1), (x_2, y_2, z_2), (x_3, y_3, z_3), where $z_1 > z_2 > z_3$ so that with respect to Q as the origin, the co-ordinates of P are $(x_1 - x_2, y_1 - y_2, z_1 - z_2)$ and that of R are $(x_3 - x_2, y_3 - y_2, z_3 - z_2)$. After the strain the co-ordinates of P and R will be as given in (3.1) so that with respect to Q the point P will move above the plane PQR and the point R below the plane. If P and R are silicon atoms and Q an oxygen atom, the motion of P will produce a moment which will be opposed to that of R. Suppose that a change in the angle PQR is produced entirely by the displacements normal to the plane. If PQ = QR, draw a line QN perpendicular to PR (Fig. 2). Before strain, $\angle NQP = \angle NQR$,

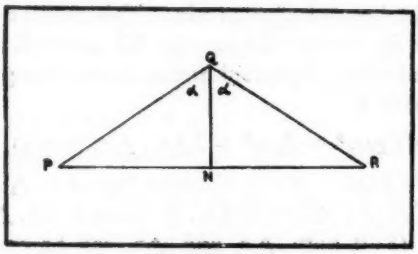

FIG. 2

but after the strain it will not be so. If $\Delta\alpha_1$ be the change in the angle NQP and $\Delta\alpha_2$ in the angle NQR after strain, then $k_1 er\Delta\alpha_1$ will be the moment

developed normal to the plane due to the motion of P and $k_2 er \Delta a_2$ due to the motion of Q. The resultant moment is $er(k_1 \Delta a_1 - k_2 \Delta a_2)$

$$= er[\tfrac{1}{2}(k_1 + k_2)(\Delta a_1 - \Delta a_2) + \tfrac{1}{2}(k_1 - k_2)(\Delta a_1 + \Delta a_2)] \quad (4.1)$$

Writing $\angle NQP = \angle NQR = a$, $r = PQ = QR$, the changes in PQ and QR as Δr_1 and Δr_2, we have $QN = v = r \cos a$.

From triangle NQP, we have $\Delta v = \Delta r_1 \cos a - r \sin a \, \Delta a_1$ and from triangle NQR, we have $\Delta v = \Delta r_2 \cos a - r \sin a \Delta a_2$

$\therefore \; r(\Delta a_1 - \Delta a_2) = (\Delta r_1 - \Delta r_2) \cot a$, which gives $(\Delta a_1 - \Delta a_2)$

If we write $PR = r_3$, and the variation of PR as Δr_3, we get from triangle PQR, $r_3 \Delta r_3 = r(\Delta r_1 + \Delta r_2)(1 - \cos 2a) + r^2 \sin 2a \cdot (\Delta a_1 + \Delta a_2)$, which gives $(\Delta a_1 + \Delta a_2)$. The average value of the moment normal to the plane will be half of the moment (4.1) which is the moment normal to the plane when the change in the angle PQR is entirely due to the displacements normal to the plane. Its value is therefore

$$\tfrac{1}{4}e\left[\tfrac{1}{2}(k_1+k_2)(\Delta r_1 - \Delta r_2)\cot a + \tfrac{1}{2}(k_1-k_2)\frac{r_3 \Delta r_3 - r(\Delta r_1 + \Delta r_2)(1-\cos 2a)}{r \sin 2a}\right] \quad (4.2)$$

5. Electric Moment of the Unit Cell

As the moments in the planes PQR are along the directions of the bonds PQ and QR and the moments normal to the planes are along the normals, we can resolve the moments along the axes of the crystal. We have now to sum up for all the planes PQR in the unit cell, and divide by the volume of the unit cell to get the electric moment per unit volume. There are six O-Si-O planes at each silicon atom, and there are six silicon atoms in the unit cell. But as each silicon atom is shared between two cells, the contributions of each of the six O-Si-O planes are equally shared between the two cells. In addition the contributions of the six Si-O-Si planes belong entirely to the cell. In summing up for all the planes, the electric moment produced by the displacement of silicon and oxygen atoms is reckoned four times. For example, the displacements of silicon atom (1) and oxygen atom (7) of the unit cell, and consequently the electric moments developed due to their motion, are counted four times if we resolve and sum up the electric moments of the planes (1, 7, 2), (1, 7, 12), and (1, 7, 10_1) and (1, 7, 9_1) which contain the atoms (1) and (7). Hence the moment per unit cell is given by:

$\frac{1}{4}[\frac{1}{2}$(moment due to 36 $\overset{O}{\underset{}{\diagdown}}$Si—O planes)+moments due to 6 Si-O-Si planes].

Let us first consider the moments in the plane which are equivalent to the electric moments along the directions of the Si-O bonds. In the six O-Si-O planes at each silicon atom, there are only four Si-O bonds each of

which is reckoned three times in summing up for the six planes. Thus as there are six silicon atoms in the unit cell, we have in all 24 Si-O bonds each of which is reckoned three times in summing up. It is immediately seen (Fig. 1) that twelve of these are identical with the other twelve as they are obtained by a mere translation of the atoms parallel to the electric axes. Hence half the moment in the plane due to thirty-six O-Si-O planes is just equivalent to the electric moment along the directions of the twelve Si-O bonds each of which is reckoned three times. Further the electric moment in the plane due to six Si-O-Si planes are equivalent to those along the twelve Si-O bonds. Thus each Si-O bond is reckoned four times. Hence the moments in the planes per unit cell are just equivalent to the moments $ke\Delta r$ along the twelve Si-O bonds, where Δr is the variation of the length of the Si-O bond.

As the silicon atoms (2), (1), (6) with their associated oxygen atoms have been obtained by a mere translation of the silicon atoms (5), (4), (3) with their associated oxygen atoms, half of the moment due to thirty-six planes is equivalent to the moments due to eighteen O-Si-O planes at silicon atoms (6), (1), (2).

We may now resolve the moments along the axes of the crystal. If (l, m, n) be the direction-cosines of the various Si-O bonds and (p, q, r) of the various normals to the O-Si-O and Si-O-Si planes, V the volume of the unit cell, e the electronic charge, we get

$$p_x = \frac{e}{\nabla}\left[\Sigma_{\text{12 Si-O bonds}}(k\Delta r \cdot l)\right] + \frac{e}{8\nabla}\left[\Sigma_{\text{18 O-Si-O and 6 Si-O-Si planes}}\left\{\tfrac{1}{2}(k_1+k_2)(\Delta r_1 - \Delta r_2)\cot\alpha + \tfrac{1}{2}(k_1-k_2)\frac{r_3\Delta r_3 - r(\Delta r_1+\Delta r_2)(1-\cos 2\alpha)}{r\sin 2\alpha}\right\}p\right] \quad (5.1)$$

with similar expressions for p_y and p_z.

This equation gives rise to equations of the form (1·1).

The values of Δr's for the various Si-O bonds in the unit cell have been given by the author (1944). Further the bonds $r_{1,7}$, $r_{1,12}$, $r_{3,9}$, $r_{5,10}$, $r_{3,8}$, $r_{5,11}$ contribute a value $k_1 e\Delta r$ to the electric moments and $r_{2,7}$, $r_{6,12}$, $r_{2,8}$, $r_{6,11}$, $r_{4,9}$ and $r_{4,10}$ contribute a value $k_2 e\Delta r$.

Knowing the direction cosines of the bonds and assuming that the direction of the moment is from silicon to oxygen we get for the first part in parenthesis in the above expression

$$\begin{aligned} p_x &= a\frac{e}{\nabla}(u_{xx} - u_{yy}) \times 10^{-8} = \lambda(u_{xx} - u_{yy}) \\ p_y &= -a\frac{e}{\nabla}u_{xy} \times 10^{-8} = -\lambda u_{xy} \\ p_z &= 0, \end{aligned} \quad (5.2)$$

where $a = \dfrac{4{\cdot}56\,k_1 - {\cdot}62\,k_2}{(1{\cdot}588)^2}$, $V = 111{\cdot}2 \times 10^{-24}$ c.c.

$$e = 4{\cdot}77 \times 10^{-10}\ e.s.u,\ \lambda = (7{\cdot}756\,k_1 - 1{\cdot}054\,k_2) \times 10^4.$$

Thus it is immediately apparent from these calculations that the moments along Si-O bonds give rise to longitudinal coefficients only.

For finding moments perpendicular to the planes of Si-O bonds we need the expressions

$$\tfrac{1}{2}(k_1 + k_2)(\Delta r_1 - \Delta r_2)\cot\alpha \text{ and}$$

$$\frac{k_1 - k_2}{2r \sin 2\alpha}[r_3 \Delta\ r_3 - r(\Delta r_1 + \Delta r_2)(1 - \cos 2\alpha)].$$

These along with the direction cosines of the normals to the various planes and the direction cosines of Si-O bonds and the variations of bond lengths are given in the appendix. The moments produced by 18 O-Si-O and six Si-O-Si planes fall into five groups. The moments in each group can be combined with others as such or with signs changed . We have seen before that the moments in the plane of the Si-O bonds do not contribute anything to the transverse piezo-electric coefficient. It may therefore be expected that the moments perpendicular to the plane of Si-O bonds will give rise to the transverse coefficient and will not contribute anything or contribute very little to the longitudinal coefficient. Also the value of k_1 should not be very different from k_2 and should be in the neighbourhood of unity. When this is kept in view there is only one way of combining them. (If we put $k_1 = k_2 = 1$ we find that the contribution of moments perpendicular to the plane of Si-O bonds is very small towards the longitudinal coefficient.) We get

$$p_x = [(-\ {\cdot}9988\,k_1 + 1{\cdot}0806\,k_2)(u_{xx} - u_{yy}) + (2{\cdot}866\,k_1 + {\cdot}202k_2)\,u_{yz}]\ \frac{e}{8V} \times 10^{-8}$$

$$p_y = [-(-\ {\cdot}9988k_1 + 1{\cdot}0806k_2)\,u_{xy} - (2{\cdot}866k_1 + {\cdot}202k_2)\,u_{xz}]\ \frac{e}{8V} \times 10^{-8}$$

$$p_z = 0, \qquad (5.3)$$

If the moments perpendicular to the plane of Si-O bonds do not contribute to the longitudinal coefficient we must have

$${\cdot}9988k_1 = 1{\cdot}0806k_2 \text{ (or } k_1 = 1{\cdot}082k_2)$$

and the resolved parts of these moments along the axes become

$$p_x = [(1{\cdot}537k_1 + {\cdot}1083k_2)\,u_{yz}] \times 10^4$$

$$p_y = [-(1{\cdot}537k_1 + {\cdot}1083k_2)\,u_{xz}] \times 10^4$$

$$p_z = \qquad 0 \qquad (5.4)$$

The total moments along the axes are the sum of the two expressions (5.2) and (5.4).

$$p_x = [(7\cdot756k_1 - 1\cdot054k_2)(u_{xx} - u_{yy}) + (1\cdot537k_1 + \cdot1083k_2)\, u_{yz}] \times 10^4$$

$$p_y = -(7\cdot756k_1 - 1\cdot054k_2)\, u_{xy} - (1\cdot537k_1 + \cdot1083k_2)\, u_{xz}] \times 10^4$$

$$p_z = 0, \tag{5.5}$$

$$\therefore \quad \epsilon_{11} = (7\cdot756k_1 - 1\cdot054k_2) \times 10^4$$

$$\epsilon_{41} = (1\cdot537k_1 + \cdot1083k_2) \times 10^4 \tag{5.6}$$

Using $\epsilon_{11} = 5\cdot1 \times 10^4$ we get $k_1 = \cdot695$, $k_2 = \cdot752$ and so $\epsilon_{41} = 1\cdot23 \times 10^4$ which is the observed value

If, however, we put $k_1 = k_2 = 1$ we get $\epsilon_{11} = 6\cdot78 \times 10^4$ and $\epsilon_{41} = 1\cdot64 \times 10^4$. Even these values are quite close to observed ones

$$\epsilon_{11} = 5\cdot1 \times 10^4 \text{ and } \epsilon_{41} = 1\cdot23 \times 10^4.$$

In this way we derive the equations of the type (1.1) from the structure and obtain satisfactory values of the piezo-electric coefficients. The value of k_1 and k_2 which are in the neighbourhood of $\cdot7$ show that the bonds are not ionic. This is also otherwise apparent since quartz is a hard crystal, showing high spectroscopic frequencies and the Si-O-Si angle is not 180°. Further it is also apparent from these calculations that the piezo-electric constants ϵ_{11} and ϵ_{41} are the true structure constants and not the modulii δ_{11} and δ_{41} which depend also on the elastic constants as in (2.1).

6. Appendix

The variations in length (Δr) of the various Si-O bonds are given by:

$1\cdot588\ \Delta r_{1,7} = \cdot6486u_{xx} + 1\cdot474u_{yy} + \cdot397u_{zz} - \cdot9777u_{xy} - \cdot7647u_{yz} + \cdot5074u_{xz}$

$1\cdot588\ \Delta r_{1,12}$ = same as above with signs of u_{xy} and u_{xz} changed.

$1\cdot588\ \Delta r_{2,7} = \cdot0155u_{xx} + 1\cdot141u_{yy} + 1\cdot364u_{zz} - \cdot1288u_{xy} - 1\cdot248u_{yz} + \cdot1408u_{xz}$

$1\cdot588\ \Delta r_{6,12}$ = same as above with signs of u_{xy} and u_{xz} changed.

$1\cdot588\ \Delta r_{2,8} = \cdot9720u_{xx} + \cdot1840u_{yy} + 1\cdot364u_{zz} + \cdot4239u_{xy} + \cdot501u_{yz} + 1\cdot152u_{xz}$

$1\cdot588\ \Delta r_{6,11}$ = same as above with signs of u_{xy} and u_{xz} changed.

$1\cdot588\ \Delta r_{4,9} = \cdot7468u_{xx} + \cdot4081u_{yy} + 1\cdot364u_{zz} + \cdot5521u_{xy} + \cdot7461u_{yz} + 1\cdot009u_{xz}$

$1\cdot588\ \Delta r_{4,10}$ = same as above with signs of u_{xy} and u_{xz} changed.

$1\cdot588\ \Delta r_{3,9} = \cdot4209u_{xx} + 1\cdot703u_{yy} + \cdot397u_{zz} + \cdot8465u_{xy} + \cdot8219u_{yz} + \cdot4087u_{xz}$

$1\cdot588\ \Delta r_{5,10}$ = same as above with signs of u_{xy} and u_{xz} changed.

$1\cdot588\ \Delta r_{3,8} = 2\cdot115u_{xx} + \cdot0083u_{yy} + \cdot397u_{zz} - \cdot1323u_{xy} - \cdot0573u_{yz} + \cdot9160u_{xz}$

$1\cdot588\ \Delta r_{5,11}$ = same as above with signs of u_{xy} and u_{xz} changed.

These Δr's are in A.U.

The direction cosines of the various Si-O bonds are:

	$r_{2,8}$	$r_{2,7}$	$r_{1,7}$	$r_{1,12}$	$r_{6,12}$	$r_{5,11}$	$r_{5,10}$	$r_{4,10}$	$r_{4,9}$	$r_{3,9}$	$r_{3,8}$	$r_{6,11}$
l ..	− ·9858	·1206	− ·8054	− ·8054	·1206	1·454	− ·6488	·8642	·8642	− ·6488	1·454	− ·9858
m ..	− ·4290	−1·068	1·214	−1·214	1·068	·091	1·305	− ·6389	·6389	−1·305	− ·091	·4290
n ..	−1·168	1·168	− ·630	·630	−1·168	− ·630	·630	−1·168	1·168	− ·630	·630	1·168
	1·588	1·588	1·588	1·588	1·588	1·588	1·588	1·588	1·588	1·588	1·588	1·588

The values of $\Sigma k\ \Delta r.l$, $\Sigma k\ \Delta r.m$, $\Sigma k\ \Delta r.n$ required for the first part in parenthesis in the expression (5.1) can then be evaluated, and are given in expressions (5.2).

The direction cosines (p, q, r) of the normals to the various planes are:

	1, 7, 12	8_6, 6, 9_6	10_2, 2, 11_2	1, 9_1, 10_1	8, 2, 7	11, 6, 12	12, 1, 10_1	9_6, 6, 11	8, 2, 10_2	7, 2, 11_2	7, 1, 9_1	8_6, 6, 12
p ..	0	·8795	·8795	0	−1·748	−1·748	−1·82	1·254	1·254	·5665	−1·82	·5665
q ..	1·015	·5073	− ·5073	2·02	1·01	−1·01	·3963	−1·379	1·379	1·774	− ·3963	−1·774
r ..	1·956	−1·956	1·956	−1·104	1·104	−1·104	−1·564	1·564	−1·564	1·564	1·564	−1·564
	2·203	2·203	2·203	2·301	2·301	2·301	2·431	2·431	2·431	2·431	2·431	2·431

	12, 1, 9_1	7, 1, 10_1	7, 2, 10_2	9_6, 6, 12	8, 2, 11_2	8_6, 6, 11	1, 7, 2	6, 12, 1	2, 8, 3	5, 11, 6	3, 9, 4	4, 10, 5
p ..	−1·82	−1·82	2·197	2·197	− ·3766	− ·3766	− ·7454	− ·7454	− ·3766	− ·3766	1·122	1·122
q ..	1·485	−1·485	·8338	− ·8338	2·319	−2·319	− ·8646	·8646	−1·077	1·077	− ·2133	·2133
r ..	·535	− ·535	·535	− ·535	− ·535	·535	− ·7135	·7135	·7135	− ·7135	− ·7135	·7135
	2·409	2·409	2·409	2·409	2·409	2·409	1·346	1·346	1·346	1·346	1·346	1·346

The values of

$$\frac{k_1 + k_2}{2}(\Delta r_1 - \Delta r_2)\cot\alpha \quad \text{and} \quad \frac{k_1 - k_2}{2r\sin 2\alpha}[r_3\Delta r_3 - r(\Delta r_1 + \Delta r_2)(1-\cos 2\alpha)]$$

are given below. The values of the moments p_x, p_y, p_z for the various groups of planes using the second part within brackets in the expression (5.1) are also being given. These values refer only to the moments perpendicular to the various planes given above.

Plane	$\frac{1}{2}(k_1+k_2)(\Delta r_1-\Delta r_2)\cot\alpha$	$\frac{k_1-k_2}{2r\sin 2\alpha}[r_3\Delta r_3-r(\Delta r_1+\Delta r_2)(1-\cos 2\alpha)]$
7, 1, 12	$k_1\{-\cdot7274u_{xy}+\cdot3779u_{xz}\}$	0
8_6, 6, 9_6	$k_1\{\cdot6311(u_{xx}-u_{yy})-\cdot3644u_{xy}$ $-\cdot3274u_{yz}+\cdot1889u_{zz}$	0
10_2, 2, 11_2	same as for 8_6, 6, 9_6 with signs of	u_{xy} and u_{xx} changed

$$p_x=[\cdot5035\,(u_{xx}-u_{yy})-\cdot2611u_{yz}]\frac{k_1e}{8V}\times10^{-8}$$

$$p_y=[-\cdot5035u_{xy}+\cdot2611u_{xz}]\frac{k_1e}{8V}\times10^{-8}$$

$$p_z=0;\qquad \cot\alpha=\cdot5913 \tag{I}$$

9_1, 1, 10_1	$k_2[\cdot4512u_{xy}+\cdot8247u_{xz}]$	0
8, 2, 7	$k_2[\cdot3909(u_{xx}-u_{yy})+\cdot2258u_{xy}$ $+\cdot7148u_{yz}+\cdot4132u_{zz}$	0
11, 6, 12	same as for 8, 2, 7 with signs of	u_{xy} and u_{xz} changed

$$p_x=[-\cdot5941\,(u_{xx}-u_{yy})-\cdot1\cdot085u_{yz}]\frac{k_2e}{8V}\times10^{-8}$$

$$p_y=[\cdot5941u_{xy}+1\cdot085u_{xz}]\frac{k_2e}{8V}\times10^{-8}$$

$$p_z=0;\ \cot\alpha=\cdot6491 \tag{II}$$

7, 1, 9_1	$\frac{k_1+k_2}{2}$ $[-\cdot04752u_{xx}+\cdot5147u_{yy}$ $-\cdot467u_{zz}-\cdot7389u_{xy}-\cdot7298u_{yz}$ $-\cdot2432u_{xz}$	$\frac{k_1-k_2}{2}$ $[\cdot6722u_{xx}-\cdot1328u_{yy}+\cdot6616u_{zz}$ $-\cdot2768u_{xy}-\cdot6598u_{yz}+\cdot7125u_{xz}]$
12_1, 1, 10_1	same as for 7, 1, 9_1 with signs of	u_{xy} and u_{xz} changed
8, 2, 10_2	$\frac{k_1+k_2}{2}$ $[-\cdot2662u_{xx}+\cdot7336u_{yy}-\cdot467u_{zz}$ $-\cdot6134u_{xy}+\cdot1584u_{yz}-\cdot7534u_{xz}]$	$\frac{k_1-k_2}{2}$ $[-1\cdot069u_{xx}+\cdot4074u_{yy}+\cdot6616u_{zz}$ $+\cdot7266u_{xy}+\cdot9461u_{yz}-\cdot2147u_{xz}]$
9_6, 6, 11	same as for 8, 2, 10_2 with signs of	u_{xy} and u_{xz} changed
7, 2, 11_2	$\frac{k_1+k_2}{2}$ $[1\cdot014u_{xx}-\cdot5478u_{yy}-\cdot467u_{zz}$ $+\cdot1261u_{xy}+\cdot5751u_{yz}-\cdot5104u_{xz}]$	$\frac{k_1-k_2}{2}$ $[-\cdot5899u_{xx}-\cdot0678u_{yy}+\cdot6616u_{zz}$ $+1\cdot017u_{xy}-\cdot2863u_{yz}-\cdot9264u_{xz}]$
8_6, 6, 12	same as for 7, 2, 11_2 with signs of	u_{xy} and u_{xz} changed

$$p_x=\left[\left(\cdot269\frac{k_1+k_2}{2}-2\cdot386\frac{k_1-k_2}{2}\right)(u_{xx}-u_{yy})+\left(1\cdot523\frac{k_1+k_2}{2}+1\cdot829\frac{k_1-k_2}{2}\right)u_{yz}\right]\frac{e}{8V}\times10^{-8}$$

$$p_y=\left[-\left(\cdot269\frac{k_1+k_2}{2}-2\cdot386\frac{k_1-k_2}{2}\right)u_{xy}-\left(1\cdot523\frac{k_1+k_2}{2}+1\cdot829\frac{k_1-k_2}{2}\right)u_{xz}\right]\frac{e}{8V}\times10^{-8}$$

$$p_z=0;\ \cot\alpha=\cdot767 \tag{III}$$

Plane	$\frac{1}{2}(k_1+k_2)(\Delta r_1-\Delta r_2)\cot\alpha$	$\frac{k_1-k_2}{2r\sin 2\alpha}\,[r_3\Delta r_3-r(\Delta r_1+\Delta r_2)(1-\cos 2\alpha)$
12, 1, 9	$\frac{k_1+k_2}{2}$ [−·0458u_{xx}+·4972u_{yy}−·451u_{zz} +·1986u_{xy}−·7049u_{yz}−·7071u_{zx}]	$\frac{k_1-k_2}{2}$ [·6507u_{xx}+·6631u_{yy}−1·304u_{zz} +·7396u_{xy}+·6725u_{yz}+·1655u_{zx}]
7, 1, 10_1	same as for 12, 1, 9_1 with signs of	u_{xy} and u_{zx} cnanged
7, 2, 10_2	$\frac{k_1+k_2}{2}$ [·1891u_{xx}+·2621u_{yy}−·451u_{zz} −·3347u_{xy}+·9656u_{yz}−·2564u_{zx}]	$\frac{k_1-k_2}{2}$ [·01934u_{xx}+1·29u_{yy}−1·304u_{zz} −·3737u_{xy}−·4789u_{yz}−·4995u_{zx}]
9_6, 6, 12	same as for 7, 2, 10_2 with signs of	u_{xy} and u_{zx} changed
8, 2, 11_2	$\frac{k_1+k_2}{2}$ [·5332u_{xx}−·0827u_{yy}−·451u_{zz} −·136u_{xy}−·2604u_{yz}−·9647u_{zx}]	$\frac{k_1-k_2}{2}$ [1·299u_{xx}+·0145u_{yy}−1·304u_{zz} +·3763u_{xy}−·1934u_{yz}+·6637u_{zx}]
8_6, 6, 11	same as for 8, 2, 11_2 with signs of	u_{xy} and u_{zx} changed

$$p_x = \left[\left(\cdot 2476\,\frac{k_1+k_2}{2} - 1\cdot 355\,\frac{k_1-k_2}{2}\right)(u_{xx}-u_{yy}) + \left(2\cdot 908\,\frac{k_1+k_2}{2} - 1\cdot 83\frac{k_1-k_2}{2}\right)u_{yz}\right]\frac{e}{8V}\times 10^{-8}$$

$$p_y = \left[-\left(\cdot 2476\,\frac{k_1+k_2}{2} - 1\cdot 355\,\frac{k_1-k_2}{2}\right)u_{xy} - \left(2\cdot 908\,\frac{k_1+k_2}{2} - 1\cdot 83\,\frac{k_1-k_2}{2}\right)u_{zx}\right]\frac{e}{8V}\times 10^{-8}$$

$$p_z = 0;\quad \cot\alpha = \cdot 7408 \qquad \text{(IV)}$$

1, 7, 2	$\frac{k_1+k_2}{2}$ [·1156u_{xx}+·0608u_{yy}−·1766u_{zz} −·155u_{xy}+·08824u_{yz}+·06694u_{zx}]	$\frac{k_1-k_2}{2}$ [−·4273u_{xx}+·4559u_{yy}−·01524u_{zz} −·°08674u_{xy}−·4501u_{yz}+·5509u_{zx}]
1, 12, 6	same as for 1, 7, 2 with signs of	u_{xy} and u_{zx} changed
2, 8, 3	$\frac{k_1+k_2}{2}$ [·2087u_{xx}−·03236u_{yy} −·1766u_{zz}−·1016u_{xy}−·102u_{yz} −·0431u_{zx}]	$\frac{k_1-k_2}{2}$ [·3099u_{xx}−·2825u_{yz}−·01524u_{zz} +·3383u_{xy}−·2693u_{yz}+·6751u_{zx}]
5, 11, 6	same as for 2, 8, 3 with signs of	u_{xy} and u_{zx} changed
3, 9, 4	$\frac{k_1+k_2}{2}$ [−·0595u_{xx}+·2364u_{yy}−·1766u_{zz} +·05375u_{xy}+·01385u_{yz}−·1096u_{zx}]	$\frac{k_1-k_2}{2}$ [·1606u_{xx}−·1289u_{yy}−·01524u_{zz} +·4279u_{xy}+·7150u_{yz}+·1266u_{zx}]
4, 10, 5	same as for 3, 9, 4 with signs of	u_{xy} and u_{zx} changed

$$p_x = \left[\left(-\cdot 3443\,\frac{k_1+k_2}{2} + \cdot 564\,\frac{k_1-k_2}{2}\right)(u_{xx}-u_{yy}) + \left(-\cdot 0176\,\frac{k_1+k_2}{2} + 1\cdot 84\,\frac{k_1-k_2}{2}\right)u_{yz}\right]\frac{e}{8V}\times 10^{-8}$$

$$p_y = \left[-\left(-\cdot 3443\,\frac{k_1+k_2}{2} + \cdot 564\,\frac{k_1-k_2}{2}\right)u_{xy} - \left(-\cdot 0176\,\frac{k_1+k_2}{2} + 1\cdot 84\,\frac{k_1-k_2}{2}\right)u_{zx}\right]\frac{e}{8V}\times 10^{-8}$$

$$p_z = 0;\quad \cot\alpha = \cdot 29 \qquad \text{(V)}$$

The sum of the moments along the axes due to these five groups is given in the expressions (5.3). These give the moments along the axes due to the moments perpendicular to the plane of Si-O bonds. The sum of the moments as given in expressions (5.2) and (5.3) or (5.4) gives the total moment along the axes and is given in (5.5). The piezo-electric constants calculated from (5.5) according to (1.1) are given in (5.6).

References

Born, M. .. *Handbuch der Phy.*, 1924, **24**, 2, 636.

Bragg and Gibbs .. *Proc. Roy. Soc.*, 1925, **109**, 425.

Cady, W. G. .. *Piezo-Electricity*, McGraw Hill Publication, 1945, p. 415.

Gibbs, R. E. .. *Proc. Roy. Soc.*, 1926, **110**, 443.

Love .. *Math. Theory of Elasticity*, pp. 38, 39.

Saksena, B. D. .. *Proc. Ind. Acad. Sci.*, A, 1944, **19**, 357.

VARIATION OF THE PIEZO-ELECTRIC CONSTANTS OF α-QUARTZ WITH TEMPERATURE*

By Bishambhar Dayal Saksena and Krishna Gopal Srivastava
(Department of Physics, University of Allahabad, Allahabad, India)

Received November 8, 1948

Abstract.—The method of finding the piezo-electric constants with the help of the variations of bond distances and bond angles on strain has been utilised in finding the variations of the piezo-electric constants ϵ_{11} and ϵ_{41} of α-quartz with temperature. It is found that the variations of ϵ_{11} with temperature can be explained on the basis of the change of co-ordinates with temperature. At 558° C. the silicon atoms are found to occupy the same positions as they do in β-quartz. As the transition temperature is reached, the longitudinal coefficient ϵ_{11} drops to zero, while the transverse coefficient ϵ_{41} decreases by only 15%. The piezo-electric constant of β-quartz has been similarly determined and its value comes out to be $1{\cdot}05 \times 10^4$ for a non-ionic crystal ($k = {\cdot}724$) and $1{\cdot}45 \times 10^4$ for an ionic crystal ($k = 1$).

1. Introduction

In the previous paper the authors have found the piezo-electric constants of α-quartz by considering the variations of Si-O bond-lengths and of the Si-O-Si and O-Si-O bond angles in a unit cell in an elastic deformation. The same method has been used to find the variations of the piezo-electric constants ϵ_{11} and ϵ_{41} of α-quartz with temperature, and also to find the piezo-electric constant of β-quartz.

2. Experimental Data on the Variation of the Piezo-Electric Constant with Temperature

According to Perrier (1916) the phenomenon was first independent of temperature and decreased sensibly from 200° C. onwards and finally at 579° C. the piezo-electric liberation of charges ceased suddenly. Dawson (1927) states that the piezo-electric effect increases by 20% from room temperature to 60° C. and then decreases slowly till 300° C. and then rapidly reaches low values at about 480° C. But according to Sculwas-Sorokina (1929) Dawson's results are affected by the electrical conductivity of quartz.

* A report of the work has appeared in *Nature*, Feb. 21, 1948.

Andreeff and others (1929) using the quartz resonator method found only a small change of about 10% between 0° C. and 500° C. Freederiscksz and Michailov (1932) have also determined the piezo-electric modulus δ_{41} by the same method. Their results are given below.

T° C.→	150	246	300	380	420	470	502	526	540	552	568
$\delta_{11}\times10^{+8}$→	6·50	6·68	6·50	6·60	6·50	6·25	6·11	4·50	3·97	3·83	3·3
$S_{11}\times10^{+12}$→	1·291	1·293	1·298	1·302	1·322	1·355	1·395	1·448	1·484	1·54	1·75
$\epsilon_{11}\times10^{-4}$→	5·035	5·154	5·007	5·070	4·915	4·607	4·380	3·107	2·675	2·487	1·88

The values of $\epsilon_{11} = \dfrac{\delta_{11}}{S_{11}}$ given by these authors are only approximate values as the piezo-electric modulus δ_{11} is related to the constant ϵ_{11} by the relation

$$\delta_{11} = \epsilon_{11}(S_{11} - S_{12}) + \epsilon_{41} S_{14}$$

so that

$$\epsilon_{11} = \frac{\delta_{11}}{S_{11}} + e_1 \text{ where } e_1 = \epsilon_{11}\frac{S_{12}}{S_{11}} - \epsilon_{41}\frac{S_{14}}{S_{11}}$$

The value of e_1 at room temperature is only 1/25th of the value of ϵ_{11} and at higher temperatures it is not likely to be very different. We have assumed the values of ϵ_{11} given by these authors, plotted them on a smooth curve, and obtained the following values at various temperatures.

T° C.→	18	118	203	280	366	418	494	525	558	567
ϵ_{11} →	5·1	5·1	5·09	5·08	5·05	4·98	4·15	3·37	2·41	$1·89\times10^{4}$

Pitt and Mackinley (1936) have not given any values but they find a weak maximum at 200° C.

There is no data for the variation of ϵ_{41} with temperature.

3. Calculation of the Piezo-Electric Constants at Various Temperatures

For the purpose of these calculations, we must know the co-ordinates of the atoms in α-quartz at various temperatures. Using the hexagonal axes, the positions of the nine atoms in the unit cell have already been given in an earlier paper. These are stated in terms of four parameters—u, x, y, z—where the value of u gives the position of the silicon atoms, and the values of x, y, z, those of the oxygen atoms. If we use rectangular co-ordinates x', y', z' (the horizontal electric axis being the x' axis) we get

$$x' = x - \frac{y}{2};\ y' = \frac{\sqrt{3}}{2}y;\ z' = z.$$

If we write $u = \dfrac{a}{2} - p$, the position of the silicon atoms become determined if we know p. Gibbs assumes that every oxygen atom is equidistant

from its silicon neighbours. If Si-O distance be taken as 'd', and if x', y', z' be the co-ordinates of the reference oxygen atom of the unit cell in rectangular co-ordinates, we can find x', y', if z' be known.

$$y' = \frac{1}{\sqrt{3}} \frac{1}{\left(\frac{a}{2}+p\right)} \left\{\left(\frac{a}{2}-3p\right)x' + \left(2ap + \frac{c^2}{9} - \frac{2}{3}cz'\right)\right\}$$

$$x' = \frac{1}{(a^2+12p^2)}\left[3\left(\frac{a^2}{4}-p^2\right)\left(\frac{a}{2}+p\right) - \left(\frac{a}{2}-3p\right)\left(2ap+\frac{c^2}{9}-\frac{2}{3}cz'\right)\right.$$

$$\left. -\sqrt{3}\left(\frac{a}{2}+p\right)\times \right.$$

$$\left.\sqrt{(a^2+12p^2)\left\{d^2-\tfrac{1}{4}\left(\frac{a^2}{4}+\frac{c^2}{9}+3p^2\right)\right\}-\left(\frac{a^2}{4}+\frac{c^2}{9}+3p^2\right)\left(\frac{c}{3}-2z'\right)^2}\right]$$

The distance $q = \sqrt{d^2 - \frac{1}{4}\left(\frac{a^2}{4}+\frac{c^2}{9}+3p^2\right)}$ is the distance of the oxygen atom from the middle point of the line joining the silicon atoms. For β-quartz, $p = 0$, $z' = c/6$; and so $x' = \frac{3a}{8} - \frac{\sqrt{3}}{2}q$, $y' = \frac{x'}{\sqrt{3}}$.

The above calculation shows that we need five parameters a, c, p, q, z' to determine the co-ordinates of quartz of various temperatures. The values of a and c at various temperatures are known from the work of Jay (1938) while the values of z' were taken from the work of Gibbs (1925), who measured the intensities of reflection of X-rays from various planes in the crystal, particularly from the (111) plane. To explain the rising part of the curve upto 575° C., Gibbs has given another curve indicating the position of the oxygen planes relative to the silicon planes. From this curve the co-ordinates of the various oxygen atoms were determined, but the shape of the curve beyond 525° C. is not definite. We have no data for the variation of p and q with temperature. From the co-ordinates of α- and β-quartz as obtained from Gibbs' data, we find that the Si-O distance in α-quartz is the same as in β-quartz. We therefore assume that it does not vary with temperature and take it as 1·5917 ($d^2 = 2{\cdot}5337$) for the purpose of our calculations. We are now left with only one parameter p and this was determined with reference to the variation of ϵ_{11} with temperature. Using a particular value of p and z' we can calculate x' and y' from the formulæ given before.

The values of ϵ_{41} have been calculated for the room temperature and for 567° C. while ϵ_{11} has been calculated for all the temperatures. The

calculations for ϵ_{41} are very long and tedious, and so they have been made for two temperatures only as shown.

T° C.	'a' A.U.	'c' A.U.	'p' A.U.	'x' A.U.	'y' A.U.	'z' A.U.	$\epsilon_{11}\times10^{-4}$	$\epsilon_{41}\times10^{-4}$
18	4·9030	5·3930	·1989	1·443	1·214	·634	5·11	1·23
567	4·9685	5·4355	0	1·496	1·012	·730	1·85	1·08

The values of k_1 and k_2 calculated on the basis that the moments perpendicular to the plane of the bonds give no contribution to the longitudinal piezo-electric coefficient ϵ_{11} are $k_1 = \cdot752$ and $k_2 = \cdot695$ at 18° C. and $k_1 = \cdot724$ and $k_2 = \cdot757$ at 567° C. There is a certain degree of inexactness in these calculations due to the fact that both z' and ϵ_{11} are not correctly known. As is to be expected, we see that both k_1 and k_2 tend to become equal at 567° C. For the intervening temperatures we have calculated ϵ_{11} by assuming a proper value of 'p'. We have assumed $k_1 = \cdot752$ and $k_2 = \cdot659$ for all the temperatures. As already explained this is not strictly true for higher temperatures, but the calculations enable us to explain the fact that the progressive diminution of ϵ_{11} with temperature can be explained by a change of co-ordinates with temperature.

T° C.	'a' A.U.	'c' A.U.	'p' A.U.	'x' A.U.	'y' A.U.	'z' A.U.	$\epsilon_{11}\times10^{-4}$ Cal.	$\epsilon_{11}\times10^{+1}$ Obs.
18	4·9030	5·3930	·1989	1·4430	1·2140	·6340	5·11	5·10
118	4·9102	5·3982	·2000	1·4540	1·2200	·6365	5·08	5·10
203	4·9172	5·4027	·2100	1·4690	1·2320	·6380	5·04	5·09
280	4·9245	5·4069	·2200	1·4840	1·2460	·6400	4·97	5·08
366	4·9334	5·4129	·2200	1·4990	1·2520	·6415	4·92	5·05
418	4·9396	5·4163	0·230	1·5170	1·2640	·6430	4·82	4·92
494	4·9503	5·4241	·1000	1·5010	1·1630	·6460	4·16	4·15
525	4·9560	5·4276	·0100	1·5150	1·0980	·6500	3·30	3·37
558	4·9642	5·4338	·0000	1·4950	1·0240	·7150	2·34	2·41
567	4·9685	5·4355	·0000	1·4960	1·0120	·7300	1·85	1·88

4. Discussion

Although the co-ordinates given above are only approximately correct, one point which can be definitely stated is that for 558° C. and 567° C. the value of 'p' is zero. This means that at these temperatures the silicon atoms occupy the same positions as they do in β-quartz. It is also clear that there is a general expansion of the lattice upto 400° C. after which the silicon atoms change their positions rather rapidly and occupy the same positions as they do in β-quartz; it is likely that this condition also exists at 525° C. But

the oxygens and silicons do not move appreciably along the 'c' axis upto 558° C. After this the oxygens move appreciably, rather rapidly, and further diminution in ϵ_{11} is due to their motion. From the room temperature to 567° C., the total change in the oxygen positions along the 'c' axis does not exceed ·066 A.U. The oxygens lie at $z' = \cdot 73$ at 567° C. while in β-quartz they lie midway between the silicon planes at $z' = c/6 = \cdot 902$ A.U. The change of ·17 A.U. takes place very close to the critical temperature, and some may take place at the critical temperature itself. An absorption of 4 grs.-calories of heat has been observed by Perrier and Wolfers (1920) at the transition temperature.

A study of the Raman spectra of α-quartz by the author (1940) has brought out the interesting fact that the lines which broaden most with temperature are those in which the movements of atoms are confined to the basal plane, while the lines in which the movements are perpendicular to the basal plane remain practically sharp even at higher temperatures. Of those lines which broaden most with temperature, the line 207 shows the phenomena to a remarkable extent, and the vibration is mostly due to the motion of the silicon atoms in the basal plane. These observations are in general agreement with the observations made above about the motions of the silicon and oxygen atoms. It is possible that the large displacements of the silicon atoms in the basal plane with temperature lead to large amplitudes of vibration of these atoms which gives rise to broadening ; while perpendicular to the basal plane the displacements of atoms are not large enough to give rise to any anharmonicity, in the vibrations.

5. Calculation of the Piezo-Electric Constant ϵ_{41} of β-Quartz

The structure of β-quartz has been investigated by Bragg and Gibbs (1925) and Wyckoff (1926). Using the values 'a' = 5·01 A.U. and 'c'= 5·466 (Jay, 1933 and Landolt Tables) and the value of $q = \cdot 35$ A.U. (Bragg and Gibbs, 1925) we get

$$u = \cdot 5\, a,\ x = \cdot 2094\, a,\ y = -\cdot 2101\, a,\ z = c/6$$

which agree with those given in Landolt's tables.

The calculations for β-quartz are shown in the Appendix. The method of procedure is just the same as in α-quartz. Resolving the moments in the direction of the Si-O bonds along the axes, we get

$$\begin{aligned} p_x &= \cdot 897\,(k_1 - k_2)\,(u_{xx} - u_{yy}) \cdot (e/\mathrm{V}) \times 10^{-8} \\ p_y &= -\cdot 897\,(k_1 - k_2)\,(u_{xy}) \cdot (e/\mathrm{V}) \times 10^{-8} \\ p_z &= 0 \end{aligned} \qquad (5.1)$$

As the coefficient of u_{yz} is zero, the moments in the plane of the Si-O bonds give no contribution to the transverse coefficient ϵ_{41}.

The moments perpendicular to the plane of the Si-O bonds when resolved along the axes give

$$p_x = [-\cdot 6838\,(k_1 - k_2)\,(u_{xx} - u_{yy}) + 2\cdot 879\,(k_1 + k_2)/2\cdot u_{yz}]\,(e/8\mathrm{V}) \times 10^{-8}$$
$$p_y = [\cdot 6838\,(k_1 - k_2)\,(u_{xy}) - 2\cdot 879\,(k_1 + k_2)/2\cdot u_{xz}]\,(e/8\mathrm{V}) \times 10^{-8}$$
$$p_z = 0 \qquad (5.2)$$

If we assume, as in α-quartz, that the moments perpendicular to the plane of the bonds give no contribution to the longitudinal coefficient ϵ_{11} we must have $k_1 = k_2$. This is also otherwise evident, for β-quartz is a hexagonal crystal so that both x and y axes are axes of two-fold symmetry. All the Si-O bonds must therefore be of the same type, so that $k_1 = k_2$. The above assumption is therefore justified. Since $k_1 = k_2$, we get

$$\epsilon_{11} = 0 \text{ and } \epsilon_{41} = 2\cdot 879\, k_1 \cdot (e/8\mathrm{V}) \times 10^{-8} \qquad (5.3)$$

It has been shown before that in α-quartz, k_1 becomes nearly equal to k_2 near the transition temperature, and in β-quartz it is so. We therefore take $k_1 = \cdot 724$ in β-quartz which is the mean of the values of k_1 and k_2 in α-quartz. Since the volume of the unit-cell in β-quartz is $118\cdot 8 \times 10^{-24}$ c.c. we get $\epsilon_{41} = 1\cdot 05 \times 10^4$.

If, however, we take $k_1 = k_2 = 1$, we get $\epsilon_{41} = 1\cdot 45 \times 10^4$. Therefore, for β-quartz, $\epsilon_{11} = 0$ and $\epsilon_{41} = 1\cdot 05 \times 10^4$. Thus in passing from α-quartz to β-quartz, ϵ_{11} drops to zero, while ϵ_{41} diminishes by nearly 15%. Using $c_{44} = 3\cdot 58 \times 10^{11}$ (Kammer and Atanasoff, 1942) and $c_{14} = 0$, we get

$$\delta_{41} = \frac{\epsilon_{41}}{c_{44}} = 2\cdot 93 \times 10^{-8}.$$

6. Appendix

The Δr's for the various Si-O bonds are given by:

$$1\cdot 587\,\Delta r_{1,7} = \cdot 8641\, u_{xx} + \cdot 8275\, u_{yy} + \cdot 83\, u_{zz} - \cdot 8457\, u_{xy} - \cdot 8287\, u_{yz} + \cdot 8468\, u_{xz}$$

$1\cdot 587\,\Delta r_{1,12}$ = same as above with signs of u_{xy} and u_{xz} changed.

$$1\cdot 587\,\Delta r_{2,7} = \cdot 1043\, u_{xx} + 1\cdot 587\, u_{yy} + \cdot 83\, u_{zz} - \cdot 4068\, u_{xy} - 1\cdot 149\, u_{yz} + \cdot 2942\, u_{xz}$$

$1\cdot 587\,\Delta r_{6,12}$ = same as above with signs of u_{xy} and u_{xz} changed.

$$1\cdot 587\,\Delta r_{2,8} = 1\cdot 569\, u_{xx} + \cdot 1225\, u_{yy} + \cdot 83\, u_{zz} + \cdot 4384\, u_{xy} + \cdot 3188\, u_{yz} + 1\cdot 141\, u_{xz}$$

$1\cdot 587\,\Delta r_{6,11}$ = same as above with signs of u_{xy} and u_{xz} changed.

$$1{\cdot}587\ \Delta\, r_{3,8} = 1{\cdot}569\, u_{xx} + {\cdot}1225\, u_{yy} + {\cdot}83\, u_{zz} - {\cdot}4384\, u_{xy} - {\cdot}3188\, u_{yz} + 1{\cdot}141\, u_{xz}$$

$1{\cdot}587\ \Delta\, r_{5,11}$ = same as above with signs of u_{xy} and u_{xz} changed.

$$1{\cdot}587\ \Delta\, r_{3,9} = {\cdot}1043\, u_{xx} + 1{\cdot}587\, u_{yy} + {\cdot}83\, u_{zz} + {\cdot}4068\, u_{xy} + 1{\cdot}149\, u_{yz} + {\cdot}2942\, u_{xz}$$

$1{\cdot}587\ \Delta\, r_{5,10}$ = same as above with signs of u_{xy} and u_{xz} changed.

$$1{\cdot}587\ \Delta\, r_{4,9} = {\cdot}8641\, u_{xx} + {\cdot}8275\, u_{yy} + {\cdot}83\, u_{zz} + {\cdot}8457\, u_{xy} + {\cdot}8287\, u_{yz} + {\cdot}8468\, u_{xz}$$

$1{\cdot}587\ \Delta\, r_{4,10}$ = same as above with signs of u_{xy} and u_{xz} changed.

The direction-cosines of the various Si-O bonds are:

	$r_{1,7}$	$r_{2,7}$	$r_{2,8}$	$r_{3,8}$	$r_{3,9}$	$r_{4,9}$	$r_{4,10}$	$r_{5,10}$	$r_{5,11}$	$r_{6,11}$	$r_{6,12}$	$r_{1,12}$
l ..	−·9296	·3229	−1·252	+1·252	−·3229	·9296	·9296	−·3229	+1·252	−1·252	·3229	−·9296
m ..	·9097	−1·26	−·35	−·35	−1·26	·9097	−·9097	1·26	·35	·35	1·26	−·9097
n ..	−·911	·911	−·911	·911	−·911	·911	−·911	·911	−·911	·911	−·911	+·911
	1·587	1·587	1·587	1·587	1·587	1·587	1·587	1·587	1·587	1·587	1·587	1·587

As before we assign to the bonds $r_{1,7}$, $r_{1,12}$, $r_{3,8}$, $r_{3,9}$, $r_{5,10}$, $r_{5,11}$ the value of the charge $k_1 \cdot e$ and to the remaining a value $k_2 \cdot e$. The moments along the bonds may now be resolved along the axes. The result is given in (5.1).

The direction-cosines of the normals to the various planes formed by the various Si-O bonds are:

	7, 1, 10_1	12, 1, 9_1	8, 2, 11_2	8_6, 6, 11	7, 2, 10_2	9_6, 6, 12	1, 7, 2	6, 12, 1	2, 8, 3	5, 11, 6	3, 9, 4	4, 10, 5
p ..	−·9097	−·9097	−·35	−·35	1·26	1·26	−·3189	−·3189	·6380	·6380	−·3189	−·3189
q ..	−·9296	·9296	1·252	−1·252	·3229	−·3229	·5527	−·5527	0	0	−·5527	·5527
r ..	0	0	0	0	0	0	·8778	−·8778	−·8778	·8778	·8778	−·8778
	1·301	1·301	1·301	1·301	1·301	1·301	1·085	1·085	1·085	1·085	1·085	1·085
	1, 7, 12	10_2, 2, 11_2	9_1, 1, 10_1	8_6, 6, 9_6	8, 2, 7	11, 6, 12	7, 1, 9_1	12, 1, 10_1	8, 2, 10_2	9_6, 6, 11	7, 2, 11_2	8_6, 6, 12
p ..	0	·7889	0	·7889	−·7889	−·7889	−·9110	−·9110	·4555	·4555	·4555	·4555
q ..	·9110	−·4555	·9110	·4555	·4555	−·4555	0	0	·7889	−·7889	·7889	−·7889
r ..	·9097	·9097	−·9097	−·9097	·9097	−·9097	·9296	−·9296	−·9296	·9296	·9296	−·9296
	1·287	1·287	1·287	1·287	1·287	1·287	1·301	1·301	1·301	1·301	1·301	1·301

The values of $\frac{1}{2}(k_1 + k_2)(\Delta r_1 - \Delta r_2)\cot\alpha$ and $\frac{k_1 - k_2}{2r \sin 2\alpha}\{r_3\Delta r_3 - r(\Delta r_1 + \Delta r_2)(1 - \cos 2\alpha)\}$ as well as of the moments perpendicular to the plane of the bonds resolved along the axes are being given below.

Plane	$\frac{1}{2}(k_1+k_2)(\Delta r_1-\Delta r_2)\cot\alpha$	$\frac{k_1-k_2}{2r\sin 2\alpha}[r_3\Delta r_3-r(\Delta r_1+\Delta r_2)(1-\cos 2\alpha)]$
1, 7, 12	$(k_1)\cdot(-\cdot7690u_{xy}+\cdot7698u_{xz})$	0
10_2, 2, 11_2	$(k_1)\cdot[\cdot6658(u_{xx}-u_{yz})+\cdot3842u_{yy}-\cdot6668u_{yz}-\cdot385u_{zz}]$	0
8_6, 6, 9_6	same as for 8_6, 6, 9_6 with signs of u_{xy}	and u_{xx} changed.

$$p_x = k_1[\cdot8158(u_{xx} - u_{yy}) - \cdot8172\,u_{yz}]\cdot e/8V \times 10^{-8}$$

$$p_y = k_1[-\cdot8158\,u_{xy} + \cdot8172\,u_{xz}]\cdot e/8V \times 10^{-8}$$

$$p_z = 0;\quad \cot\alpha = \cdot7216 \qquad (1)$$

9_1, 1, 10_1	$=k_2(\cdot7690u_{xy}+\cdot7698u_{xz})$	0
8, 2, 7 =	$k_2[\cdot6658(u_{xx}-u_{yy})+\cdot3842u_{xy}+\cdot6668u_{yz}+\cdot385u_{zz}$	0
11, 6, 12	same as for 8, 2, 7 with signs of	u_{xy} and u_{xz} changed.

$$p_x = k_2[-\cdot8158(u_{xx} - u_{yy}) - \cdot8172\,u_{yz}]\cdot e/8V \times 10^{-8}$$

$$p_y = k_2[\cdot8158\,u_{xy} + \cdot8172\,u_{xz}]\cdot e/8V \times 10^{-8}$$

$$p_z = 0;\quad \cot\alpha = \cdot7216 \qquad (2)$$

7, 1, 9_1	$\frac{k_1+k_2}{2}[-\cdot7446u_{xy}-\cdot7295u_{yz}]$	$\frac{k_1-k_2}{2}[\cdot76u_{xx}-1\cdot492u_{yy}+\cdot731u_{zz}+\cdot7452u_{xz}]$
12_1, 1, 10_1	same as for 7, 1, 9_1 with signs of	u_{xy} and u_{xz} changed
8, 2 10_2	$\frac{k_1+k_2}{2}[-\cdot6445(u_{xx}-u_{yy})-\cdot372u_{xy}+\cdot365u_{yz}-\cdot6316u_{xz}]$	$\frac{k_1-k_2}{2}[-\cdot9291u_{xx}+\cdot197u_{yy}+\cdot731u_{zz}+\cdot9755u_{xy}+\cdot646u_{yz}+\cdot3725u_{xz}]$
9_6, 6, 11_6	same as for 8, 2, 10_2 with signs of	u_{xy} and u_{xz} changed
7, 2, 11_2	$\frac{k_1+k_2}{2}[\cdot6445(u_{xx}-u_{yy})+\cdot372u_{xy}+\cdot365u_{yz}-\cdot6316u_{xz}]$	$\frac{k_1-k_2}{2}[-\cdot9291u_{xx}+\cdot197u_{yy}+\cdot731u_{zz}+\cdot9755u_{xy}-\cdot646u_{yz}-\cdot3725u_{xz}]$
8_6, 6, 12	same as for 7, 2, 11_2 with signs of	u_{xy} and u_{xz} changed

$$p_x = \left[-2\cdot364\,\frac{k_1 - k_2}{2}(u_{xx} - u_{yy}) + 1\cdot531\,\frac{k_1 + k_2}{2}u_{yz}\right]\frac{e}{8V} \times 10^{-8}$$

$$p_y = \left[2\cdot364\,\frac{k_1 - k_2}{2}u_{xy} - 1\cdot531\,\frac{k_1 + k_2}{2}u_{xz}\right]\frac{e}{8V} \times 10^{-8}$$

$$p_z = 0;\quad \cot\alpha = \cdot6987 \qquad (3)$$

Plane	$\frac{1}{2}(k_1+k_2)(\Delta r_1-\Delta r_2)\cot\alpha$	$\frac{k-k_2}{2r\sin 2\alpha}[r_3\Delta r_3-r(\Delta r_1+\Delta\gamma_2)(1-\cos 2\alpha)]$
7, 1, 10_1	$\frac{k_1+k_2}{2}[-\cdot7310u_{yz}+\cdot7469u_{zz}]$	$\frac{k_1-k_2}{2}[\cdot763u_{xx}+\cdot73u_{yy}-1\cdot493u_{zz}-\cdot746u_{xy}]$
12 , 1, 9_1	same as for 7, 1, 10_1 with signs of	u_{xy} and u_{zz} changed
8, 2, 11_2	$\frac{k_1+k_2}{2}[-\cdot2812u_{yz}-1\cdot007u_{zz}]$	$\frac{k_1-k_2}{2}[1\cdot385u_{xx}+\cdot1082u_{yy}-1\cdot493u_{zz}+\cdot3871u_{xy}]$
8_6, 6, 11	same as for 8, 2, 11_2 with signs of	u_{xy} and u_{zz} changed
7, 2, 11_2	$\frac{k_1+k_2}{2}[1\cdot013u_{yz}-\cdot2595u_{zz}]$	$\frac{k_1-k_2}{2}[\cdot092u_{xz}+1\cdot399u_{yy}-1\cdot493u_{zz}-\cdot3591u_{xy}]$
9_6, 6, 12	same as for 7, 2, 11_2 with signs of	u_{xy} and u_{zz} changed

$$p_x=\left[-1\cdot632\frac{k_1-k_2}{2}(u_{xx}-u_{yy})+3\cdot135\frac{k_1+k_2}{2}u_{yz}\right]\frac{e}{8V}\times10^{-8}$$

$$p_y=\left[1\cdot632\frac{k_1-k_2}{2}u_{xy}-3\cdot135\frac{k_1+k_2}{2}u_{xz}\right]\frac{e}{8V}\times10^{-8}$$

$$p_z=0;\quad\cot\alpha=\cdot7002 \tag{4}$$

1, 7, 2	$\frac{k_1+k_2}{2}[\cdot1033(u_{xx}-u_{yy})-\cdot05969u_{xy}+\cdot04341u_{yz}+\cdot07515u_{zz}]$	$\frac{k_1-k_2}{2}[-\cdot405u_{xx}+\cdot161u_{yy}+\cdot236u_{zz}-\cdot489u_{xy}-\cdot278u_{yz}+\cdot160u_{xz}]$
6, 12, 1	same as for 1, 7, 2 with signs of	u_{xy} and u_{zz} changed
2, 8, 3	$\frac{k_1+k_2}{2}[-\cdot1192u_{xy}-\cdot08672u_{yz}]$	$\frac{k_1-k_2}{2}[\cdot444u_{xx}-\cdot6857u_{yy}+\cdot236u_{zz}+\cdot324u_{xz}]$
5, 11, 6	same as for 2, 8, 3 with signs of	u_{xy} and u_{zz} changed
3, 9, 4	$\frac{k_1+k_2}{2}[-\cdot1033(u_{xx}-u_{yy})-\cdot05969u_{xy}+\cdot04341u_{yz}-\cdot07515u_{zz}]$	$\frac{k_1-k_2}{2}[-\cdot405u_{xx}+\cdot161u_{yy}+\cdot236u_{zz}+\cdot489u_{xy}+\cdot278u_{yz}+\cdot160u_{xz}]$
4, 10, 5	same as for 3, 9, 4 with signs of	u_{xy} and u_{zz} changed

$$p_x=\left[\cdot9970\frac{k_1-k_2}{2}(u_{xx}-u_{yy})-\cdot153\frac{k_1+k_2}{2}u_{yz}\right]\frac{e}{8V}\times10^{-8}$$

$$p_y=\left[-\cdot9970\frac{k_1-k_2}{2}u_{xy}+\cdot153\frac{k_1+k_2}{2}u_{xz}\right]\frac{e}{8V}\times10^{-8}$$

$$p_z=0;\quad\cot\alpha=\cdot2159 \tag{5}$$

The sum of the moments (1), (2), (3), (4), (5) is given in (5.2) and the piezo-electric constants are calculated in (5.3).

References

Perrier	..	*Arch. de Sc. Phy. et Nat.*, 1916, **41**, 423.
Dawson	..	*Phy. Rev.*, 1927, **29**, 532.
Schulwas-Sorkina	..	*Ibid.*, 1929, **34**, 1448.
Andreeff and others	..	*Zs. f. Phy.*, 1929, **54**, 577.
Freederiscksz and Michailov	..	*Ibid.*, 1932, **76**, 334.
Pitt and Mackinley	..	*Canad. Jour. Res.*, 1936, **14**, 57.
Gibbs, R. E.	..	*Proc. Roy. Soc.*, 1926, **110**, 443.
————	..	*Ibid.*, 1925, **107**, 561.
Jay, A. H.	..	*Ibid.*, 1933, **142**, 237.
Bragg and Gibbs	..	*Ibid.*, 1925, **109**, 425.
Saksena, B. D.	..	*Proc. Ind. Acad. Sci.*, A, 1940, **12**, 93.
Wyckoff	..	*Zs. f. Krys.*, 1926, **63**, 512.
Kammer and Atanasoff	..	*Phy. Rev.*, 1942, **62**, 395.
Perrier and Wolfers	..	*Arch. de Sc. Nat. et Phy.*, 1920, **2**, 372.

THE THERMO-OPTIC BEHAVIOUR OF MICA

By T. Radhakrishnan

(From the Department of Physics, Indian Institute of Science, Bangalore)

Received November 15, 1948

(Communicated by Prof. R. S. Krishnan, F.A.Sc.)

1. Introduction

The micas are biaxial crystals of the monoclinic system, and as is well known, they exhibit a perfect cleavage parallel to the (001) plane. It is easy to obtain cleavage laminæ a few hundredths of a millimetre thick. Such laminæ yield striking interference phenomena which have been noticed and discussed by Lord Rayleigh (1906), Chinmayanandam (1914) and Tolansky (1946). These phenomena can be utilised to give a wealth of information regarding the birefringence of the crystal, the topographical details of its cleavage faces and even the lattice spacing perpendicular to the cleavage plane. In the present investigation, the author has employed the interference method for the measurement of the temperature variation of two of the three principal refractive indices of mica, the thermo-optic behaviour of which has not been investigated before. The results obtained have been discussed with special reference to the theory of thermo-optic behaviour proposed by G. N. Ramachandran (1947) and applied by him with striking success to a large number of transparent solids.

2. Principle of the Method

The usual way of studying the dependence of refraction on temperature is to obtain the refractive indices of a prism of the substance at different temperatures. This is an arduous task in any case, and it is out of the question for substances like diamond and mica where large prisms are not available. The interference method, on the other hand, directly measures the *change* in refractive index caused by a given variation in temperature. Transmitted interference fringes are provided by a thin and fairly uniform plate of the substance, coated on both sides with a reflecting film to enhance the contrast and sharpness of the bands. On heating the crystal, the fringes shift in position, the shift depending on the change in the refractive index as well as the thickness of the substance. If the change in thickness is known, and the fringe shift measured, the change in refractive index can be computed. The method therefore requires a knowledge of the linear expansion of the substance.

The fringes used may be of the Haidinger or Newtonian variety; but in the present investigation the well-known Edser-Butler fringes have been used for the first time in the determination of thermo-optic behaviour. A parallel beam of white light, after traversing the crystal normally, is incident on the slit of a spectrograph. In the field of view of the spectrograph a banded spectrum will be seen, the distance in wave numbers between successive fringes decreasing with decrease in wave-length. Heating the crystal causes a shift in the position of the fringes and by photographing the banded spectra at different temperatures on the same negative, using a Hartmann diaphragm, the fringe shifts for any desired wavelength can be measured. The advantage of this method over using Haidinger or Newtonian fringes is that all wave-lengths are simultaneously recorded in the same picture, the spectrograph serving as a monochromator for each wave-length.

A birefringent crystal will give two sets of banded spectra, owing to the presence of two orthogonally polarised rays having slightly different refractive indices, thus giving rise to a complicated fringe system. But in the case of mica, the axis X of the index ellipsoid (which is the acute bisectrix of the angle between the optic axes) is perpendicular to the cleavage plane. Thus the two rays into which unpolarized light is divided on normally entering the crystal have their directions of vibration *in the plane of the mica.* Their refractive indices are the principal refractive indices n_2 and n_3 in the usual notation. Since their vibration directions are in the plane of the mica, a suitably oriented Nicol placed in front of the crystal will cut off one of the rays completely. There are two positions of the Nicol (at right angles to each other) for which the spectrum will consist of only one set of bands. This is to be expected since the directions of vibration of the two rays are at right angles. The banded spectrum corresponding to a particular ray could be identified from the separation of the bands. It will be shown later that the separation between the bands (in wave-lengths) is inversely proportional to the refractive index of the ray. Hence, in a given wave-length range, there will be a greater number of bands of the ray with the higher refractive index than of the ray with the lower one.

3. Experimental Details

A sheet of muscovite mica (0·03 mm.) was obtained by cleavage and its thickness accurately measured. The mica was coated on both sides with an aluminium film by the usual evaporation method. The thickness of the films was adjusted so that the transmission coefficient was about twenty per cent. The crystal was then cemented at one end with sodium silicate inside a longitudinal slot cut in a glass rod. The other end of the glass rod slid tightly into a hole in a wooden block which was clamped to a stand

loaded down with weights. The same stand carried an electric heater provided with windows for observation. The heater could be slid over the glass rod so that the mica was at the level of the windows. Temperatures were measured with the aid of a thermo-couple kept nearly touching the mica and having a calibrated galvanometer in series.

Light from a hundred-watt lamp with a frosted bulb, restricted by means of suitable apertures, was focussed on to the slit of a Fuess spectrograph by means of a long focus lens in the $2f$–$2f$ position, the convergence of the beam being very small. The mica was placed normally in the path of the beam before it entered the spectrograph. A Nicol placed with its axis perpendicular to the mica served to cut out one ray. Using a Hartmann diaphragm, photographs of the banded spectrum were obtained on the same negative first at room temperature and then at a steady temperature of 180°C. A spectrum of the iron arc was also taken on the same negative, using the Hartmann diaphragm, to indicate the wave-length at different regions. A typical photograph is reproduced in Fig. 1. Photographs were taken with

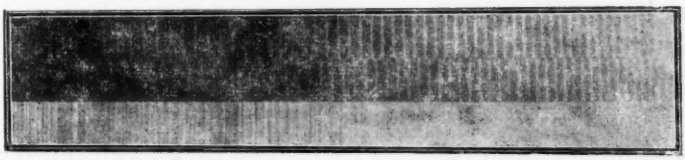

FIG. 1

Photograph of the bands from λ 4400 to λ 6400, showing
(*a*) bands at room temperature
(*b*) bands at about 180° C.
(*c*) iron arc spectrum

panchromatic plates for the red-green region and selochrome plates for the green-blue region. The Nicol was then rotated through 90° to obtain the other ray and photographs taken in a similar manner.

To identify the refractive indices along the principal vibration directions of the mica, photographs of the two band systems at room temperature were taken one below the other on the same negative, using the Hartmann diaphragm. The number of bands in one system corresponding to 10 bands in the other was carefully measured and hence the orientation of the Nicol corresponding to the smaller refractive index n_2 and the greater index n_3 ascertained.

The measurements of the band-widths at different wave-lengths were carried out with the aid of a Hilger cross-slide micrometer. On heating the crystal, each fringe was found to have shifted to a slightly longer wave-

length. By taking photographs at a few intermediate temperatures, it was ascertained that the shift for a temperature change of 145° was much less than a band-width. The fringe shift was measured as a fraction of the band-width in that region, the mean wave-length of the region being measured from the spectrum of the iron arc.

4. Results

The calculation of results can be carried out in the following manner. The bright bands satisfy the relation

$$2\mu l = N\lambda, \tag{1}$$

where μ is the refractive index and l the thickness of the crystal. N, the number of waves in the crystal decreases in steps of unity as we proceed, band by band towards longer wave-lengths. Thus, if we take the next bright band at the higher wave-length $(\lambda + \lambda_m)$, we can write

$$2\mu l = (N - 1)(\lambda + \lambda_m) \tag{2}$$

the dispersion of the mica over this range of wave-length being negligible.

From (1) and (2) we get

$$N\lambda_m = \lambda + \lambda_m \simeq \lambda$$

$$\text{or} \quad \lambda_m = \frac{\lambda}{N} = \frac{\lambda^2}{2\mu l} \tag{3}$$

which shows that the band-widths for the two rays are inversely proportional to their refractive indices.

If, on heating the crystal by $\Delta t°$ C., the band of chromatic order N shifts by a wave-length $\Delta\lambda$, we have, on differentiating (1)

$$\left(2\frac{d\mu}{dt}l + 2\mu\frac{dl}{dt}\right)\Delta t = N\,\Delta\lambda$$

$$\text{or} \quad \frac{d\mu}{dt} = \frac{N}{2l}\frac{\Delta\lambda}{\Delta t} - \frac{\mu}{l}\frac{dl}{dt} = \frac{N}{2l}\frac{\Delta\lambda}{\Delta t} - \mu\alpha \tag{4}$$

$$\text{Since} \quad \frac{1}{l}\frac{dl}{dt} = \alpha \tag{5}$$

where α is the linear expansion perpendicular to the cleavage plane.

We have determined $\Delta\lambda$ as a fraction of the band-width, *i.e.*,

$$\Delta\lambda = \Delta N \cdot \lambda_m \text{ (say)}$$

$$= \Delta N \cdot \frac{\lambda}{N} \qquad \text{from (3)}$$

$$\text{Thus, from (4)}, \quad \frac{d\mu}{dt} = \frac{\lambda}{2l}\frac{\Delta N}{\Delta t} - \mu\alpha. \tag{6}$$

The thickness l can be accurately measured and knowing α, $\frac{d\mu}{dt}$ can be evaluated for the indices n_2 and n_3. α has been recently measured by Hidnert and Dickson (1945). While the average value for muscovite mica seems to be about 17×10^{-6}, individual samples show enormous variations in expansion, especially at high temperatures. For this reason, measurements of thermo-optic behaviour at higher temperatures have not been made in this investigation. Even in the determinations made at low temperatures, there may be an error in the value of α assumed here, so that the absolute values of $\frac{d\mu}{dt}$ may not be correct. But the error is only a constant one and will not affect the *course* of the curve of $\frac{d\mu}{dt}$ against λ, which is the focus of theoretical interest.

The data are reproduced in Table I and plotted graphically in Fig. 2.

TABLE I

Wavelength Å.U.	$-10^6\frac{dn_2}{dt}$	Wavelength Å.U.	$-10^6\frac{dn_3}{dt}$
4330	4·40	4320	3·77
4530	5·20	4512	4·55
4790	6·14	4790	4·94
5050	6·41	5060	5·40
5250	6·70	5260	5·87
5587	7·45	5590	6·10
6100	7·75	6100	6·32
6380	7·94	6350	6·84

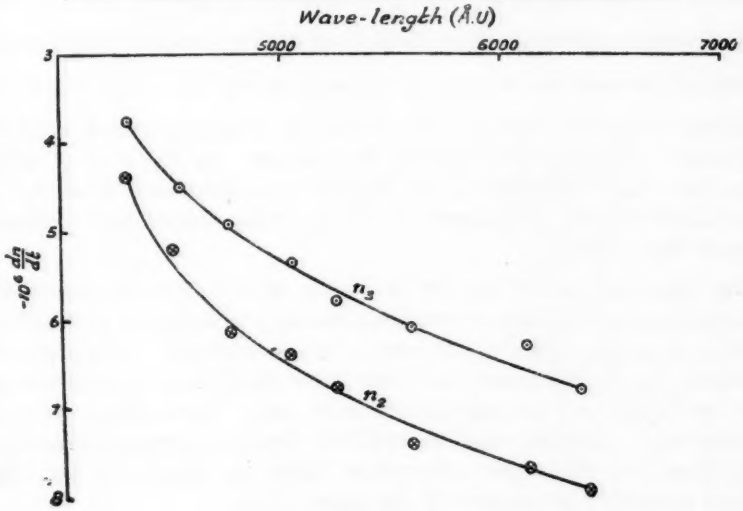

FIG. 2

5. Discussion

The thermo-optic behaviour of a solid and the course of the curve of $\frac{d\mu}{dt}$ against λ can be discussed most fruitfully from the standpoint of a theory proposed by G. N. Ramachandran (1947). He shows that the change in refractive index can be regarded as a superposition of two effects. The first effect is a *decrease* in refractive index with increasing temperature, caused by the decrease in density and hence the number of oscillators in unit volume. The second effect arises from the shift of the absorption frequencies of the solid which are responsible for its dispersion. This shift is in general towards *higher* wave-lengths for absorption frequencies in the nearer ultra-violet and hence tends to *increase* the refractive index. For our purpose, it is sufficient to lump all ultra-violet frequencies into a single term, while contributions from infra-red absorptions are negligible.

The first effect is negative and independent of the wave-length of the light, but the second effect is positive and proportional to a term of the type

$$\frac{1}{(\nu_0^2 - \nu^2)^2}$$

where ν_0 is the ultra-violet absorption frequency. The magnitude of this increases rapidly with decreasing wave-length.

Superposing the two effects, we find that at long wave-lengths the second term is small so that $\frac{d\mu}{dt}$ is large and negative. As the wave-length decreases, however, the second term rapidly becomes larger so that $\frac{d\mu}{dt}$ becomes less and less negative at a steeply rising rate. This is just what is observed in the two curves. The behaviour of mica is typical of that of many other substances like quartz, for instance. In the case of quartz, studies have been extended to the remote ultra-violet and show that the second effect becomes so powerful as to make the temperature coefficients zero and then positive.

The behaviour of the two rays is similar, showing that the second term is characterized by the same absorption frequency in both, but with different oscillator strengths. This is just what is to be expected. It is apparently anomalous that the ray having the larger index should have a smaller temperature coefficient, but an explanation is at once forthcoming when we remember that a smaller negative coefficient implies a larger *positive* contribution from the ultra-violet absorption frequency caused by the higher oscillator strength which goes with the larger index.

Thus all the experimental features can be qualitatively explained on the basis of Ramachandran's theory. A quantitative explanation is not possible without the knowledge of the dispersion, birefringence and ultra-violet characteristic frequencies of muscovite.

I wish to express my gratitude to Prof. R. S. Krishnan for his guidance during this investigation.

Summary

The temperature variation of two of the refractive indices of muscovite mica has been determined by an interference method which can be utilised for other solids as well. The experimental values have been discussed theoretically and shown to conform to the general behaviour of transparent solids as given by Ramachandran's thermo-optic theory.

References

Lord Rayleigh .. *Phil. Mag.*, 1906, **12**, 489.
Chinmayanandam .. *Proc. Roy. Soc.*, A, 1919, **95**, 176.
Tolansky .. *Ibid.*, 1946, **186**, 262.
Ramachandran .. *Proc. Ind. Acad. Sci.*, A, 1947, **25**, 266.
Hidnert and Dickson .. *J. Sc. Res. Bur. Stand.*, 1945, **35**, 309.

THE DYNAMICAL THEORY OF THE VIBRATION SPECTRA OF CRYSTALS

Part V. The Fluorspar Structure

By K. G. Ramanathan

(From the Department of Physics, Indian Institute of Science, Bangalore)

Received November 10, 1948

(Communicated by Prof. R. S. Krishnan, F.A.SC.)

1. Introduction

Recently a rigorous method was developed (Ramanathan, 1947) for the calculation of the frequencies of the various modes of vibration of a crystal in terms of a general set of force constants, based on the theory of crystal dynamics first put forward by Sir C. V. Raman (1943). The method which is applicable to all crystals was used there to calculate the frequencies of the normal modes of vibration of several cubic structures like that of the diamond, rocksalt, cæsium chloride and the face-centred and body-centred cubic lattices. The success of the method in satisfactorily explaining the experimental results obtained with various crystals (Raman, *et al.*, 1947) encourages us to proceed further and apply it also to crystals for which much experimental data is not available. We shall here consider the fluorspar structure which is typical of a number of crystals.

2. The Force Constants

The structure of fluorspar consists of three interpenetrating face-centred cubic lattices, two of which are of fluorine and the third of calcium. Considering a unit cube of calcium atoms, the fluorines are situated at the body centres of the eight small cubes formed by joining the midpoints of the edges of the unit cube. In such a structure every calcium atom is surrounded by eight fluorines and every fluorine by four calciums. The nearest neighbours of any atom are always situated along the trigonal directions of the cube. The twelve next-nearest neighbours of every calcium atom are also calciums situated at the midpoints of the twelve edges of a cube of twice the linear dimensions as that of the unit cube, with the atom under consideration at its centre. The six next nearest neighbours of every fluorine and its twelve neighbours next to it are also fluorines, the former situated at the six face-centres and the latter at the midpoints of the twelve cube edges of a unit cube described with the atom under consideration at the body centre.

In the following calculation the forces acting on every calcium atom due to its own displacement and the displacements of the 20 atoms nearest to it are considered as also the forces acting on every fluorine atom due to

its own displacement and the displacements of the 22 nearest atoms surrounding it. The total number of force-components 384, $(3 + 9 \times 20 + 3 + 9 \times 22)$ are reduced to 14 independent force-constants by applying the principles of symmetry already described in the work referred to above. The 14 force-constants thus obtained are described in Tables I and II.

TABLE I

Description of the forces acting on any calcium atom due to its own displacement and due to the displacements of its 20 nearest neighbours

Atoms responsible for the forces	Symbol	Description of Force Constants
0 ..	P_1	Force on any calcium atom proportional to its own displacement
1 to 8 (Fluorines) ..	Q	Direction of both force and displacement along any one of the three cube axes
,, ..	R	Direction of displacement along a cube axis and that of force along any one of the other two cube axes
9 to 20 Calciums ..	S_1	Both force and displacement in a direction perpendicular to the cubic plane containing the two atoms
,, ..	T_1	Direction of both force and displacement along any one of the three cube axes, the plane containing the two being the cubic plane containing the two atoms
,, ..	U_1	Force and displacement along different cube axes, the plane containing the two being the cubic plane containing the two atoms

TABLE II

Description of the forces acting on any fluorine atom due to its own displacement and the displacements of its 22 nearest neighbours

Atoms responsible for the forces	Symbol	Description of Force Constants
0 ..	P_2	Force on any fluorine atom proportional to its own displacement
1 to 4 (Calciums) ..	Q, R	Described in Table I
5 to 10 (Fluorines)	S_2	Force and displacement perpendicular to the cubic plane containing the two atoms
,, ..	T_2	Force and displacement parallel to each other and to the line joining the two atoms
11 to 22 (Fluorines)	U_2	Force and displacement perpendicular to the cubic plane containing the two atoms
,, ..	V	Force and displacement along the same cubic axis, the plane containing the two being the cubic plane containing the two atoms
,, ..	W	Force and displacement along different cube axes, the plane containing the two being the cubic plane containing the two atoms

It is now possible to derive some relations between the force constants by using the fact that a translation of the entire crystal by an infinitesimally small amount involves no work and the fact that the work involved in a translation of all the calcium atoms alone by a very small amount δx will be the same as the work to be done in translating all the fluorine atoms by the same amount, the calcium atoms now remaining at rest. Or

$$\delta x \{(P_1 + 8Q + 4S_1 + 8T_1) + 2(P_2 + 4Q + 4S_2 + 2T_2 + 4U_2 + 8V)\} = 0 \quad (1)$$

and

$$(P_1 + 4S_1 + 8T_1)\,\delta x = 2(P_2 + 4S_2 + 2T_2 + 4U_2 + 8V)\,\delta x \quad (2)$$

Combining (1) and (2) we have

$$(P_1 + 4S_1 + 8T_1) = -8Q = 2(P_2 + 4S_2 + 2T_2 + 4U_2 + 8V). \quad (3)$$

3. The Frequency Expressions

The normal modes of vibration of the structure of fluorspar can be derived from a consideration of the four modes of vibration of a face-centred cubic lattice having one atom per unit cell, *viz.*, the normal and tangential oscillations of the octahedral planes of atoms and the normal and tangential oscillations of the cubic planes of atoms having degeneracies of 4, 8, 3 and 6 respectively. We have here to consider the three possibilities: (i) The Ca and the two F atoms in any unit cell in the same phase of vibration; (ii) The Ca atom in one phase and the two F atoms in the opposite phase; and (iii) the two F atoms move in opposite phases the Ca atom remaining at rest. Therefore corresponding to every distinct mode of the face-centred cubic lattice, we have here three distinct modes. In addition to the 12 modes thus obtained, there will be two more oscillations of the lattice, in one of which the Ca lattice oscillates against the two F lattices while in the other, the two F lattices oscillate against each other, the Ca lattice remaining at rest. A description of the fourteen modes is contained in Columns 2 and 3 of Table III. Expressions for the frequencies of vibration of the fourteen modes obtained in terms of the force-constants described in Tables I and II are also contained in Table III. As the method of arriving at the frequency expressions is already described fully in the earlier work referred to above, details are not given here.

TABLE III

Expressions for the Frequencies of the fourteen normal modes of fluorspar structure

Degeneracy	Oscillating Units	Direction of oscillation	Expressions for the frequencies $4\pi^2c^2\nu^2$
3	Ca lattice against the F lattices	Arbitrary	$\left(\frac{8Q}{m_1}+\frac{4Q}{m_2}\right)=\left[\frac{P_1+4S_1+8T_1}{m_1}+\frac{P_2+4S_2+2T_2+4U_2+8V}{m_2}\right]$
3	The two F lattices against each other	do	$(P_2-4S_2-2T_2+4U_2+8V)/m_2$
4	(111) planes	[111]	$\left.\begin{matrix}\\ \\ \end{matrix}\right\}\frac{P_1-8U_1}{2m_1}+\frac{P_2-8W}{2m_2}\pm\left\{\left[\frac{P_1-8U_1}{2m_1}-\frac{P_2-8W}{2m_2}\right]^2+\frac{2\,(2Q-4R)^2}{m_1m_2}\right\}^{\frac{1}{2}}$
4	(111) do	[111]	
4	(111) do	[111]	$(P_2-8W)/m_2$
8	(111) dc	Tangential	$\left.\begin{matrix}\\ \\ \end{matrix}\right\}\frac{P_1+4U_1}{2m_1}+\frac{P_2+4W}{2m_2}\pm\left\{\left[\frac{P_1+4U_1}{2m_1}-\frac{P_2+4W}{2m_2}\right]^2+\frac{2\,(2Q+2R)^2}{m_1m_2}\right\}^{\frac{1}{2}}$
8	(111) do	do	
8	(111) do	do	$(P_2+4W)/m_2$
3	(100) do	[100]	$(P_1+4S_1-8T_1)/m_1$
3	(100) do	[100]	$(P_2+4S_2-2T_2+4U_2-8V)/m_2$
3	(100) do	[100]	$(P_2+4S_2+4U_2)/m_2$
6	(100) do	Tangential	$(P_1-4S_1)/m_1$
6	(100) do	do	$(P_2+2T_2-4U_2)/m_2$
6	(100) do	do	$(P_2+2S_2+2T_2+4V)/m_2$

4. SOME FURTHER SIMPLIFICATIONS

The twelve constants appearing in the frequency formulæ of Table III are connected by the two relations (3). It is possible to simplify the formulæ further by making some justifiable assumptions, *viz.*, that those forces in which the directions of both force and displacement are perpendicular to the cubic plane containing the two atoms are of negligible magnitude. We can thus eliminate the constants S_1, S_2 and U_2. Further, if the forces are strictly central, then $Q = R$, $T_1 = U_1$ and $V = W$. Even if the force field deviates slightly from central forces, the above relations hold as a good approximation to the real state of affairs. We thus have the fourteen frequencies expressed in terms of five constants connected by the relation.

$$(P_1 + 8T_1) = -8Q = 2(P_2 + 2T_2 + 8V) \qquad (4)$$

The simplified formulæ are contained in Column 4 of Table IV.

TABLE IV

Simplified Expressions for the fourteen modes of vibration using 5 constants

Degeneracy	Oscillating units	Direction of oscillation	Frequency expressions $4\pi^2c^2\nu^2$
3	Ca and F lattices	Arbitrary	$\left\{\frac{P_1+8T_1}{m_1}+\frac{P_2+2T_2+8V}{m_2}\right\}=-\left\{\frac{8Q}{m_1}+\frac{4Q}{m_2}\right\}$
3	F lattices	do	$(P_2-2T_2+8V)/m_2$
4	(111) planes	Normal	$\left(\frac{{}^7/_3P_1-3T_1}{m_1}\right)+\left(\frac{{}^1/_4P_2-3V+{}^1/_4T_2}{m_2}\right)$
4	do	do	$\left(\frac{{}^1/_3P_1-5T_1}{m_1}\right)+\left(\frac{{}^1/_4P_2-5V-{}^1/_4T_2}{m_2}\right)$
4	do	do	$(P_2-8V)/m_2$
8	do	Tangential	$\left(\frac{P_1+6T_1}{m_1}\right)+\left(\frac{P_2+T_2+6V}{m_2}\right)$
8	do	do	$-\left\{\frac{2T_1}{m_1}+\frac{2V+T_2}{m_2}\right\}$
8	do	do	$(P_2+4V)/m_2$
3	(100) planes	Normal	$(P_1-8T_1)/m_1$
3	do	do	$(P_2-2T_2-8V)/m_2$
3	do	do	P_2/m_2
6	do	Tangential	P_1/m_1
6	do	do	$(P_2+2T_2)/m_2$
6	do	do	$(P_2+2T_2+4V)/m_2$

SUMMARY

Exact expressions for the frequencies of the fourteen normal modes of the fluorspar structure are derived in terms of 12 force constants which take account of the influence of the 20 nearest neighbours of each calcium atom and 22 nearest neighbours of each fluorine atom. Simplified formulæ are also given which involve only five constants connected by an additional relation.

REFERENCES

1. Raman, C. V. .. *Proc. Ind. Acad. Sci.*, A, 1943, **18**, 237.
2. Raman, *et al.* .. *Ibid.*, 1947, **26**, 339.
3. Ramanathan, K. G. .. *Ibid.*, 1947, **26**, 481.

DYNAMICAL THEORY OF THE VIBRATION SPECTRA OF CRYSTALS

Part VI. The Zinc Sulphide Structure

By K. G. Ramanathan

(From the Department of Physics, Indian Institute of Science, Bangalore)

Received November 17, 1948

(Communicated by Prof. R. S. Krishnan, F.A.SC.)

1. Introduction

The zinc sulphide structure is typical of many crystals and therefore expressions for the frequencies of its eigenvibrations are derived in what follows by using the method described in Part I of this series (Ramanathan, 1947).

2. The Force Constants

As is well known, the structure of this crystal is similar to that of diamond and consists of two interpenetrating face-centred cubic lattices of zinc and sulphur atoms. Each zinc and sulphur atom in the structure has as its nearest neighbours, four atoms of the other kind situated along trigonal directions of the crystal. The next nearest neighbours of any atom are twelve atoms of the same kind situated at the midpoints of the twelve edges of a unit cube described with the atom under consideration at its centre. The $294\,[= 2\,(3 + 16 \times 9)]$ force-components arising out of a consideration of the influence of the 16 atoms surrounding every atom in the crystal can be reduced by applying the principles of symmetry, to 14 force-constants of which only 10 appear in the frequency formulæ, as will be seen later. A description of these 10 constants is contained in Table I below.

The fact that a translation of the entire crystal by an infinitesimally small amount δx involves no restoring forces, leads us to the two relations:

$$P_1 + 4Q + 4S_1 + 8U_1 = 0 \qquad (1)$$

$$P_2 + 4Q + 4S_2 + 8U_2 = 0 \qquad (2)$$

Or

$$(P_1 + 4S_1 + 8U_1) = -4Q = (P_2 + 4S_2 + 8U_2) \qquad (3)$$

TABLE I

Description of the force-constants appearing in the frequency formulæ

*Atoms responsible for the forces	Symbol	Description of the Constants
0	P_1, P_2	Force on any atom proportional to its own displacement along any one of the three cube axes
1 to 4	Q	Direction of both force and displacement along any one of the three cube axes
do	R	Direction of both force and displacement along any two different cube axes
5 to 16	S_1, S_2	Direction of both force and displacement along the same cube axis which is also perpendicular to the cubic plane containing the two atoms
do	U_1, U_2	Both force and displacement along any one of the three cube axes contained in the cubic plane containing the two atoms
do	W_1, W_2	Force and displacement along different cube axes, the directions of the two being contained in the cubic plane containing the two atoms

* Atom 0 may refer to either zinc or sulphur and the other numbers accordingly. The symbols P_1, S_1, U_1 and W_1 refer to zinc atoms, P_2, S_2, U_2 and W_2 to sulphur atoms and Q and R to both.

3. THE FREQUENCY FORMULAE

As in the case of diamond, the normal modes of the zinc sulphide structure can also be derived from a consideration of the four modes of a face-centred cubic lattice, *viz.*, the normal and tangential oscillations of the octahedral planes and the normal and tangential oscillations of the cubic planes,

TABLE II

Showing the complete expressions for the frequencies of the nine normal modes of vibration of the zinc sulphide structure

Degeneracy	Oscillating units	Direction of oscillation	*Expressions for the frequencies $4\pi^2c^2\nu^2$
3	The two lattices	Arbitrary	$(P_1+4S_1+8U_1)/\mu = (P_2+4S_2+8U_2)/\mu = -\frac{4Q}{\mu}$
4	(111) planes	Normal	$\frac{P_1-8W_1}{2m_1} + \frac{P_2-8W_2}{2m_2} \pm \left\{\left[\frac{P_1-8W_1}{2m_1} - \frac{P_2-8W_2}{2m_2}\right]^2 + \frac{(2Q-4R)^2}{m_1m_2}\right\}^{\frac{1}{2}}$
4	do	do	
8	do	Tangential	$\frac{P_1+4W_1}{2m_1} + \frac{P_2+4W_2}{2m_2} \pm \left\{\left[\frac{P_1+4W_1}{2m_1} - \frac{P_2+4W_2}{2m_2}\right]^2 + \frac{(2Q+2R)^2}{m_1m_2}\right\}^{\frac{1}{2}}$
8	do	do	
3	(100) planes	Normal	$(P_1+4S_1-8U_1)/m_1$
3	do	do	$(P_2+4S_2-8U_2)/m_2$
6	do	Tangential	$\frac{P_1-4S_1}{2m_1} + \frac{P_2-4S_2}{2m_2} \pm \left\{\left[\frac{P_1-4S_1}{2m_1} - \frac{P_2-4S_2}{2m_2}\right]^2 + \frac{16R^2}{m_1m_2}\right\}^{\frac{1}{2}}$
6	do	do	

* m_1 refers to the mass of the zinc atom, m_2 to the mass of the sulphur atom and μ to the reduced mass given by $\left(\frac{1}{\mu} = \frac{1}{m_1} + \frac{1}{m_2}\right)$.

the phase of the vibration being reversed at each successive equivalent layer of atoms. Since there are two non-equivalent atoms per unit cell in the present case, there will be two possibilities corresponding to every one of the above four. Finally there will be one more vibration, which is the oscillation of the zinc and sulphur lattices against each other along any three orthogonal directions. All the nine modes of vibration are described in Columns 2 and 3 of Table II. Column 4 of Table II contains the expressions for the frequencies of the nine normal modes derived in terms of the 10 constants described in Table I.

4. Some Further Simplifications

The quantities S_1 and S_2 are bound to be negligible because they are forces in which the directions of both force and displacement are perpendicular to the cubic plane containing the two interacting atoms and consequently involve no change in their distance. We can further put $U_1 = W_1$ and $U_2 = W_2$, under the assumption that the forces are along the line joining the two atoms for the more distant neighbours. Thus, we are left with the constants P_1, P_2, Q, R, U_1 and U_2 connected by the relation

$$(P_1 + 8U_1) = (P_2 + 8U_2) = -4Q. \qquad (4)$$

Table III

Showing simplified expressions for the frequencies of the various modes of vibration

Degeneracy	Oscillating units	Direction of oscillation	Simplified Expressions $4\pi^2 c^2 \nu^2$
3	The two lattices	Arbitrary	$\frac{P_1+8U_1}{m_1} + \frac{P_2+8U_2}{m_2} = -\frac{4Q}{\mu}$
4	(111) Planes	Normal	$\frac{P_1-8U_1}{m_1} + \frac{P_2-8U_2}{m_2} - \frac{(P_1-8U_1)(P_2-8U_2) - (2Q-4R)^2}{(P_1-8U_1)m_2 + (P_2-8U_2)m_1}$
4	do	do	$\frac{(P_1-8U_1)(P_2-8U_2) - (2Q-4R)^2}{(P_1-8U_1)m_2+(P_2-8U_2)m_1}$
8	do	Tangential	$\frac{P_1+4U_1}{m_1} + \frac{P_2+4U_2}{m_2} - \frac{(P_1+4U_1)(P_2+4U_2) - (2Q+2R)^2}{(P_1+4U_1)m_2 + (P_2+4U_2)m_1}$
8	do	do	$\frac{(P_1+4U_1)(P_2+4U_2) - (2Q+2R)^2}{(P_1+4U_1)m_2 + (P_2+4U_2)m_1}$
3	(100) Planes	Normal	$\frac{(P_1-8U_1)}{m_1}$
3	do	do	$\frac{(P_2-8U_2)}{m_2}$
6	do	Tangential	$\frac{P_1}{m_1} + \frac{P_2}{m_2} - \frac{P_1P_2-16R^2}{P_1m_2+P_2m_1}$
6	do	do	$\frac{P_1P_2-16R^2}{P_1m_2+P_2m_1}$

Also, since by the nature of the forces $P_1 \gg U_1$ and $P_2 \gg U_2$ and further U_1 and U_2 are of the same sign, it follows that $P_1 \simeq P_2$. Under these simplifying assumptions the frequencies of the nine normal modes can be expressed as shown in Table III in terms of six independent constants connected by two additional relations (4).

Summary

Expressions for the frequencies of the nine normal modes of the zinc sulphide structure are derived in terms of 10 force-constants taking account of the interaction of each atom with its 16 nearest neighbours. The formulæ, after simplification contain only six constants which are further connected by two additional relations.

Reference

Ramanathan, K. G. .. *Proc. Ind. Acad. Sci.*, A, 1947, 26, 481.

PHOTOMETRY OF RAMAN SPECTRA OF CRYSTALS

BY P. S. NARAYANAN

(From the Department of Physics, Indian Institute of Science, Bangalore)

Received November 19, 1948

(Communicated by Prof. R. S. Krishnan, F.A.SC.)

1. INTRODUCTION

OWING to the extreme feebleness with which many of the Raman lines are recorded even after long exposures, an accurate determination of their intensities, absolute as well as relative is beset with many difficulties. Also it is well known that the data available on the subject are so inconsistent and contradictory that it is not possible to come to any definite conclusions regarding the validity of the existing theory of Raman effect in its entirety. The observations concerning the variation of the intensity of Raman lines in carbon tetrachloride by K. S. Krishnan, (1929), R. Anantha Krishnan (1938) and Sirkar (1943) showed that the intensity of the Stokes line did not increase with temperature. Brickwedde and Peters (1929) concluded from a study of the temperature variations of the Raman effect in quartz that the Stokes lines became weaker at higher temperatures. Landsberg and Mandelstamm (1930) reinvestigated the problem in the case of crystalline quartz and reported an increase of intensity for the Stokes component of the Raman line at 465 cm.$^{-1}$ in the ratio 1 : 1·29 when the temperature was raised from 295° to 810° T. Although the expected increase was in the ratio 1 : 1·6 they concluded that the deviation was well within the limits of accuracy attainable in the measurement. More recent work by Ornstein and Went (1935) and K. Venkateswarlu on a few crystals including calcite and quartz confirms the observations of the earlier workers. The general inferences of all these workers are that : (1) the ratio of the intensity of the Stokes and the anti-Stokes lines are in fair agreement with the theoretically calculated values; (2) the absolute intensity of the Stokes lines showed a marked decrease with rise of temperature; (3) the intensity of the anti-Stokes lines increased with rise of temperature but far slower than predicted by theory (except in the case of calcite); and (4) the deviations are most pronounced in the case of low frequency shift lines.

2. THEORETICAL

On the basis of Placzek's theory of Raman effect, the aggregate intensities of the Stokes and the anti-Stokes Raman lines are given by

$$I_{(\nu-\nu_j)} = \frac{64\pi^4}{3c^3}\{4A_{1j}^2 - 7B_{1j}^2\}(\nu-\nu_j)^4 \frac{1}{1-e^{-\frac{h\nu_j}{kT}}}$$

and

$$I_{(\nu+\nu_j)} = \frac{64\pi^4}{3c^3}\{4A_{1j}^2 - 7B_{1j}^2\}(\nu+\nu_j)^4 \frac{1}{e^{\frac{k\nu_j}{kT}} - 1},$$

where A_{1j} and B_{1j} are the invariants of the symmetric tensor $\left(\frac{\partial\alpha}{\partial q_j}\right)_0$. The ratio of the intensity of the Stokes Raman line to that of the corresponding anti-Stokes line is given by

$$\frac{I_{(\nu-\nu_j)}}{I_{(\nu+\nu_j)}} = \left(\frac{\nu-\nu_j}{\nu+\nu_j}\right)^4 e^{\frac{k\nu_j}{kT}}.$$

It is evident that the experimental results regarding the individual intensities are in sharp disagreement with the values calculated from formulæ (1) and (2). R. Ananthakrishnan (1938) pointed out that the effect of anharmonicity is not explicitly taken into account in Placzek's theory. $\left(\frac{\partial\alpha}{\partial q_j}\right)_0$ which determines the intensity of the Raman line cannot be assumed to be independent of the internuclear distances; on the contrary it decreases with increasing nuclear separation. K. Venkateswaralu (1947) showed that by assuming $\left(\frac{\partial\alpha}{\partial q_j}\right)_0$ to be a function of the amplitude of vibration, the experimental results could be satisfactorily explained. As the contribution to the intensity of the Raman lines from transitions involving higher quantum numbers become more and more important with increasing temperature, in the case of low frequency shifts, the effect of the increased amplitude of vibration on the change in polarisability cannot be neglected.

However, the ratio of the Stokes to the anti-Stokes intensity can be expected to be in agreement with expression (3) as the factor involving $\left(\frac{\partial\alpha}{\partial q_j}\right)_0$ is absent and the experiments of K. Venkateswaralu (1942, 1943) have shown that the ratio of the Stokes to the anti-Stokes lines is in better agreement with the modified formula than the classical Boltzmann formula alone on the basis of which the earlier workers interpreted their results. As only low frequency shift lines have been measured so far, the difference between the two does not amount to more than 10% and is quite within the limits of experimental error. The question can be taken to be settled beyond a doubt only when the intensity ratio has been measured for a few high frequency shift lines where the factor $\left(\frac{\nu-\nu_j}{\nu+\nu_j}\right)^4$ will differ considerably from unity. With the help of a new technique, a detailed investigation has therefore been undertaken by the author.

3. Experimental Technique

The chief difficulty experienced by the earlier investigators was their inability to record the anti-Stokes lines of faint Raman lines, as also those with frequency shifts greater than 480 cm.$^{-1}$, the exciting radiation being λ 4047 or λ 4358 of mercury. But the ultra-violet technique developed and perfected by R. S. Krishnan in this laboratory may with decided advantage be used instead and the enormously increased scattering power of the resonance radiation arising from its exceptional intensity as compared with the other mercury radiations and from the λ^{-4} law make it possible to record the anti-Stokes lines of even very faint Raman lines. Further, as the λ 2536·5 Å.U. radiation from the light scattered by the medium is effectively suppressed by absorption in a long column of mercury vapour, the Raman lines are obtained on a clear background and no correction need be made for the continuous background.

Another obstacle in the way of an accurate measurement of the relative intensity of the Stokes and anti-Stokes components for frequency shifts greater than 350 cm.$^{-1}$ is the great disparity in their intensities so that a direct comparison of the lines on one and the same plate is unlikely to yield any reliable result. But by taking a series of exposures for the Stokes line of different time intervals a comparison may be made with the intensity of the anti-Stokes line recorded in another exposure. For this a complete knowledge of the characteristics of the photographic plate used is necessary and fluctuations in the intensity of the light source during the exposure will vitiate the result considerably. All these difficulties and errors get automatically eliminated by the use of an ultra-violet Spekker photometer in conjunction with a medium quartz spectrograph. The experimental technique used in this case enables one to determine with a fair accuracy the intensity ratios even in the case of high frequency shift Raman lines. The results obtained with the Spekker in the case of Raman lines of small shifts were checked with the help of the direct method and the values never differed by more than 5%.

The Raman spectra of the crystals investigated were excited by means of the resonance radiation of mercury from a water-cooled magnet controlled quartz arc. The scattered light from the crystal was focussed on the tungsten-steel spark gap of the Spekker photometer with the help of the ivory indicator. The image acted as the source for the Spekker and the light from it was divided into two paths by a suitable arrangement of prisms. Each one contained an aperture, one being fixed and the other one being variable by means of a shutter mechanism operated by a calibrated screw

directly giving the value of $\log_{10} \frac{I_0}{I}$, where $\frac{I_0}{I}$ is the ratio of the intensities of the beams passing through the two apertures. The beams were then focussed by means of quartz lenses and the light paths were brought into close juxtaposition on the slit of the quartz spectrograph by means of quartz rhombs. Thus the spectrograph was illumined by two beams of light having the same origin, the intensity of one reduced by a known amount. It becomes now possible to compare the intensity of the Stokes line recorded from the light passing through the reduced aperture with the intensity of the anti-Stokes line recorded with the full aperture. The actual ratio can be calculated from a knowledge of the $\log_{10} \frac{I_0}{I}$ value. No error can occur because of fluctuation in the intensity of the quartz arc. The Spekker photometer though specially designed to work at high density values cannot be relied upon to give intensity ratios over 250 with very great accuracy as in those regions any small error in the photographic estimate will be magnified hundredfold when the actual ratio is calculated.

Ilford Special Rapid plates used throughout this work were calibrated by the method of varying slit-widths with the help of a tungsten lamp provided with a quartz window. A measurement of the ratio of the slopes of the characteristic curves of the photographic plate at 2 or 3 different wavelengths in the neighbourhood of λ2537 showed that the Schwarzschild constant p was practically constant. Further the work of G. R. Harrison (1925) shows that for about 100 Å.U. on either side of λ2537 the photographic sensitivity for a similar type of plate remains fairly uniform. As such no attempt was made to draw the characteristic curves at wavelengths corresponding to the different Raman lines and all the intensities were computed from the characteristic curves drawn for a mean wavelength of λ2540. The plates were developed in the same stock developer, for the same time and the photographs were restricted to the centre of the plate to avoid any error due to the difference in the rate of development near the edges.

4. Results and Discussion

A preliminary report of the results that have so far been obtained in the case of quartz, calcite, barytes and ammonium di-hydrogen phosphate has been given below along with the theoretically computed values from the Boltzmann formula alone and also from the modified formula. For the purpose of comparison the values obtained by K. Venkateswaralu in the visible region have also been included in the table.

The temperature was taken as 27° C. (room temperature) though as a result of the close proximity of the arc it is quite possible for the temperature of the crystal to have been a few degrees higher in spite of the efficient fan cooling.

Quartz

$$A = e^{\frac{h\nu_j}{kT}} \qquad B = \left(\frac{\nu - \nu_j}{\nu + \nu_j}\right)^4 \qquad C = e^{\frac{h\nu_j}{kT}}\left(\frac{\nu - \nu_j}{\nu + \nu_j}\right)^4$$

ν cm.$^{-1}$	A	B	C	Expl. value	A	C	Expl. value
127	1·834	·9745	1·79	1·78	..	..	..
207	2·687	·9594	2·58	2·43	..	..	..
267	3·58	·9471	3·4	3·2	..	..	..
358	5·53	·9298	5·14	4·95	..	..	..
400	6·75	·9221	6·23	6·0	..	..	..
467	9·31	·9095	8·47	7·00	8·72	7·42	7·68

Calcite

ν cm.$^{-1}$	A	B	C	Expl. value	A	C	Expl. value
155·5	2·102	·9683	2·04	2·01	2·07	1·96	2·00
284	3·88	·9436	3·66	3·61	3·73	3·38	3·30

Barytes

ν cm.$^{-1}$	A	B	C	Experimental value
64	1·36	·9872	1·34	1·53
73·6	1·42	·9854	1·4	1·7
88·3	1·525	·9817	1·5	1·75
127·4	1·84	·9745	1·79	1·83
150·0	2·05	·9701	1·99	1·98
189·0	2·467	·962	2·37	2·45
462·2	9·09	·9103	8·27	10·0

Ammonium di-hydrogen phosphate

ν cm.$^{-1}$	A	B	C	Experimental value
172	2·27	·9656	2·2	2·36

The values obtained for the 465 cm.$^{-1}$ line of quartz and 462·2 cm.$^{-1}$ line of barytes deviate considerably from the theoretical values and the

author is at present unable to say if they are genuine. The Spekker photometer has not yet been calibrated with any standard source and the reading on the drum has been taken to represent the correct value. In the case of barytes most of the low frequency Raman lines are doublets and as the intensity ratios have been determined only for the peak intensities, they are bound to be less accurate than in the case of sharp lines like those of calcite. Yet it is obvious that the results are in good agreement with those obtained from the modified formula.

Even after long exposures of the order of a week, the anti-Stokes line of 1158 cm.$^{-1}$ (quartz) was not recorded. This is not surprising in view of the fact that in R. S. Krishnan's spectrogram of the Raman spectrum of quartz (1945) even after the second order lines have made their appearance with considerable intensity the anti-Stokes of 1158 cm.$^{-1}$ is absent.

In conclusion, the author's respectful thanks are due to Prof. R. S. Krishnan for his kind interest and suggestions in the course of this work.

Summary

Using the ultra-violet Spekker photometer and the resonance radiation of mercury as exciter the relative intensities of the Stokes and anti-Stokes Raman lines in the case of calcite, quartz, barytes and ammonium di-hydrogen phosphate have been measured. It is found that the results obtained confirm the theoretical relation that the intensity is proportional to the fourth power of the emission frequency. The new method outlined in this paper makes it possible to measure the intensity ratios in case of high frequency shift Raman lines.

References

Ananthakrishnan, R. .. *Proc. Ind. Acad. Sci.*, **A**, 1938, **22** 329.
Brickwedde and Peters .. *Phy. Rev.*, 1929, **33**, 116.
Harrison, G. R. .. *J. O. S. A.*, 1925, **11**, 341.
Krishnan, K. S. .. *Nature*, 1928, **122**, 650.
Krishnan, R. S. .. *Proc. Ind. Acad. Sci.*, **A**, 1945, **22** 329.
Landsberg and Mandelstamm .. *Z. f. Phy.*, 1930, **60**, 364.
Ornstein and Went .. *Physica*, 1935, **2**, 503.
Sirkar .. *Ind. Journ. Phys.*, 1944, **17**, 309.
Venkateswaralu, K. .. *Proc. Ind. Acad. Sci.*, **A**, 1944, **19** 111.
———— .. *Ibid.*, 1941, **14** 529.
———— .. *Ibid.*, 1942, **16** 45.
———— .. *Current Science*, 1947, **16**, 15.
———— .. *Nature*, 1947, **159**, 96.

RAMAN SPECTRUM OF AMMONIUM DI-HYDROGEN PHOSPHATE

By P. S. Narayanan

(From the Department of Physics, Indian Institute of Science, Bangalore)

Received November 30, 1948

(Communicated by Prof. R. S. Krishnan, F.A.SC.)

1. Introduction

Ammonium di-hydrogen phosphate ($NH_4H_2PO_4$) has in recent years been subjected to many investigations to elucidate the origin and cause of the Seignette electric anomaly that exists in the case of crystals isomorphic with Rochelle salt and the phosphates and arsenates of the tetragonal class. The elastic, piezo-electric and dielectric constants show analogous variations within the range of stress and temperature in which measurements have so far been carried out (Mason, 1946). Stephenson and Zettlemoyer (1944) noticed a transition point in the specific heat curve at 147·9° K, while Klug and Johnson (1937) and later Jean Jaffray (1944) claim to have observed a second order transformation of the ammonia type at about 19° C. In view of the importance of the subject and as a study of the Raman spectrum of ammonium di-hydrogen phosphate in the form of single crystals can yield valuable information concerning the structure as well as the interatomic forces, an investigation of its Raman spectrum using λ 2536·5 radiation of mercury as exciter, has been undertaken.

The earlier investigations on the Raman spectra of the acids of phosphorus and their salts are not very numerous and the results obtained are very meagre. The solutions of the primary phosphates have been studied by C. S. Venkateswaran (1936) and in the case of $NH_4H_2PO_4$ 30% solution, only 4 lines with frequency shifts 360, 515, 885 and 1090 cm.$^{-1}$, corresponding to the internal oscillations of the PO_4 group, have been reported. The chief difficulty experienced by the earlier workers in recording the Raman spectra of the phosphates is the strong continuous spectrum which appears on every plate obliterating all the faint lines. C. S. Venkateswaran attributed this to the mercury arc itself and by a proper design of the arc and by the use of fan cooling directed towards the cathode, he reduced this to a minimum. However, as C. S. Venkateswaran himself has remarked in his paper, with crystals of the primary phosphates of sodium, potassium and ammonium, he was unable to get any satisfactory picture even after prolonged exposures. Apart from this, no work on $NH_4H_2PO_4$ has so far been reported. The use of the ultraviolet technique removes this difficulty at

once as the intense unmodified light is quenched completely from the scattered light before its entry into the spectrograph by a cool mercury vapour filter. This combined with the enormously increased scattering power owing to the use of ultraviolet radiation, made it possible to study the Raman spectrum of ammonium di-hydrogen phosphate.

2. Experimental Details and Results

Two fine transparent specimens of $NH_4H_2PO_4$ with fully developed faces, one of size $1\frac{1}{2}$ cm. × 1 cm. × $\frac{3}{4}$ cm. and the other $7'' \times 2\frac{1}{2}'' \times 2\frac{1}{2}''$ made in the Bell Telephone Company's laboratories at Murray Hill and presented to Sir C. V. Raman were used in the present investigation, the smaller one being cut suitably to enable a study of the effect of orientation on the Raman spectrum. The spectra were excited by the resonance radiation of mercury from a water-cooled magnet-controlled quartz arc and the scattered light was focussed on to the slit of a Hilger medium quartz spectrograph, all precautions being taken to eliminate parasitic light from fogging the plate.

Fig. 1 (*a*) is a reproduction of the picture obtained with the big crystal and with a slit width of 5 div. (0·025 mm). For this slit width exposures

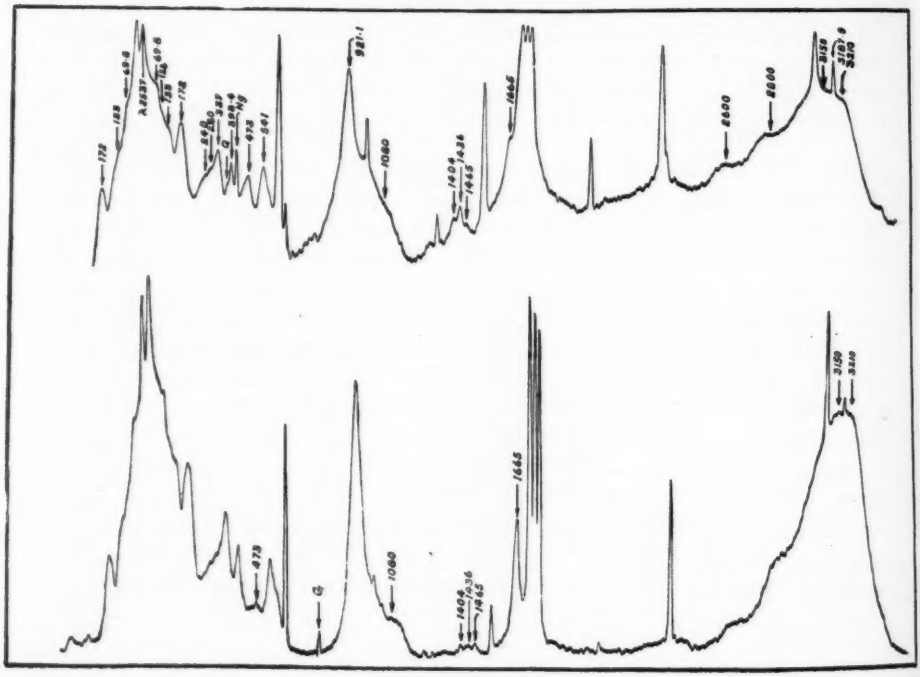

Fig. 2

of the order of 12 hours were found to be necessary to bring out the salient features of the spectrum, while 24 hours were sufficient to get a fairly intense picture. This is a really surprising and noteworthy point, for in the case of the ammonium halides, the exposure times were of the order of 4 hours (R. S. Krishnan, 1947). The characteristic feature of the Raman spectrum of ammonium di-hydrogen phosphate is that all the lines including those due to the internal oscillations of the PO_4 group as well as the NH_4 group are broad though fairly intense.

For a comparative study of the effect of orientation on the Raman spectrum, a picture with the scattered light taken along the tetragonal axis has also been reproduced in Fig. 1 (*c*). Fig 1 (*b*) is the mercury spectrum enlarged to the same extent as the other two. The first spectrogram was recorded with the direction of the scattered light normal to the fourfold axis of symmetry. As is to be expected, the pictures taken with the incident light being respectively along *a* and *b* axes, the direction of the scattered light being along the tetragonal axis, were found to be identical.

The frequency shifts of the Raman lines were evaluated by a comparison with the superposed iron arc spectrum and also by a direct measurement under a Hilger comparator. The Raman shifts of the feeble lines and bands, however, were computed from the microphotometer curves. The frequency shifts and the intensities of the principal Raman lines are listed in Table I.

TABLE I

Principal Raman lines of ammonium di-hydrogen phosphate

Serial No.	Group	Frequency shift in cm.$^{-1}$	Nature of the lines
1	lattice	69·8 (4)	very broad
2	do	124 (2)	broad
3	do	133 (2)	..
4	do	172 (4)	broad
5	phosphate	240 (1)	do
6	do	280 (1)	..
7	do	337 (3)	broad and diffuse
8	do	398·4(2)	sharp
9	do	473 (2)	diffuse
10	do	541 (3)	do
11	do	921·1 (10)	sharp
12	do	1080 (1)	very broad
13	NH_4	1404 (1)	..
14	do	1436 (1)	..
15	do	1465 (1)	..
16	do	1665 (3)	sharp
17	do	2600 (1)	Extremely broad
18	do	2800 (1)	do
19	do	3150 (5)	diffuse
20	do	3210 (5)	..

The Raman lines with frequency shifts 1404, 1435, 1465 and 473 cm.$^{-1}$ were found to be influenced enormously by the direction of scattering and the intensity is considerably greater when the scattered light is taken along the fourfold axis of symmetry.

In the low frequency region the spectrum exhibits two broad bands and one line. The bands extend from 0 to 69·8 cm.$^{-1}$ and from 70 to 133 cm.$^{-1}$ with a sharp cut off at the upper limit. Of these the former is the more intense one. The line at 172 cm.$^{-1}$ is also intense and has a width of about 10 cm.$^{-1}$

3. Discussion

Ammonium di-hydrogen phosphate is isomorphous with KH_2PO_4, KH_2AsO_4 and $NH_4H_2AsO_4$ and crystallises in the tetragonal scalenohedral class. The space group is V_d^{12}. The X-Ray analysis has been carried out by O. Hassel (1920) and he found that the phosphate groups consist of a phosphorus atom tetrahedrally surrounded by four oxygens and that each group is surrounded tetrahedrally by four other groups. Neighbouring PO_4 groups are connected by hydrogen bonds. Like the PO_4 group, the NH_4 group retains its tetrahedral structure. The number of molecules in the unit cell is 4.

From a comparative study of the spectra of the aqueous solutions of the phosphates and the ammonium salts with the frequency shifts observed in the spectrum of $NH_4H_2PO_4$, we may broadly classify the observed lines into three groups, *viz.*, (1) the lattice spectrum, (2) the spectrum of the PO_4 ion and (3) the spectrum of the NH_4 ion. The classification is indicated in Table I.

Lattice spectrum.—The appearance of the two broad bands in the lattice spectrum with continuous distribution of intensity from the exciting line suggests that the ions PO_4 and NH_4 are capable of hindered rotation more or less as in a liquid, the lower frequency band corresponding to the heavier ion. It is quite probable that the bands split up into lines at lower temperatures.

Spectrum of the PO_4 ion.—The PO_4 ion in the free state possesses full cubic symmetry and has only four distinct modes of oscillation with frequency shifts 361 (2), 515 (3), 980 (1) and 1080 (3) cm.$^{-1}$, the figures within brackets giving the degeneracies. In the crystal the PO_4 ion has only the symmetry of the crystal which is lower than that of the free ion. One might therefore expect some of the degeneracies of the characterestic frequencies of the free ion to be removed in the crystal, as indicated in Table II.

TABLE II

Raman frequencies of the PO_4 ion

Nature	$\nu_1(1)$	$\nu_2(2)$	$\nu_3(3)$	$\nu_4(3)$
Free state ..	980	363	1082	515
$NH_4H_2PO_4$..	921·1	337 ; 398·4	1080	473 ; 541

The splitting of ν_2 and ν_4 into two lines with widely different frequency shifts indicates the strong influence of the hydrogen bond on the PO_4 group. Further investigation has to be carried out before any satisfactory explanation can be given for the presence of the two lines with frequency shifts 240 and 280 cm.$^{-1}$ respectively.

Spectrum of the NH_4 ion.—Because of its tetrahedral symmetry, NH_4 ion in the free state should have only four distinct modes of oscillation of which ν_1 is single, ν_2 is doubly degenerate and ν_3 and ν_4 are triply degenerate. The corresponding Raman shifts are 3033, 1685, 3134 and 1397 cm.$^{-1}$ In the spectra of the ammonium compounds, the most intense line usually corresponds to the totally symmetric oscillation ν_1. Contrary to this, there is no line in the Raman spectrum of $NH_4H_2PO_4$ at room temperature, with a frequency shift 3030 cm.$^{-1}$ It is quite likely that it has shifted to higher frequency and is lost in the intense background due to the Raman lines at 3150 cm.$^{-1}$

TABLE III

Raman frequencies of the NH_4 ion

State	$\nu_1(1)$	$\nu_2(2)$	$\nu_3(3)$	$\nu_4(3)$
Free ion ..	3033	1685	3134	1397
NH_4 Br Crystal ..	3037	1686	3121	1398 ; 1429
NH_4Cl Crystal ..	3041	1710 ; 1765	3146	1400 ; 1418 ; 1440
$NH_4H_2PO_4$ ..	..	1665	3150 ; 3210	1404 ; 1437 ; 1465

The partial removal of the degeneracies of the characteristic frequencies of the penta-atomic group in the spectrum of ammonium di-hydrogen phosphate suggests that in the crystal lattice the vibrating NH_4 ion possesses lower symmetry evidently due to the presence of potential fields of the neighbouring ions, although the NH_4 ion has full tetrahedral symmetry when the atoms are at rest.

As in the spectra of the ammonium halides, there are two extra bands, one at 2600 cm.$^{-1}$ and the other at 2800 cm.$^{-1}$ In the case of $NH_4H_2PO_4$ the band with a shift 2600 cm.$^{-1}$ might be due to P–H oscillation. The origin of the other band is at present not clear.

In conclusion, the author wishes to express his grateful thanks to Prof. R. S. Krishnan for his kind interest and valuable suggestions in the course of the work.

Summary

Using the λ 2536·5 mercury resonance radiation as exciter, the Raman spectrum of ammonium di-hydrogen phosphate has been investigated. The spectrum consists of 20 lines of which (1) 4 are lattice lines, (2) 8 are due to internal oscillations of the PO_4 group and (3) 8 due to NH_4 groups. The continuous distribution of intensity in the lattice spectrum indicates the possibility of the existence of hindered rotation of the NH_4 and PO_4 groups. The splitting up of some of the degenerate lines of both PO_4 and NH_4 groups might be due to the strong influence of the hydrogen bonds.

References

Hassel, O. .. *Zeits. fur. Electrochemie*, 1920, **31**, 523.

Hibben .. *The Raman Effect and its Chemical Applications*, 1939, 381–84.

Jean Jaffray .. *Comp. rendus*, 1944, **218**, 798.

Klug and Johnson .. *Journ. Amer. Chem. Soc.*, 1937, **59**, 2061.

Krishnan, R. S. .. *Proc. Ind. Acad. Sci.*, A, 1947, **26**, 432.

———— .. *Ibid.*, 1948, **27**, 321.

Mason, W. P. .. *Phys. Rev.*, 1946, **69**, 173–94.

Schaefer, Matossi and Aderhold .. *Z. Physik*, 1930, **65**, 289.

Stephenson and Zettlemoyer *Journ. Amer. Chem. Soc.*, 1944, **66**, 1405–8.

Venkateswaran, C. S. .. *Proc. Ind. Acad. Sci.*, A, 1936, **3**, 25.

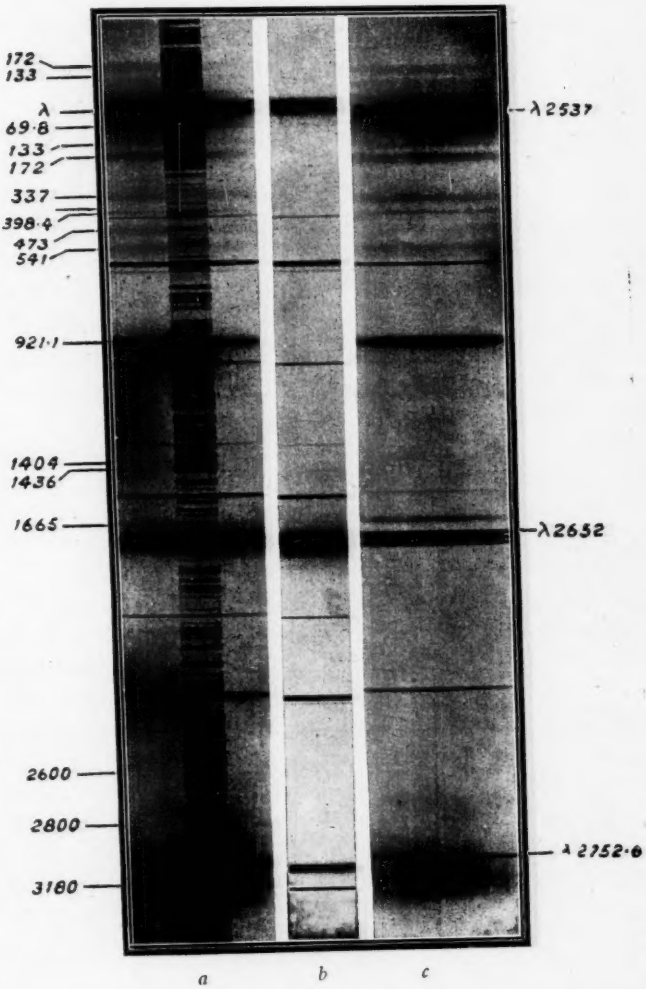
172
133
λ
69·8
133
172
337
398·4
473
541
921·1
1404
1436
1665
2600
2800
3180
λ 2537
λ 2652
λ 2752·6
a
b
c

FIG. 1

A MODIFIED METHOD FOR THE DETERMINATION OF ELASTIC CONSTANTS OF CRYSTALS

By R. V. G. Sundara Rao

(From the Department of Physics, Andhra University, Waltair)

Received November 26, 1948

(Communicated by Prof. S. Bhagavantam, F.A.SC.)

1. Introduction

By exciting a piezo-electric wedge, Bhagavantam and Bhimasenachar[1] obtained a continuous range of ultrasonic frequencies. The elastic constants of several crystalline substances, available only in small sizes, have been successfully determined using such wedges.

It has been found, however, that a wedge often contains a number of discrete frequencies for which the amplitude of piezo-vibration is high. These frequencies are superposed on the continuous spectrum. When a crystal plate is driven by such a wedge, in addition to the natural frequencies of the plate, the wedge maxima force themselves through, giving spurious indications, especially when the frequency is in the region of the lower harmonics of the plate. Analysis of the data in such cases becomes a little difficult, unless the higher harmonics of the plate are excited, when the spurious maxima become few. Efforts have been made recently in this laboratory to get at a wedge without spurious maxima, by working with different shapes and sizes, and considerable success has been achieved. These results will be published in another communication.

In the present paper, a slightly different method of determining the elastic constants of crystals is described. It has been found that under suitable conditions, even a piezo-electric plate of uniform thickness can be thrown into forced vibrations giving a continuous frequency spectrum, the spurious maxima appearing with a wedge being thus altogether absent. Using such a plate, the elastic constants of ammonium alum, barium nitrate and two varieties of beryl have been determined.

2. Experimental Technique

A Z-cut tourmaline plate is ground to uniform thickness of about 2 mm. and silvered on the two flat sides. If R.F. oscillations from a sufficiently powerful oscillator are impressed on it, it would execute what may be

called " pure " piezoelectric thickness oscillations of the same frequency as the impressed R.F. oscillations, provided we are fairly remote from a resonance frequency. The amplitude would naturally be very much smaller than that which the plate would acquire while in resonance. However, with a sufficiently powerful H.F. oscillator to drive the plate, these " pure " oscillations may themselves be used for exciting in their turn the mechanical resonant frequencies of a non-piezo-electric plate. Such oscillations are then communicated to a liquid and the rest of the procedure is identical with that in the wedge method referred to in the introduction.

The oscillator used is a Hartley shunt-feed type using R.C.A. 807 valve. The mean thickness of the tourmaline plate used is $(2{\cdot}18 \pm {\cdot}02)$ mm. The oscillations of the plate alone are studied in the first place. The mean fundamental frequency is found to be $(1{\cdot}82 \pm {\cdot}02)$ Mc/sec. A resonant oscillation can be easily distinguished from the " pure " one from the nature of the diffraction pattern. At resonance, the pattern contains as many as 10 orders (using transformer oil as the liquid) at the fundamental frequency and more than 4 at the higher harmonics. On the other hand, the pattern due to the " pure " vibration contains only one bright first order, a very feeble second order appearing very rarely near the fundamental frequency range, *i.e.*, between 1·6 to 1·8 and 1·84 to 2 Mc/sec. For the rest, the plate gives only a single bright order from approximately 0·8 to 7 Mc/sec. After 7 Mc/sec, the pattern becomes rather faint but remains continuous up to 8 Mc/sec.

This plate is used to measure the elastic constants of (*a*) Ammonium alum,[2] (*b*) Barium nitrate,[3] and (*c*) two varieties of beryl* which have all been worked previously by the wedge method.

3. Experimental Observations and Results

The following observations may be mentioned. Firstly, when the piezo-plate is used to excite the natural frequencies of the crystals, no spurious maxima appeared in diffraction so that every diffraction pattern observed corresponds to a vibration mode of the crystal. Secondly, round every frequency of a mode of oscillation of the crystal, a group of frequencies, differing very minutely from each other occur. This is due to minute variations in thickness. All the frequencies observed fall, however, into definite groups, and the groups can in turn be classified into two or three types, each type containing a fundamental mode and its harmonics. Table I

* The wedge method values for beryl have been taken from unpublished work done by B. Ramachandra Rao, in these Laboratories.

gives the complete data obtained with a Z-cut beryl plate and is intended to illustrate how the analysis of the data is done:

TABLE I

Green variety beryl; Z-cut plate

Thickness = 1·495 mm.; density 2·720 gm/cm.³

Frequencies		Mode	Corresponding Elastic constant
With a good tourmaline wedge	With a tourmaline plate		
1·7 .. I	..1·7 } .. I	torsion (t)	C_{44}
1·73 .. I	1·72 }		
*1·9 .. S	x 1·82 .. I	(fundamental of the piezo-plate)	—
*2·9 .. S	..		
3·1 .. V. I	3·12 }		
3·15 .. V. I	3·15 } ..V. I	longitudinal (l)	C_{33}
3·18 .. I	3·18 }		
*3·3 .. S	..		
3·4 .. I	3·38 }		
3·45 .. S	3·40 } .. I	2 × (t)	C_{44}
	3·42 }		
*4·28 .. S	..		
5·07 .. I	5·07 }		
5·08 .. S	5·072 } .. I	3 × (t)	C_{44}
*5·28 .. S	..		
*5·4 .. W	..		
6·3 .. V. I	6·3 }		
	6·31 } ..V. I	2 × (l)	C_{33}
*6·5 .. S	..		
*6·8 .. W	..		
*8·98 .. W	..		
*9·12 .. W	..		
9·48 .. I	9·47 }		
9·49 .. I	9·48 } .. S	3 × (l)	C_{33}
9·50 .. I	9·49 }		

In the above Table, V.I. denotes very intense and more than one order; I, intense; S, strong but less than intense; W, weak; and frequencies marked with (*) are spurious wedge maxima. In the wedge method, the spurious maxima are minimized by a careful selection of the wedge; and finally scored off in analysis since their harmonics do not appear. Table I also shows that using the plate there are no spurious maxima except the one at 1·82 which is the fundamental frequency of the plate itself. Its second harmonic does not occur. After sorting out the frequencies, the mean value corresponding to each mode is found, and the effective elastic constant calculated in the usual way.

Thus, from the table, the longitudinal fundamental comes out as 3·153 Mc/sec, and the torsional one as 1·7 Mc/sec giving respectively $C_{33} = 24·18$ and $C_{44} = 7·03$ in units of 10^{11} dynes/cm.^{2}

A third observation of interest is that if the plate under investigation is very thick and non-uniform in structure, with cracks in the material, the intensity of the pattern obtained with a piezo-plate is considerably less than that with a wedge. In the extreme case, with a plate 2 mm. thick of a micro-crystalline aggregate like quartzite with a highly inhomogeneous structure, the response is very poor. Also the thinner plates of beryl were more easy to work with by this method than the thicker ones.

The elastic constants obtained with various crystals are given in Table II in units of 10^{11} dynes/cm^2.

TABLE II

Substance	C_{11}		C_{33}		C_{44}		C_{12}		C_{13}	
	With Wedge	With Plate	With Wedge	With Plate	With Wedge	With Plate	With Wedge	With Plate	With Wedge	With Plate
1. Ammonium Alum	2·50	2·51	..	..	0·8	0·81	1·06	1·08	..	..
2. Barium Nitrate ..	6·02	6·04	..	..	1·21	1·22	1·86	1·86	..	..
3. Beryl (spotted green variety)	27·81	28·00	24·8	24·80	6·61	6·58	10·01	9·9	6·77	6·70
4. Beryl (Sea-green variety)	29·71	28·73	26·50	24·18	7·54	7·02	10·26	9·91	7·39	7·29
Voigt's values for Beryl by static Methods	26·95		23·61		6·54		9·60		6·61	

It may be noted here that for the successful working of this method, the crystal plate under investigation should be sufficiently thin, so that absorption of the comparatively small ultrasonic energy in the medium is minimised. As has already been mentioned, plates like that of quartzite with many crevices and cavities cannot be investigated by this method without increasing the electrical load on the piezo-plate beyond safe limits.

The elastic constants obtained in the case of ammonium alum, and barium nitrate with the plate agree very well with those obtained by the wedge methods. The agreement in the case of beryl is fairly good.

Voigt's[4] values for beryl are considerably lower than those obtained in the present investigation. The values of elastic constants obtained by using static methods (Voigt) are usually lower than those obtained by

dynamic methods. Moreover, beryl occurs in a large variety of slightly differing compositions giving slightly differing elastic constants.

4. Summary

A modified method of finding the elastic constants of crystalline substances using a piezo-electric plate of uniform thickness is described in the present paper. The conditions under which the method can be successfully employed have been discussed. The elastic constants of ammonium, alum, barium nitrate and beryl have been determined by using this method. Results compare well with those obtained by the wedge method.

Acknowledgement

The author expresses his thanks to Prof. S. Bhagavantam under whose guidance this work was done.

References

1. Bhagavantam, S., and Bhimasenachar, J. .. *Proc. Ind. Acad. Sci.*, 1941, **20**, 298.
2. Sundara Rao, R. V. G. .. *Curr. Sci.*, February 1948, **17**, 50.
3. Bhagavantam, S., and Sundara Rao, R.V.G. *Ibid.*, October 1948, **17**, 296.
4. Voigt, W. .. *Lehrbuch Der Krystal Physik*, 748.

ELASTIC CONSTANTS OF AMMONIUM CHLORIDE AND AMMONIUM BROMIDE

By R. V. G. Sundara Rao and T. S. Balakrishnan

(From the Department of Physics, Indian Institute of Science, Bangalore)

Received November 17, 1948

(Communicated by Prof. R. S. Krishnan, F.A.SC.)

1. Introduction

Many of the physical properties of the alkali halides, like the thermal expansion coefficients, molecular refractions, etc., have been determined by various authors and summarised by Wooster (1938). Recently, the Raman effect (R. S. Krishnan, 1947) and the Faraday effect (S. Ramaseshan, 1947) for some of the single crystals of these were studied in this laboratory, so that there is a large amount of available data concerning them. The comparatively simple structure of these crystals has also made it possible to attempt a theoretical correlation between the structure and the observed data. Among the elastic properties of these substances, the cubical compressibilities have been determined for almost all of them; but the separate elastic constants of the single crystals are determined for only a few.

It is proposed therefore to determine the separate constants of ammonium chloride and ammonium bromide. A word about the choice of these ammonium halides is not out of place. Though the cation is really complex, the hydrogen ions, imbedded in the distribution of the negative charge in a symmetrical tetrahedral arrangement do not greatly affect the structure so that they can be considered along with the other alkali halides, as is usually done. Another point of interest regarding these two halides is that they have the body centred caesium chloride structure at room temperature and change over to the rock-salt type at high temperatures.

The single crystals of ammonium chloride are of fairly good size for the method of investigation used, being about ·8 cm. × ·8 cm. × ·5 cm., without any inclusions in them. Those of NH_4Br, however, have a number of inclusions in the material so that observations on them are rather tentative and approximate.

2. Experimental Technique

The method of determining the elastic constants is to send an ultrasonic wave, using a piezo-electric plate of uniform thickness, developed in the Andhra University laboratories. The details of the experimental technique

are given in another paper by one of the authors (Sundara Rao) appearing in this Symposium. The outlines of the method may be given as follows. The inverse piezo-electric effect for a piezo-plate of uniform thickness is given by the relation:

$$\delta = d_{ij} \cdot U \tag{1}$$

for the thickness displacement of the plate, where δ is the amount of contraction or expansion; U, the difference of potential applied to the faces normal to the thickness direction, and d_{ij} the appropriate piezo-electric modulus for that direction. If therefore U is of the form:

$$U = U_0 \cos \nu t, \tag{2}$$

the plate executes forced vibrations with approximately the same frequency as ν. Therefore, if an oscillator of a sufficiently good R.F. voltage and power output of variable frequency is used as a driver for the piezo-plate, we have at once a source of continuous frequency ultrasonic energy. The latter output, however small, was found to be sufficient to work with, when a non-piezo-plate, under investigation, of uniform thickness, is acoustically coupled to the piezo-plate. This is effected by forming a condenser with two parallel metallic plates, between which is placed the combination of the piezo- and the non-piezo-plates placed with their thicknesses parallel, and with a drop of transformer oil in between them to accomplish the acoustic contact. This condenser is now connected in parallel with the variable condenser of the oscillator. At the natural mechanical frequency (or a harmonic) of the crystal plate, it acts as a resonator to the driving piezo-electric oscillations of the small amplitude, given by (1) and (2) above, when the frequency of the oscillator coincides with that of the former. In other words, it is the resonator principle that makes it possible to utilize the forced oscillations of the piezo-plate to throw the crystal plate into ultrasonic vibrations at the latter's natural frequency. These ultrasonic vibrations are communicated to a transparent liquid, touching the underneath of the non-piezo-plate. The detection of the ultrasonic waves in the liquid is effected by using Debye Sears' phenomenon.

As regards the necessary crystal sections, since the crystals belong to the cubic symmetry, a plate cut normal to the cube edge, (100) section and another cut parallel to one of the edges and making equal intercepts on the other two axes, (110) section, are enough to determine C_{11}, C_{12}, and C_{44}, which are the three non-vanishing elastic constants required to describe the elastic behaviour of a cubic crystal under stress. Specifically, the sections and the effective elastic constants associated with them are given in Table I below.

TABLE I

Section	Effective Elastic Constants
(100)	C_{11} ; C_{44}
(110)	$\frac{1}{2}(C_{11}+C_{12}+2C_{44})$; C_{44} ; $\frac{1}{2}(C_{11}-C_{12})$
(111)	$\frac{1}{3}(C_{11}+2C_{12}+4C_{44})$; $\frac{1}{3}(C_{11}-C_{12}+C_{44})$

The third section (111), if available, can be used to check the results obtained from the other two. The effective elastic constants can be computed from the relation:

$$f_r = \frac{1}{2d}\left(\frac{C_E}{\rho}\right)^{\frac{1}{2}}, \tag{3}$$

where f_r is the fundamental resonance frequency, d, the thickness of the plate, C_E, the effective elastic constant, and ρ the density of the plate.

A push-pull Hartley oscillator of variable frequency for R.F. power generation, and plates of about 1 mm. to 1·5 mm. thickness are used.

3. EXPERIMENTAL RESULTS

As mentioned in the introduction, the crystals of NH_4Br are not very good, so that the diffraction patterns were not as sharp as in the case of NH_4Cl. However, a sort of average frequency is made out of repeated observations, and by selecting the most intense of the patterns as corresponding to the resonance frequency. In any case, the deviation as calculated from the entire frequency data would not be more than 8 to 10 per cent. and in all probability, the tabulated values are lower than the possible actual ones by so much. With this degree of uncertainty about the values for NH_4Br, the following Table II gives the values obtained in the case of the two halides. In the last two columns, the calculated and the observed (Bleick, 1934) values of the bulk modulus are given, the former having been obtained from

$$K = \tfrac{1}{3}(C_{11} + 2C_{12}) \tag{4}$$

All the values are given in units of 10^{11} dynes cm.$^{-2}$

TABLE II

No.	Substance	C_{11}	C_{12}	C_{44}	K (calculated)	K (observed)
1	NH_4Cl	3·90	0·72	0·68	1·77	1·736
2	NH_4Br	2·96	0·59	0·53	1·38	1·630

4. Discussion of the Results

Though it is not possible to draw many quantitative conclusions from the above data, firstly because data concerning no other crystals having the CsCl structure type are available in the literature, and secondly because of the uncertainty of the values of NH_4Br, we can see, that they exhibit the same sort of gradation in the values as do the other alkali halides. Another point of interest comes out if we compare the values with the lattice spacings. Thus for NH_4Cl, the interionic distance *i.e.*, the distance between one ion and the nearest neighbour of opposite sign is 3·34 and that for NH_4Br, 3·51 (Slater, 1939) in angstroms. A comparison of these values with the elastic constants shows that as the interionic distance increases, the elastic resistance of the crystals decreases (ionic charge remaining the same). In other words, the closer the packing of the ions in the crystal, which means a lesser interionic distance, the larger are the elastic constants. An examination of the elastic constants of the other alkali halides, for which values are available in the literature (R.F.S. Hearmon, 1946) and tabulated below, also shows the same variation.

Table III

Substance	r_0 in Angstroms	C_{11}	C_{12}	C_{44}
LiF ..	2·01	9·81	3·61	6·28
Nacl ..	2·81	6·23	1·37	1·28
NaBr ..	2·98	3·26	1·31	1·33
KCl ..	3·14	3·72	0·81	0·79
KBr ..	3·29	3·33	0·58	0·62
KI ..	3·53	2·67	0·43	0·42

The substances in Table III, all belong to the rock-salt structure, but the regular decrease of the elastic constants with the increasing interionic distance r_o (Slater, 1939) is quite obvious. In fact, from the above table, we see after a little calculation, that for most of the crystals (LiF being an outstanding exception) the relation

$$C_{ij} \simeq a_{(ij)}\, r_0^{-4} \tag{5}$$

holds good, where C_{ij} represents C_{11}, C_{12} or C_{44}, and a_{ij} is a typical constant for each (ij), for a particular structure type. In other words, the relation (5) gives

$$\frac{C_{ij}^{ak}}{C_{ij}^{a'k}} \simeq \left(\frac{r_0^{ak}}{r_0^{a'k}}\right)^{-4} \tag{6}$$

where C_{ij}^{ak} stands for the elastic constant C_{ij} of the alkali halide with cation 'a' and anion 'h' and similarly for $c_{ij}^{a\,k}$. Thus if we take NaCl and KCl, we have, for instance,

$$\frac{C_{12}^{NaCl}}{C_{12}^{KCl}} = \frac{1{\cdot}37}{{\cdot}81} = \left(\frac{2{\cdot}81}{3{\cdot}14}\right)^{-4.096} \simeq \left(\frac{r_0^{NaCl}}{r_0^{KCl}}\right)^{-4}$$

and so on.

A similar calculation for NH_4Cl and NH_4Br, belonging to CsCl structure type can be made, and we have:

$$\frac{C_{11}}{C_{11}'} = \frac{3{\cdot}9}{2{\cdot}96} = \left(\frac{3{\cdot}34}{3{\cdot}51}\right)^{-5.302}$$

$$\frac{C_{12}}{C_{12}'} = \frac{{\cdot}72}{{\cdot}59} = \left(\frac{3{\cdot}34}{3{\cdot}51}\right)^{-3.864}$$

$$\frac{C_{44}}{C_{44}'} = \frac{{\cdot}68}{{\cdot}53} = \left(\frac{3{\cdot}34}{3{\cdot}51}\right)^{-4.787}$$

where the undashed constants belong to NH_4Cl and dashed ones to NH_4Br. Except in the case of C_{12}'s, we see that the value of the index is about -5; but this is inconclusive because of the probably low values of NH_4Br. Accurate determination of the elastic constants with better specimens of NH_4Br crystals might yield better results for 'n' the index.

Another point of interest in the above results is that Cauchy's relations are nearly satisfied for these crystals, as in the case of the other alkali halides. For cubic crystals, Cauchy's relations give $C_{12} = C_{44}$. Table II shows that it is approximately so. It is in a sort of agreement with the theoretical requirements (Born, 1932) of a crystal in which all the atoms or (ions) are at the centres of symmetry.

In conclusion, the authors wish to thank Prof. R. S. Krishnan for his kind encouragement and guidance.

5. Summary

The elastic constants of NH_4Cl and NH_4Br single crystals are determined by using the ultrasonic piezo-plate method. The relation between the elastic constants and the interionic distances for the alkali halides and the ammonium halides in question has been discussed. Cauchy relation has been verified in the case of NH_4Cl and NH_4Br.

References

1. Bleick, W. E. .. *J. Chem. Phy.*, 1934, **2**, 162.
2. Born, M. .. *Atom theorie des Festen Zustandes*, 1932.
3. Hearmon, R. F. S. .. *Rev. Mod. Phy.*, 1946, **18**, 409.
4. Krishnan, R. S. .. *Proc. Ind. Acad. Sci.*, 1948, **26**, 419, 432; 1948, **27**, 321.
5. Ramaseshan, S. .. *Ibid.*, 1947, **25**, 464.
6. Slater, J. C. .. *Introduction to Chemical Physics*, Mc-Graw Hill, 1939.
7. Wooster, W. A. .. *Crystal Physics*, Cambridge, 1938.

RAMAN SPECTRA OF SODIUM AND POTASSIUM TARTRATES

By V. M. Padmanabhan

(From the Department of Physics, Indian Institute of Science, Bangalore)

Received November 20, 1948

(Communicated by Prof. R. S. Krishnan, F.A.Sc.)

1. Introduction

Studies on the Raman spectra of crystalline tartrates are of great theoretical interest as they may be expected to throw some light on the peculiar electric properties of such crystals. Special mention may be made of crystals like potassium tartrate ($K_2C_4H_4O_6$, $\frac{1}{2}H_2O$) and ethylene diamine tartrate ($C_6H_{14}N_2O_6$) which are finding increasing application as piezo-electric oscillators. In view of the fact that large clear crystals of tartrates can be easily grown from solutions, it is surprising to note that very little systematic work has been done on their Raman spectra. The author has therefore undertaken a systematic investigation of the Raman spectra of crystalline tartrates and the present paper describes the results obtained with sodium and potassium tartrates.

Working with a single crystal, Gupta (1938) was the first to record the spectrum of sodium tartrate which exhibited five lines with frequency shifts 889, 990, 1071, 1118 and 1215 cm.$^{-1}$ The Raman spectrum of potassium tartrate has been investigated by Canals and Peyrot (1938) using the powder technique and by Laksmana Rao (1941) using a single crystal. While the former authors recorded nine frequency shifts all lying above 1200 cm.$^{-1}$, Rao reported no less than 17 lines including 3 low frequency lines and 1 water band. In view of the complicated nature of both sodium and potassium tartrate crystals, the results obtained by earlier authors are evidently incomplete. This may be attributed to the fact that they used the λ4047 and λ4358 radiations of the mercury arc for excitation.

2. Experimental Details

Single crystals of sodium and potassium tartrates were grown by the method of slow evaporation from aqueous solutions of the pure salts. Great care had to be taken in adjusting the saturation of the solution and

maintaining constancy of the temperature of the room. The largest crystal grown had the following dimensions: $3 \times 2 \times 1$ cm. In the case of sodium tartrate the longer side of the crystal was parallel to the (100) face. The (010) face was not well developed. In the case of potassium tartrate also, the length of the crystal was along the (100) face.

As the tartrates are transparent to the ultra-violet, the 2536 Hg resonance radiation was used for exciting the Raman spectrum from a specially designed quartz arc. As will be evident from the later sections, this has helped to get a wealth of data regarding the Raman spectrum especially in the region of low frequency shifts.

The crystal under investigation was held facing the most intense portion of the arc, near the front wall of the quartz tube towards which the discharge was deflected. The light scattered from the crystal was condensed on the slit of a Hilger E3 Quartz Spectrograph. In the case of sodium tartrate, light was incident along the '*a*' axis, and the scattered light was taken along the *c*-axis. In the case of potassium tartrate, light was incident along the '*a*' axis and the scattered light was taken along the direction perpendicular to this axis. The 2536 radiation in the scattered light was suppressed before its entry into the spectrograph by absorption. With a slit width of 0·035 mm. and using special rapid plates, exposures of the order of 48 hours were given to get intense photographs of the Raman spectra of both the tartrates. During such long exposures a disturbing effect was noticed, namely that the portion of the crystal facing the arc became frosted due to heating, in spite of efficient cooling by a fan. Therefore, fresh crystals had to be used every five hours. In replacing the crystals care was taken to see that the same orientation was adopted. The plates were measured under a Hilger cross-slide micrometer.

3. Results

Photographs of the Raman spectra of sodium and potassium tartrates are reproduced in Fig. 1 (*a*), (*c*), together with a spectrum of the mercury arc for purposes of comparison, Fig. 1 (*b*). The corresponding microphotometric records are shown in Fig. 2. The positions of the lines are marked for clarity. The frequency shifts are listed below in Table I. The figures given in brackets represent visual estimates of the relative intensities of the lines. Laksmana Rao's values for the frequency shifts in the case of potassium tartrate are shown in column 3. The author's results are in close agreement with those of Laksmana Rao.

TABLE I

Sodium tartrate (Frequency shifts in cm.$^{-1}$) Author		Potassium tartrate (Frequency shifts in cm.$^{-1}$) Author		Potassium tartrate (Laksmana Rao)
42	(5)	33	(15)	
83	(5)	78	(8)	77
110	(4)	106	(15)	103
134	(8)	153	(5)	150
188	(8)	172	(15)	
205	(3)			
231	(3)	235	(2)	
248	(5)			
279	(4)	281	(4)	
302	(5)	309	(3)	
		339	(4)	
353	(3)			
		379	(4)	
488	(4)	493	(6)	493
532	(8)	528	(8)	531
		603	(2)	603
697	(4)	697	(3)	
813	(15)	809	(10)	807
849	(5)	850	(6)	846
893	(8)	897	(6)	889
917	(4)	919	(8)	
		955	(5)	
990	(2)	992	(2)	995
1037	(3)			
1072	(8)	1072	(2)	1073
1112	(15)	1110	(8)	1110
1209	(8)	1218	(10)	1219
1247	(3)	1244	(8)	
1287	(3)	1281	(2)	
		1315	(3)	
		1322	(2)	1323
1352	(5)			1351
1381	(3)	1397	(4)	
1404	(4)	1418	(15)	
1432	(6)	1429	(20)	1425
1463	(8)			
1496	(2)			
1560	(3)	1560	(5)	
1585	(6)	1585	(5)	
1604	(3)	1602	(2)	
		1628	(2)	
		1659	(3)	
2935	(20)	2926	(20)	2926
2981	(20)			
3285		3283		
3399		3336		3336
3471		3435		
3514				

The displaced lines are clearly seen on the microphotometric record. Most of them can be identified on the reproduced photographs. The recorded spectra show 40 frequency shifts in the case of sodium tartrate, and 39 in the case of potassium tartrate. Of these, 31 lines and 4 water

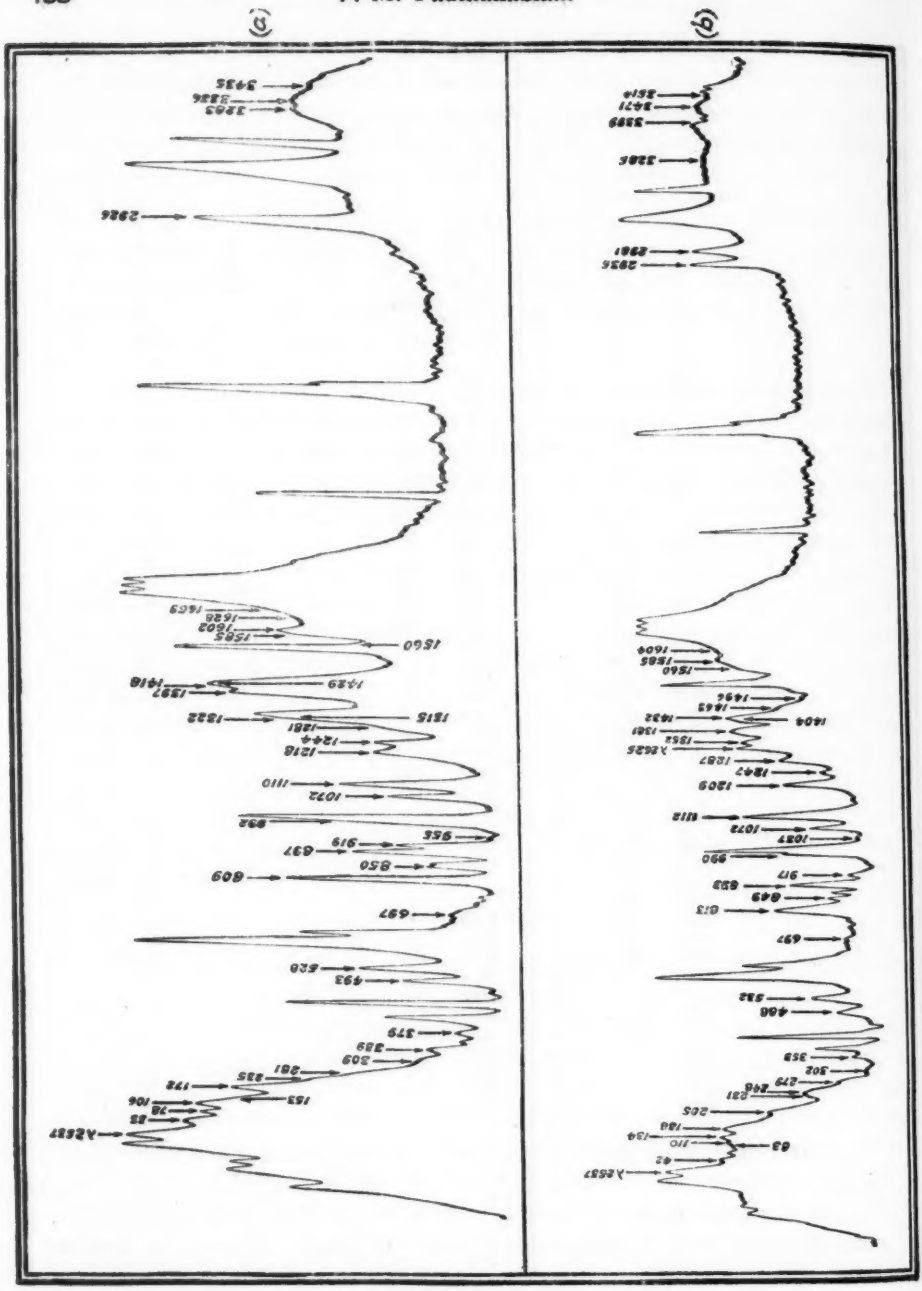

FIG. 2
Micro-photometric record— (*a*) Potassium Tartrate (*b*) Sodium Tartrate.

bands in sodium tartrate and 19 lines and 2 water bands in potassium tartrate have been recorded for the first time. As is to be expected, there is a close correspondence between the Raman spectrum of sodium tartrate and that of potassium tartrate in the region of frequency shifts 230 to 3500 cm.$^{-1}$ The Raman lines falling in this region are evidently due to the internal oscillations of the tartrate ion and that of the water molecule. The existence of a line at 603 cm.$^{-1}$ reported by Laksmana Rao could not be identified in the spectra taken by the author since it coincides with the mercury line λ 2576. Besides the Raman lines given in Table I, a weak band in the neighbourhood 1400 cm.$^{-1}$ appears to be present in the case of sodium tartrate, though it is not present in the case of potassium tartrate. Of the three water bands observed with potassium tartrate, the band at 3283 cm.$^{-1}$ is the weakest. In the case of sodium tartrate, on the other hand, the band at 3399 cm.$^{-1}$ is the most intense, and the one at 3285 is the least intense. The bands at 3471 and 3514 are less broad than the other two.

The low frequency lines can be clearly seen in the spectra of both the crystals, though they are more intense in the case of potassium tartrate. The two lattice lines at 33 and 172 cm.$^{-1}$ of potassium tartrate, and all the six lattice lines of sodium tartrate have been recorded for the first time. The lines 134 and 188 cm.$^{-1}$ in sodium tartrate are more intense than the other lattice lines. The line 188 cm.$^{-1}$ is rather broad. This may be attributed to the superposition of the weak low frequency water band at 170 cm.$^{-1}$ The lines 33, 106 and 172 cm.$^{-1}$ observed in the spectrum of the potassium tartrate are more intense and broader than the lines 78 and 153 cm.$^{-1}$

4. Discussion

Sodium tartrate belongs to the orthorhombic class and has two molecules of water of crystallisation. Potassium tartrate belongs to the monoclinic system, and has one molecule of water of crystallisation for two molecules of potassium tartrate. Their chemical constitutional formula is given as

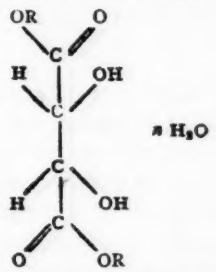

where R represents the metallic ion and n the number of water molecules.

The structures of both sodium and potassium tartrates have not been fully worked out by X-ray analysis.

The observed Raman lines can be roughly classified into three groups—lattice lines, frequencies due to the tartrate ion and water bands.

Lattice Oscillations.—Table II shows lattice frequencies observed in the spectra of sodium tartrate, potassium tartrate, Rochelle salt and tartaric acid.

TABLE II

Sodium tartrate (Author)	Potassium tartrate (Author)	Rochelle Salt (Nedungadi) (1940)	Tartaric acid (Gupta)
42	33	39	36
83	76	88	80
110	106		103
134	153	132	124
188	172		
205			

As can be seen from the above table, the lattice frequencies in the case of potassium tartrate have lower values as compared with the corresponding frequencies in the case of sodium tartrate and Rochelle salt. The lowering of frequency in the case of potassium tartrate may be attributed to the heavier mass of the potassium ion than sodium or sodium and potassium combined. A more complete study of the spectra of Rochelle salt and tartaric acid using the ultra-violet technique is necessary before one can attempt to give a proper interpretation of the observed lattice lines in sodium and potassium tartrates.

Frequencies due to the tartrate ion.—Table III gives the frequency shifts of the Raman lines due to the internal oscillations of the tartrate ion as observed in the spectra of crystalline sodium and potassium tartrates (author), Rochelle salt (Nedungadi) and of sodium tartrate solution (Edsall) (1937).

The most intense line at 2926 cm.$^{-1}$ observed in potassium tartrate and the lines at 2935 and 2981 cm.$^{-1}$ in sodium tartrate are obviously due to C–H oscillation. The interesting fact is that whereas only one line is observed in the case of potassium tartrate, two lines appear in sodium tartrate. Sodium tartrate belongs to the orthorhombic class, whereas potassium tartrate belongs to the monoclinic system. The appearance of two lines in the case of sodium tartrate cannot be attributed to any splitting

TABLE III

Sodium tartrate	Potassium tartrate	Rochelle salt	Sodium tartrate solution
231	235		239
248		249	
279	281		
302	307		
	339		
353			
	379		378
488	493	485	491
532	528	532	532
	603	611	618
		641	
697	697	691	
813	809	811	805
849	850		
893	897	891	893
	919	915	
917	955		
990	992	990	992
1037			
1072	1072	1070	1068
1112	1110	1112	1121
1209	1218	1210	1224
1247	1244		
1287	1281	1292	
	1315		1310
	1322		
1352		1347	
1381		1379	1370
	1397		
1404	1418		1418
1432			
1463	1429	1425	
1496			
1560	1560		
1585	1585		
1604	1602		1617
	1628		
	1659		
2935	2926	2935	2936
2981		2979	

of the oscillations due to lower symmetry, because sodium tartrate is more symmetric than potassium tartrate. The group of lines in the neighbourhood of 900 cm.$^{-1}$ (lines 813, 849, 893, 917, 990 in sodium tartrate, and lines 809, 850, 897, 919, 955 and 992 in potassium tartrate) is obviously due to linear *C–C* oscillations of the ion. The three lines at 239, 491 and 532 cm.$^{-1}$, observed in the spectrum of the solution, have been attributed to the deformation oscillations of the carbon chain. The appearance of these three lines in the spectra of crystalline sodium tartrate, potassium tartrate and Rochelle salt without appreciable change in frequency shifts indicates that ionisation

has no effect on these frequencies. The three lines appearing in the region 275–350 cm.$^{-1}$ in the spectra of both sodium and potassium tartrates may also be attributed to deformation oscillation of the carbon chain arising from its increased complexity. The group of lines falling in the region 1035–1380 cm.$^{-1}$ may be attributed to the oscillations of the $-\overset{|}{\underset{|}{C}}-OH$ group. The carbonyl frequency ~ 1700 cm.$^{-1}$ observed in other organic acids and compounds does not appear in the spectra of tartrates. Hibben (1939) attributed the line 1617 cm.$^{-1}$ observed in the spectrum of tartaric acid, to the ionised carboxyl group. So the group of lines appearing in the region 1560–1604 cm.$^{-1}$ in the spectra of both the salts can likewise be attributed to oscillations of the ionised carboxyl group. The lines 1432 and 1463 of sodium tartrate, and 1429 of potassium tartrate may be attributed to C-H bond-bending oscillations.

The ionised carboxyl group resembles a bent triatomic molecule $\left[R-C\begin{matrix}O\\O\end{matrix}\right]^-$. The calculated frequency of the symmetric valence oscillation of this group falls at 1400. The line 1381 in the case of sodium tartrate and the one 1397 in the case of potassium tartrate correspond to this oscillation. The lines 1404 and 1418 can then be attributed to asymmetric valence oscillation of this group. A symmetric deformation oscillation at 600 must also be present. This could not be detected in the spectra taken with λ 2537 excitation as it would fall on the intense mercury line λ 2576.

The spectrum of potassium tartrate exhibits two faint lines at 1659 and 1628 cm.$^{-1}$ which may be assigned as the combination of the intense lines 809 and 850, and the overtone of the line 809.

The four water bands observed in the case of sodium tartrate have nearly the same frequency shifts as the four water bands of Rochelle salt (3262, 3400, 3468 and 3534) recorded by Nedungadi. It is of some interest to point out that the band with the lowest frequency shift corresponds with the band 3200 cm.$^{-1}$ observed in the case of pure water.

In conclusion, the author wishes to express his grateful thanks to Prof. R. S. Krishnan for his guidance and encouragement.

5. Summary

Using λ 2536 for excitation, the Raman effect of single crystals of sodium and potassium tartrates has been investigated. The recorded spectra exhibit forty Raman lines in the case of both sodium and potassium tartrates.

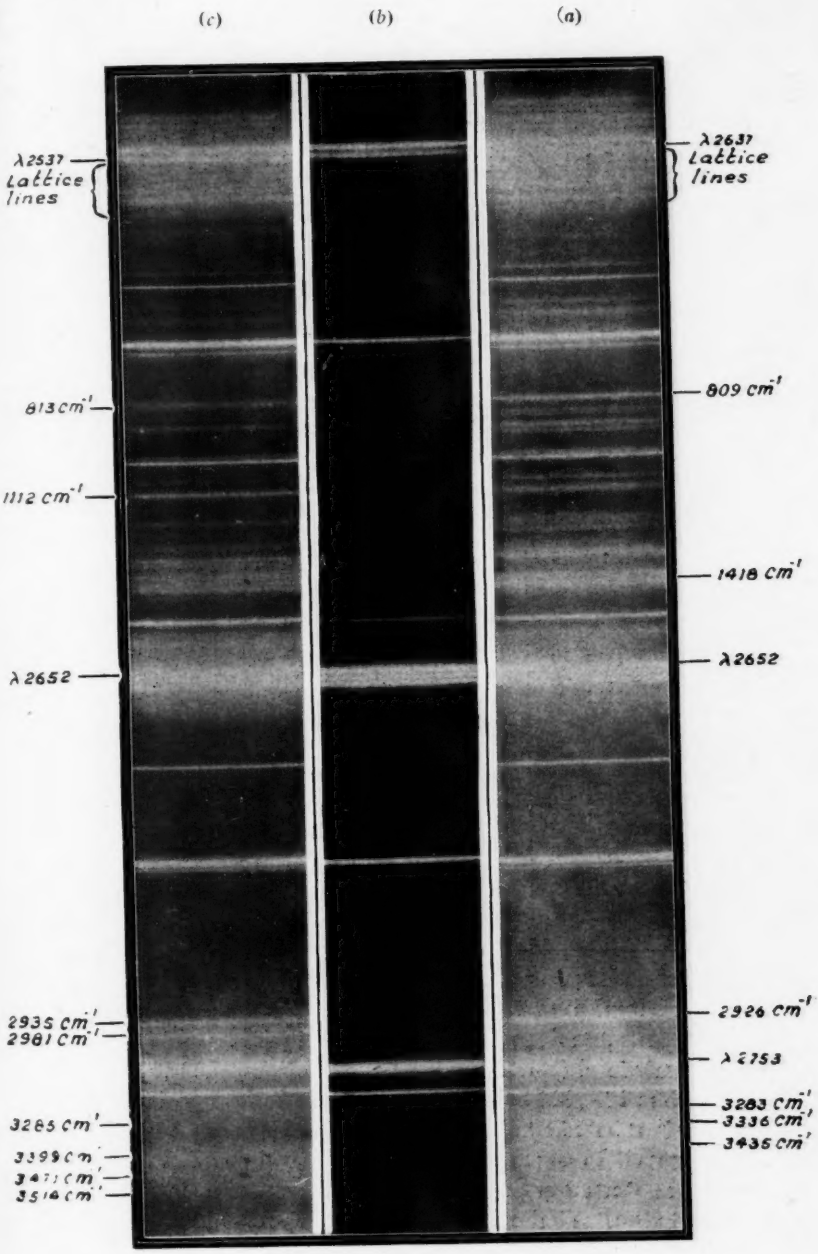

FIG. 1. (*a*) Raman spectrum of potassium tartrate
(*b*) Comparison spectrum of mercury arc
(*c*) Raman spectrum of sodium tartrate

As many as thirty-four lines in the case of sodium tartrate, and twenty-two in the case of potassium tartrate, have been recorded for the first time. The observed frequencies can be classified under three heads—namely, lattice spectrum, internal frequencies due to tartrate ion, and water bands. A tentative assignment has been given to important groups of lines appearing in the spectrum.

References

Canals and Peyrot	..	*Compt. Rend.*, 1938, **206**, 1179.
Edsall	..	*J. Chem. Phys.*, 1937, **5**, 508.
Gupta	..	*Ind. Jour. of Phys.*, 1938, **12**, 355.
————	..	*Ibid.*, 1936, **10**, 117.
Hibben	..	*Raman Effect and its Chemical Application*, 1939, p. **195**.
Laksmana Rao	..	*Proc. Ind. Acad. Sci.*, A, 1941, **14**, 42.
Nedungadi	..	*Ibid.*, 1940, **11**, 413.

RAMAN SPECTRUM OF ETHYLENE DIAMINE TARTRATE

By V. M. Padmanabhan

(From the Department of Physics, Indian Institute of Science, Bangalore)

Received November 30, 1948

(Communicated by Prof. R. S. Krishnan, F.A.Sc.)

1. Introduction

It is known that ethylene diamine tartrate ($C_6H_{14}N_2O_6$) has elastic modes of vibration with zero temperature coefficient of frequency and high electro-mechanical coupling constants. Because of these special properties, this crystal is finding increasing application as filters in oscillators in place of quartz which is difficult to obtain in large sizes. A detailed study of its Raman spectrum may be expected to throw some light on the mechanism of its peculiar electric behaviour. Besides, it will also give some information regarding the existence or otherwise of "free rotation" about the C-C bond. Surprisingly enough, so far no one has studied the Raman spectrum of ethylene diamine tartrate. A detailed investigation on the Raman spectrum of ethylene diamine tartrate and also the effect of crystal orientation on its spectrum has therefore been undertaken by the present author and the results are given in this paper.

2. Experimental

The specimen of ethylene diamine tartrate used in the present investigation had well developed faces with the following dimensions—$9 \times 6 \times 4$ cm. This crystal was grown in the Bell Telephone Laboratories, Murray Hills, New Jersey, U.S.A., and was presented to Prof. Sir C. V. Raman, who very kindly placed the same at the disposal of the author. Though the major portion of the crystal was clear, imperfections existed in certain places, probably due to the conditions and the mode of growth of the specimen. As the crystal got coloured intensely yellow on exposure to ultra-violet light and became opaque to λ 2536 radiation, λ 4358 and λ 4047 excitation had to be used for recording the Raman spectrum. Light from a quartz mercury arc was focussed on the crystal by a glass condenser. The scattered light was condensed on the slit of a two-prism glass spectrograph. A trial exposure taken with the 4047 and 4358 excitation exhibited a continuum due

to fluorescence extending over λ 4500–5000. This was found to overpower the Raman lines and thus prevented the latter from being recorded properly. The use of a filter, made up of a weak solution of iodine in carbon tetrachloride in the path of the incident light reduced the intensity of the continuous spectrum to some extent. Using a slit width of 0·075 mm. and Ilford Selochrome plates, exposures of the order of 36 hours were found to be sufficient to get pictures with reasonable intensity.

Six different spectrograms can be got by varying the orientation of the crystal relatively to the directions of incidence and scattered beams. Only three spectrograms were taken in the present case, with the following orientations:—(1) incident light being perpendicular to 100 face, and scattered light being perpendicular to 001 face, (2) incident light being perpendicular to 100 face, and scattered light being perpendicular to $\bar{1}\bar{1}0$ face, and lastly incident light being perpendicular to 001 face and scattered light being perpendicular to $\bar{1}\bar{1}0$ face. The plates were measured by direct comparison with a standard iron arc spectrum, on a Hilger cross-slide micrometer.

3. Results

Three spectrograms obtained by the use of unpolarised light for different orientations of the crystal are reproduced as Fig. 1 *a*, *b* and *c*, in Plate XI. Fig. 1 *c* is particularly clear and more intense than the other two. As there was a continuum near λ 4358, Raman lines arising from the excitations of λ 4047 alone are marked on the Plate. The frequency shifts and the visual estimate of the intensities of the lines in the three orientations are given in Table I.

On the whole, thirty-five distinct frequency shifts have been recorded in the present investigation. It must be mentioned that a correct assignment of these lines in the spectrum is difficult as some of the C–H valence oscillations excited by λ 4046 are superposed over other lines excited by λ 4358. Further, lines due to N–H oscillation also fall in the same region.

An interesting observation made in the present investigation is that the Raman lines undergo marked changes in intensity for different orientations of the crystal even when the incident light is unpolarised. The lines 3010, 2985, 2946, 1459, 1432, 1110, 1060, 992, 920, 144 and 85 undergo marked changes in intensity, whereas the lines 1677, 1380, 1203, 798, 758, 723 and 102 do not show fluctuations in intensity with the three orientations of the crystal. The rest of the lines show correspondingly only slight changes in intensity. The very low frequency lines also show this behaviour.

TABLE I

Line	Intensities of the lines		
	I. L.—100 S. L.—$\bar{1}10$	I. L.—100 S. L.—001	I. L.—001 S. L.—$\bar{1}10$
45	5	1	3
85	9	2	6
102	3	2	3
144	5	3	10
232	3	1	5
328	5	2	8
394	1	..	3
428	1	..	3
477	6	..	2
520	2	6	3
562	2	2	8
610	2	..	3*b*
642	5	..	4
723	3	5	5
758	2	3	2
798	5	5	6
897	8	3	10
920	6	2	6
992	2	1	10
1060	5	5	10
1110	4	1	2
1162	2	2	4
1203	2	3	3
1328	3	3	6
1352	3	8	5*b*
1380	2	3	3
1432	5	3	10
1459	6	2	8
1523	2	4	2
1570	1	1	3
1640	3	8	5
1677	2	4	3
2946	6	8	10
2985	10	8	20
3010	4	4	8

I. L. — incident light perpendicular to
S. L. — Scattered „ „ „ } *b* = broad

4. DISCUSSION

The frequency shifts observed in ethylene diamine tartrate are listed in Table II, along with the shifts in crystalline sodium tartrate (Padmanabhan, 1948) and in liquid ethylene diamine (Ananthakrishnan, 1937).

TABLE II

Ethylene diamine tartrate	Sodium tartrate (Crystal)	Ethylene diamine (liquid)
45	42	
85	83	
102	110	
144	134	
	188	186
	205	
232	231	
	248	
	279	
328	302	333
394	353	
428		
477	488	467
520	532	510
562		
610		
642		
	697	
723		
758		
798		
	813	
	849	837
897	893	
920	917	
992	990	987
	1037	
1060	1072	1051
1110	1112	1093
1162		
1203	1209	
	1247	1240
	1287	1296
1328		
1352	1352	1360
1380	1381	
1432	1432	
1459	1463	1445
	1496	
1523		
	1560	
1570		
	1585	
	1604	
1640		
1677		
		2661
		2743
		2848
		2898
2946	2935	2932
2985	2981	
3010		
	3285 }	3299
	3399 } Water	3366
	3471 } bands	
	3514 }	

A perusal of the figures given in Table II reveals the following special features. Most of the Raman lines observed in the spectrum of sodium tartrate appear with very nearly the same frequency shifts in the specimen of ethylene diamine tartrate. This is particularly true of the lines 2985, 2946, 1459, 1432, 1380, 1352, 1110, 992, 920, 897 and 232 of ethylene diamine tartrate, suggesting thereby that they are due to the internal oscillations of the tartrate ion. In contrast to this, many of the Raman lines with frequency shifts higher than 2660 appearing in the spectra of ethylene diamine are not recorded in the case of ethylene diamine tartrate. Similar observations have been reported by Ananthakrishnan (1936, 1937) in the case of hydroxylamine compounds, who attributed the absence of N–H oscillations (above 3100 $cm.^{-1}$) to the ionic nature of the crystal. If the explanation is correct, the binding between ethylene diamine and tartaric acid in the ethylene diamine tartrate crystal is ionic in nature.

The low frequency lines (45, 85, 102 and 144) observed near the unmodified line, are due to lattice oscillations. Out of these four, 144 may be due to the mutual oscillations of the two groups of ethylene diamine ($C_2H_4N_2H_4$) and tartaric acid ($C_4H_6O_6$) against each other, and 85 may be due to rotation. In order to give proper assignment for the remaining ones, it is necessary to know the crystal structure of ethylene diamine tartrate.

Effect of crystal orientation.—The changes in the intensity of many of the Raman lines with orientation of the crystal have already been mentioned. This kind of behaviour of the Raman lines is to be expected in the case of monoclinic crystals. Saxena (1940) has indicated that the Raman lines observed with a crystal may be regarded as due to deformation of the optical polarisability ellipsoid of the solid produced by internal vibrations and they can be expressed in terms of the six components of the change of polarisability tensor. The selection rules for these vibrations give the particular tensor components that are responsible for them, and on these depend the intensities of the corresponding lines. From considerations of symmetry, all the vibrations in a monoclinic crystal can be classified as either symmetric or antisymmetric. The intensities of the lines due to symmetric oscillations should undergo marked changes with orientation of the crystal, whereas the lines due to antisymmetric oscillations do not undergo changes in intensity. Accordingly, the lines mentioned above which change in intensity markedly, can be treated as due to symmetric oscillations, while those which do not show changes in intensity may be classed as antisymmetric oscillations.

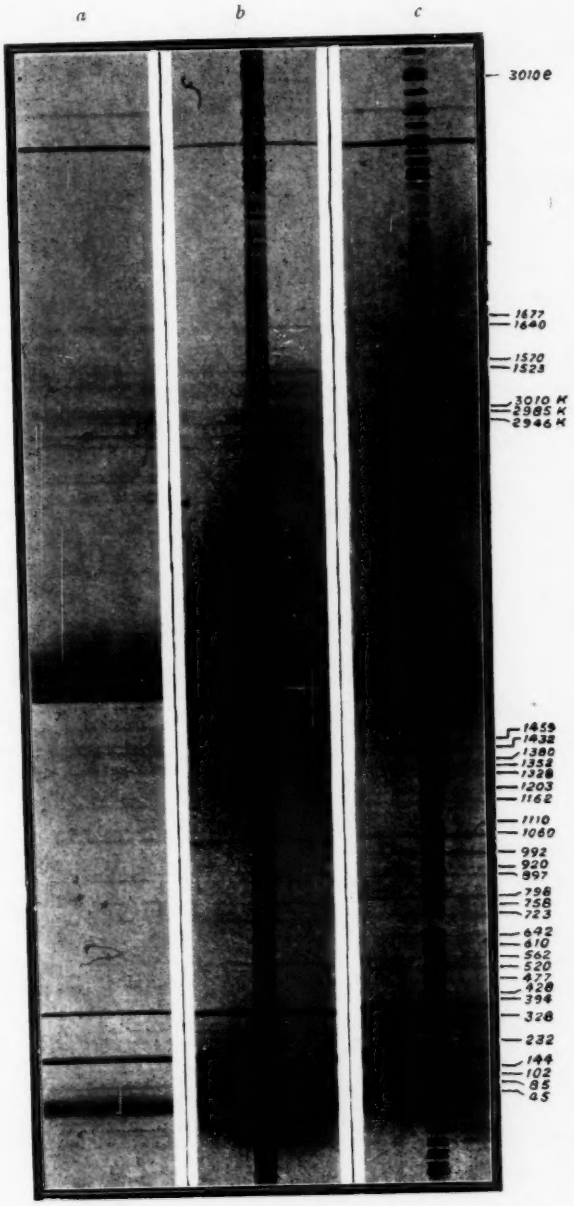
a
b
c
3010 e
1677
1640
1520
1523
3010 K
2985 K
2946 K
1459
1432
1380
1358
1328
1203
1162
1110
1060
992
920
897
798
758
723
692
610
562
520
477
428
394
328
232
144
102
85
65

FIG. 1

In conclusion, the author wishes to record his grateful thanks to Prof. R. S. Krishnan for his keen interest and encouragement during the course of this work.

5. Summary

The Raman spectrum of ethylene diamine tartrate, in the form of a single crystal has been recorded for the first time. Thirty-five distinct Raman shifts are observed. Many of them have been identified as due to tartrate frequencies by comparison with the spectrum of sodium tartrate. A study of the effect of orientation of the crystal relative to the directions of incidence and observation is also made. Many of the Raman lines show marked changes in intensity by varying the orientation of the crystal. In accordance with Saxena's analysis, those lines which show change in intensity are classified as symmetrical oscillations, while those which do not show any change in intensity are regarded as due to antisymmetric oscillations.

References

Ananthakrishnan, R. .. *Proc. Ind. Acad. Sci.*, A, 1937, **5**, 285 and 87.

———— .. *Ibid.*, 1936, **4**, 204.

Padmanabhan, V. M. .. *Ibid.*, 1948, **28**, 485.

Saxena, B. D. .. *Ibid.*, 1940, **11**, 209.

Description of Plate

Fig. 1. Raman spectrum of ethylene diamine tartrate.

a. Incident light perpendicular to 100 face, scattered light perpendicular to $\bar{1}10$ face.

b. " " 100 " " " 001 "

c. " " 001 " " " $\bar{1}10$ "

e — excitation due to λ 4358.

k — " " λ 4047.

RAMAN SPECTRUM OF SODIUM CHLORATE

By C. Shanta Kumari

(From the Department of Physics, Indian Institute of Science, Bangalore)

Received November 22, 1948

(Communicated by Prof. R. S. Krishnan, F.A.SC.)

1. Introduction

The studies on the Raman effect in sodium chlorate are not very numerous. Among the earlier workers, Dickenson and Dillon (1929), S. T. Shen, Y. T. Yao and T. Y. Wu (1937), Venkateswaran (1938) and Kujumzelis (1938) recorded the spectrum of the aqueous solutions of sodium chlorate which exhibited four lines with frequency shifts, 930, 615, 975 and 479 cm.$^{-1}$ Daure (1929), Krishnamurthy (1930) and Venkateswaran (1938) worked on crystal powders. Among them, Daure recorded the maximum number of lines, namely eight including two low frequency lines. Recently, a more detailed investigation has been made of the Raman spectrum of sodium chlorate in the form of single crystals by Rousset, Laval and Lochet (1943). They have recorded thirteen Raman lines due to the internal frequencies of the chlorate ion and three low frequency lines. They have also measured the depolarisation factors for the intense Raman lines. From a perusal of the results obtained by the earlier workers, it is evident that very little information is available regarding the lattice spectrum of sodium chlorate, although the spectrum of the chlorate ion appears to have been very thoroughly studied. This may be attributed to the fact that the earlier workers have invariably used λ 4358 and λ 4046 radiations of the mercury arc for excitation. It was therefore felt desirable to undertake a detailed study of the Raman spectrum of sodium chlorate crystal using λ 2537 as exciter, which is specially suited for recording the lattice spectrum. The results are presented in this paper.

2. Experimental Details

Crystals of sodium chlorate were prepared by the method of slow evaporation from aqueous solutions of the salt. The crystallisation was carried out in a chamber, the temperature of which was kept constant at about 27° C. A little quantity of urea was added to the solution to facilitate the growth of crystals of large size. The crystals were in the form of rectangular plates. The average dimensions of the crystals grown here for the present purpose were $1 \times 1 \times 0{\cdot}5$ cm.

The specimen to be investigated was mounted with its broad face vertical and facing the most intense portion of a water-cooled, magnet-controlled quartz arc which emitted the λ 2537 radiation with exceptional intensity. The light scattered transversely and emerging out through the edge of the crystal was focussed on the slit of a Hilger E3 quartz spectrograph. As usual, the resonance radiation from the scattered light was effectively suppressed by a mercury vapour filter. Using Ilford Special Rapid plates and a slitwidth of 0·035 mm., exposures of the order of three hours were sufficient to get a spectrogram which exhibited all the features. Photographs were taken with exposures of the order of one day; but they did not exhibit any new features. It was noticed that, due to prolonged exposure, the crystal got slightly coloured. Hence, while taking long exposure photographs, fresh crystals were used every three hours. In order to exhibit the doublet nature of some of the Raman lines more clearly, lightly exposed photographs were also taken using a fine slit (0·02 mm.).

3. Results

As is evident from the photographs reproduced in Fig. 1, the Raman spectrum of sodium chlorate consists of a series of sharply defined Raman lines, the frequency shifts of which are entered in Table I. The sharpness of the lines is more clearly seen in the microphotometric record reproduced in Fig. 2. The figures given in brackets against the frequency shifts in Table I represent visual estimates of the relative intensities of the lines. The values

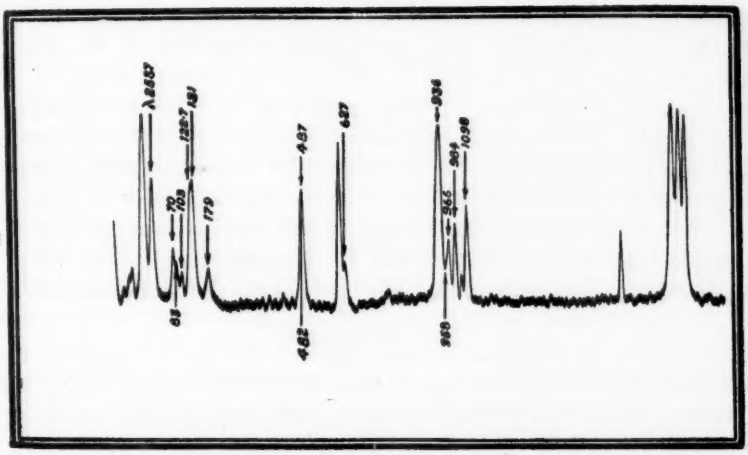

Fig. 2. Microphotometric Record of Raman Spectrum of Sodium Chlorate.

TABLE I

Raman Spectrum of Sodium Chlorate

Internal Oscillations				Lattice Oscillations			
Author		Rousset, Laval and Lochet (1943)		Author		Rousset, Laval and Lochet (1943)	
482 } 487 }	[10]	482 } 487 }	[6]	70	[6]		
				83	[4]		
627	[4]	625	[3]				
..		665	[1]	103	[2]		
..		925	[0]				
933 } 936 }	[20]	933 } 936 }	[10]	122·7 } 131 }	[15]	122·5 } 131 }	[3]
959 } 966 }	[3] [5]	963 } 966 }	[27]	179	[4]	179	[0]
984	[6]	984	[5]				
..		1003	[0]				
1028	[8]	1025	[5]				
		1285	[0]				

of the frequency shifts of the Raman lines of sodium chlorate recorded by Rousset, Laval and Lochet are included in the same table. The author's results agree reasonably well with those reported by Rousset, Laval and Lochet.

The spectrum recorded by the author exhibits nine frequency shifts due to the internal oscillations of the chlorate ion as compared to thirteen observed by Rousset, Laval and Lochet. The existence of lines of negligible intensity namely, 665, 925, 1003 and 1285 cm.$^{-1}$ reported by Rousset, Laval and Lochet could not be confirmed. Of these, the line at 1003 cm.$^{-1}$, even if present, cannot be identified in the present case, as it would fall adjacent to the mercury line λ 2603·2. In agreement with their observations, the doublet nature of the lines 482–87, 933–36 and 959–66 can be clearly seen in the enlarged photograph reproduced in Fig. 3. As compared with three lattice lines reported by Rousset, Laval and Lochet, the spectrum recorded here exhibits not less than six lattice lines of which the doublet 122·7–131 cm.$^{-1}$ (Fig. 3) is the most intense one. The line 179 cm.$^{-1}$ is rather broad.

4. DISCUSSION

Sodium chlorate crystallises in the cubic tetrahedral class. Zachariasen has shown by X-ray analysis that there are four molecules of sodium chlorate in the unit cell (Wyckoff, 1931). They are so arranged as to give the crystal rotatory power. Each molecule consists of three oxygen atoms

arranged in the form of an equilateral triangle with a separation of 2·38 A between the oxygen centres. The chlorine atom is located at a distance of 0·48 A above the plane of the oxygen atoms in a line through their centre of gravity. The sodium atom lies above the chlorine at a distance of 6·12 A. as in Fig. 4. The O–Cl distance is 1·476 A.

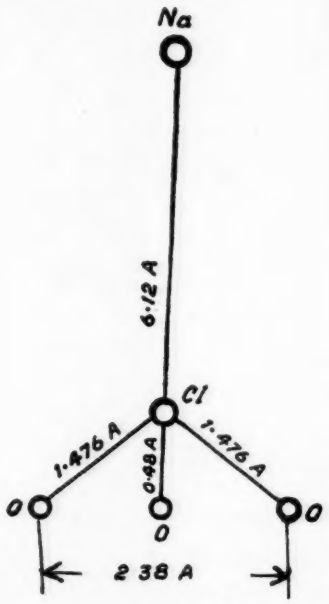

FIG. 4. Structure of $NaClO_3$ Molecule.

On semi-theoretical grounds and later, by quantum mechanical considerations it has been shown by Zachariasen that the chlorate ion in the free state has a pyramidal structure of point group C_{3v}. This has been confirmed by Venkateswaran and Shen, Yao and Wu by experimental studies. Such a unit possesses two totally symmetric vibrations ν_1 and ν_3 and two doubly degenerate vibrations ν_2 and ν_4, all of which are active in Raman effect. The four frequency shifts observed with solutions, namely, 930, 975, 615 and 479 cm.$^{-1}$ have been identified as ν_1, ν_2, ν_3 and ν_4 respectively.

Measurements on the Faraday effect in sodium chlorate by Ramaseshan (1948) indicate that the bond between Na and Cl atoms in the crystalline state is more of a covalent type than of ionic type. On the basis of this, the sodium chlorate molecule should belong to the symmetric class C_{3v}. such a molecule will have 3 vibrations which are symmetric with respect to

the axis, called parallel vibrations and 3 perpendicular vibrations, namely, ν_1, ν_3, and ν_5, and ν_2, ν_4 and ν_6 respectively. The latter vibrations are doubly degenerate. These vibrations are graphically represented in Fig. 5. As the interaction between Na and o atoms is negligible, ν_1 of the

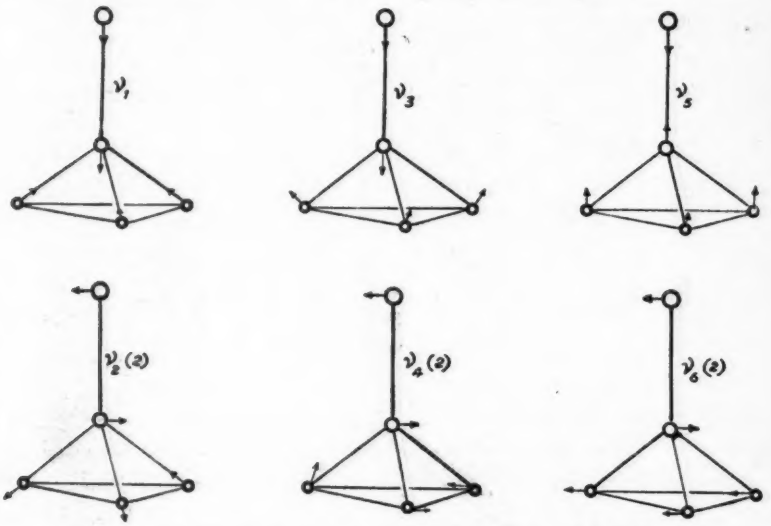

FIG. 5. The different modes of vibrations of the $NaClO_3$ Molecule.

$NaClO_3$ molecule is approximately the valence vibration ν_1 of the free ClO_3-ion (930 cm.$^{-1}$); ν_3 will correspond to the deformation vibration ν_3 of the free ClO_3-ion (615 cm.$^{-1}$) and ν_5 is the group movement of ClO_3 ion against Na. Of the three perpendicular vibrations, ν_2 and ν_4 correspond respectively to the valence vibration ν_2 (975 cm.$^{-1}$) and the deformation vibration ν_4 (479 cm.$^{-1}$) of the free ClO_3^- ion. ν_6 is the vibration of the chlorine atom with respect to the rest of the molecule, perpendicular to the symmetry axis. Comparing the frequencies observed in crystalline sodium chlorate with those of the ClO_3 ion, it is possible to give the following assignments.

ν_1	933–36 cm.$^{-1}$	ν_2	966 and 984 cm.$^{-1}$
ν_3	627 cm.$^{-1}$	ν_4	482–487 cm.$^{-1}$
ν_5	959 cm.$^{-1}$	ν_6	1028 cm.$^{-1}$

As is to be expected, because of the lower symmetry of $NaClO_3$ molecule in the lattice, the degeneracies of ν_2 and ν_4 of the free $NaClO_3$ molecule are removed and appear as double lines. The doubling of the principal frequency ν_1 (933–36 cm.$^{-1}$) may be attributed to the fact that there are four molecules in the unit cell.

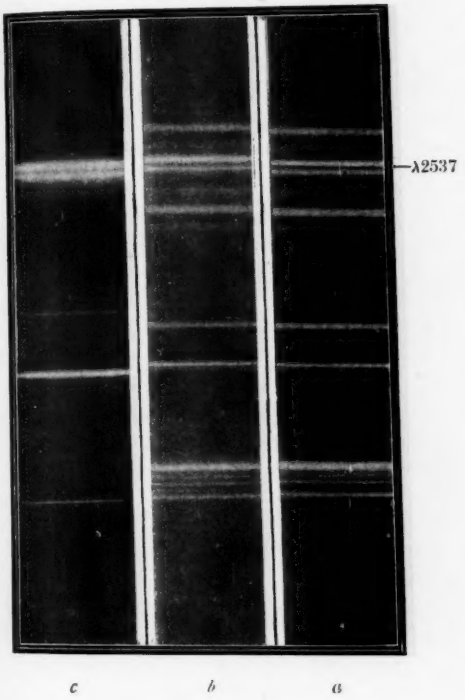

FIG. 1. *a* Raman spectrum of sodium chlorate (heavily exposed)
b „ (light picture)
c Mercury spectrum

FIG. 3. Raman spectrum of sodium chlorate (taken with E3 quartz-spectrograph)

The six lattice lines observed in the spectrum of sodium chlorate crystal are due to the external oscillations. These external oscillations are both of the rotatory type and the translatory type and there will be some interaction between the two. As the translatory type of oscillations are likely to be of low frequencies and low intensities, the lines 70, 83 and 103 cm.$^{-1}$ may come under this class. The rotatory type of oscillations will result in intense Raman lines especially if the rotatory groups are strongly optically anisotropic. The intense doublet 122·7–131 cm.$^{-1}$ and the line at 179 cm.$^{-1}$ observed in the spectrum may be assigned to oscillations of the rotatory type.

In conclusion, the author desires to record her grateful thanks to Prof. R. S. Krishnan for his valuable guidance and encouragement in the present work.

5. Summary

The Raman spectrum of sodium chlorate in the form of single crystal has been studied using λ 2537 radiation for excitation. The recorded spectrum exhibits nine Raman lines due to internal oscillations and six lines due to lattice oscillations, of which three lattice lines 70, 83 and 103 cm.$^{-1}$ are recorded for the first time by the author. Assignments have been given to all the fifteen Raman lines.

References

1. P. Daure .. *Ann. de Physique*, 1929, **2**, 375.
2. Dickenson and Dillon .. *Proc. Nat. Acad. Sci.*, 1929, **15**, 334.
3. Krishnamurthy .. *Ind. Jour. Phy.*, 1930, **5**, 633.
4. Kujumzelis .. *Zeit. für. Physik*, 1938, **110**, 760.
5. Ramaseshan .. *Proc. Ind. Acad. Sci.*, A, 1948, **28**, 360.
6. Rousset, Laval and Lochet *Comp. Rend.*, 1943, **216**, 886.
7. S. T. Sheu, Yao and Wu.. *Phy. Rev.*, 1937, **51**, 235.
8. Ta – You Wu .. *Vibrational Spectra and Structure of Polyatomic Molecules*, 1946, p. 235.
9. Venkateswaran .. *Proc. Ind. Acad. Sci.*, A, 1938, **7–8**, 144.
10. Wyckoff .. *The Structure of Crystals*, 1931, 276.

DER EINFLUSS DES KATIONS AUF DIE INTENSITÄT DES RAMANSPEKTRUMS VON SALZPULVERN

VON OTTO THEIMER

(Aus dem Physikalischen Institut der Technischen Hochschule, Graz)

Received November 15, 1948

(Communicated by Prof. K. W. F. Kohlrausch)

Synopsis.—Der Ausdruck $\delta\alpha/\delta q$, der die Abhängigkeit der Polarisierbarkeit von der Normalkoordinate einer Molekülschwingung beschreibt, wird nach der wellenmechanischen Störungsrechnung mit Hilfe eines Variationsprinzips behandelt. Es ergibt sich dabei eine Formel, die das Verhalten von $\partial\alpha/\partial q$ in starken Feldern erkennen läßt:

$$\partial\alpha/\partial q = \partial\alpha_0/\partial q \cdot (1 - kf^2)$$

Der Index Null bezieht sich auf die Feldstärke $f = 0$. Die Formel enthält ein "Verfestigungsglied" kf^2, das die Abnahme von $\partial\alpha/\partial q$ mit wachsender Feldstärke zum Ausdruck bringt. Der Proportionalitätsfaktor k hängt von der Polarisierbarkeit des unverzerrten Moleküls ab. Die Abnahme kann bei den großen Feldstärken innerhalb von Ionenkristallen bis 50% des Grenzwertes, den $\partial\alpha/\partial q$ bei unendlich kleiner Feldstärke annimmt, betragen. Angewandt auf das Ramanspektrum von Salzpulvern bedeutet dies, daß die Intensität des Ramanspektrums bei gleichbleibendem komplexen Anion mit wachsendem Ionenpotential des Kations abnimmt. Dies wird durch das Experiment im großen und ganzen bestätigt.

1. EINLEITUNG

Im Physikalischen Institut der Technischen Hochschule Graz wurden in den letzten Jahren die Ramanspektren zahlreicher kristallisierter organischer und anorganischer Salze in Pulverform aufgenommen. Die Streufähigkeit im Ramaneffekt ist bei diesen Salzen sehr verschieden. Dies liegt zum Teil an wechselnden Versuchsbedingungen wie z.B. Korngröße und Fluoreszenz. Es scheint aber auch ein systematischer Kationeneinfluß zu bestehen dergestalt, daß in kristallisierten Salzen die Intensität der Ramanstreuung eines komplexen Anions mit wachsendem Ionenpotential der umgebenden Kationen abnimmt.

2. PROBLEMSTELLUNG

Nach der Polarisierbarkeitstheorie von *G. Placzek*[1] ist die Intensität einer Ramanlinie gegeben durch:

[1] *G. Placzek*, Handbuch der Radiologie IV / 2. Leipzig, 1934.

$$I \sim \left(\frac{\partial \alpha}{\partial q}\right)^2 \qquad \alpha = \text{Polarisierbarkeit}$$

q = Normalkoordinate der Molekülschwingung

Angeregt durch den eingangs beschriebenen, experimentell allerdings recht wenig gesicherten Befund, ist es das Ziel dieser Arbeit zu zeigen, daß $\partial\alpha/\partial q$ und damit die Streufähigkeit im Ramaneffekt mit wachsendem Ionenpotential der Kationen merklich abnimmt.

Eine derartige Abnahme ist von der Polarisierbarkeit selbst schon seit langem bekannt.[2] Sie läßt sich auch quantenmechanisch erklären.[3] Die folgende Untersuchung wird zeigen, daß nach der Quantenmechanik auch $\partial\alpha/\partial q$ eine Funktion der Feldstärke ist und aus dem gleichen Grunde mit wachsender Feldstärke abnimmt wie α.

3. Allgemeine Bemerkungen über die Berechnung der Polarisierbarkeit und die wellenmechanische Störungsrechnung

Das Verhalten von $\partial\alpha/\partial q$ in starken Feldern läßt sich ziemlich leicht überblicken, wenn man eine von *H. Hellmann*[3] angegebene Formel für die Polarisierbarkeit des H-Atoms nach q differenziert. Es ergibt sich dabei unmittelbar, daß $\partial\alpha/\partial q$, wie schon gesagt, genauso mit der Feldstärke abnimmt wie α.

Die Formel von *Hellmann* ist jedoch in der mir zugänglichen Literatur nicht so abgeleitet, daß man sie für Probleme der Lichtstreuung ohneweiters verwenden kann, da die Polarisierbarkeit nicht durch das induzierte Dipolmoment, sondern durch die Polarisationsenergie definiert ist. Es läßt sich auch der Einfluß gewisser Näherungen und der Zusammenhang zwischen α und q nicht überblicken.

Es erschien mir daher notwendig, die bekannten Ergebnisse für die Polarisierbarkeit, in einer für das vorliegende Thema geeigneten Form neu abzuleiten und sie erst dann auf den noch nicht behandelten Ausdruck $\partial\alpha/\partial q$ anzuwenden.

Im allgemeinen wird die Polarisierbarkeit eines Atoms oder Moleküls so ermittelt, daß man nach den Methoden der wellenmechanischen Störungsrechnung das durch ein äußeres elektrisches Feld f induzierte Dipolmoment μ berechnet. Daraus findet man α mit Hilfe der Definitionsgleichung: $\mu = \alpha f$.

---

[2] *K. Fajans u. G. Joos*, Z. Physik, 23, I (1924).

[3] *H. Hellmann*, Einführung in die Quantenchemie, Leipzig, 1937.

Ich werde zur Berechnung von α in dieser Arbeit ein Variationsverfahren der Störungsrechnung verwenden. Dies wird wahrscheinlich allen denen, die die wellenmechanische Behandlung des Ramaneffektes kennen, als eigenartiger Umweg erscheinen. Denn für die allgemeine Theorie des Ramaneffektes ist es wesentlich, jene Form der Störungsrechnung anzuwenden, bei der die gestörte Eigenfunktion nach den Eigenfunktionen des ungestörten Systems entwickelt wird. Nur bei diesem Verfahren treten die für alle Wechselwirkungen zwischen Licht und Materie so wichtigen Übergangsfrequenzen ν_{ik} des Systems in Erscheinung. Beim Schwingungsramaneffekt ist es zwar erlaubt, gewisse Ausdrücke, die sich auf die Elektronenhülle beziehen, zur makroskopischen Polarisierbarkeit zusammenzufassen; trotzdem bedeutet es eine gewisse Sinnwidrigkeit dieses α, das schon eine ganz bestimmte, auf die Lichtstreuung besonders zugeschnittene, quantenmechanische Gestalt besitzt, nun mit Hilfe einer anderen Form der Störungsrechnung, z.B. mit Hilfe eines Variationsverfahrens, neu zu bestimmen. Dieser Vorgang kann nur durch seine mathematische Zweckmäßigkeit entschuldigt werden Er gestattet es, die fehlende Kenntnis der Eigenwerte und Eigenfunktionen des ungestörten Systems durch ein Variationsprinzip zu ersetzen. Dies ist folgendermaßen gemeint:

Die gestörte ψ-Funktion eines Systems läßt sich immer darstellen als Produkt der ungestörten Eigenfunktion mit einem Störfaktor:

$$\psi = \psi_0 (1 + v).$$

Für v ergibt sich bei Entwicklung nach Eigenfunktionen:

$$v = \frac{1}{\psi_0} \Sigma' \frac{\int \psi_n^* \, u \, \psi_0 \, d\tau}{E_0 - E_n} \cdot \psi_n$$

ψ_n und E_n sind die meist unbekannten Eigenwerte und Eigenfunktionen des ungestörten Systems.

Man kann v aber auch so bestimmen, daß man den Mittelwert der Energie

$$\bar{H} = \frac{\int \psi^* H_{o\varphi} \psi \, d\tau}{\int \psi^* \psi \, d\tau} = \bar{H}_0 + \bar{H}_1$$

zu einem Minimum macht.

$\underline{H}_{o\varphi} \equiv H_{o\varphi,\varrho} + u$ bedeutet den gestörten Energieoperator; u ist das Störpotential, $\bar{H}_1$ die mittlere Eigenwertstörung.

Der Strich über einer Größe bedeutet Mittelwertbildung, z.B.

$$\bar{u} = \frac{\int \psi^* u \psi \, d\tau}{\int \psi^* \psi \, d\tau}$$

Die Minimumsbedingung läßt sich auch in einer anderen, für die Variation bequemeren Fassung anschreiben, deren etwas umständliche Ableitung hier nicht angegeben wird (*loc. cit.* 3). Sie lautet:

$$\bar{H}_1 = \frac{\bar{u} + 2\overline{uv} - 2\bar{u}\bar{v} + \overline{uv^2} - \bar{u}\bar{v}^2 + \frac{ae^2}{2}\,\overline{(\text{grad } v)^2}}{1 + 2\bar{v} + \bar{v}^2} \qquad (1)$$

$$(\text{grad } v)^2 = \sum_{i=1}^{3N} \left(\frac{\partial v}{\partial x_i}\right)^2$$

a = Radius des H-Atoms

e = elektrisches Elementarquantum

x_i = Lagekoordinaten aller zum System gehörigen Partikel.

Wählt man nun v so, daß H_1 ein Minimum wird, dann ist dieses v das für das betreffende Störungsproblem richtige Störglied. Es ergibt sich als Funktion nur bekannter Größen und zwar der Koordinaten, der ungestörten Eigenfunktion und des Störpotentials u.

Der Störfaktor $(1 + v)$ hat einr ziemlich anschauliche Bedeutung. Sein Quadrat beschreibt z.B. im Fall der Elektroneneigenfunktion eines Moleküls die Verzerrung, die die Ladungswolke durch die Störung erleidet.

4. Die Polarisierbarkeit des H-Atoms

Da die Berechnung der Polarisierbarkeit mit Hilfe des Variationsprinzipes der Störungsrechnung zu einem Spezialgebiet gehört, das den meisten Lesern nicht geläufig sein dürfte, werde ich das Verfahren zuerst für den einfachsten Fall, das Wasserstoffatom, erläutern.

Zunächst müssen alle in Formel (1) auftretenden Größen festgesetzt werden.

Legt man die z-Achse eines an sich willkürlichen, kartesischen Koordinatensystems in die Richtung eines homogenen elektrischen Feldes f und den Koordinatenursprung in den Kern des H-Atoms, dann wird das Störpotential an der Stelle z

$$u = efz;$$

denn diese Energie wird frei, wenn man ein Elektron von einer Stelle $z = 0$ im Feld nach z verschiebt.

v setzt man in erster Näherung an:

$$v = \lambda z$$

λ ist eine Konstante, die erst durch Minimisieren der Eigenwertstörung $\bar{H}_1$ bestimmt wird.

Man wählt diesen Ansatz deshalb, weil v, wie schon gesagt, im wesentlichen die durch die Störung bedingte Deformation der Ladungswolke beschreiben soll. Diese Deformation wird im homogenen Feld, zumindest

in erster Näherung, nur in der z-Richtung erfolgen. Will man den Absolutwert der Polarisierbarkeit genauer ermitteln, dann muß man für v einen Ansatz mit mehreren Variationsparametern machen, z.B. $v = \lambda z(1 + \sigma r)$. Eine solche hohe Näherung ist jedoch im Rahmen dieser Arbeit nicht notwendig, da nur ein allgemeiner Überblick über das Verhalten der Ableitung $\partial\alpha/\partial q$ in starken Feldern gewonnen werden soll.

Mit obigen Ansätzen für u and v vereinfacht sich Formel (1) wesentlich, da wegen der Kugelsymmetrie des Wasserstoff-Grundzustandes alle Ausdrücke mit ungeraden Potenzen von z bei der Mittelwertsbildung verschwinden. Man erhält:

$$\overline{H}_1 = 2\overline{uv} + \frac{ae^2}{2}\,\frac{\overline{(\text{grad } v)^2}}{1 + \overline{v^2}}. \tag{2}$$

Für die Mittelwerte findet man:

$$\overline{uv} = \lambda ef\overline{z^2},\quad \overline{v^2} = \lambda^2\overline{z^2},\quad \overline{(\text{grad } v)^2} = \overline{(\partial v/\partial z)^2} = \lambda^2.$$

Damit wird aus (2):

$$\overline{H}_1(\lambda) = \frac{2\lambda ef\overline{z^2} + \frac{ae^2}{2}\lambda^2}{1 + \lambda^2\overline{z^2}} \tag{3}$$

Differenzieren nach λ und Nullsetzen des Differential-quotienten $\partial\overline{H}_1(\lambda)/\partial\lambda$ liefert entsprechend dem früher besprochenen Variationsprinzip die richtigen Werte für λ:

$$\frac{\partial\overline{H}_1(\lambda)}{\partial\lambda} = (1 + \lambda^2\overline{z^2})(2ef\overline{z^2} + ae^2\lambda) - (2\lambda ef\overline{z^2} + \frac{ae^2}{2}\lambda^2)\,2\lambda\overline{z^2} = 0.$$

Durch Ausmultiplizieren und Ordnen nach Potenzen von λ erhält man:

$$2ef\overline{z^2}\lambda^2 - ae^2\lambda - 2ef\overline{z^2} = 0$$

$$\lambda_{1,2} = \frac{ae^2}{4ef(\overline{z^2})^2}\left(1 \pm \sqrt{1 + \frac{16f^2(\overline{z^2})^3}{a^2e^2}}\right)$$

Der Ausdruck $16f^2(\overline{z^2})^3/a^2e^2$ unter der Wurzel ist in allen praktischen Fällen klein gegen 1. Dies erkennt man, wenn man z.B. für f jene Feldstärke einsetzt, die durch ein einfach geladenes positives Ion im Abstand $4a \sim 2$ Å hervorgerufen wird: $f^2 = e^2/16^2a^4$ und bedenkt, daß im Fall des H-Atoms $\overline{z^2}$ definitionsgemäß identisch a^2 ist. Der Ausdruck unter der Wurzel wird dann $1 + 1/16$. Man kann die Wurzel daher nach der binomischen Reihe entwickeln und die Reihe nach dem 3. Glied abbrechen und findet dann für λ:

$$\lambda_{1,2} = \frac{ae^2}{4ef(\overline{z^2})^2}\left[1 \pm \left(1 + \frac{8f^2(\overline{z^2})^3}{a^2e^2} - \frac{32f^4(\overline{z^2})^6}{a^4e^4}\right)\right]$$

Von den beiden Ausdrücken für λ führt nur der mit negativem Vorzeichen vor der runden Klammer zu einer physikalisch sinnvollen Lösung, da bei positivem Vorzeichen λ unendlich wird, wenn f gegen Null geht.

Die Lösung des Variationsproblems lautet also:

$$\lambda = -\frac{2f\overline{z^2}}{ae} + \frac{8f^3(\overline{z^2})^4}{a^3e^3}. \tag{4}$$

Damit läßt sich der Mittelwert des induzierten Diplomomentes leicht berechnen:

$$\bar{\mu} = e\int z\psi^*\psi\, d\tau = e\int z(1+v)^2\psi_0^*\psi_0 d\tau. \tag{5}$$

Setzt man für $v = \lambda z$ aus Formel (4) ein und berücksichtigt man, daß Ausdrücke mit ungeraden Potenzen von z wegen der Kugelsymmetrie von $\psi_0^*\psi_0$ bei der Mittelwertbildung wegfallen, dann wird:

$$\mu = \frac{4(\overline{z^2})^2}{a} f - \frac{16(\overline{z^2})^5}{a^3e^2} f^3 = \alpha f$$

$$\alpha = \frac{4(\overline{z^2})^2}{a} - \frac{16(\overline{z^2})^5}{a^3e^2} f^2$$

Dies läßt sich in übersichtlicher Weise schreiben:

$$\alpha = \alpha_0\left(1 - \frac{f^2\,\alpha_0^{3/2}}{2a^{1/2}e^2}\right) \tag{6}*$$

$\alpha_0 \equiv \left(\frac{4(\overline{z^2})^2}{a}\right)$ ist der Grenzwert der Polarisierbarkeit, wenn f gegen Null geht.

Das im Rahmen dieser Untersuchung wichtigste Ergebnis der Rechnung, ist die Abhängigkeit der Polarisierbarkeit von der Feldstärke f. Die Polarisierbarkeit zeigt bei großer Feldstärke Verfestigungserscheinungen, d.h. sie nimmt mit dem Quadrat der Feldstärke ab und zwar umso mehr, je größer α_0 ist. Es ist leicht abzuschätzen, daß bei Feldsterken, wie sie an den Ionenschwerpunkten in kristallisierten Salzen auftreten, die Abnahme der Polarisierbarkeit bis 50% betragen kann. Dies erkennt man, wenn man z.B. für f etwa $3e/16a^2$ und für α_0 die Polarisierbarkeit des Iod-ions einsetzt ($\alpha_{J^-} \simeq 64a^3$).

Wenn man die eben gefundenen Ergebnisse für Probleme der Lichtstreuung und Brechung an Kristallen heranzieht, dann muß man bedenken, daß die induzierende Feldstärke aus zwei Teilen besteht. Aus dem schwachen Feld f_1 des Lichtes und aus dem starken Feld f_2 der Ionen. Wäre das elektrische Feld des

* Diese Formel läßt sich viel einfacher ableiten, wenn man α durch die Polarisationsenergie $H_1 = \frac{\alpha}{2} f^2$ definiert. Da für das Problem der Ramanstreuung aber vor allem das induzierte Dipolmoment interessiert, war obige etwas komplizierte Ableitung angemessen.

Lichtes statisch, dann brauchte man in den Formeln (4–6) bloß f durch $(f_1 + f_2)$ ersetzen, ohne sonst an dem Resultat irgend etwas zu ändern. Im elektrischen Wechselfeld liegen die Dinge nicht so einfach. Man könnte z.B. annehmen, daß der Verfestigungseffekt nur bei jener Phase der elektromagnetischen Schwingung voll zur Wirkung kommt, bei der Ionen—und Lichtfeld gleichgerichtet sind. Der durchschnittliche Verfestigungseffekt wäre dann im Wechselfeld geringer als im statischen Feld. Ich möchte jedoch auf diese undurchsichtigen Verhältnisse hier nicht näher eingehen.

5. Die Polarisierbarkeit eines beliebigen Moleküls

In diesem Kapitel soll untersucht werden, wie weit die für das H-Atom abgeleiteten Ergebnisse auch für beliebige Moleküle gelten. Es wird sich zeigen, daß die Polarisierbarkeit α eines Moleküls im wesentlichen mit der gleichen Näherung als Summe der von den einzelnen Elektronen herrührenden Polarisierbarkeitsanteile α_e dargestellt werden darf, mit der es erlaubt ist die Eigenfunktion ψ des ganzen Moleküls als Produkt der einzelnen Elektroneneigenfunktionen ψ_e anzusetzen, wobei jedes einzelne ψ_e nur von den Koordinaten des e-ten Elektrons abhängen darf.

Nach *Hellmann* darf man diesen Ansatz ohne einen großen Fehler zu begehen dann machen, wenn sich die Elektronen des Moleküls in Gruppen ungefähr gleich stark gebundener Elektronen einteilen lassen, innerhalb derer die einzelnen Elektronenspins nicht parallel sind. Der Anteil der um eine Grössenordnung fester gebundenen Rumpfelektronen an der Polarisierbarkeit werde vernachlässigt. Dann kommen als Gruppen ähnlicher Bindefestigkeit nur die Valenzelektronen in Frage, von denen sowohl die nicht-anteiligen, als auch die anteiligen der homöopolaren Bindung in Paaren mit antiparallelem Spin auftreten.

Ich werde mich daher im Folgenden nur auf die Behandlung der Polarisierbarkeit von einfachen homöopolaren Bindungen beschränken, doch möchte ich schon hier bemerken—eine ausführlichere Kritik folgt am Schluß—, daß die hier vor allem interessierenden Verfestigungseffekte auch dann immer auftreten, wenn der einfache Produktansatz nicht mehr erlaubt ist und der Absolutwert der Polarisierbarkeit daher nicht mehr so einfach ermittelt werden kann.

Die Berechnung verläuft wie folgt:

Man geht wieder von der allgemeinen Formel (1) aus, legt die Werte für u und v fest und macht die mittlere Eigenwertstörung $\bar{H}_1$ durch Variation der Konstanten zu einem Minimum. u ergibt sich dabei eindeutig aus dem betreffenden Störungsproblem, während für v ein Ansatz gemacht werden

muß, der geeignet ist die Deformation der Ladungswolke passend zu beschreiben.

Mit dem Index *e* für die Elektronen und a für die Atomkerne wird das Störpotential:

$$u = ef(\Sigma z_e - \Sigma N_a z_a) \qquad (N_a = \text{Kernladung}),$$

worin *e* über alle Elektronen und a über alle Kerne läuft. Die *z*-Koordinate wurde willkürlich in die Richtung des Feldes gelegt.

Die von den Kernen abhängigen Anteile von u sind Konstante bezüglich der Mittelwertsbildung mit der Elektroneneigenfunktion und fallen daher in der Gleichung (1) heraus. Die Invarianz von Gleichung (1) gegenüber Hinzufügen beliebiger Konstanten zu *u* gestattet es auch, den Koordinatenursprung für jede Schale des Moleküls, also auch für die von uns betrachtete Schale einer einfachen homöopolaren Bindung, in den Schwerpunkt der zugehörigen Ladungsverteilung zu legen. Dadurch wird Formel (1) wesentlich vereinfacht, weil alle Glieder, die $\bar{u}$ enthalten, herausfallen.

Für *v* setzt man wieder:

$$v = \sum_e \lambda_e z_e$$

Für die Mittelwerte erhält man wegen des Produktansatzes

$\psi = \psi_1 \cdot \psi_2 \ldots \psi_e$

$$\overline{uv} = ef \sum_{ek} \lambda_e \overline{z_e z_k} = ef \sum_e \lambda_e \overline{z_e^2}, \qquad \overline{v^2} = \sum_{ek} \lambda_e \lambda_k \overline{z_e z_k} = \sum_e \lambda_e^2 \overline{z_e^2}$$

$$\overline{(\text{grad } v)^2} = \sum_e \overline{\left(\frac{\partial v}{\partial z_e}\right)^2} = \sum_e \lambda_e^2$$

$\overline{uv^2}$ enthält nur Glieder mit $\overline{z_e^3}$: Wegen der Verlegung des Koordinatenursprunges in den negativen Ladungsschwerpunkt wird auch im allgemeinsten Fall von Elektronenschalen ohne Symmetrieebene senkrecht zur Feldrichtung $\overline{uv^2}$ so klein, daß man es mit dem gleichen Recht wie die Wechselwirkung zwischen den einzelnen Elektronenschalen des Moleküls vernachlässigen kann. Die Berechnung von α läßt sich übrigens in einer höheren Näherung auch mit Berücksichtigung von $\overline{uv^2}$ durchführen, doch wird dabei der Gang der Rechnung unübersichtlich kompliziert, ohne am Ergebnis bezüglich des Verfestigungseffektes etwas Wesentliches zu ändern.

Mit obigen Werten für die Mittelwerte erhält man als Eigenwertstörung:

$$\overline{H_1}(\lambda_e) = \frac{2ef \sum_e \lambda_e \overline{z_e^2} + \frac{ae^2}{2} \sum_e \lambda_e^2}{1 + \sum_e \lambda_e^2 \overline{z_e^2}}$$

Durch partielles Differenzieren nach den λ_ε und Nullsetzen der Ableitungen erhält man e Gleichungen für die λ_ε:

$$\frac{\partial H_1(\lambda_k)}{\partial \lambda_k} = (1 + \lambda_k^2 \overline{z_k^2} + \sum_\varepsilon{}' \lambda_\varepsilon^2 \overline{z_\varepsilon^2})\,(2ef\overline{z_k^2} + ae^2\lambda_k) -$$

$$- (2ef\,\lambda_k \overline{z_k^2} + 2ef \sum_\varepsilon{}' \lambda_\varepsilon \overline{z_\varepsilon^2} - \frac{ae^2}{2}\lambda_k^2 - \frac{ae^2}{2}\sum_\varepsilon{}' \lambda_\varepsilon^2)\, 2\lambda_k \overline{z_k^2}.$$

Der Strich am Summenzeichen bedeutet, daß über den Index k nicht mehr summiert wird.

Durch Ausmultiplizieren und Ordnen nach Potenzen von λ_k erhält man näherungsweise:

$$2ef\overline{z_k^2}\lambda_k^2 - \lambda_k(ae^2 - 4ef z_k^2 \sum_\varepsilon{}' \lambda_\varepsilon \overline{z_\varepsilon^2}) - 2ef\overline{z_k^2} = 0.$$

Damit wird

$$\lambda_k = \frac{ae^2}{4ef(z_k^2)^2}\left(1 - \frac{4ef\overline{z_k^2}\sum_\varepsilon{}' \lambda_\varepsilon \overline{z_\varepsilon^2}}{ae^2} \pm \sqrt{1 - \frac{8ef z_k^2 \sum_\varepsilon{}' \lambda_\varepsilon \overline{z_\varepsilon^2}}{ae^2} + \frac{16f^2(z_k^2)^3}{a^2e^2}}\right)$$

Berücksichtigt man wieder nur die Lösung mit negativer Wurzel und entwickelt man die Wurzel bis zum dritten Glied der binomischen Reihe, dann findet man:

$$\lambda_k = -\frac{2f\overline{z_k^2}}{ae}\left[1 + \frac{(\sum_\varepsilon{}' \lambda_\varepsilon^2 \overline{z_\varepsilon^2})^2}{z_k^2}\right] + \frac{8f^3(\overline{z_k^2})^4}{a^3e^3} \tag{7}$$

Setzt man die eckige Klammer näherungsweise gleich 1, was wegen der Kleinheit der λ_ε in Rahmen der schon durchgeführten Näherungen ohneweiters erlaubt ist, dann erhält man für λ_k und damit für alle λ_ε die gleiche Formel, die schon beim Wasserstoffatom abgeleitet wurde.

Das induzierte Dipolmoment errechnet sich nun ganz einfach. Wegen des Produktansatzes $\psi = \psi_1 \cdot \psi_2 \ldots \psi_\varepsilon$ wird

$$\mu = e\int \sum_\varepsilon z_\varepsilon(1 + z_\varepsilon\lambda_\varepsilon)^2 \psi_\varepsilon^* \psi_\varepsilon d\tau_\varepsilon = e\int \sum_\varepsilon (z_\varepsilon + 2z_\varepsilon^2\lambda_\varepsilon + z_\varepsilon^3\lambda_\varepsilon^2)\,\psi_\varepsilon^*\psi_\varepsilon d\tau_\varepsilon.$$

Infolge der schon mehrfach beschriebenen Wahl des Koordinatenursprunges verschwindet das Integral über z_ε exakt und das über $z_\varepsilon^3\lambda_\varepsilon^2$ näherungsweise und es gilt:

$$\mu = e\int \sum_\varepsilon 2z_\varepsilon^2 \lambda_\varepsilon \psi_\varepsilon^* \psi_\varepsilon d\tau = \sum_\varepsilon 2\lambda_\varepsilon \overline{z_\varepsilon^2} = \sum_\varepsilon \mu_\varepsilon. \tag{8}$$

Nach Formel (8) läßt sich das in beliebigen Molekülen induzierte Dipolmoment und damit auch die Polarisierbarkeit additiv aus Anteilen der einzelnen Elektronen zusammensetzen, allerdings nur dann, wenn ein Produktansatz für die Eigenfunktion erlaubt ist, wie z.B. bei den Bindungselektronen einer einfachen homöopolaren Bindung.

Man sieht in diesem Fall unmittelbar, daß die hier vor allem interessierenden Verfestigungseffekte auch bei beliebigen Molekülen und beliebigen Elektronenschalen, z.B. auch bei den für die Ramanstreung maßgebenden Bindungselektronen auftreten, da die λ_e in Formel (8) nach (7) die gleiche Abhängigkeit von der Feldstärke zeigen wie beim H-Atom.

Ist der Produktansatz nicht mehr angebracht, dann werden zwar die in der Rechnung auftretenden Mittelwerte kompliziertere Ausdrücke; die allgemeine Form der Lösung für die λ_e und damit die Verfestigungseffekte bleiben jedoch erhalten, da letztere unabhängig vom Einzelproblem im wesentlichen mit dem Nenner der allgemeinen Störformel (1) zusammenhängen.

6. Quantenmechanische Behandlung des Ausdruckes $\partial\alpha/\partial q$

Im vorigen Kapitel wurde gezeigt, daß sich die Polarisierbarkeit eines beliebigen Moleküles bzw. einer homöopolaren Einfachbindung, näherungsweise als Summe von Elektronenanteilen darstellen läßt, für die einzeln Formel (6) gilt. Ich werde daher im Folgenden die beim H-Atom abgeleiteten Formeln für λ und α verwenden und den Elektronenindex e und die Summierung über alle e weglassen, ohne Rücksicht darauf, wieviel Elektronen das behandelte System besitzt.

Das eigentliche Problem dieser Arbeit, die Frage ob auch der Ausdruck $\partial\alpha/\partial q$ Verfestigungserscheinungen zeigt, ist nun sehr einfach zu lösen.

Wenn man überhaupt annimmt, daß α eine Funktion der Normalkoordinate q ist, dann ist in Formel (6) a_0 die *einzige* Große, die von q abhängig sein kann. Damit ergibt sich für die Ableitung nach q:

$$\frac{\partial\alpha}{\partial q} = \frac{\partial a_0}{\partial q} - \frac{5f^2 a_0^{3/2}}{4a^{1/2}e^2}\frac{\partial a_0}{\partial q} = \frac{\partial a_0}{\partial q}\left(1 - \frac{5f^2 a_0^{3/2}}{4a^{1/2}e^2}\right) \qquad (9)$$

$\partial\alpha/\partial q$ zeigt also bis auf einen Zahlenfaktor die gleichen Verfestigungserscheinungen wie α.

Die Begründung dieser Behauptung durch einfache Differentiation von Formel (6) ist zwar, wie sich zeigen wird, ziemlich korrekt, doch nicht sehr befriedigend, da nichts über den Mechanismus des Zusammenhanges zwischen α und q ausgesagt wird und der Verdacht besteht, das Ergebnis könnte anders ausfallen, wenn man α nicht als Funktion von a_0 ausdrückt, sondern entsprechend der Ableitung, unmittelbar als Funktion von λ und $\bar{r}^2$, die beide von q abhängen können.

Ich werde daher zum Abschluß Formel (9) auf korrektere und physikalisch durchsichtigere Weise ableiten, auch auf die Gefahr hin, den Leser durch die etwas umständlichen Rechnungen noch weiter zu ermüden.

Behandelt man die Verzerrungen des schwingenden Moleküls als Störung des ruhenden Moleküls, dann kann man die durch die Verzerrung gestörte Elektronen-eigenfunktion nach dem Variationsprinzip darstellen als:

$$\psi = \psi_0 (1 + \epsilon q)$$

ϵ ist ein Variationsparameter, der auf alle Fälle klein gegen 1 ist und nur bei einer Absolutberechnung von $\partial a/\partial q$ interessieren würde; q ist die Normalkoordinate der Molekülschwingung, die die Verzerrung des Moleküls aus der Ruhelage beschreibt.

ψ ist nun eine Funktion von q.

Wirkt auf ein so verzerrtes Molekül ein elektrisches Feld ein, dann wird die Eigenfunktion zusätzlich gestört und erhält im Anschluß an die früheren Rechnungen die Form:

$$\psi = \psi_0 (1 + \epsilon q)(1 + \lambda z)$$

Damit wird das Dipolmoment

$$\mu = e \int z (1 + \epsilon q)^2 (1 + \lambda z)^2 \psi_0^* \psi_0 d\tau$$

Legt man den Koordinatenursprung wie immer so, daß $\bar{z}$ verschwindet, und vernachlässigt man die Glieder mit λ^2, dann wird

$$\mu = 2e\lambda \overline{z^2} (1 + \epsilon q)^2 \tag{10}$$

Nimmt man zunächst an, daß λ durch die der Schwingung entsprechende Verzerrung des Moleküls nicht verändert wird, dann kann man λ aus Formel (4) in Formel (10) einsetzen und erhält:

$$\mu = 2e\overline{z^2}(1 + \epsilon q)^2 [-2f\overline{z^2}/ae + 8f^3(\overline{z^2})^4/a^3e^3]$$

$$\alpha = -\mu/f = 2e\overline{z^2}(1 + \epsilon q)^2 (2z^2/ae - 8f^2(\overline{z^2})^4/a^3e^3) =$$

$$= \alpha_0 \left(1 - \frac{f^2 \alpha_{0,0}^{3/2}}{2a^{1/2}e^2}\right) \tag{11}$$

$$\text{mit } \alpha_0 = \frac{4(\overline{z^2})^2 (1 + \epsilon q)^2}{a} \text{ und } \alpha_{0,0} = \frac{4(\overline{z^2})^2}{a} \text{ (vergl. Formel 6)}$$

$\alpha_{0,0}$ bedeutet in dieser Formel den Grenzwert von α für unendlich kleine Feldstärke des ruhenden unverzerrten Moleküls.

Nur α_0 ist eine Funktion von q, dargestellt durch Multiplikation mit dem Faktor $(1 + \epsilon q)^2$; $\alpha_{0,0}$ dagegen ist unabhängig von q.

Der Ausdruck $\partial a/\partial q$ läßt sich nun leicht durch Differenzieren ermitteln:

$$\frac{\partial \alpha}{\partial q} = 4e\overline{z^2}\epsilon (1 + \epsilon q)(2z^2/ae - 8f^2(\overline{z^2})^4/a^3e^3) = \frac{\partial \alpha_0}{\partial q}\left(1 - \frac{f^2 \alpha_{0,0}^{3/2}}{2a^{1/2}e^2}\right) \tag{12}$$

Es bleibt nur noch zu untersuchen, ob die sicher bestehende Abhängigkeit des λ von q irgend etwas Wesentliches an dem Resultat ändert.

Da bei der Bestimmung von λ, die zu Formel (4) bzw. (*F*) führte, keine speziellen Annahmen über die Eigenfunktion der betrachteten Elektronenschale gemacht wurden, bleibt Formel (4) auch erhalten, wenn die Eigenfunktion durch die Schwingung verzerrt wird. Es ändert sich dabei bloß der Mittelwert $\overline{z^2}$. Diese Änderung läßt sich leicht ermitteln. Man geht von Formel (4) aus:

$$\lambda_0 = \frac{-2f\overline{z^2}}{ae} + \frac{8f^3(\overline{z^2})^4}{a^3e^3}.$$

Der Index 0 deutet an, daß sich λ auf das unverzerrte Molekül bezieht.

Um das λ des verzerrten Moleküls zu erhalten, ersetzt man jetzt

$$\overline{z^2} \equiv \int z^2\psi^*\psi d\tau \text{ durch } \overline{z^2} = \int z^2(1+\epsilon q)^2\psi_0^*\psi_0\, d\tau$$

Damit wird

$$\lambda = -\frac{2f}{ae}\int z^2(1+\epsilon q)^2\psi_0^*\psi_0\, d\tau + \frac{8f^2}{a^3e^3}\left[\int z^2(1+\epsilon q)^2\psi_0^*\psi_0\, d\tau\right]^4$$

Vernachlässigt man bei der Mittelwertbildung alle Glieder mit höheren Potenzen von ϵ als ϵ^2, dann erhält man näherungsweise:

$$\lambda = \lambda_0[1+\epsilon q(2+\epsilon q)]$$

Setzt man diesen Wert für λ in (10) ein, dann gewinnt man einen Ausdruck der gleichen Form wie Formel (11):

$$a = 2e\overline{z^2}(1+\epsilon q)^4(2\overline{z^2}/ae - 8f^2(\overline{z^2})^4/a^3e^3) = a_0\left(1 - \frac{f^2 a_{0,0}^{3/2}}{2a^{1/2}e^2}\right) \qquad (13)$$

In Formel (13) hat sich gegenüber (11) nur a_0 geändert, während $a_{0,0}$ gleich geblieben ist.

Aus diesem Grund bleibt Formel (12), die den Verfestigungseffekt von $\partial a/\partial q$ beschreibt, vollkommen erhalten, abgesehen davon, daß $\partial a_0/\partial q$ gegenüber (12) einen anderen Wert annimt.

Mit dieser Feststellung ist die Untersuchung des Verhaltens von $\partial a/\partial q$ in starken Feldern beendet. Das Ergebnis, das in Formel (12) mathematisch formuliert ist, konnte nur nach zahlreichen Näherungen in einfacher Form gewonnen werden. Es erscheint mir daher wichtig, den möglichen Einfluß der verschiedenen Vernachlässigungen klarzustellen.

Wesentlich an allen Ableitungen in dieser Arbeit sind die Ansätze für das Störpotential u and das Störglied v, als Funktionen von z. Dadurch gehen in alle Formeln dieser Arbeit, auch bei beliebig hoher Näherung, als *einzige* Moleküleigenschaft nur die Mittelwerte der Potenzen von z ein. Auch der Verfestigungseffekt ist grundsätzlich unabhängig vom Einzelfall, d.h. von der speziellen Form der Elektroneneigenfunktion und von den mehr oder weniger groben Vernachlässigungen insbesondere auch vom Produktansatz für die Eigenfunktionen. Er hängt nur mit dem Nenner der

allgemeinen Störformel (1) zusammen, der bei der Differentiation nach λ die negativen Glieder bewirkt.

Da, wie schon gesagt, nur eine einzige Moleküleigenschaft, nämlich $\overline{z^2}$, in die Formeln eingeht, bleibt der Verfestigungseffekt auch bei Differentiation nach q unabhängig von den gemachten Vernachlassigungen immer erhalten.

Im *inhomogenen* Feld der Ionen ist allerdings die Voraussetzung dieser Beweisführung nicht mehr gegeben. u and v hängen nicht nur von z sondern auch vom Abstand r der Elektronen von der Molekülachse ab. Diese Abhängigkeit ist zwar meist vernachlässigbar klein (*loc. cit.* 3), ihre Vernachlässigung bedeutet aber immerhin eine Näherung, deren Einfluß auf die Abnahme von $\partial\alpha/\partial q$ genauer untersucht werden müßte.

Zum Schluß möchte ich die physikalischen Konsequenzen von Formel (12) noch einmal zusammenfassen. Sie besagt, daß der Ausdruck $\partial\alpha/\partial q$, der die Abhängigkeit der Polarisierbarkeit von der Normalkoordinate einer Molekülschwingung beschreibt, eine Funktion der Feldstärke ist. Diese Funktion ist so beschaffen, daß ein Verfestigungsglied mit dem Quadrat der Feldstärke zunimmt, wobei die Polarisierbarkeit selbst abnimmt. Die Abnahme ist umso stärker, je größer die Polarisierbarkeit $\alpha_{0,0}$ des unverzerrten Moleküls bei unendlich kleiner Feldstärke ist und kann bei den großen Feldstärken im Inneren von Ionenkristallen bis zu 50% des Grenzwertes $\lim_{f\to 0} \partial\alpha/\partial q$ betragen.

Wendet man diesen Satz auf das Ramanspektrum von Salzpulvern an, dann bedeutet er, daß nach Ausschaltung aller anderen Einflüsse die Intensität des Ramanspektrums, bei gleichem komplexen Anion, mit wachsendem Ionenpotential des Kations abnimmt. Ein Ergebnis, das im großen und ganzen mit dem experimentellen Befund in Einklang steht.

Ich möchte Herrn Prof. Dr. *K. W. F. Kohlrausch* danken, der mich auf die Möglichkeit aufmerksam machte, die Intensität der Ramanstreuung in Kristallpulvern nach obigem Verfahren zu behandeln.

1180 48. Printed at the Bangalore Press, Bangalore City, by G. Srinivasa Rao, Superintendent and Published by The Indian Academy of Sciences, Bangalore

NOTICE TO AUTHORS

Scientific papers intended for publication in the *Proceedings of the Indian Academy of Sciences* can be accepted only when they are communicated by Fellow of the Academy whose duty shall be to satisfy himself that such communications are fit to be read at the Meeting of the Academy and published in its *Proceedings*.

Papers should not ordinarily exceed fifty pages of foolscap. MSS. should be either typewritten or written in legible hand on one side of the paper. All papers should be carefully revised by the authors and should be absolutely in final form for printing. Position for text-figures should be indicated. Each paper shall conclude with a critical summary not exceeding 350 words.

Drawings, diagrams or other illustrations should be made on larger scale (preferably) twice the size than the ones in which they are intended to appear. They should be done in Indian ink on bristol board with lettering in pencil. Scale of magnification of camera lucida tracings should be indicated by the side of drawings. In certain special cases arrangements will also be made for monochrome lithographic and other colour plates. Reduction of illustrations desired should be indicated in pencil. Appropriate legends should accompany all drawings. Names of authors are to be marked in pencil on the left-hand corner of drawing sheets. Photomicrographs should be securely mounted with colourless paste.

All tables, quotations and footnotes which will be set hereafter (beginning from Vol. I, No. 2) in types smaller than the text, should be typewritten on separate sheets and placed with the text in proper sequence. Footnotes should be numbered in Arabic numerals.

References to literature in the text should be given, whenever possible, in chronological order, only the names of authors and years of publication, in brackets, being given. They should be cited in full after the summary, the authors' names following in alphabetical order. Thus,

Name or Names of author; Name of Journal (abbreviation) with a single underline; Year of publication; Number of Volume with a double underline, and lastly page. The following would be a useful illustration:—

Bergmann and Stather . . . . . Z. Physiol. Chem., 1926, 152, 189.

Two copies of slip-proof and wherever possible, a page proof for final revision will be sent to authors. All corrections are best made on the slip-proof which should be transmitted to the Office of the Academy. All proof corrections involve heavy expenses which would be negligible if the papers are carefully revised by the authors before submission.

Authors will be supplied with reprints of their papers at cost price, intimation is given at the time of returning the slip-proof.

All the blocks printed in the *Proceedings* will be offered to the respective authors at a price of 25% of the actual cost of preparing the blocks *plus* the packing and postal charges or railway freight to be incurred for despatching them, it being understood that authors should give due acknowledgment to the Academy whenever such blocks are reproduced in other journals.

The original drawings and plates of blocks appearing in the *Proceedings* will be returned to such of the authors as may require them provided the cost of despatching such originals is borne by them.

Intending new subscribers for the PROCEEDINGS of the Academy (Section A), beginning with Volume XXVIII, will on payment of the usual annual subscription of Rs. 18 or £. 1/10/- receive the enlarged Number for November 1948 (SYMPOSIUM ON CRYSTAL PHYSICS) without extra cost. Separate copies of the same can also be had in the usual paper covers from the Indian Academy of Sciences, Malleswaram P.O., Bangalore–3 (S. India), at Rs. 10 or £. 1 per copy. Calico bound copy will cost Rs. 15 or £. 1/10/-.